ISSN 0021-9673

VOL. 356 NO. 2 APRIL 4, 1986

JOURNAL OF CHROMATOGRAPHY

INTERNATIONAL JOURNAL ON CHROMATOGRAPHY, ELECTROPHORESIS AND RELATED METHODS

ELSEVIER

JOURNAL OF CHROMATOGRAPHY

Scope. The *Journal of Chromatography* publishes papers on all aspects of chromatography, electrophoresis and related methods. Contributions consist mainly of research papers dealing with chromatographic theory, instrumental development and their applications. The section *Biomedical Applications,* which is under separate editorship, deals with the following aspects: developments in and applications of chromatographic and electrophoretic techniques related to clinical diagnosis (including the publication of normal values); screening and profiling procedures with special reference to metabolic disorders; results from basic medical research with direct consequences in clinical practice; combinations of chromatographic and electrophoretic methods with other physicochemical techniques such as mass spectrometry. In *Chromatographic Reviews,* reviews on all aspects of chromatography, electrophoresis and related methods are published.

Submission of Papers. Papers in English, French and German may be submitted, in three copies. Manuscripts should be submitted to: The Editor of *Journal of Chromatography,* P.O. Box 681, 1000 AR Amsterdam, The Netherlands, or to: The Editor of *Journal of Chromatography, Biomedical Applications,* P.O. Box 681, 1000 AR Amsterdam, The Netherlands. Review articles are invited or proposed by letter to the Editors and will appear in *Chromatographic Reviews* or *Biomedical Applications.* An outline of the proposed review should first be forwarded to the Editors for preliminary discussion prior to preparation. Submission of an article is understood to imply that the article is original and unpublished and is not being considered for publication elsewhere. For copyright regulations, see below.

Subscription Orders. Subscription orders should be sent to: Elsevier Science Publishers B.V., P.O. Box 211, 1000 AE Amsterdam, The Netherlands. The *Journal of Chromatography* and the *Biomedical Applications* section can be subscribed to separately.

Publication. The *Journal of Chromatography* (incl. *Biomedical Applications, Chromatographic Reviews* and *Cumulative Author and Subject Indexes, Vols. 326–350*) has 38 volumes in 1986. The subscription prices for 1986 are:

J. Chromatogr. (incl. *Chromatogr. Rev.* and *Cum. Indexes, Vols. 326–350*) + *Biomed. Appl.* (Vols. 346–383): Dfl. 6080.00 plus Dfl. 912.00 (postage) (total *ca.* US$ 2589.75)

J. Chromatogr. (incl. *Chromatogr. Rev.* and *Cum. Indexes, Vols. 326–350*) only (Vols. 346–373): Dfl. 5040.00 plus Dfl. 672.00 (postage) (total *ca.* US$ 2115.50)

Biomed. Appl. only (Vols. 374–383): Dfl. 1850.00 plus Dfl. 240.00 (postage) (total *ca.* US$ 774.00).

Journals are automatically sent by airmail at no extra costs to Argentina, Australia, Brasil, Canada, China, Hong Kong, India, Israel, Japan, Malaysia, Mexico, New Zealand, Pakistan, Singapore, South Africa, South Korea, Taiwan, Thailand and the U.S.A. Back volumes of the *Journal of Chromatography* (Vols. 1 through 345) are available at Dfl. 219.00 (plus postage). Claims for issues not received should be made within three months of publication of the issue. If not, they cannot be honoured free of charge. Customers in the U.S.A. and Canada wishing information on this and other Elsevier journals, please contact Journal Information Center, Elsevier Science Publishing Co. Inc., 52 Vanderbilt Avenue, New York, NY 10017. Tel. (212) 916-1250.

Abstracts/Contents Lists published in Analytical Abstracts, Biochemical Abstracts, Biological Abstracts, Chemical Abstracts, Chemical Titles, Current Contents/Physical, Chemical & Earth Sciences, Current Contents/Life Sciences, Deep-Sea Research/Part B: Oceanographic Literature Review, Index Medicus, Mass Spectrometry Bulletin, PASCAL-CNRS, Referativnyi Zhurnal and Science Citation Index.

See page 3 of cover for Publication Schedule, Information for Authors and information on Advertisements.

0021-9673/86/$03.50

Printed in The Netherlands

CONTENTS

(Abstracts/Contents Lists published in Analytical Abstracts, Biochemical Abstracts, Biological Abstracts, Chemical Abstracts, Chemical Titles, Current Contents/Physical, Chemical & Earth Sciences, Current Contents/Life Sciences, Deep-Sea Research/Part B: Oceanographic Literature Review, Index Medicus, Mass Spectrometry Bulletin, PASCAL-CNRS, Referativnyi Zhurnal and Science Citation Index)

(Continued overleaf)

. . . Attend HPLC '86

The 10th International Symposium On Column Liquid Chromatography

San Francisco, May 18-23, 1986

For the first time this prestigious symposium will be held on the West Coast. With the large number of presentations, there will be something that should appeal to everyone.

Specific Scientific Sessions planned on:

- *New Separation & Detection Principles*
- *Sample Preparation/Robotics*
- *New Columns/Column Switching*
- *Ion Chromatography*
- *Preparative LC*
- *Separation of Cells*
- *Proteins, Peptides & Amino Acids*
- *Drugs/Endogenous Compounds in Biological Fluids*
- *Latest Advances in Size Exclusion Chromatography*
- *Characterization of Bonded Phases*
- *Applications (Industrial, Food, Agricultural, etc.)*

. . . And More!

- *Sponsored by all major chemical and chromatography societies throughout the world*
- *Exhibition of latest instrumentation, columns, & accessories . . . Over 70 exhibitors*
- *Over 500 papers submitted — Oral, poster, scientific roundtable presentations*
- *Full social program*

For full details, preliminary program, and registration information, send to:

HPLC '86 SAN FRANCISCO

Ms. Shirley Schlessinger
Symposium Manager
of HPLC '86
400 E. Randolph Drive
Chicago, IL 60601 U.S.A.

NAME _____

TITLE _____

AFFILIATION _____

ADDRESS _____

_____

TELEPHONE _____

220g

Journal of Chromatography, 356 (1986) 231–245
Elsevier Science Publishers B.V., Amsterdam — Printed in The Netherlands

CHROM. 18 398

THE GOUY–CHAPMAN THEORY IN COMBINATION WITH A MODIFIED LANGMUIR ISOTHERM AS A THEORETICAL MODEL FOR ION-PAIR CHROMATOGRAPHY

JAN STÅHLBERG*
Astra Pharmaceutical Production AB, Quality Control, S-151 85 Södertälje (Sweden)
(First received September 20th, 1985; revised manuscript received December 10th, 1985)

SUMMARY

A theory for ion-pair chromatography is developed, based on a Langmuir-like adsorption isotherm and the Gouy–Chapman theory for an electrically charged surface. It is found that the predictions made by the theory agree qualitively and semi-quantitatively with experimental results. A useful consequence of the theory is that when the charges of ions Y and R are of equal magnitude but of opposite signs

$$k'_Y k'_R = K_1$$

and when the charges are of equal magnitude and sign

$$k'_Y / k'_R = K_2$$

where the constants are independent of the concentration of amphiphilic modifier in the mobile phase.

INTRODUCTION

Liquid chromatographic analysis of organic ions is often carried out with a mobile phase modified with amphiphilic molecules. This analytical technique is usually called ion-pair chromatography. There are a number of different theories concerning the physico-chemical interpretation of the experimental findings. The theoretical and experimental findings have been summarized in ref. 1.

Most of the published theories define a scheme for the various equilibria that may exist in the system. Relationships between the capacity factor, k', and the corresponding equilibrium constants are then derived. However, it is generally found that when long-range forces between the molecules are of importance the equilibrium constants vary with the composition of the system. A well known example is the Debye–Hückel corrections made for ionic systems.

* Affiliated to the Institute of Physical Chemistry, University of Uppsala, Uppsala, Sweden.

0021-9673/86/$03.50

This work presents a theory where the contributions from the chemical and electrostatic energies are separated. In ion-pair chromatography the electrostatic energy is related to the electrostatic potential of the surface, which in turn depends on the charge density on the surface, *i.e.*, the concentration of adsorbed amphiphilic ions. The importance of this electrostatic potential for the retention of solute molecules has also been proposed by Cantwell[2]. He writes that "there appears to have been little recognition of the role played by the surface potential created by the sorption of P^+ in enhancing the surface sorption of S^-". An interesting work by Deelder and Van den Berg[3] shows that the Stern–Gouy–Chapman theory well describes the adsorption of sodium 1-dodecanesulphonate on octadecyl modified silica.

This paper derives equations for the adsorption isotherm of the amphiphilic ion used as modifier in the mobile phase. The adsorption isotherm is then used to derive equations for the capacity factor for solute ions. It is of the Langmuir type and has been applied to calculate adsorption isotherms for amphiphilic ions at the oil–water interface[4]. The Gouy–Chapman theory for a plane surface is used to derive the equations relating the amount of adsorbed amphiphilic ions to the electrostatic potential of the surface.

THEORETICAL

The general assumption is that the adsorption of a charged organic molecule, Q^{z_Q}, on the stationary phase is primarily governed by two factors: the electrostatic repulsion (attraction) from (to) the surface, governed by the electrostatic potential of the surface, ψ_0, and the charge of the molecule, z_Q; and the free energy of adsorption of the molecule, $-\Delta G_Q^\circ$ (kJ/mol), when $\psi_0 = 0$. Assuming that the maximum possible concentration of Q^{z_Q} molecules on the surface is n_0 mol/m^2 and using the isotherm that applied previously for adsorption of surfactants at the oil–water interface[4], one obtains

$$n_Q = \frac{Bc_Q \cdot \exp[(-\Delta G_Q^\circ - z_Q F\psi_0)/RT]}{1 + B(c_Q/n_0) \cdot \exp[(-\Delta G_Q^\circ - z_Q F\psi_0)/RT]} \tag{1}$$

where n_Q is the concentration (mol/m^2) of molecule Q^{z_Q} on the surface, c_Q is the concentration (mol/m^3) of the amphiphilic modifier Q^{z_Q} in the mobile phase, F is the Faraday number and B is a constant representing the thickness of the surface layer.

If Q^{z_Q} is added to the solvent as the salt QX and X^{-z_Q} is not adsorbed, the concentration of Q^{z_Q} on the surface determines the electrostatic potential of the surface. To calculate the adsorption isotherm for Q^{z_Q} the relationship between n_Q and ψ_0 has to be determined. This is obtained from the Poisson–Boltzmann equation for a planar surface and the well known Gouy–Chapman theory[5]. Since it is essential for a proper understanding of the final results, a derivation of the equations will be given here. Readers not interested in the derivation may proceed to eqn. 11 which is the isotherm obtained.

To maintain electroneutrality in the system, the charge of the surface is the same as the charge in the solution but of opposite sign. When performing chromatography with amphiphilic ions as modifiers, the solvent usually contains inorganic ions too and this has to be considered in order to obtain the general solution

of the equations. It is assumed that these ions contribute to the double layer but are not adsorbed on the surface. To be able to obtain an explicit solution we must restrict ourselves to the case where all ions in the system have charges of equal magnitude, *i.e.*, $+z$ and $-z$. The condition of electroneutrality is

$$n_Q z_Q F = -|z_Q| F \int_0^\infty \left[\left(\sum_{i,+} c_{0,i} \right) \cdot \exp\left(-\frac{|z_i| F\psi(x)}{RT} \right) - \left(\sum_{j,-} c_{0,j} \right) \cdot \exp\left(\frac{|z_i| F\psi(x)}{RT} \right) \right] dx \tag{2}$$

where x is the distance from the surface, $\psi(x)$ is the electrostatic potential at x, $|z_i| = |z_Q|$, $c_{0,i}$ represents the concentration of the positively charged ion i at infinite distance from the surface and $c_{0,j}$ is concentration of the corresponding negatively charged ion j; to simplify the equations the concentration unit is mol/m^3. The summation symbols indicate that a number of different positively and negatively charged ions may be present. It is important to point out that the concentration of Q^{z_Q} is included in the summation. Furthermore, there is electroneutrality at infinite distance from the surface, *i.e.*

$$\sum_{i,+} c_{0,i} = \sum_{j,-} c_{0,j} = \sum_i c_{0,i} \tag{3}$$

since all the charges are of the same magnitude. By using the definition of $\sinh(x)$ we can now rewrite eqn. 2 as:

$$n_Q z_Q F = 2|z_Q| F \left(\sum_i c_{0,i} \right) \cdot \int_0^\infty \sinh \frac{|z_Q| F\psi(x)}{RT} dx \tag{4}$$

According to the Poisson equation the following relationship holds

$$\frac{d^2\psi}{dx^2} = \frac{-\rho(x)}{\varepsilon_0 D} \tag{5}$$

where $\rho(x)$ is the charge density (C/m^3) in the mobile phase at a distance x from the surface, ε_0 is the permittivity in a vacuum and D is the dielectric constant of the mobile phase. The charge density at x can also be written as follows:

$$\begin{aligned} \rho(x) &= |z_Q| F \left[\left(\sum_{i,+} c_{0,i} \right) \exp\left(-\frac{|z_i| F\psi(x)}{RT} \right) - \left(\sum_{j,} c_{0,j} \right) \exp\left(\frac{|z_i| F\psi(x)}{RT} \right) \right] \\ &= -2|z_Q| F \left(\sum_i c_{0,i} \right) \sinh \frac{|z_Q| F\psi(x)}{RT} \end{aligned} \tag{6}$$

Combining eqns. 4–6 one obtains

$$n_Q z_Q F = \varepsilon_0 D \int_0^\infty \frac{d^2\psi}{dx^2} dx = -\varepsilon_0 D \left(\frac{d\psi}{dx}\right)_{x=0} \tag{7}$$

since $d\psi/dx \to 0$ as $x \to \infty$. Integration of eqn. 5, after inserting the expression for $\rho(x)$ in eqn. 6, gives:

$$\frac{d\psi}{dx} = \left[\frac{8\left(\sum_i c_{0,i}\right)RT}{\varepsilon_0 D}\right]^{1/2} \sinh \frac{|z_i|F\psi(x)}{2\,RT} \tag{8}$$

At the surface $\psi = \psi_0$ and combining eqns. 7 and 8 gives:

$$n_Q z_Q F = \left(8\varepsilon_0 DRT \sum_i c_{0,i}\right)^{1/2} \sinh \frac{|z_i|F\psi_0}{2\,RT} \tag{9}$$

This is the equation obtained from the Gouy–Chapman theory.

Inverting this equation and using the relationship $\sinh^{-1} x = \ln[x + (x^2 + 1)^{1/2}]$, see, *e.g.*, ref. 6, one obtains:

$$\psi_0 = \frac{2\,RT}{|z_i|F} \ln\left\{\frac{n_Q z_Q F}{\left(8\varepsilon_0 DRT \sum_i c_{0,i}\right)^{1/2}} + \left[\frac{(n_Q z_Q F)^2}{8\varepsilon_0 DRT \sum_i c_{0,i}} + 1\right]^{1/2}\right\} \tag{10}$$

When eqn. 10 is substituted into eqn. 1 and considering that it is an odd function, eqn. 11 is obtained:

$$n_Q = \frac{Bc_Q \cdot \exp\left(-\dfrac{\Delta G_Q^\circ}{RT}\right)}{\left\{\dfrac{n_Q|z_Q|F}{\left(8\varepsilon_0 DRT \sum_i c_{0,i}\right)^{1/2}} + \left[\dfrac{(n_Q|z_Q|F)^2}{8\varepsilon_0 DRT \sum_i c_{0,i}} + 1\right]^{1/2}\right\}^2 + Bc_Q/n_0 \cdot \exp\left(-\dfrac{\Delta G_Q^\circ}{RT}\right)} \tag{11}$$

Solving this equation for n_Q for different values of c_Q gives the adsorption isotherm for $Q^{z}{}_{Q}$.

The theory used to calculate the adsorption isotherm for $Q^{z}{}_{Q}$ may also be used to calculate the retention of a solute molecule, $Y^{z}{}_{Y}$, as a function of the concentration of $Q^{z}{}_{Q}$ on the surface and, thus indirectly, as a function of the concentration of $Q^{z}{}_{Q}$ in the mobile phase. The starting equation is again eqn. 1, with all the subscripts Q changed to Y. The next step is to evaluate the relationship between ψ_0 and the

concentrations of adsorbed ions on the surface, n_Q and n_Y. This can be done by using eqn. 10 by adding the concentrations of the absorbed species, with proper consideration of their charges, and we obtain the following equation:

$$\psi_0 = \frac{2\,RT}{|z_i|F} \ln\left\{ \frac{F(n_Q z_Q + n_Y z_Y)}{\left(8\varepsilon_0 DRT \sum_i c_{0,i}\right)^{1/2}} + \left(\frac{[F(n_Q z_Q + n_Y z_Y)]^2}{8\varepsilon_0 DRT \sum_i c_{0,i}} + 1 \right)^{1/2} \right\} \qquad (12)$$

This equation has then to be introduced in the equations for the isotherms of n_Q and n_Y, respectively. It is readily seen that it is not possible to obtain an equation where n_Y is solely dependent on n_Q. Thus, it can be concluded that the general case has to be treated by an iteration procedure.

It is the influence on ψ_0 of the adsorbed Y^{z_Y} ions that makes the evaluation difficult. In the limit where this influence is negligible, *i.e.*, when $n_Q z_Q \gg n_Y z_Y$, the equation for the adsorption isotherm of Y simplifies to:

$$n_Y = Bc_Y \cdot \exp[(-\Delta G^\circ_Y - z_Y F\psi_0)/RT] \qquad (13)$$

Since ψ_0 is assumed to be determined by n_Q, eqn. 10 applies giving

$$n_Y = Bc_Y \cdot \exp\left(-\frac{\Delta G^\circ_Y}{RT}\right) \cdot \left\{ \frac{n_Q|z_Q|F}{\left(8\varepsilon_0 DRT \sum_i c_{0,i}\right)^{1/2}} + \left[\frac{(n_Q|z_Q|F)^2}{8\varepsilon_0 DRT \sum_i c_{0,i}} + 1 \right]^{1/2} \right\}^{-2z_Y/z_Q} \qquad (14)$$

since $|z_Q| = |z_i|$. From the definition of the capacity factor we obtain

$$k'_Y = A' \cdot \exp\left(-\frac{\Delta G^\circ_Y}{RT}\right) \cdot \left\{ \frac{n_Q|z_Q|F}{\left(8\varepsilon_0 DRT \sum_i c_{0,i}\right)^{1/2}} + \left[\frac{(n_Q|z_Q|F)^2}{8\varepsilon_0 DRT \sum_i c_{0,i}} + 1 \right]^{1/2} \right\}^{-2z_Y/z_Q} \qquad (15)$$

where $A' = BA_s/V_m$ and A_s/V_m is the phase ratio. We have thus obtained an equation for the capacity factor of a solute molecule as a function of the concentration of amphiphilic modifier on the surface, which through eqn. 11 is related to the concentration of amphiphilic modifier in the mobile phase.

RESULTS AND DISCUSSION

The adsorption isotherm

From eqn. 11 it is possible to calculate the adsorption isotherm for the amphiphilic modifier $Q^{z}o$. The relationship between n_Q and c_Q is slightly complex, so when c_Q is known the equation has to be evaluated by suitable numerical methods. Eqn. 11 is derived from eqn. 1 from which it is seen that the amount of $Q^{z}o$ adsorbed depends on the following parameters: the concentration of $Q^{z}o$ in the mobile phase, c_Q; the free energy of adsorption for $Q^{z}o$, $-\Delta G^{\circ}_{Q}$; the electrostatic potential of the surface, ψ_0; the thickness of the surface layer, B; the maximum possible concentration of $Q^{z}o$ on the surface, n_0, and the charge of $Q^{z}o$, z_Q. However, according to eqn. 10, the electrostatic potential of the surface, ψ_0, also depends on a number of parameters: the surface concentration of $Q^{z}o$, n_Q; the charge of $Q^{z}o$; the dielectric constant of the mobile phase, D, and the concentration of ions in the mobile phase, $\sum_i c_{0,i}$.

A number of parameters must thus be considered. A few numerical examples are given to demonstrate how some of these parameters influence the adsorption isotherm. These examples are compared with adsorption isotherms from the literature.

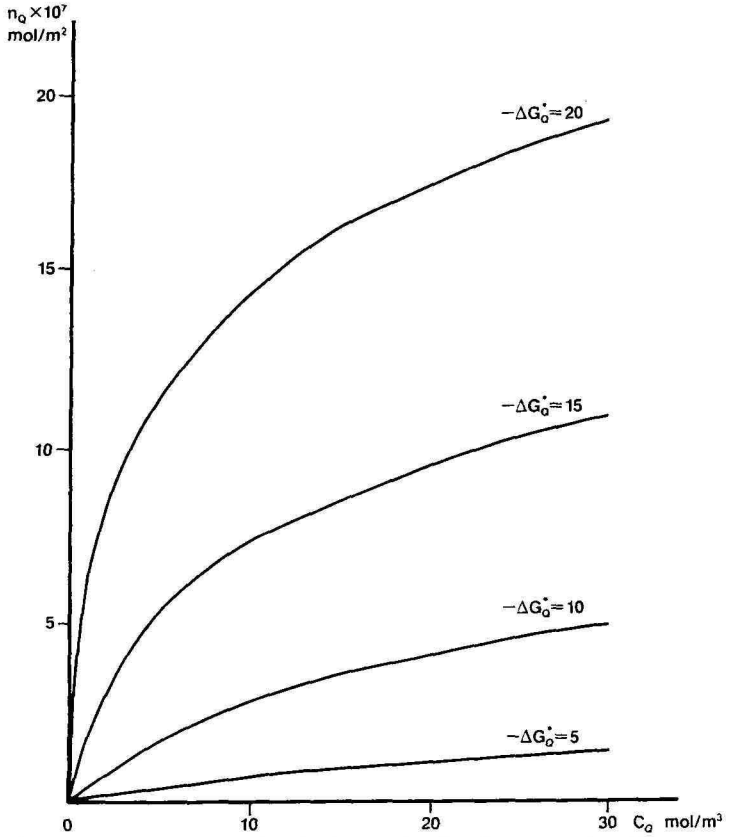

Fig. 1. Calculated adsorption isotherms for $Q^{z}Q$ from eqn. 11 with $z_Q = \pm 1$, for different values of ΔG°_{Q} (kJ/mol). T = 298K; D = 80; $\Sigma c_{0,i}$ = 500 mM; $n_0 = 3.321 \cdot 10^{-6}$ mol/m²; $B = 2 \cdot 10^{-9}$ m.

It is important to note that the theory cannot be expected to give a full quantitative description of an adsorption isotherm as determined by liquid chromatographic (LC) methods. Its validity is determined by the limitations of the Gouy–Chapman theory and the use of a Langmuir-like isotherm. Some of these limitations are:

the theory is derived for a planar surface but the particles used in LC are highly porous. The measured adsorption will therefore depend on the distribution of pore radii

the thickness of the surface layer, B, and the value of ΔG_Q° are unknown

the theory is a mean-field approximation and as such it does not consider correlation effects between the ions

the ΔG_Q° value may depend on the concentration of Q^{z_Q} at the surface

It is also important to note that if the pH of the system is such that the silanol groups on the surface are ionized, a proper correction must be made for the corresponding electrostatic potential.

Fig. 1 shows calculated adsorption isotherms for various values of $-\Delta G_Q^\circ$ (kJ/mol). It is seen that a plateau is reached and that its value increases when the hydrophobicity of the ion Q increases; this is in accordance with experimental findings, *e.g.*, ref. 7. The logarithmic derivatives of these curves, Fig. 2, can be compared to the adsorption isotherm for various quaternary ammonium ions, Fig. 3, obtained by Bartha and Vigh[7]. The qualitative information in the two figures is the same, *e.g.*, as $-\Delta G_Q^\circ$ increases the slope of the curve decreases. Another way to change the value of $-\Delta G_Q^\circ$ is to change the composition of the mobile phase. In the same paper[7], the adsorption isotherm of tetrabutylammonium bromide from mobile phases containing

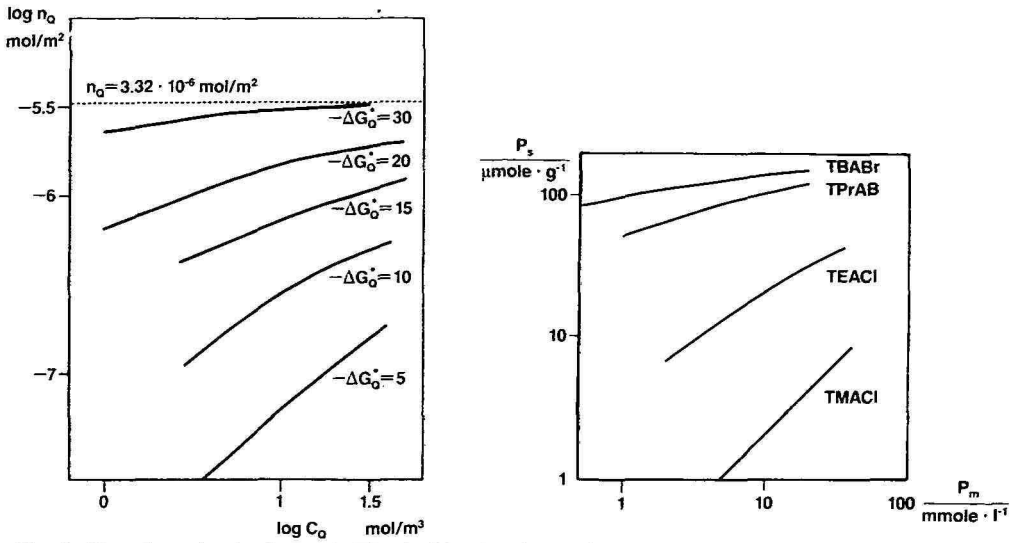

Fig. 2. The adsorption isotherms in Fig. 1 with a log–log scale.

Fig. 3. Adsorption isotherms of tetramethylammonium chloride (TMACl), tetraethylammonium chloride (TEACl), tetrapropylammonium bromide (TPrAB) and tetrabutylammonium bromide (TBABr) on LiChrosorb RP-18 from 25 mM orthophosphoric acid–25 mM sodium dihydrogenphosphate (pH = 2.1) buffer at constant bromide concentration (200 mM) at 25°C (from ref. 7) (P_s = concentration of quaternary ions on the surface; P_m = concentration of quaternary ions in the mobile phase).

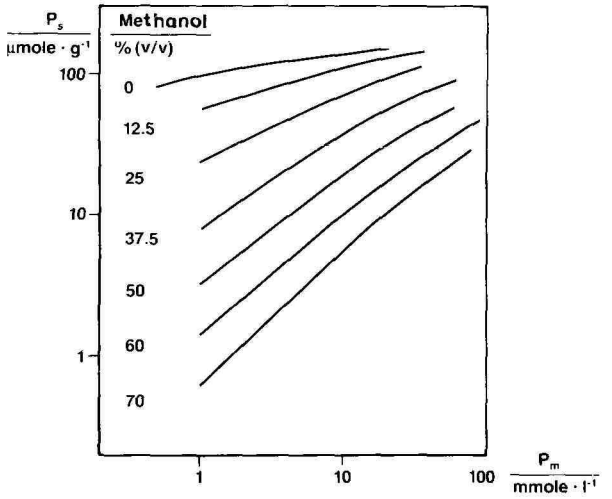

Fig. 4. Adsorption isotherms of tetrabutylammonium bromide on LiChrosorb RP-18 from 0, 12.5, 25, 37.5, 50, 60 and 70% (v/v) methanol–aqueous phosphate buffer eluents (25 m*M* orthophosphoric acid–25 m*M* sodium dihydrogenphosphate; pH = 2.1–3.4; $[Br^-]$ = 200 m*M*; 25°C) (from ref. 7).

different concentrations of methanol was reported, Fig. 4. An increase in the concentration of methanol will give a lower $-\Delta G^\circ_Q$, so the results can also be qualitatively compared to Fig. 2.

The adsorption isotherms of the different quaternary ammonium ions are not suitable for a quantitative comparison with the theory because the unknown parameters ΔG°_Q and n_0 are difficult to predict. However, these parameters are semi-quantitatively predictable for linear amphiphilic molecules by comparison of data from

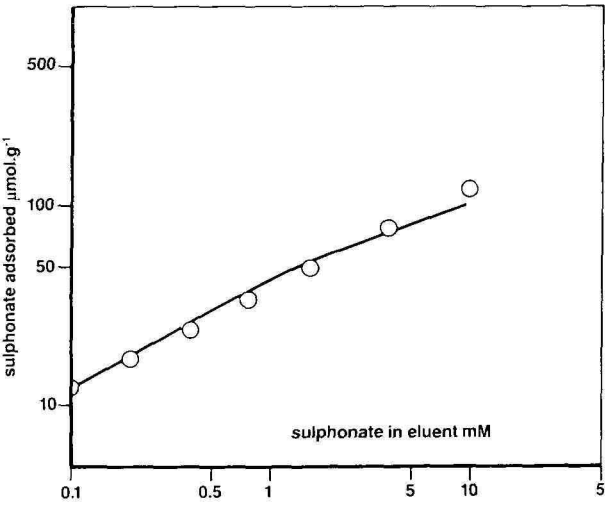

Fig. 5. Comparison between the calculated (full line) and experimental (○) adsorption isotherms for sodium 1-octanesulphonate on octadecylsilica at 40°C. Eluent: phosphate buffer (50 m*M* Na^+; pH = 3.00). Experimental points from ref. 3.

a water–oil interface[4]. Deelder and Van den Berg[3] measured the adsorption isotherms of octanesulphonate and dodecanesulphonate in the RP-18–water system. A semi-quantitative comparison of the theoretical adsorption isotherm with the reported adsorption isotherm is made in the following way:

the value of n_0 is set to $3.32 \cdot 10^{-6}$ mol/m^2 (50 Å^2 per molecule), approximately the same as that found for linear molecules at the oil–water interface (45–55 Å^2 per molecule)[9];

the thickness of the surface layer is set to 20 Å;

the reported value for n_Q at the lowest concentration, c_Q, is used to calculate ψ_0 according to eqn. 10;

the value of ΔG°_Q is then calculated from eqn. 1;

the value obtained for ΔG°_Q is then used in eqn. 11 to calculate the complete adsorption isotherm.

Calculation of $-\Delta G^\circ_Q$ according to this procedure gives ≈ 16 kJ/mol for octanesulphonate and ≈ 37 kJ/mol for dodecanesulphonate. From measurements at the oil–water interface, these values are expected to be 20–25 and 30–38 kJ/mol, respectively[4]. So the calculated value for $-\Delta G^\circ_Q$ is lower than expected for octanesulphonate but is in the expected range for dodecanesulphonate.

In Figs. 5 and 6 the theoretical adsorption isotherms for octanesulphonate and dodecanesulphonate are compared with the results of Deelder and Van den Berg[3]. Despite the previously mentioned limitations of the theory, the quantitative agreement between the theoretical and experimental data is good.

Eqn. 11 shows that the concentration of Q^{z}_0 on the surface, n_Q, increases with the concentration of non-adsorbed ions in the mobile phase, $\Sigma c_{0,i}$, when the concentration of Q^{z}_0 in the mobile phase is kept constant. This is in agreement with the experimental findings, *e.g.*, ref. 1.

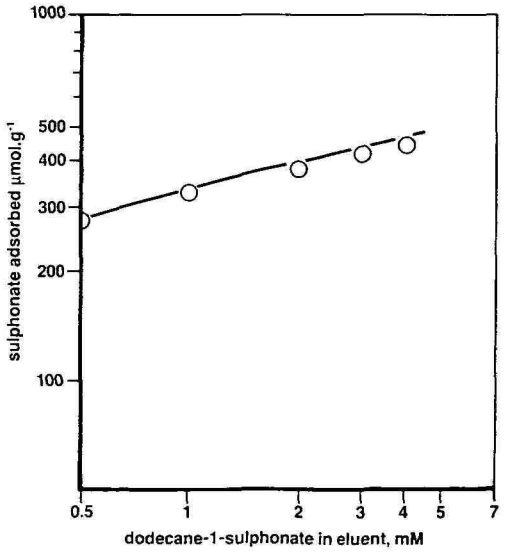

Fig. 6. Comparison between the calculated (full line) and experimental (O) adsorption isotherms for sodium 1-dodecanesulphonate on octadecyl silica from phosphate buffer at 40°C (10 mM Na^+; pH = 3.00). Experimental points from ref. 3.

The capacity factors of solute molecules

The reservations made concerning the validity of the equation for the adsorption isotherm also apply to the equation for the capacity factor. Another important restriction of eqn. 15 is that it is valid only when adsorption of the solute molecule does not change the electrostatic potential of the surface. If this condition is not fulfilled in the chromatographic system, the adsorption isotherm for the solute will depend on its concentration in the mobile phase.

Eqn. 15 gives the relationship between the capacity factor for a solute molecule and the concentrations of the amphiphilic molecules on the surface. It is seen that, with all factors kept constant, the capacity factor depends only on the surface concentrations of the amphiphilic molecules. It is shown in ref. 10 that this is the case for various alkanesulphonates.

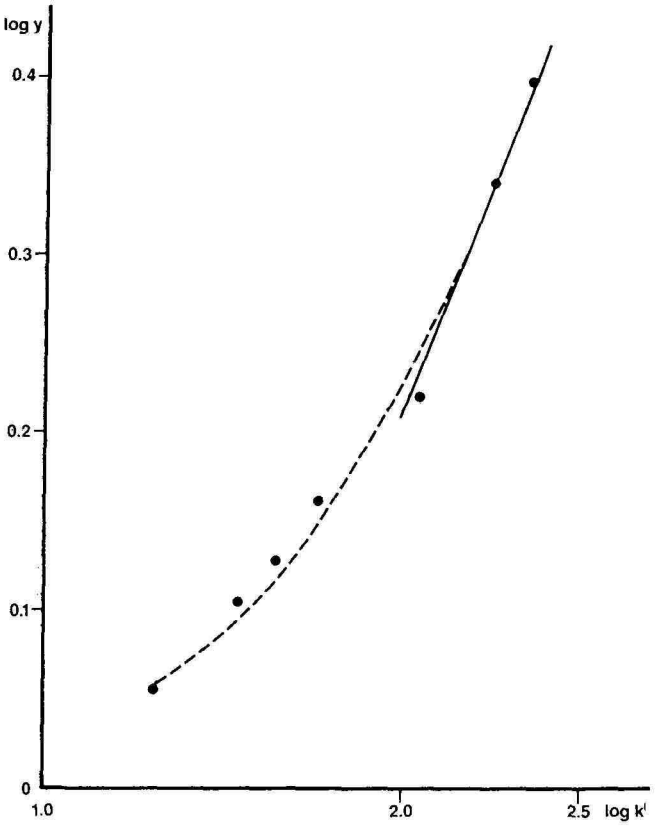

Fig. 7. Comparison between the limiting law, eqn. 16, and experimental results from ref. 11 where:

$$y = \frac{n_Q|z_Q|F}{(8\varepsilon_0 DRT\Sigma c_{0,i})^{1/2}} + \left[\frac{(n_Q|z_Q|F)^2}{8\varepsilon_0 DRT\Sigma c_{0,i}} + 1\right]^{1/2}$$

For experimental conditions, see Table I.

For comparison of eqn. 15 with experimental data we rewrite it as follows

$$\log\left\{\frac{n_Q|z_Q|F}{(8\varepsilon_0 DRT\Sigma c_{0,i})^{1/2}} + \left[\frac{(n_Q|z_Q|F)^2}{8\varepsilon_0 DRT\Sigma c_{0,i}} + 1\right]^{1/2}\right\} = -\frac{z_Q}{2z_Y}\log k' + \alpha \qquad (16)$$

where α is unknown and is assumed to be a constant and independent of n_Q. Since, eqn. 16 only holds in the limit $(n_Y z_Y/n_Q z_Q) \rightarrow 0$, an experimental plot according to this equation will give a slope $(-z_Q/2z_Y)$ in the high concentration limit. Fig. 7 shows experimental adsorption data obtained by Tilly-Melin[11] which are expressed in accordance with eqn. 16 where Q = tetrabutylammonium ion and Y = naphthalenesulphonate ion. The numerical value for D in this mixture of solvents is estimated to be 78 from $(X_1D_1 + X_2D_2)$ where X_i is the mole fraction of solvent component i and D_i is the dielectric constant of the pure solvent i. The full line represents the theoretical line with slope $= \frac{1}{2}$ and it is seen that the slope of the experimental curve tends to this value in the high concentration limit of Q. The values for c_Q and c_Y for the experimental point with the lowest concentration of amphiphilic modifier are $5.6 \cdot 10^{-5}$ and $\approx 1 \cdot 10^{-5}$ M respectively. So eqn. 16 cannot be expected to hold for the lower concentrations.

From eqn. 11 it is possible to calculate n_Q for a given c_Q, and the obtained value may be inserted in eqn. 15 giving k'_Y as a function of c_Q.

Fig. 8 presents calculated curves for the case when the charge of the solute

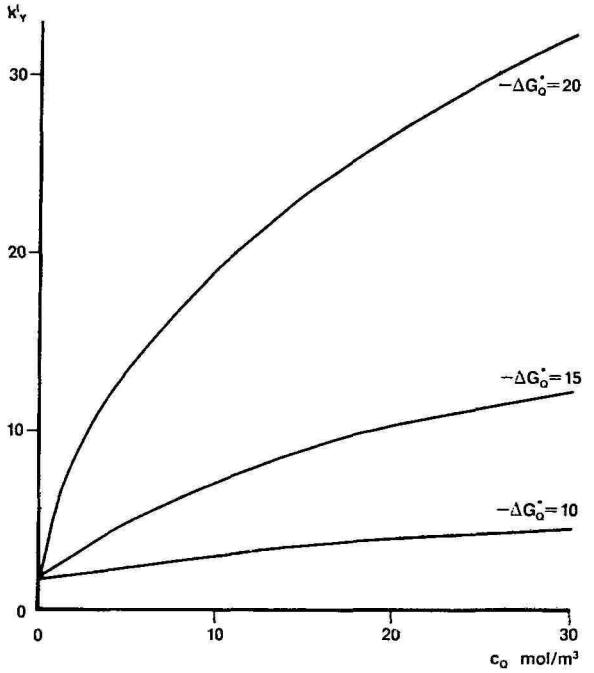

Fig. 8. Capacity factors calculated from eqns. 15 and 11 as a function of c_Q for different values of ΔG°_Q (kJ/mol). $z_Q = -z_Y = \pm 1$; $-\Delta G^\circ_Y = 5$ kJ/mol; $\Sigma c_{0,i} = 500$ mM; $D = 80$; $T = 298$ K; $n_0 = 3.321 \cdot 10^{-6}$ mol/m²; $A' = 0.2$.

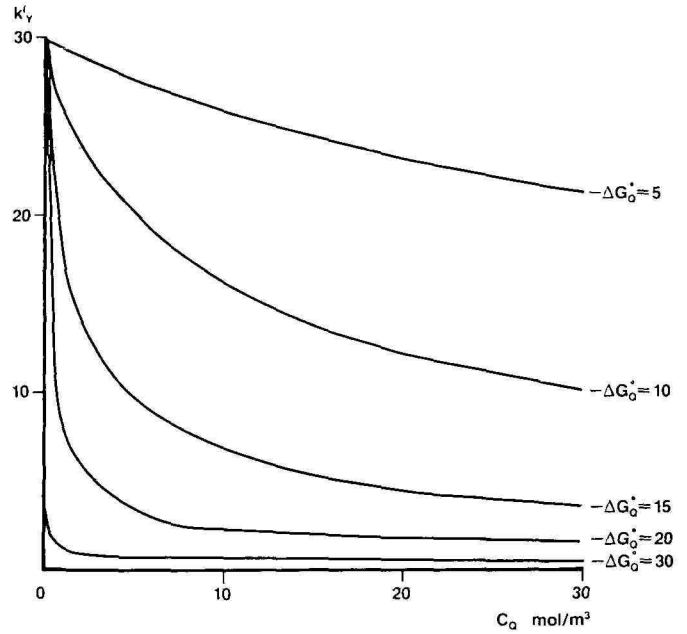

Fig. 9. Capacity factors calculated from eqns. 15 and 11 as a function of c_Q for different values of ΔG°_Q (kJ/mol). $z_Q = z_Y = \pm 1$; $-\Delta G^\circ_Y = 12.4$ kJ/mol; $\Sigma c_{0,i} = 500$ mM; $D = 80$; $T = 298$ K; $n_0 = 3.321 \cdot 10^{-6}$ mol/m²; $A' = 0.2$.

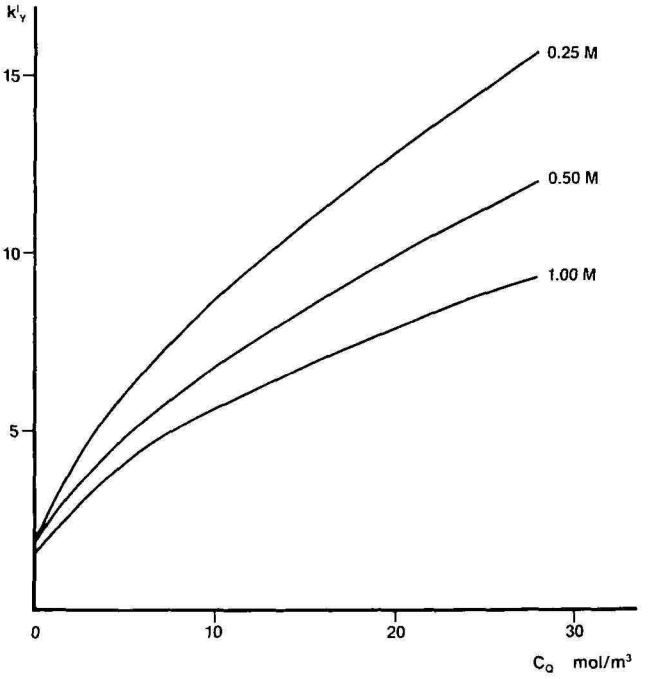

Fig. 10. Capacity factors calculated from eqns. 15 and 11 as a function of c_Q for different values of $\Sigma c_{0,i}$. $-\Delta G^\circ_Q = 15$ kJ/mol; $-\Delta G^\circ_Y = 5$ kJ/mol; $z_Q = -z_Y = \pm 1$; $D = 80$; $n_0 = 3.321 \cdot 10^{-6}$ mol/m²; $T = 298$ K; $A' = 0.2$.

molecule is of the opposite sign, and Fig. 9 the same sign, as the amphiphilic modifier, for different values of the free energy of adsorption of the amphiphilic modifier. The curves are similar to those usually obtained in chromatographic experiments. It is also seen that the capacity factor changes sensibly with the value for $-\Delta G^{\circ}_{Q}$, see *e.g.*, refs. 10 and 12. In Fig. 10 is shown an example calculated from eqns. 11 and 15 of how the ionic strength influences the capacity factor. It is found that, when the ionic strength increases, the capacity factor decreases when the charge of the solute ion is opposite to that of the amphiphilic modifier, but when the charge of the solute ion is the same as that of the amphiphilic modifier k' increases. Both of these trends are in accord with the experimental findings[8].

From eqns. 10 and 13 it can be concluded that for two solute molecules, Y and R, the following relationships hold

$$k'_{Y}k'_{R} = A'^{2} \cdot \exp(-\Delta G^{\circ}_{R} - \Delta G^{\circ}_{Y}) \approx \text{constant} \tag{17}$$

where the charges of R and Y are of equal magnitude and of opposite sign and

$$\frac{k'_{Y}}{k'_{R}} = \exp(+\Delta G^{\circ}_{R} - \Delta G^{\circ}_{Y}) \approx \text{constant} \tag{18}$$

where the charges of R and Y are of equal magnitude and sign. These relationships are easily obtained by considering the fact that the electrostatic potential, ψ_0, is independent of the solute molecule. The experimental data[11,13] presented in Tables I and II are in accordance with the obtained equations. It must be pointed out that eqn. 15 holds only in the limit $(n_{Y}z_{Y}/n_{Q}z_{Q}) \rightarrow 0$. Since c_{Y} is $\approx 1 \cdot 10^{-5}$ M this condition is not fulfilled which may explain the small trend observed. These data give strong support to one of the hypotheses made in this work, *i.e.*, when varying c_{Q} it is the electrostatic potential of the surface that determines the changes in the capacity factor for organic ions.

A phenomenon that is not included in the present theory is the effect of sec-

TABLE I

THE DEPENDENCE OF k'_{Y}, k'_{R} AND $k'_{Y}k'_{R}$ ON c_{Q}

Y = Naphthalenesulphonate; R = ω-diethylamino-2,6-dimethylacetanilide; QX = tetrabutylammonium phosphate. Data are from ref. 11. Experimental conditions: mobile phase, acetonitrile–water (10:90); phosphate buffer pH = 3.0; $\sum_{i} c_{0,i} = 0.1$ M; column, μBondapak C_{18}, surface area = 150 m^2/g (according to the manufacturer), dimensions 200 × 3 mm; 296 K.

10^4 c_Q (M)	k'_Y	k'_R	$k'_Yk'_R$
0.563	20.3	5.28	107
1.90	34.7	3.17	110
2.85	43.3	2.76	120
4.76	57.4	2.24	129
19.0	111	1.21	134
47.5	178	0.782	139

TABLE II

THE DEPENDENCE OF k'_Y, k'_R AND k'_Y/k'_R ON c_Q

Y = D-propoxyphene; R = Transergan®; QX = tetrabutylammonium phosphate. Mobile phase: acetonitrile–water (25:75), pH = 3.0; $\Sigma c_{0,i}$ = 0.1 *M*. The data are from ref. 13.

$10^3\ c_Q$ (*M*)	k'_Y	k'_R	k'_Y/k'_R
1.50	7.19	5.81	1.24
2.99	5.54	4.50	1.23
4.99	4.53	3.71	1.22
6.99	3.94	3.28	1.20

ondary ions[14]. Since similar effects are well known in colloid chemistry as the Hofmeister or lyotropic series this deviation from the theory is expected.

CONCLUSIONS

It can be concluded that the theory described is in good agreement with the general observations made in chromatographic practice. Since the theory is developed from the Gouy–Chapman theory and from the Langmuir isotherm it is also well founded in physical chemistry.

An observation that has been the subject of many discussions is that k' reaches a plateau and may even decrease when the concentration of the amphiphilic modifier in the mobile phase increases, *e.g.*, refs. 1,10. In some cases the decrease is explained by the fact that the concentration of amphiphilic modifier is above the critical micelle concentration[1]. The possibility of solute-induced micelle formation at concentrations below the critical micelle concentration of the amphiphilic modifier must also be considered. However, these effects may not explain all the cases where a decrease is found and an additional explanation is required. That a plateau is reached is explained by the present theory, since it is based on the Langmuir isotherm. It is shown in ref. 10 that the decrease in k' is mainly due to an increase in the ionic strength of the mobile phase. Thus, the decrease in k' may be explained on the basis of eqn. 15 by a combination of three effects: the concentration of $Q^z{}_Q$ on the surface, n_Q, approaches the maximum possible, n_0; the increase in QX in the mobile phase decreases k' because $\Sigma c_{0,i}$ increases and it is usually found that for uncharged molecules k' decreases with increasing concentration of $Q^z{}_Q$ on the surface[10]. This indicates that the adsorption energy for these solute molecules decreases. A corresponding decrease in ΔG°_Y is expected.

ACKNOWLEDGEMENTS

The author is most greatful to Dr. A. Tilly-Melin who has kindly put her unpublished data at my disposal, Professor M. Almgren for most valuable discussions during the preparation of this work and Drs. L. Uppström and A. Furängen for valuable discussions of the manuscript.

REFERENCES

1 R. H. A. Sorel and A. Hulshoff, *Adv. Chromatogr. (N.Y.)*, 21 (1983) 87.
2 F. Cantwell, *J. Pharm. Biomed. Anal.*, 2 (1984) 153.
3 R. S. Deelder and J. H. M. van den Berg, *J. Chromatogr.*, 218 (1981) 327.
4 J. T. Davies and E. K. Rideal, *Interfacial Phenomena*, Academic Press, New York, 2nd ed., 1963, Ch. 4.
5 A. W. Adamson, *Physical Chemistry of Surfaces*, Wiley, New York, 4th ed., 1982, Ch. V.
6 *Standard Mathematical Tables*, CRC Press, Cleveland, OH, 19th ed., 1971.
7 A. Bartha and Gy. Vigh, *J. Chromatogr.*, 260 (1983) 337.
8 A. Bartha, H. A. H. Billiet, L. de Galan and Gy. Vigh, *J. Chromatogr.*, 291 (1984) 91.
9 R. D. Vold and M. J. Vold, *Colloid and Interface Chemistry*, Addison-Wesley, London, 1983.
10 A. Bartha, Gy. Vigh, H. A. H. Billiet and L. de Galan, *J. Chromatogr.*, 303 (1984) 29.
11 A. T. Melin, unpublished results.
12 C. T. Hung, R. B. Taylor and N. Paterson, *J. Chromatogr.*, 240 (1982) 61.
13 A. T. Melin, M. Ljungcrantz and G. Schill, *J. Chromatogr.*, 185 (1979) 225.
14 L. R. Snyder and J. J. Kirkland, *Introduction to Modern Liquid Chromatography*, Wiley, New York, 2nd ed., 1979, Ch. 11.

Journal of Chromatography, 356 (1986) 247–259
Elsevier Science Publishers B.V., Amsterdam — Printed in The Netherlands

CHROM. 18 395

HYDROPHOBIC INTERACTION CHROMATOGRAPHY OF SIMPLE COMPOUNDS ON ALKYL-AGAROSES WITH DIFFERENT ALKYL CHAIN LENGTHS AND CHAIN DENSITIES

MECHANISM AND THERMODYNAMICS

P. M. BRANDTS*, C. M. MIDDELKOOP, W. J. GELSEMA and C. L. DE LIGNY
Analytical Chemistry Laboratory, State University of Utrecht, Croesestraat 77A, 3522 AD Utrecht (The Netherlands)
(First received November 19th, 1985; revised manuscript received December 9th, 1985)

SUMMARY

The retention of homologous *n*-alcohols in dilute phosphate buffer solution was determined on pentyl-, octyl- and dodecyl-agarose as a function of the degree of substitution of the alkyl-agaroses. The occurrence of two retention determining processes, *i.e.*, liquid–liquid distribution and bimolecular association, is revealed by the retention data. The standard thermodynamic functions for the interaction were calculated and are discussed.

INTRODUCTION

In previous papers we have demonstrated for the sorbent Octyl-Sepharose that both the sorption of *n*-alcohols[1] and the chromatographic retention of simple test substances with varying amounts of co-solvents in the eluent[2,3] can be described by a simple partition model. The agarose behaves as an inert support for the layer of octylglycidyl (OG) groups. The activity coefficients of the solutes in this layer are close to unity and they do not vary with the eluent composition. The OG layer has properties closely resembling those of liquid *n*-octanol. The chromatography of simple model compounds on Octyl-Sepharose can therefore be considered as a form of liquid–liquid chromatography (LLC), the retention being governed by an equilibrium much like that for a solute between two liquid phases. In this paper we refer to this mechanism as to LLP (liquid–liquid partition). Thus, the behaviour of the alkyl-agarose (at least, of the commercial product Octyl-Sepharose) is totally different from that of the alkyl-silicas used in reversed-phase high-performance liquid chromatography (HPLC).

At first sight, an LLP mechanism is unexpected as the degree of substitution, *P*, of Octyl-Sepharose is relatively low, *i.e.*, 0.40 mol OG per mol disaccharide[4]. However, if the multi-chain agarose fibres[5,6] remain intact during the synthesis of Octyl-Sepharose[7], the resulting high surface coverage[2] may produce a coherent,

0021-9673/86/$03.50

liquid-like film around the fibres. It is anticipated that the properties of such a layer depend on the chain length and the amount of alkyl groups per unit of fibre surface area (henceforth denoted as "chain density"), and that at very low chain densities the LLP mechanism breaks down. It is the aim of this paper to investigate whether such a dependence exists.

We used home-made pentyl-, octyl- and dodecyl-agaroses with widely varying chain densities as adsorbents and simple compounds as model sorbates. The chromatographic retention data obtained enabled us to calculate the relevant thermodynamic data. Other studies on the influence of the alkyl chain length and chain density[8–12] dealt mainly with protein sorption. The results of these studies are of course important for practical purposes, but are less suitable for interpretation in terms of hydrophobic interaction.

THEORETICAL

From basic chromatographic theory it follows that

$$V_g = K_B V_s \tag{1}$$

where V_g is the specific retention volume (ml g^{-1} of OG), K_B is the molar distribution constant of a test substance B and V_s is the volume of 1 g of OG. With the approximation[13,14] that the specific weights of OG and of other alkylglycidyl (AG) ethers are equal to to 1 g ml^{-1}, it follows that V_g is numerically equal to K_B. With the low P values used in this study, a correction of V_g for the interaction between B and unsubstituted agarose is necessary, yielding a corrected specific retention volume:

$$V_g^* = \frac{(V_e - V^0) - (V_a - V_a^0)}{w_{AG}^0} \tag{2}$$

Here, V_e and V^0 denote the elution volumes, corrected for the out-of-column dead volume, of B and a supposedly unretarded compound on a column containing $(1 + w_{AG}^0)$ g of alkyl-agarose with 1 g of agarose and w_{AG}^0 g of AG groups. V_a and V_a^0 denote the same data for a column containing 1 g of unsubstituted agarose. Note that it is assumed that the AG groups do not hinder the interaction of B with agarose and that eventual cooperative interactions between B, AG and agarose are not taken into account.

Values of K_B (or of V_g) at several temperatures can be used to calculate the partial molar standard thermodynamic data for the partition of B over the eluent and the AG layer. (The uncertainty in the temperature coefficient of the specific weight of this layer introduced errors of only minor importance.) In this paper, the same procedure[2] is applied to V_g^* values obtained on agarose with high P.

The LLP model predicts that the V_g^* values do not depend on P. However, it should be realized that models based on other mechanisms (adsorption, bimolecular association) also predict constant V_g^* values. Additional information about the sorption mechanism can be obtained from the value of the activity coefficient of B infinitely diluted in the layer of AG, $\gamma_{B,AG}^{\infty}$, which can be calculated from the mole

fraction partition constant, $K_{X,B}$, as described in ref. 3. The expression for $\log \gamma^{\infty}_{B,AG}$ is as follows:

$$\log \gamma^{\infty}_{B,AG} = \log \gamma^{\infty}_{B,aq} - \log K_{X,B} = \log \gamma^{\infty}_{B,aq} - \log 5.55 \cdot 10^{-2} M_{AG} V^{*}_{g} \quad (3)$$

Thus, values of $\log \gamma^{\infty}_{B,AG}$ can be calculated from V^{*}_{g}, the molecular weight of the AG group, M_{AG}, and the (literature) value of the activity coefficient of B in the aqueous eluent, $\gamma^{\infty}_{B,aq}$, which is about equal to that in water. The values obtained in this way can be compared with predictions from solubility theories if the bonded AG groups are considered as mobile molecules.

Constant V^{*}_{g} values at extremely low P values are interpreted in terms of bimolecular association. If we represent the complex formation as

$$AG + B, aq \leftrightarrows AGB$$

we can define:

$$K_{AS} = C_{AGB} C^{-1}_{AG} C^{-1}_{B,aq} \quad (4)$$

Here, $C_{B,aq}$, C_{AG} and C_{AGB} denote the molar concentrations of B, AG and the complex AGB, respectively, in the eluent. In this case, the capacity ratio is equal to the ratio of C_{AGB} and $C_{B,aq}$ and it follows from basic chromatographic theory and from eqn. 2 that:

$$\frac{C_{AGB}}{C_{B,aq}} = \frac{(V_e - V^0) - (V_a - V^0_a)}{V^0} = \frac{V^{*}_{g} w^0_{AG}}{V^0} \quad (5)$$

The standard free energy of association of 1 mol of solute is given by $\Delta G^0_{AS} = -RT \ln K_{AS}$ or

$$\Delta G^0_{AS} = -RT \ln \frac{V^{*}_{g} w^0_{AG}}{V^0 C_{AG}} = -RT \ln 10^{-3} M_{AG} V^{*}_{g} \quad (6)$$

Values of ΔH^0_{AS} and $\Delta C^0_{p,AS}$ can be obtained from a Van 't Hoff plot.

EXPERIMENTAL

Preparation and characterization of alkyl-agarose

Pentyl-, octyl- and dodecyl-agaroses were synthesized from one single batch of Sepharose CL-4B (Pharmacia, Uppsala, Sweden) according to ref. 7. Their alkyl concentration was determined by ^{1}H NMR spectroscopy (90 MHz)[8]. We added a small quantity of trifluoroacetic acid in order to shift the interfering water signal[11] to lower field.

Chromatographic experiments

Column experiments were performed as described before[2,3]. The 30-ml bed volumes contained *ca.* 1 g of dry alkyl-agarose. The sample dose was 0.1–0.5 mg

depending on the retention time. The gels with the lowest alkyl contents were packed in 60-ml beds, and the sample dose was reduced to 10 μg, the smallest dose possible with the differential refractive index detector. Low doses are necessary to avoid overloading of the column, as can be seen as follows. With $P = 0.010$, there are *ca.* 10^{-6} mol of AG groups per ml of gel bed. This value must be sufficiently large with respect to the solute concentration in the column. A 10-μg dose of *n*-nonanol corresponds to *ca.* $3 \cdot 10^{-8}$ mol per ml of gel bed. The fraction of octanol-bonded AG groups is thus less than 3%. So the concentration of free AG groups in eqn. 6 can be taken to be equal to the total concentration of AG groups, C_{AG}. The gel beds were slightly compressed prior to use, to avoid contraction during experiments. The test substances were eluted with a phosphate buffer (ionic strength 0.1, pH = 7.0). The elution peaks were symmetrical.

RESULTS

In Table I, P values are given for the alkyl-agaroses used; also listed are values of w^0_{AG}. The experimental error in the P values is estimated from duplicate determinations to be 4% or 0.004 for low values of P.

The dry specific weight and the hydrophobicity of the alkyl-agarose increase with increasing P. The latter fact makes the highly substituted gels less able to swell in water, *cf.*, ref. 8. Fig. 1 shows the bed volumes, V_{bed}, of $(1 + w^0_{AG})$ g of swollen alkyl-agarose as a function of w^0_{AG}. In the extreme case, the gel did not swell at all.

In Table II, the retention volumes, $(V_e - V^0)$, of some *n*-alcohols on various alkyl-agaroses (dry weights $1 + w^0_{AG}$ g) are listed. We estimate the precision of these values to be 0.08 ml or 0.8% for large values of $(V_e - V^0)$. The values of V^0 and

TABLE I

DEGREE OF SUBSTITUTION, P, AND MASS OF ALKYLGLYCIDYL GROUPS PER GRAM OF AGAROSE OF ALKYL-AGAROSES

*Gel**	*P***	w^0_{AG}***	*Gel*	*P*	w^0_{AG}
a	0.000	0.000	O6	0.170	0.103
P1	0.050	0.024	O7	0.190	0.115
P2	0.095	0.045	O8	0.22	0.134
P3	0.115	0.054	O9	0.43	0.261
P4	0.212	0.100	D1	0.035	0.028
P5	0.275	0.129	D2	0.048	0.038
P6	0.47	0.221	D3	0.060	0.047
P7	0.71	0.334	D4	0.084	0.066
P8	0.74	0.348	D5	0.167	0.132
O1	0.010	0.006	D6	0.223	0.176
O2	0.025	0.015			
O3	0.060	0.036	Ph	0.40	0.243
O4	0.070	0.043			
O5	0.090	0.055			

* a = Unsubstituted agarose; P = pentyl-agarose; O = octyl-agarose; D = dodecyl-agarose and Ph = Octyl-Sepharose CL-4B.

** Moles of alkyl per mol of disaccharide.

*** Mass of alkylglycidyl groups (g per g of agarose).

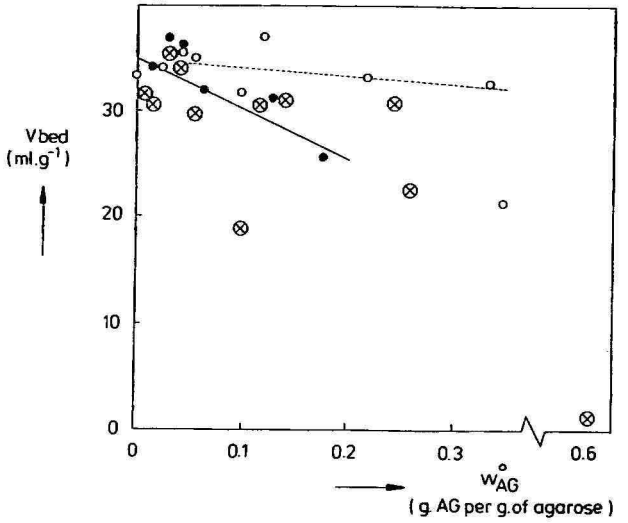

Fig. 1. Bed volumes (ml per g of agarose) of various alkyl-agaroses as a function of w^{0}_{AG} (g AG per g of agarose). Symbols: ○, ..., pentyl-agarose; ⊗, ——, octyl-agarose; ●, ——, dodecyl-agarose.

TABLE II

RETENTION VOLUMES, $(V_e - V^0)$ (ml/g OF AGAROSE) OF *n*-ALCOHOLS AT 25°C ON ALKYL-AGAROSES

*Gel**	*n***					*Benzene*
	5	*6*	*7*	*8*	*9*	
S		0.00	0.17	0.47	1.37	
P1			0.55	1.18	1.99	
P2		0.41	0.86	1.77	3.47	
P3	0.39	0.63	1.49	2.53	8.54	
P4	0.79	1.93	5.44	14.7	45.0	3.51
P5	1.19	3.76	11.9	36.3		
P6	3.76	11.5	38.1	119.7		22.4
P7	5.96	19.7	72.8	242.9		
P8	6.20	20.9	71.1	248.4		42.3
O1			0.42	0.85	1.80	
O2		0	0.74	1.51	3.62	
O3		0.73	1.83	4.57	12.43	
O4	0.33	0.77	1.54	3.40	7.75	
O5	1.08	3.00	9.04	27.7		
O6	2.16	6.80	22.2	74.4		
O7	2.35	7.58	25.8	86.0	274.8	
O8	2.91	9.75	34.3	104.1		
O9	6.31	22.2	75.4	240.9		
D1		1.73	4.45	11.9	30.4	2.64
D2		2.16	6.93	18.9	61.8	3.37
D3	1.35	4.52	14.0	41.1	133.1	6.79
D4	1.50	5.66	20.2	63.0		
D5	3.41	12.6	42.8	138.8		
D6	4.89	16.9	58.7	195.9		28.5

* See Table I.

** Number of carbon atoms in the solute molecule.

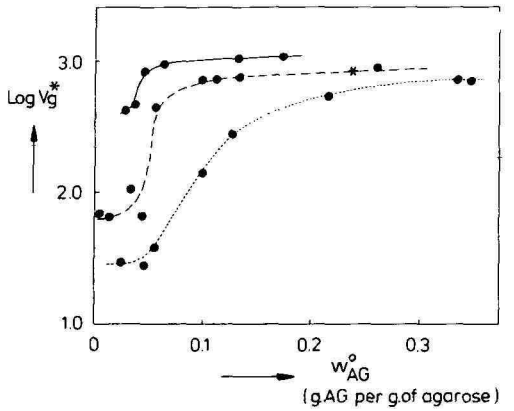

Fig. 2. Specific retention volumes of *n*-octanol as a function of w^0_{AG} (g AG per g of agarose). The asterisk denotes the Pharmacia gel. Curves: ....., pentyl-; ----, octyl-; and ——, dodecyl-agarose.

V^0_a were determined with ethanol and potassium bromide, and are in close agreement with the calculated amount of eluent in the column. For comparison, some values for a non-polar solute, *i.e.*, benzene, are also given.

Values of log V^*_g for *n*-octanol are plotted as a function of w^0_{AG} in Fig. 2. The correction for retention on agarose is significant only for the gels O1-4, P1-3.

Fig. 3 shows values of log $\gamma^\infty_{B,AG}$, calculated from the data in Tables I and II with eqn. 3, as a function of $P^{-\frac{1}{2}}$. Values of log $\gamma^\infty_{B,aq}$ in the eluent were obtained from a data compilation in ref. 15 as the logarithm of the reciprocal of the mole fraction solubility in water. Vertical bars denote the errors caused by the uncertainty in the retention volumes. Tilted bars show the impact of the uncertainty in P on both $P^{-\frac{1}{2}}$ and log $\gamma^\infty_{B,AG}$ values.

With some alkyl-agaroses, *i.e.*, P8, D6, O2, O3 and O5, and with unsubstituted

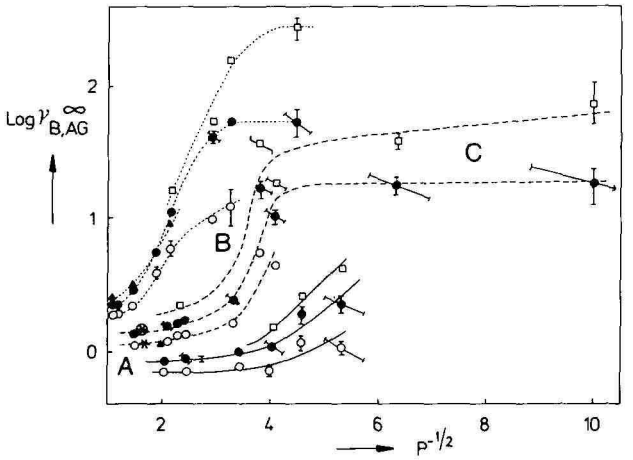

Fig. 3. Activity coefficients of *n*-hexanol (○), *n*-octanol (●), *n*-nonanol (□) and benzene (▲) in the sorbed state as a function of $P^{-\frac{1}{2}}$. Curves: ....., pentyl-; ----, octyl- and ——, dodecyl-agarose.

TABLE III

RETENTION VOLUMES, $(V_e - V^0)$ (ml/g OF AGAROSE) OF *n*-ALCOHOLS AT DIFFERENT TEMPERATURES ON ALKYL-AGAROSES

Gel	*T* (°C)	*n*				
		5	*6*	*7*	*8*	*9*
a	2.5			0.00	0.10	0.21
	11.5			0.02	0.29	0.80
	20.5			0.18	0.42	1.30
	32.0			0.22	0.59	1.39
	39.0			0.41	0.60	1.60
	45.0			0.50	0.82	1.51
P8	3.9	4.38	15.0	51.5	182	
	10.5	5.08	17.3	59.5	207	
	17.7	5.91	20.0	67.9	234	
	25.5	6.33	21.4	72.9	254	
	32.6	7.10	23.4	77.5	271	
	40.5	7.38	24.1	80.8	275	
O2	3.6				0.75	1.70
	12.5				0.86	2.73
	19.0				1.23	3.33
	27.0				1.61	3.92
	39.2				2.14	4.35
	47.0				2.46	4.66
O4	2.5			0.73	1.51	3.78
	13.6			1.11	2.18	5.56
	18.2			1.22	2.89	6.84
	27.6			1.61	3.23	8.23
	34.8			1.95	4.18	9.53
	43.2			1.84	4.09	9.81
D6	3.9	3.41	12.7	44.4	155	
	10.4	4.00	14.0	50.5	171	
	18.3	4.59	16.0	54.8	186	
	24.8	4.80	16.9	57.2	194	
	28.8	5.03	17.3	58.3	195	
	33.5	4.96	17.2	58.9	195	
	40.4	5.09	17.8	59.2	198	

agarose, measurements at different temperatures were performed. The values of $(V_e - V^0)$ and of $(V_a - V_a^0)$ are listed in Table III; V^0 and V_a^0 were determined with ethanol, and are independent of the temperature.

DISCUSSION AND CONCLUSIONS

Fig. 1 shows that the bed volume in water decreases gradually with increasing w_{AG}^0, *i.e.*, with increasing hydrophobicity of the gel. The decrease is stronger with octyl- and dodecyl-agarose than with pentyl-agarose. If it is assumed that the fibre

structure of the agarose remains intact during the synthesis of the alkyl derivative, then the surface area of 1 g of agarose is independent of P. Hence, $P^{-\frac{1}{2}}$ (Fig. 3) is a measure of the mean distance between the points of attachment of the AG groups on the agarose fibres. The use of this unit greatly improves the legibility of Fig. 3 at low P values.

Retention on unsubstituted Sepharose

It is seen in Tables II and III that *n*-alcohols are little retained on unsubstituted agarose. Nevertheless, the very low AG-group concentrations of some of our adsorbents give rise to retention volumes of comparable magnitude and in these cases the contribution of the interaction with agarose cannot be neglected. The interaction with agarose shows features of hydrophobic interaction: (i) the retention volumes increase with the number of carbon atoms, n, in the alcohols [Table II; in addition $n = 10$ yields $(V_a - V_a^0) = 3.0$ ml g^{-1}] and (ii) retention increases with temperature (Table III).

The methylene increment in the log $(V_a - V_a^0)$ values, *i.e.*, 0.40, is smaller than the corresponding increment for Octyl-Sepharose, *i.e.*, 0.60.

Retention on alkyl-agarose

Fig. 2 shows the log V_g^* values of *n*-octanol on alkyl-agarose. They depend strongly on the chain density of the AG groups. At large values of w_{AG}^0 (for dodecyl-, octyl- and pentyl-agarose: w_{AG}^0 greater than, say, 0.05, 0.10 and 0.25, respectively), log V_g^* is approximately constant and the retention is proportional to the mass of the AG groups in the column. This is in agreement with, but not a proof of an LLP mechanism.

LLP mechanism. In Fig. 3, values of log $\gamma_{B,AG}^{\infty}$ in the LLP region appear in the lower left corner, at relatively short distances between the bonded alkyl chains, in the region denoted by A. It appears that the values of log $\gamma_{B,AG}^{\infty}$ range from -0.2 to 0.4, which corresponds to $0.7 < \gamma_{B,AG}^{\infty} < 2$. Such values are commonly encountered for solutes in solvents that resemble the pure solute. If we consider the bonded AG groups as mobile molecules, these features can be compared with the predictions of

TABLE IV

COMPARISON OF CALCULATED AND EXPERIMENTAL ACTIVITY COEFFICIENTS IN THE LAYER OF ALKYLGLYCIDYL GROUPS AT HIGH P (REGION A IN FIG. 3)

Solute	$\bar{V}_B$ *(ml)*	δ_B*	*log* $\gamma_{B,AG}^{\infty}$					
			Adsorbent P8		*Adsorbent O9*		*Adsorbent D6*	
			*Calc.***	*Exptl.*	*Calc.*	*Exptl.*	*Calc.*	*Exptl.*
n-Hexanol	126	21.7	0.16	0.26	0.00	0.05	−0.10	−0.16
n-Octanol	157	20.9	0.36	0.34	0.11	0.14	−0.05	−0.08
Benzene	89	18.8	0.45	0.41			−0.08	+0.04

* $\delta_B^2 = (\Delta H_{vap}^0 - RT)/\bar{V}_B$; ΔH_{vap}^0 from ref. 17.

** $\log \gamma_{B,AG}^{\infty} = \log \frac{\bar{V}_B}{\bar{V}_{AG}} + \frac{1}{2.30}\left(1 - \frac{\bar{V}_B}{\bar{V}_{AG}}\right) + \frac{\bar{V}_B}{2.30\,RT}(\delta_B - \delta_{AG})^2$, from ref. 16. $\delta_{AG} = 22$, 23 and 24.5 for dodecyl-, octyl- and pentylglycidyl groups, respectively.

solubility theories. We used the Flory–Huggins–Hildebrand–Scott equation, already successfully adopted before by Tewari *et al.*[16] and by the present authors[1]. Values for the molar volumes, $\bar{V}$, of the AG groups were calculated as the ratio of the molecular weights and the densities of the corresponding alkylglycidyl ethers[14]. The best results were obtained with adopted values of the solubility parameter for the AG groups, δ_{AG}, equal to 22, 23 and 24.5 $J^{\frac{1}{2}}$ $mol^{-\frac{1}{2}}$ m for dodecyl-, octyl- and pentyl-agarose, respectively. These values correspond to slightly more polar liquids than the related *n*-alcohols with n = 12, 8 and 5, respectively. Results for the solutes *n*-hexanol, *n*-octanol and benzene are given in Table IV. It is seen that the agreement between calculated and experimental values of log $\gamma^{\infty}_{B,AG}$ is good. The mean deviation is 0.06. We conclude that the retention of simple compounds can be described with the LLP model in region A.

This conclusion enabled us to calculate the values of the thermodynamic standard data of LLP for *n*-alcohols over the aqueous eluent and the layer of AG. This was performed for the adsorbents P8, D6 and Octyl-Sepharose CL-4B (ref. 13). Standard free energy values were calculated as $\Delta G^0_{AG} = -RT \ln K_B = -RT \ln V^*_g$ from data in Table III. Results for ΔG^0_{AG} and ΔH^0_{AG} at 25°C, obtained with Van 't Hoff plots, are presented in Fig. 4 as a function of n. They will be discussed together with the thermodynamic data for bimolecular association.

Bimolecular association. The increase in log $\gamma^{\infty}_{B,AG}$ with increasing $P^{-\frac{1}{2}}$ in region B in Fig. 3 reflects a decreasing cooperation between the AG chains interacting with a solute. In region C in Fig. 3, log γ again becomes approximately constant. Here, the AG groups may be so far apart that the solute can interact with only one bonded alkyl chain.

Thermodynamic standard data for bimolecular association were calculated

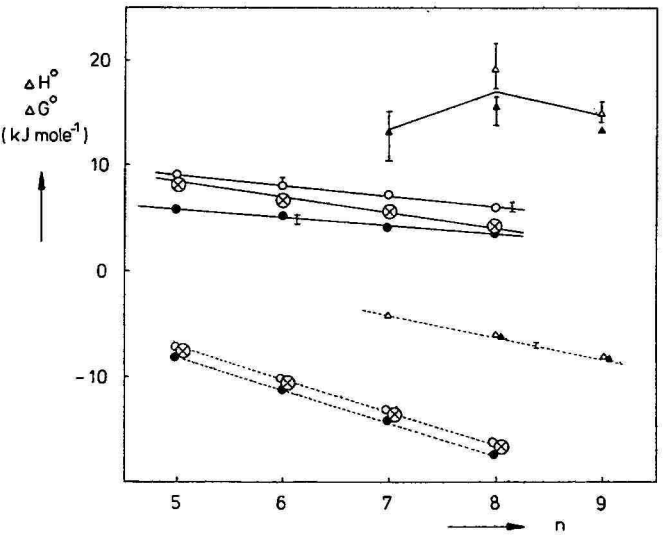

Fig. 4. Standard free energies and enthalpies for the interaction of *n*-alcohols with alkyl-agarose as a function of the number of carbon atoms, n, of the *n*-alcohol. Symbols: ○, P8; ⊗, Octyl-Sepharose CL-4B (ref. 13); △, O2; ▲, O4 and ●, D6. The full lines refer to ΔH^0 values, dotted lines to ΔG^0 values. Models: partition (○, ⊗, ●); bimolecular association (△, ▲).

from the data for absorbents O2 and O4 in Table III, with eqn. 5 and a Van 't Hoff plot. The correction for interaction with agarose was performed with values obtained from a least-squares parabola through the data points (Table III) for Sepharose as a function of temperature. Values of ΔG^0_{AS} and ΔH^0_{AS} are shown in Fig. 4.

The free energy values for adsorbents O2 and O4 are identical within 0.2 kJ mol^{-1}, which is consistent with identical retention mechanisms. The same conclusion holds for the densely substituted gels P8, Octyl-Sepharose and D6. The methylene increment of the ΔG^0_{AS} values from $n = 7$ to $n = 9$ is -2.0 ± 0.2 kJ mol^{-1}, and is thus considerably less negative than the corresponding value for LLP, *i.e.*, -3.2 kJ mol^{-1}. Such a difference between the methylene increments for bimolecular association on the one hand and for multimolecular association or partition on the other hand is in agreement with data in the literature. For multimolecular associations, values close to -3.3 kJ mol^{-1} are the rule[2], whilst for bimolecular association between alkyl chains the following values have been found: -1.5 kJ mol^{-1} for the association of alkyltrimethylammonium ions with alkyl carboxylates[18]; -1.3 kJ mol^{-1} for the dimerization of carboxylic acids in water[19]; -2.8 kJ mol^{-1} for the association of alkyl sulphate and S-alkylisothiuronium ions[20].

To the best of our knowledge, no information exists about the free energies of bimolecular association of *n*-alcohols with neutral alkyl chains. However, we may compare our results with those for the association of cyclohexanol and cyclohexane[21,22] in water. The former compound is approximately as lipophilic as *n*-pentanol. With our standard state, ΔG^0_{AS} is equal to 0.2 kJ mol^{-1}. Extrapolation of our ΔG^0_{AS} values to $n = 5$ (Fig. 4) yields a similar value.

The enthalpy values for adsorbents O2 and O4 do not differ significantly. They are strongly endothermic, as found before[19,22,23] for the association of non-polar (parts of) molecules in water. The value for the bimolecular association of cyclohexanol with cyclohexane in water[21,22] has the same magnitude, *i.e.*, 14.4 kJ mol^{-1}. The process of bimolecular association is in our case much more endothermic than LLP, where negative methylene increments of ΔH^0 have been found (*cf.* Fig. 4, refs. 2, 13 and references therein). In the case of *n*-octanol we find a difference of *ca.* 13 kJ mol^{-1} between ΔH^0 for bimolecular association and that for partition. The dimerization of benzene and the interaction of cyclohexane with cyclohexanol are also found to be more endothermic than related partition processes, *i.e.*, by 19 and 15 kJ mol^{-1}, respectively[21].

The heat capacities for bimolecular association (not shown) were arbitrarily set equal to zero for the lowest member of the series. Results for *n*-nonanol are -0.3 and -0.4 kJ mol^{-1} K^{-1}, and for *n*-octanol, -0.5 kJ mol^{-1} K^{-1}. These strongly negative values are in agreement with literature data[22,23]. For LLP, the heat capacity change is about -0.3 kJ mol^{-1}, as found before[2,13]. Thus, also in our case, it holds that the interaction between *n*-alcohols and single OG groups becomes exothermic at temperatures near 60–70°C, exactly as found previously[22] (if ΔC^0_p is assumed to be constant up to this temperature).

We conclude that the thermodynamics of the interaction of *n*-alcohols with octylglycidyl groups at low values of *P* show all the features of a bimolecular association of hydrophobic, mobile moieties in water. The strength of this strongly endothermic interaction is much lower than of cooperative interactions between several OG chains and the solute.

Mixed mechanisms govern the retention in region B in Fig. 3, where log $\gamma^{\infty}_{B,AG}$ strongly depends on $P^{-\frac{1}{2}}$ and on the length of the bonded chains. The latter dependence is much stronger than can be accounted for with the simple model of a homogeneous distribution of bonded chains on the surface of the agarose fibres. In that case, upon increasing the mean distance between the points of attachment by lowering P, water is expected to penetrate the layer of AG independently of the chain length, and the change from LLP to bimolecular association should take place at about the same values of P. This is clearly not observed in Fig. 3: the same increase in log $\gamma^{\infty}_{B,AG}$ for *n*-octanol of, say, 0.40 (with respect to values in region A) is brought about by taking $P^{-\frac{1}{2}} = 2$, 3.5 and 5 for pentyl-, octyl and dodecyl-agarose, respectively. Approximately the same ratio of $P^{-\frac{1}{2}}$ values —nearly equal to the corresponding ratio of the lengths of the alkyl chains— is found for other solutes. Apparently, upon increasing $P^{-\frac{1}{2}}$, the layer of AG breaks up into clusters of a few mutually interacting chains and cooperative interaction with a solute is much stronger than bimolecular association. This is especially so for dodecyl-agarose: at $P^{-\frac{1}{2}} = 3$ an LLP model is still valid, whereas for pentyl-agarose a bimolecular association model would be more approximate. It is caused by the much stronger association of the longer dodecyl chains.

Comparison with alkyl-silicas

Alkyl-silicas are frequently used in reversed-phase HPLC. Several studies on the influence of the chain length and chain density of the bonded alkyl groups have revealed a complex retention mechanism (see, *e.g.*, refs. 25–28 and references therein).

Berendsen and De Galan[26] studied the effect of the chain length at maximum surface coverage. We calculated log V_g^* values from their capacity ratios for *n*-propanol and *n*-butanol with water as the eluent using the characteristics of their bonded phases described in ref. 25. The results are plotted as a function of the bonded chain length in Fig. 5. Also shown are our log V_g^* values for *n*-pentanol and *n*-hexanol in

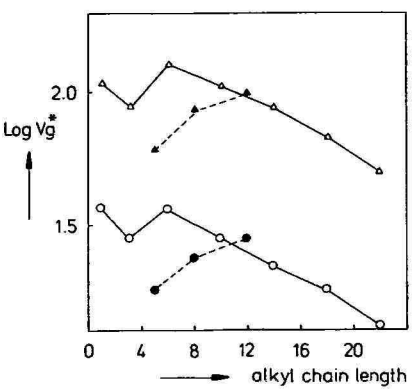

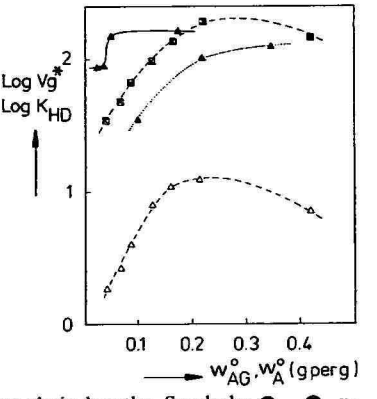

Fig. 5. Comparison of alkyl-agaroses and alkyl-silicas with different chain lengths. Symbols: ●--●, *n*-pentanol; ▲--▲, *n*-hexanol; both on alkyl-agarose in the partition region; ○—○, *n*-propanol; △—△, *n*-butanol; both on alkyl-silicas with maximum surface coverage and water as the eluent[26].

Fig. 6. Comparison of alkyl-agaroses and alkyl-silica with different chain densities. Symbols: ▲, benzene on pentyl-agarose (.....) and on dodecyl-agarose (——), with water as eluent; △, benzene; ⊠, pyrene; both on octadecyl-agarose, with methanol–water (70:30, v/v) as eluent[27,28].

the partition region. First, there exists a large discrepancy between the log V_g^* values for, *e.g.*, *n*-butanol on both types of sorbents. (This follows from extrapolation of our data to $n = 4$.) We observed and discussed this in previous work[1]. Secondly, it is seen in Fig. 5 that extension of the bonded alkyl chains has the opposite effect on the log V_g^* values. Recalculated log V_g^* values for all the other model substances (also for methanol–water eluents) in ref. 26 also decrease with increasing chain length of the bonded alkyl groups. According to Berendsen and De Galan, a solute molecule interacts only with the outer parts of the alkyl chains, keeping its most polar part (if present) in the eluent[26]. They named this mechanism "compulsory absorption". Clearly, this mechanism is not operative on alkyl-agarose, where steric factors favouring such a mechanism are absent.

Hennion *et al.*[27] investigated octadecyl-silicas of lower surface coverage, using methanol–water (70:30) as eluent. In such an eluent, silanophilic interactions can contribute to the retention, especially at low surface coverages. Nikolov[28] eliminated these contributions from the data of Hennion *et al.* in his "partial partition coefficient", K_{HD}. Values of log K_{HD}, which are comparable with our values of log V_g^*, are plotted in Fig. 6 as a function of the weight of the octadecyl chains per g of silica. The solutes are benzene and pyrene (other solutes give the same picture). For comparison, our data for benzene are shown.

It is seen that the influence of the chain density at w^0 values less than 0.25 is qualitatively the same on pentyl-agarose in water and on octadecyl-silica in 70% methanol. We explain this as follows. In the 70% methanol eluent, the association between the octadecyl chains that occurs in water is virtually absent[28]: the chains are solvated. This is also the case with pentylglycidyl chains in water (except at very high w^0); these short chains mutually interact weakly and are solvated by water. Hence, the solute retention on pentyl-agarose and on octadecyl-silica is governed by comparable mechanisms in this region; *i.e.*, the mixed mechanism discussed before. This is in contrast to the interaction with dodecyl-agarose in water. Although these alkyl groups are much shorter than octadecyl groups, the horizontal curve for this sorbent up to low alkyl densities clearly shows the cooperative interactions between the dodecyl groups. The difference in behaviour between dodecyl-agarose and octadecyl-silica is probably caused by the difference in solvating power of the two eluents for alkyl chains. At high values of w_A^0, steric effects[25,26,29] apparently cause a reduction in the retention on octadecyl-silica. The solute is (partially) squeezed out of the alkyl layer and a transformation to the "compulsory absorption" mechanism takes place. In this respect it is noteworthy that values of log V_g^* for benzene on alkyl-silicas with 50% surface coverage (corresponding to $w_A^0 = ca.\ 0.2$ for octadecyl-silica; see Fig. 6) in methanol–water eluents are linearly related to the alkyl chain length ($n = 6$–18) in the same way as on alkyl-agarose in the LLP region, contrary to the maximally substituted alkyl-silicas (calculated from data in ref. 27).

ACKNOWLEDGEMENT

We are much indebted to Mr. A. V. E. George for his kind and skilful assistance and valuable advice during the NMR analyses.

REFERENCES

1 P. M. Brandts, W. J. Gelsema and C. L. de Ligny, *J. Chromatogr.*, 322 (1985) 399.
2 W. J. Gelsema, P. M. Brandts, C. L. de Ligny, A. G. M. Theeuwes and A. M. P. Roozen, *J. Chromatogr.*, 295 (1984) 13.
3 P. M. Brandts, W. J. Gelsema and C. L. de Ligny, *J. Chromatogr.*, 333 (1985) 41.
4 *Octyl- and Phenyl-Sepharose CL-4B for Hydrophobic Interaction Chromatography*, Pharmacia, Uppsala, 1976.
5 T. Låås, *Acta Univ. Upsaliens (dissertation)*, 1975.
6 A. Amsterdam, Z. Er-el and S. Shaltiel, *Arch. Biochem. Biophys.*, 171 (1975) 673.
7 S. Hjertén, J. Rosengren and S. Påhlman, *J. Chromatogr.*, 101 (1974) 281.
8 J. Rosengren, S. Påhlman, M. Glad and S. Hjertén, *Biochim. Biophys. Acta*, 412 (1975) 51.
9 H. P. Jennissen, *Hoppe-Seyler's Z. Physiol. Chem.*, 357 (1976) 1727.
10 W. Kissing and R. Reiner, *J. Solid Phase Biochem.*, 4 (1979) 211.
11 G. Halperin, M. Breitenbach, M. Tauber-Finkelstein and S. Shaltiel, *J. Chromatogr.*, 215 (1981) 211.
12 S. Shaltiel, *Methods Enzymol.*, 104 (1984) 69.
13 P. M. Brandts, W. J. Gelsema and C. L. de Ligny, *J. Chromatogr.*, 354 (1986) 19.
14 V. Ulbrich, J. Makěs and M. Jureček, *Collect. Czech. Chem. Commun.*, 29 (1964) 1466.
15 M. H. Abraham, *J. Chem. Soc., Faraday Trans 1*, 80 (1984) 153.
16 Y. B. Tewari, M. M. Miller and S. P. Wasik, *J. Res. Natl. Bur. Stand. (U.S.)*, 87 (1982) 155.
17 M. Ducros, J. F. Grunson and H. Sannier, *Thermochim. Acta*, 36 (1980) 39.
18 D. G. Oakenfull and D. E. Fenwick, *J. Phys. Chem.*, 78 (1974) 1759.
19 A. Ben-Naim, *Hydrophobic Interactions*, Plenum, New York, 1980, Ch. 3.
20 Y. A. Mirgorod, *Russ. J. Phys. Chem. (Engl. Transl.)*, 56 (1982) 524.
21 E. E. Tucker, E. H. Lane and S. D. Christian, *J. Solution Chem.*, 10 (1981) 1.
22 S. D. Christian and E. E. Tucker, *J. Solution Chem.*, 11 (1982) 749.
23 G. Nemethy and H. A. Sheraga, *J. Phys. Chem.*, 66 (1962) 1773.
24 W. H. Scouten, in *Chemical Analysis 59*, Wiley, New York, 1981, Ch. 9.
25 G. E. Berendsen, *Thesis*, Delft University of Technology, 1980.
26 G. E. Berendsen and L. de Galan, *J. Chromatogr.*, 196 (1980) 21.
27 M. C. Hennion, C. Picard and M. Caude, *J. Chromatogr.*, 166 (1978) 21.
28 R. N. Nikolov, *J. Chromatogr.*, 286 (1984) 147.
29 G. E. Berendsen, K. A. Pikaart and L. de Galan, *J. Liq. Chromatogr.*, 3 (1980) 1437.

Journal of Chromatography, 356 (1986) 261–269
Elsevier Science Publishers B.V., Amsterdam — Printed in The Netherlands

CHROM. 18 396

CHROMATOGRAPHY WITH SUB- AND SUPERCRITICAL ELUENTS

INFLUENCE OF THE SEPARATION CONDITIONS ON SELECTIVITY, PLATE NUMBER AND RESOLUTION

FRANZ P. SCHMITZ
Lehrstuhl für Makromolekulare Chemie der RWTH Aachen, Worringerweg, D-5100 Aachen (F.R.G.)
(Received December 4th, 1985)

SUMMARY

The contributions of the selectivity, α, and plate number, n, to the dependence of chromatographic resolution on the pressure and temperature have been studied. It is demonstrated that these contributions depend on the separation conditions and on the substrates, with changes in α being in some cases responsible for changes in resolution rather than changes in n. Increasing pressure may cause the selectivity to increase, while plate numbers are lowered. For the separation of oligomers, a pressure may be found where a maximum in the overall resolution occurs.

INTRODUCTION

Studies on the chromatographic behaviour of various mobile phases in different physical states (liquid, gaseous and supercritical) with respect to the parameters temperature and pressure have produced interesting results[1–7]. In some of these studies[2,3,5,7], particular attention was paid to the effects of pressure and temperature on the chromatographic resolution, R, as a measure of the separation quality. Since R is influenced both by the elution times of the peaks relative to each other, *i.e.*, the selectivity, α, and by the peak widths, the latter information being contained in the plate number, n, knowledge of changes in the values of α and n are of additional interest. In this communication, some results are presented concerning the relationship between α, n and R and its dependence on the temperature and pressure.

THEORETICAL

For determination of resolution, a modified resolution equation was used:

$$R_{ij}^{*} = P_{ij} + \frac{d_{ij}}{w_i' + w_j'} \sqrt{\ln 4} \qquad (1)$$

with $d_{ij} > 0$

0021-9673/86/$03.50

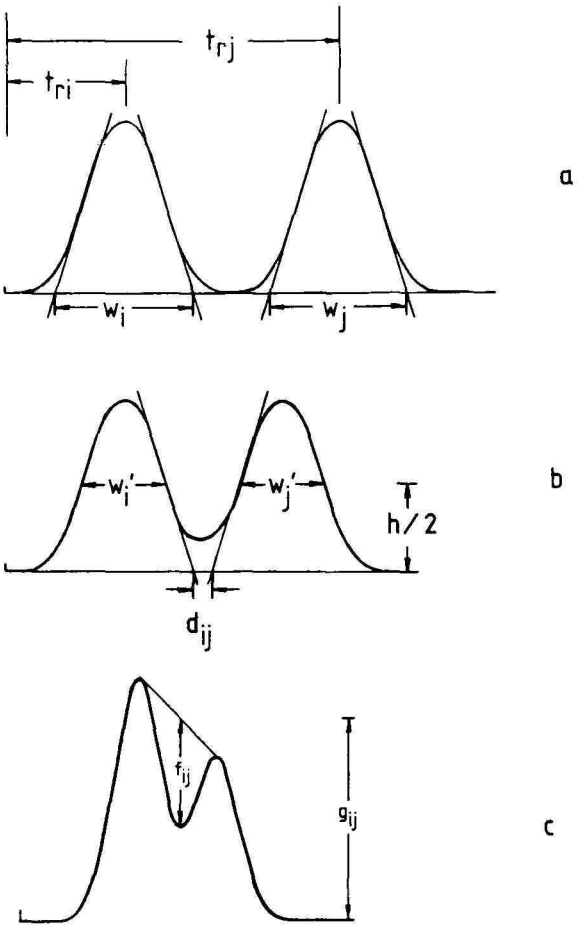

Fig. 1. Different types of peak pairs: (a) fully resolved; (b) incompletely resolved; (c) severely overlapped.

Here, P_{ij} is the ratio of the depth of a peak valley to the average peak height[8] (*cf.*, Fig. 1c)

$$P_{ij} = f_{ij}/g_{ij} \tag{2}$$

d_{ij} is the portion of the baseline intercepted between the tangents to two peaks and w' is the peak width at half height (*cf.*, Fig. 1b). For $d_{ij} = 0$ and $d_{ij} < 0$, R^* was calculated according to:

$$R_{ij}^* = P_{ij} \tag{3}$$

Eqn. 1, which resembles an equation proposed by Bhattacharjee[9], was derived from the well known resolution equation (*cf.*, Fig. 1a)

$$R_{ij} = \frac{2(t_{rj} - t_{ri})}{w_i + w_j} \tag{4}$$

with eqn. 5 (*cf.*, Fig. 2a)

$$t_{rj} - t_{ri} = d_{ij} + \frac{w_i + w_j}{2} \tag{5}$$

yielding:

$$R_{ij} = 1 + \frac{2\,d_{ij}}{w_i + w_j} \tag{6}$$

Replacing peak widths, w, by peak widths at half height, w', leads to:

$$R_{ij} = 1 + \frac{d_{ij}}{w_i' + w_j'}\sqrt{\ln 4} \tag{7}$$

For the calculation of resolution, peaks are generally treated as having trapezoidal shapes (*cf.*, Fig. 2b) for which both R_{ij} and P_{ij} are equal to unity when $d_{ij} = 0$. The value of P_{ij} remains equal to unity when d_{ij} assumes positive values. Thus, eqn. 7 may be written in the form of eqn. 1.

Calculating R^* by means of eqn. 1 for peak pairs where $d_{ij} > 0$ and by eqn. 3 when $d_{ij} \leqslant 0$ has the advantage that in plots of resolution *vs.* a selected chromatographic parameter no abrupt change is produced, since there is a smooth transition from eqn. 1 to eqn. 3. Compared to eqn. 4, the resolution values calculated using eqn. 1 are more sensitive to peak asymmetries with closely neighbouring peaks. Thus, from a practical point of view, the R^* values are more "realistic". The difficult construction of tangents to overlapped peaks is avoided when using the procedure described above.

For peaks which are resolved so poorly that their widths cannot be determined, the plate numbers can be estimated from resolution values using the relation

$$n_j = 16\left(\frac{t_{rj}}{t_{rj} - t_{ri}}\right)^2 R_{ij}^2 \tag{8}$$

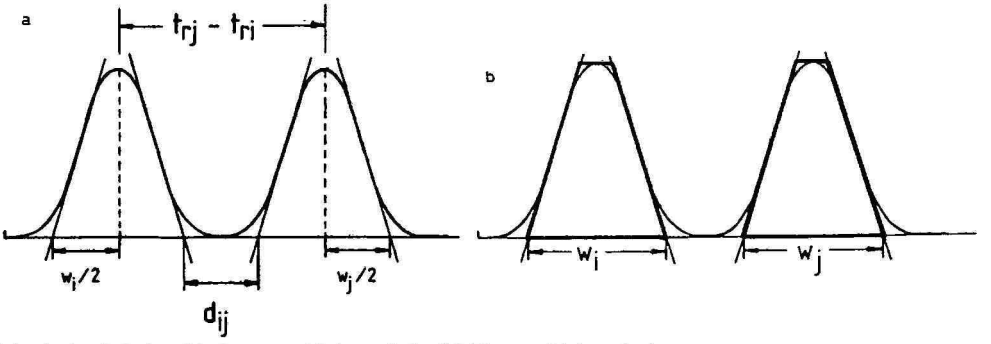

Fig. 2. (a) Relationship between $(\Delta t_r)_{ij}$ and d_{ij}. (b) Trapezoidal peak shapes.

which can be obtained from eqn. 9

$$R_{ij} = \frac{1}{4} \cdot \frac{\alpha - 1}{\alpha} \cdot \frac{k_j}{1 + k_j} \sqrt{n_j} \tag{9}$$

which is valid for closely neighbouring peaks.

Here, α is the selectivity

$$\alpha = \frac{t_{rj} - t_0}{t_{ri} - t_0} \tag{10}$$

k_j is the capacity factor of the jth peak

$$k_{rj} = \frac{t_{rj} - t_0}{t_0} \tag{11}$$

and t_0 is the dead time.

EXPERIMENTAL

The instrument used for supercritical-fluid chromatography (SFC) has been described previously[10]. It consisted of a high-performance liquid chromatograph, Type 1084 B, from Hewlett-Packard, which had been modified for SFC.

Stainless-steel columns (25 cm × 4.6 mm I.D.) were packed with LiChrosorb Si 60, 10 μm (Merck, Darmstadt, F.R.G.) using a slurry method[11]. UV detection (254 nm) was carried out at ambient temperature in the liquid state. The flow-rate was 1 ml/min at the pumps at ambient temperature. The eluents *n*-pentane and 1,4-dioxane were purified before use by drying, distillation and degassing. The chromatographic substrates were PS 800, an oligostyrene sample with a number-average molecular weight of 810 g/mol (Pressure Chemical, Pittsburgh, PA, U.S.A.), and a mixture of the aromatic compounds naphthalene, anthracene, pyrene and chrysene (*cf.*, ref. 2); the sample solvent was *n*-hexane.

The chromatographic data used for the calculation of resolution values shown in Fig. 3 are taken from studies reported previously[3,7].

RESULTS AND DISCUSSION

Fig. 3 shows isobaric plots of resolution *vs.* temperature for a sample mixture consisting of naphthalene, anthracene, pyrene and chrysene, chromatographed with *n*-pentane as the eluent. Curves 1 and 3 show the temperature dependence of the average resolution, $\overline{R^*}$, calculated according to

$$\overline{R^*} = \frac{\Sigma R^*_{ij}}{n} \tag{12}$$

where n = total number of adjacent peak pairs. Curves 2 and 4 are plots of the

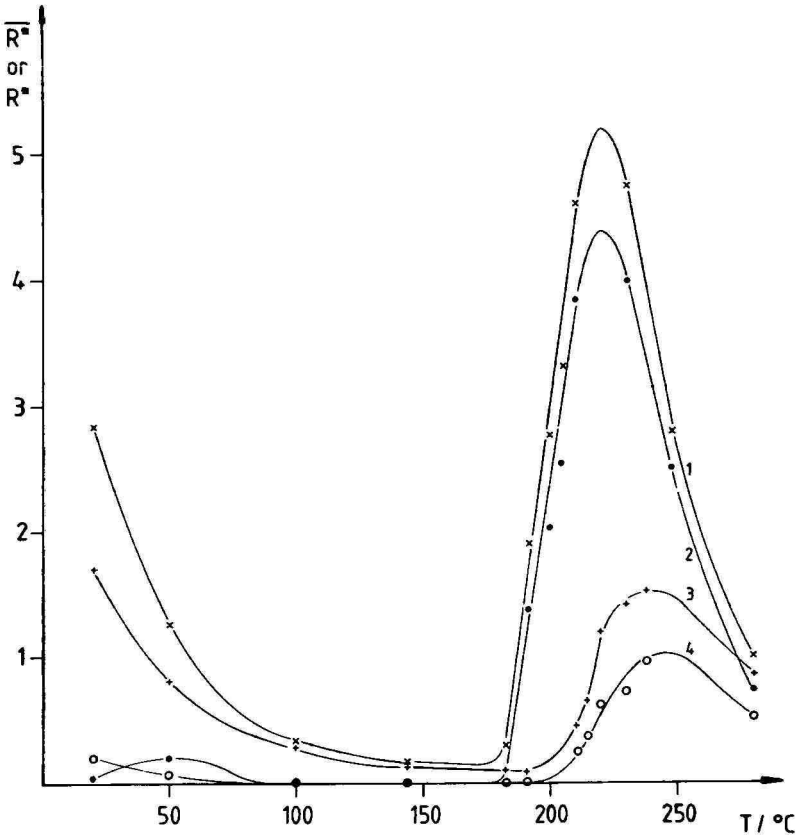

Fig. 3. Plots of mean resolution, $\overline{R^*}$, *vs.* temperature for a mixture of naphthalene, anthracene, pyrene and chrysene in *n*-pentane as the eluent at 20 bar (curve 1) and 36 bar (curve 3), and of resolution, R_{ij}^*, *vs.* temperature for anthracene/pyrene at 20 bar (curve 2) and 36 bar (curve 4).

resolution, R_{ij}^*, between anthracene and pyrene. Values of R_{ij}^* were calculated by the combination of eqns. 1 and 3 as described above.

As is seen from Fig. 3, the overall resolution, $\overline{R^*}$, for the three peak pairs naphthalene/anthracene, anthracene/pyrene and pyrene/chrysene decreases when the temperature is raised, as long as the mobile phase is in the liquid state (curves 1 and 3). Beyond the boiling or the critical temperature, $\overline{R^*}$ increases again and exhibits a maximum. Further increase in temperature leads to decreasing resolution. The lower the pressure the more pronounced is this behaviour, (*cf.*, refs. 5, 7). In contrast, the separation of anthracene and pyrene is rather poor in the liquid phase. Good separation can be achieved only when the mobile phase is in the sub- or supercritical gaseous state.

This behaviour can be ascribed partly to changes in the plate numbers, which were estimated by means of eqn. 8. In the experiments at 20 bar (curves 1 and 2), plate numbers obtained at 230°C, *i.e.*, near the maximum of the resolution curve,

TABLE I

RELATIVE VALUES FOR PARAMETERS AT THE RESOLUTION MAXIMA (*cf.*, FIG. 3)

Referred to corresponding values in the liquid phase at ambient temperature. N = Naphthalene; A = anthracene; P = pyrene; C = chrysene.

Conditions	*Peak pair*	*n (rel.)*	$\frac{\alpha - 1}{\alpha}$ *(rel.)*	$\frac{k_j}{1 + k_j}$ *(rel.)*
20 bar,	N/A	1.6	1.9	3.4
230°C	A/P	2.3	5.2	5.7
	P/C	2.2	1.2	6.8
36 bar,	N/A	0.6	1.5	1.0
240°C	A/P	0.8	4.5	1.4
	P/C	0.7	0.8	1.1

exceed those obtained in the liquid phase by a factor of about two (*cf.*, Table I). This is accompanied by increasing values of both the α and k terms of the resolution equation 9, with the increase in α for anthracene/pyrene being particularly high. Contrary to this, at 36 bar, the plate numbers at 20 and 240°C are comparable, even for the pair anthracene/pyrene, for which the resolution is considerably higher at 240°C. Here, the increase in resolution is due to changes in the selectivity of the separation, as is seen from the increase in the selectivity term. Similar results are obtained for the lower alkanes butane and propane.

It has been shown that, for SFC separations of oligomers, in addition to pres-

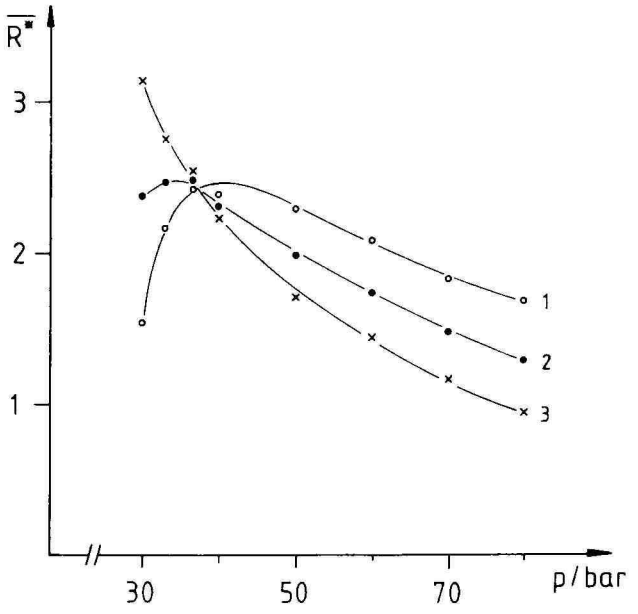

Fig. 4. Resolution of oligostyrenes as a function of column pressure. Curves: 1, overall resolution, $\overline{R^*}$, of peak 10–18; 2, overall resolution, $\overline{R^*}$, for peaks 1–18; 3, overall resolution, $\overline{R^*}$, for peaks 1–9. T = 210°C. Pressure, p, at the column exit at the start of the chromatographic experiments.

TABLE II

GRADIENT PROGRAM FOR THE POLYSTYRENE SEPARATIONS

	Time (min)								
	0	*10*	*20*	*30*	*40*	*50*	*60*	*70*	*80*
Dioxane (%, v/v)	5.0	7.1	9.1	11.0	12.9	14.6	16.2	17.9	19.4

sure programming which is most frequently used, gradients in eluent composition can be applied[10]. Fig. 4 shows the separations of oligostyrenes with *n*-pentane–1,4-dioxane as the eluent; the dioxane content in the eluent mixture is given in Table II. While the gradient and the temperature were kept the same, at the start of the chromatograms the pressure at the column exit was varied between 30 and 80 bar. It is seen from Fig. 4 that the average resolution for the first nine peaks decreases steadily with increasing pressure. Nevertheless, for both the average resolution of the last nine peaks and the overall resolution, maxima occur at pressures of *ca.* 35–40 bar.

These resolution effects are produced by changes in the selectivity, α, and plate number, n, the capacity factor term (*cf.*, eqn. 9) being only of minor importance. For the higher oligomers, *i.e.*, from a degree of oligomerization of *ca.* 6, the plate numbers were found to decrease with increasing pressure, while increasing α values were observed. Thus, with increasing pressure, the quality of the oligostyrene separations was governed more and more by selectivity. From these results it is obvious that, for an oligomer separation, a pressure may be found where the separation is optimal. A comparison of curves 1 and 2 in Fig. 5 shows that such optimum pressures are shifted to higher values with increasing molecular weight of the sample.

It should be mentioned that, with the oligostyrene separation shown here, the critical temperature of the eluent mixture may exceed the applied temperature of 210°C owing to the increase in dioxane content (*cf.*, Table III). Thus, a transition of the mobile phase from a dense (supercritical) gas to a liquid occurs during the experiment, especially where the pressure is low and, therefore, higher dioxane contents are necessary to elute the whole sample (*cf.*, Table IV). Yet, a transition from a state with a lower density to one where the density is higher does not seem to have a detrimental effect on the separation[11]. In contrast, pressures below the critical pres-

TABLE III

CRITICAL DATA FOR MIXTURES OF *n*-PENTANE AND 1,4-DIOXANE

Calculated according to the methods described by Chueh and Prausnitz[12].

	Dioxane (%, v/v)				
	0	*5*	*10*	*15*	*20*
T_c (°C)	196.5	203.9	211.2	218.3	225.2
P_c (bar)	33.7	37.4	40.8	43.9	46.7

TABLE IV

DATA FOR THE OLIGOSTYRENE SEPARATIONS

P_e (bar)*	t_{max}** (min)	Dioxane content at t_{max} (%, v/v)	P_e at t_{max} (bar)
30	78.1	18.4	41
33	68.0	16.7	43
37	56.2	14.8	46
40	52.9	14.2	49
50	35.4	11.1	57
60	31.7	10.5	66
70	25.5	9.2	75
80	22.9	8.7	85

* Column exit pressure at the start of the chromatogram.
** Retention time of the 18th peak.

sure might have a greater effect. Since, however, the column pressure is set at the start of the experiment by use of a valve at the column outlet and since the increasing dioxane content leads to a higher viscosity of the mobile phase, the pressure increases to some extent during the experiment.

This pressure increase due to the higher dioxane contents is almost parallel to the dioxane content in the eluent mixture[13]; the pressures resulting at the column exit at the elution time of the last peak, t_{max}, are summarized in Table IV. It is seen from Tables III and IV that if at the start of the chromatogram the pressure, p_e, is above the critical pressure of the eluent mixture, it will remain above critical during the separation irrespective of the increasing dioxane content. Thus, the increase in pressure prevents the transition to the subcritical gaseous state which would have occurred in some instances.

For Fig. 4, the pressure at the column exit, set at the start of the separation, was chosen as the parameter for two reasons. First, this pressure is of interest from a practical point of view since it can easily be set and controlled. Secondly, for the quality of a separation, this pressure is most important in SFC because elution is slowest at the column exit due to the lower eluent density compared to that in the preceding parts of the column; the pressure drop along the column was in the range of 10–15 bar.

ACKNOWLEDGEMENTS

Thanks are expressed to Professor E. Klesper for kindly supporting this work, to Mr. B. Lorenschat for experimental aid and to the Arbeitsgemeinschaft Industrieller Forschungsvereinigungen (AIF) for financial support.

REFERENCES

1 M. Novotný, W. Bertsch and A. Zlatkis, *J. Chromatogr.*, 61 (1971) 17.

2 F. P. Schmitz, D. Leyendecker and E. Klesper, *Ber. Bunsenges. Phys. Chem.*, 88 (1984) 912.
3 F. P. Schmitz, H. Hilgers, D. Leyendecker, B. Lorenschat, U. Setzer and E. Klesper, *J. High Resolut. Chromatogr. Chromatogr. Commun.*, 7 (1984) 590.
4 Y. Hirata and F. Nakata, *J. Chromatogr.*, 295 (1984) 315.
5 D. Leyendecker, F. P. Schmitz and E. Klesper, *J. Chromatogr.*, 315 (1984) 19.
6 Y. Hirata, *J. Chromatogr.*, 315 (1984) 31.
7 D. Leyendecker, F. P. Schmitz, D. Leyendecker and E. Klesper, *J. Chromatogr.*, 321 (1985) 273.
8 R. Kaiser, *Chromatographie in der Gasphase, Erster Teil: Gas-Chromatographie*, Zweite Auflage, Bibliographisches Institut, Mannheim, 1973, p. 56.
9 A. Bhattacharjee, *Fuel Sci. Technol.*, 2 (1983) 129.
10 F. P. Schmitz, H. Hilgers and E. Klesper, *J. Chromatogr.*, 267 (1983) 267.
11 F. P. Schmitz, H. Hilgers, B. Lorenschat and E. Klesper, *J. Chromatogr.*, 346 (1985) 69.
12 P. L. Chueh, J. M. Prausnitz, *AIChE J.*, 13 (1967) 1099; cited in R. C. Reid, J. M. Prausnitz and T. K. Sherwood, *The Properties of Gases and Liquids*, McGraw-Hill, New York, 3rd ed., 1977, p. 140.
13 F. P. Schmitz and E. Klesper, *Makromol. Chem., Rapid Commun.*, 2 (1981) 735.

Journal of Chromatography, 356 (1986) 271–284
Elsevier Science Publishers B.V., Amsterdam — Printed in The Netherlands

CHROM. 18 397

HIGH-RESOLUTION PREPARATIVE GAS CHROMATOGRAPHY

I. A MICROPROCESSOR-CONTROLLED SYSTEM FOR AUTOMATED FRACTION COLLECTION

J. ROERAADE*, S. BLOMBERG and H. D. J. PIETERSMA
Royal Institute of Technology, Department of Analytical Chemistry, S-100 44 Stockholm (Sweden)
(Received November 6th, 1985)

SUMMARY

A control system for automated high-resolution preparative gas chromatography is described. On the basis of recorded data from a reference chromatogram, the computer-controlled device automatically corrects for the drift in retention that may occur within a run or during extended operation, and synchronizes fraction collection. Failure to track the reference chromatogram activates an error status and protects the traps for contamination. A specified number of consecutive tracking failures discontinues the repetitive fractionation process. The system can be operated in a simulated mode to facilitate optimization and also includes a control routine to drive auxiliary devices such as an automatic on-column injector or flow switching valves.

Cyclic preparative high-resolution fractionation of an essential oil was carried out to evaluate the system. Retention shifts of several seconds were adequately corrected for by the real-time synchronization process, which allowed the precision trapping of closely spaced fractions. Trapping accuracy was also maintained during nearly 800 unattended high-resolution separations of *cis*- and *trans*-isopiperitenol. This resulted in the isolation of milligram amounts of the purified isomers and enabled ^{13}C NMR spectra of the components to be recorded.

INTRODUCTION

A considerable proportion of current research in organic analytical chemistry is focused on the characterisation of trace components, notably in fields such as aroma, pheromone and environmental chemistry, where many of the components that occur in very low concentrations are of key importance. In addition to various pattern recognition studies and quantitative determinations of known components, the structural elucidation of unknown ultra-trace constituents is a central activity in the disciplines mentioned. When dealing with complex natural products or samples of biological origin, such work is a demanding analytical task and requires extensive clean-up and fractionation of the starting material, usually followed by capillary gas

0021-9673/86/$03.50

chromatography–mass spectrometry (GC–MS) and other on-line techniques such as GC coupled with Fourier transform infrared spectrometry.

However, the information obtained in this way is seldom sufficient for the structural elucidation of unknown compounds. It is frequently necessary to obtain complementary chemical and/or spectroscopic (*e.g.*, ^{1}H NMR, ^{13}C NMR, UV) data, which necessitates the isolation of the individual components. Isolation is also imperative if the biological or toxicological properties of unknown compounds are to be evaluated. Isolation is usually accomplished by high-performance liquid chromatography (HPLC). However, the resolving power of this technique is not always sufficient when dealing with very complex samples. Moreover, recovery problems are encountered when the total amount of material is at the micro- or nanogram level. Particularly for volatiles the recovery becomes very poor, notably when reversed-phase systems are used.

Preparative GC would be a more suitable method in such instances, but the separation efficiency of the packed columns that are usually employed is not adequate. Adsorption of polar compounds on the packing material is another factor that limits the applicability of packed columns. Capillary columns provide an attractive alternative and have been used by a number of workers (*e.g.*, refs. 1–5). Most systems described involve manual collection techniques. However, the sample capacity of high-resolution capillary columns is very limited, and the collection of fractions for NMR studies, where micro- to milligram amounts of material are required, may involve more than 1000 repetitive runs. It is obvious that the use of an automated system is a more realistic approach for such work.

In a previous paper[6], we reported a system where the external event outputs of an integrator were used to control automated fraction collection from capillary columns. However, during practical work it was found that retention shifts can occur, particularly during long-term operation. Hence the accurate collection of narrow-spaced fractions was not possible unless frequent timing adjustments were made. Retention instability caused considerable disturbances when complex samples having a wide volatility range were fractionated.

The recovery of the small amounts of sample can be associated with difficulties[7]. Various trapping methods have been described (*e.g.*, refs. 8–10), and some workers have reported close to 100% trapping efficiency. However, the recovery studies were carried out under various conditions and are therefore not readily comparable. In particular, the handling and transfer of microgram or submicrogram amounts of (volatile) fractions is a critical step, which can lead to serious losses. Little systematic work has been devoted to this aspect.

In this series of papers, we shall explore the potential of preparative high-resolution GC and present improved methodology to allow a more versatile use of the technique. This paper describes a microprocessor-based control system, where a real-time correction of the trapping events allows unattended repetitive fractionation over extended periods. It is demonstrated that milligram amounts of pure compounds can be isolated from complex mixtures.

INSTRUMENTAL

Control system

In order to obtain a flexible system, computerized control was regarded as necessary. Precise timing of the trapping events is of critical importance when capillary columns are employed owing to the narrow width of the eluting peaks. A fraction collection period in an area with closely spaced or fused peaks may be as short as a few seconds, and a timing delay of a fraction of a second can significantly influence the composition of the trapped material. Therefore, a system for automatic time correction of the trapping events was constructed. Fig. 1 shows a schematic diagram of the hardware setup.

A home-made printed circuit board configured around a Motorola 6809 microprocessor was used. The program (mainly in assembler language) was stored in EPROM memory (32 kb), whereas the chromatographic data were stored in RAM memory (8 kb). Four VIAs (Mos-Tech 6522) were used in interfacing a printer (Epson RX-80), an ASCII keyboard (Cherry G-80) and a trapping unit (driving micro valves or rotary valves). A remote auxiliary keyboard was used to evoke the trapping events and to start or stop the recording process. A video display unit (NEC JB-902M) was interfaced to the processor bus via a video processor unit, configured around a Motorola M 6845. Apart from the control of the trapping valves, four inputs and twelve opto-coupled power outputs were installed to control auxiliary devices such as an automatic on-column injector.

The analogue detector signal from the chromatograph is transferred to the microprocessor via an instrumental amplifier and a V/f converter (INA 101 AN and VFC 320 BM, respectively; Burr-Brown). When a start pulse is obtained at the moment of sample injection (manually or from the auto-injector), the signal level is sampled every 20 ms and the measured values are compared over a specific time interval. Thus, the slope of the baseline (dV/dT) can be determined. With suitable criteria for dV and dT, the start, the end and the maximum of a peak can be distinguished from baseline drift and noise. This principle of peak detection is commonly employed in commercial integrators.

In order to allow a real-time correction of the trapping events, a reference chromatogram of the sample is first recorded. All retention data (0.1 s resolution), peak heights (in mV) and peak widths (0.1 s resolution) are stored in the RAM memory of the data system. Trapping events are evoked manually by pressing a function key, and the corresponding event times are thereby also stored in the computer memory.

A suitable number of recorded peaks are selected to serve as references, and identification windows are defined. During automatic fraction collection, the peak data are continuously compared and synchronized with the corresponding data of the stored reference chromatogram. The principle of this procedure is depicted in Fig. 2.

In principle, every peak in the reference chromatogram can be employed for the time correction procedure. However, this is usually neither necessary nor recommendable. Poorly separated or very small peaks are unsuitable for reference purpose.

Automatic fraction collection can be simulated in order to check the trapping

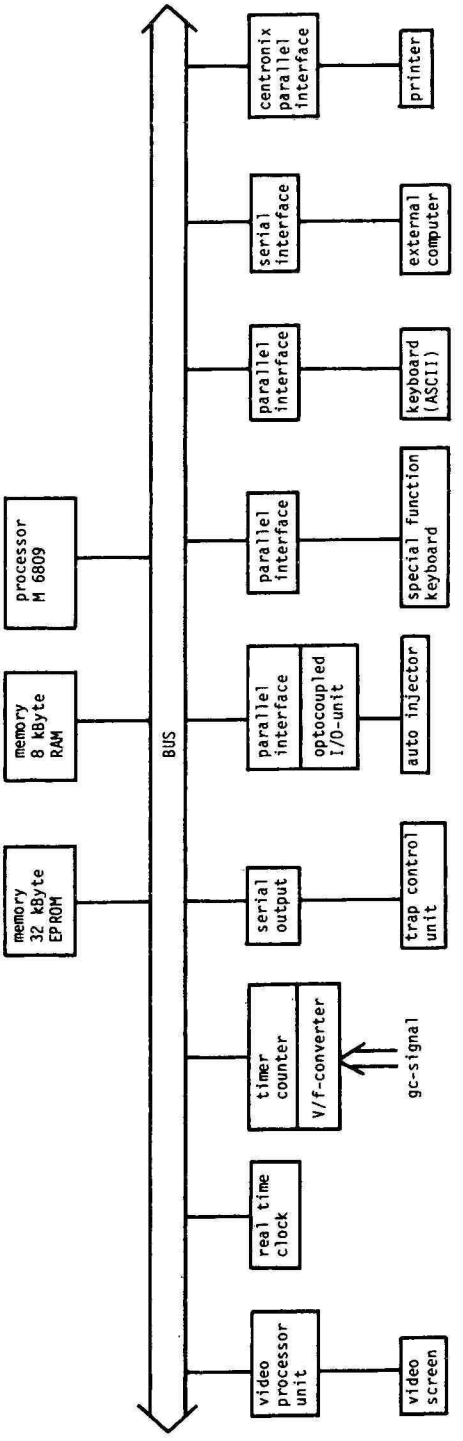

Fig. 1. Hardware configuration of the microprocessor-operated control unit.

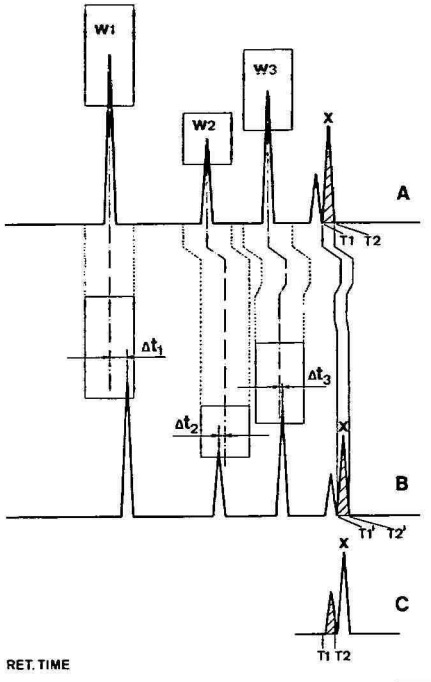

Fig. 2. Schematic principle of the fraction collection synchronization. A represents a model of a reference chromatogram, where the first three peaks are used as references. Time/height windows for each of those peaks are indicated by the areas W1, W2 and W3. The hatched area represents the region of fraction collection (compound X). B represents a chromatogram of a subsequent run, where sampling inaccuracy has resulted in reduced peak heights. However, the reference peaks still fall within the specified windows. A drift in retention is additively adjusted for, and a correct fraction collection is accomplished. C shows the last part of chromatogram B, and indicates how the fraction is collected when no retention adjustment is made.

precision and to verify that the chromatogram is properly tracked. In the simulated mode of operation, the eluting compounds are guided to a "waste" trap, to protect the individual collection tubes for contamination with unwanted material. After simulation (or any forced interruption of the process), the trapping and reference data can be edited and simulation can be repeated until satisfactory operating conditions have been created. Flexibility for optimization is obtained by using a menu-structured program. A flow sheet of the principal elements of this program is shown in Fig. 3.

Fraction collection

Trapping of the eluted fractions was accomplished according to the same principle as described previously[6]. However, some hardware modifications were made, as illustrated in Fig. 4. The effluent from the capillary column was guided to a three-way tee, where make-up gas (2 ml/min) was added, and further connected to a manifold (five or fifteen outlet ports). Part of the effluent (1/30) was guided to a flame ionization detector. Both the make-up tee and the manifold were made of fused-silica tubing, which was precision-fitted into polyimide bodies and glued with polyimide

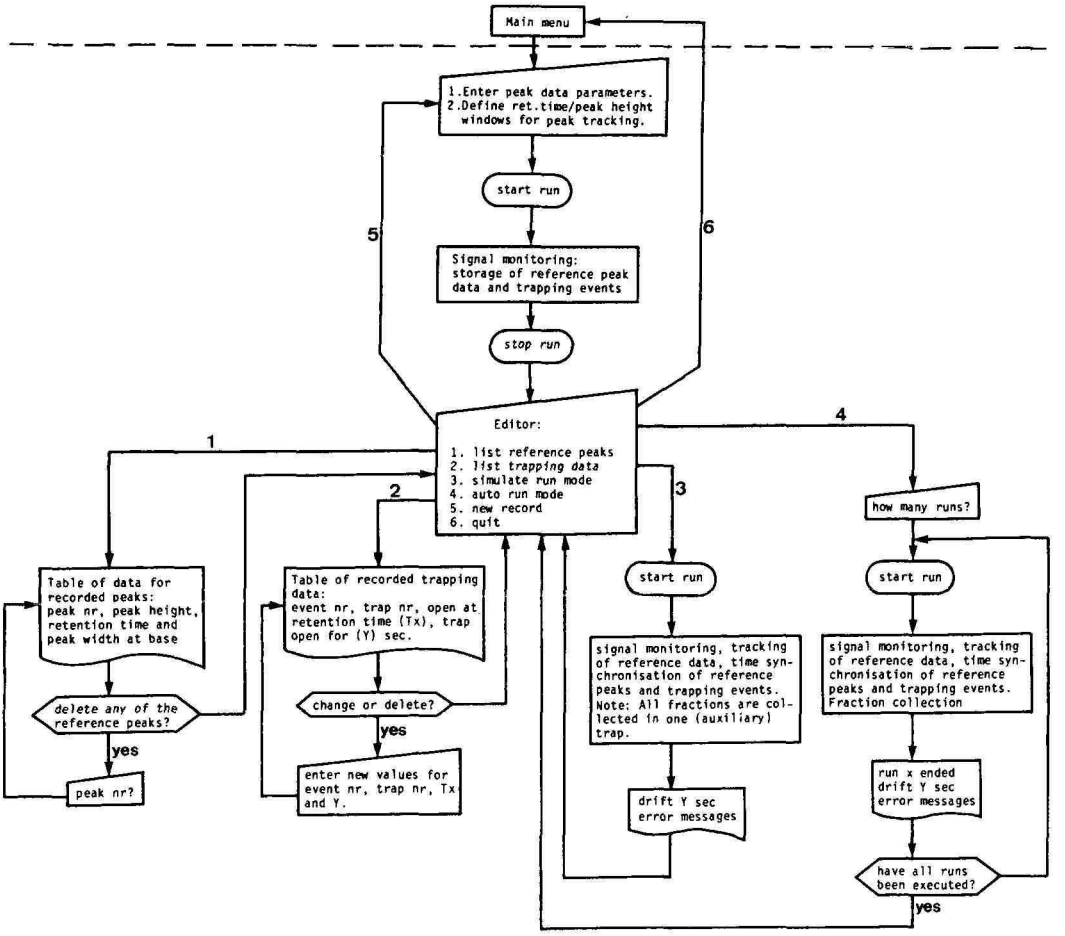

Fig. 3. Flow sheet showing the operative procedure of the control unit. The program sequence is entered via a "main menu", which comprises auxiliary entries for control of the individual functions of an auto-injector, flow switching, etc. Automatic injection is normally initiated at the "start run" command, but can also be delayed or repeated any time during the run. The cycle time for a run is automatically defined when the recording process is stopped. The recorded trapping events are numbered in consecutive order (default), but can be renumbered by using editor-2 (*e.g.*, to create mixtures of fractions). The tracking process (simulated or auto-run mode) can be interrupted at any instance. The program will then return to the editor.

prepolymer according to a procedure described by Sandra *et al.*[11]. Thus an inert flow distribution system was obtained.

Coiled glass capillary tubes (2 m × 0.6–0.7 mm I.D., coil diameter 130 mm) were used to trap the effluent. The tubes were straightened at both ends over a length of approximately 20 cm to facilitate connection. The inlet ends of the traps were drawn down to the same outer diameter as the tubes from the manifold. Connection was accomplished using shrinkable Teflon or miniature connectors[12]. The connections were positioned in a gradient-heated aluminium interface tube to reduce problems with condensation and fog formation. The outlet of the traps were connected

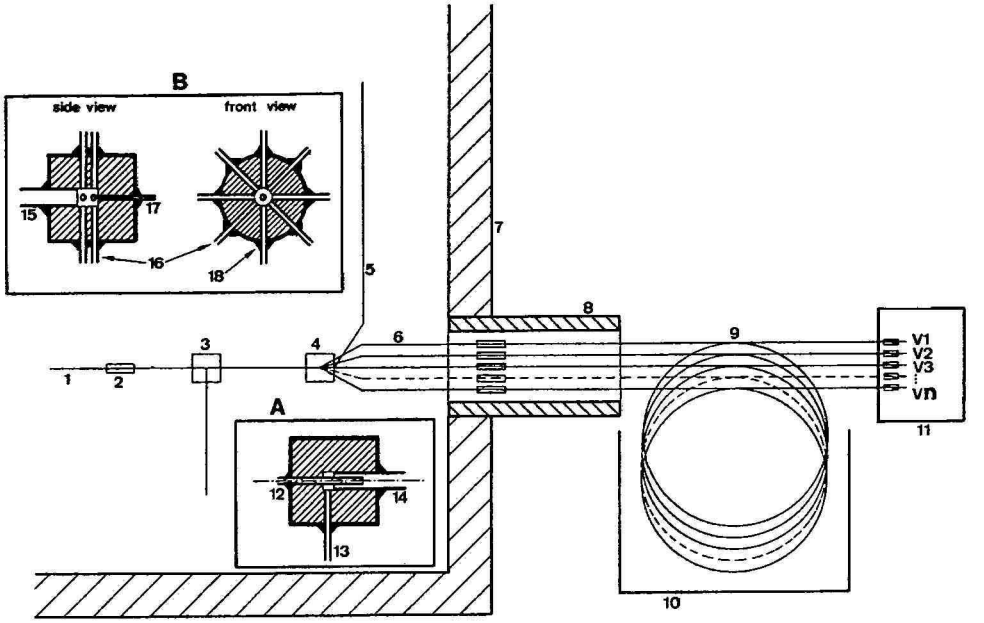

Fig. 4. Manifold and trapping arrangement. 1 = Capillary column; 2 = miniature connector; 3 = polyimide make-up tee; 4 = multi-channel manifold; 5 = outlet tube to detector; 6 = outlet tubes to the traps; 7 = GC oven wall; 8 = heated aluminium tube; 9 = glass capillary traps; 10 = Dewar (dry-ice–ethanol); 11 = trapping control unit with magnetic valves (V1, V2, V3, etc.). (A) Enlarged view of the polyimide make-up tee. 12 = Inlet tube connected to the capillary column (I.D. 0.32 mm); 13 = inlet for make-up gas (I.D. 0.32 mm); 14 = outlet tube to the manifold (I.D. 0.5 mm). (B) Enlarged view of the multi-channel manifold. 15 = Outlet from the make-up tee; 16 = outlets to the traps (I.D. 0.2 mm); 17 = outlet to the detector (I.D. 0.1 mm); 18 = polyimide glue.

to micro-magnetic valves (Brunswick Scientific, Model 407-C). A maximum of 32 valves could be driven from the processor unit via an opto-coupled serial input driver (MM5451; National Semiconductors). The setting of the valves was indicated by corresponding light-emitting diodes. The control unit can also be used to drive a rotary valve system instead of magnetic valves. However, the use of a manifold splitter and a common waste trap offers several advantages. First, there are no moving parts in the region of the sample passage. Second, the fractions can be guided to any of the traps in an optional sequence. This offers the attractive possibility of collecting mixtures of substances in their original proportions. Such a procedure is of particular value in flavour and pheromone chemistry when searching for key combination of compounds.

An important aspect in a system for unattended automated fraction collection is the elimination of trapping errors and associated risks of contamination of the collected material. A subroutine was included in the control program to protect the trapped material in events of failure. Under normal collection conditions, the common waste valve V1 (and corresponding trap) is kept open as long as no other valve is activated. During recording of the reference chromatogram and during test runs in the simulated mode, the fractions to be trapped are collected in a second waste trap (V2). Thus, flow conditions identical with those in the automated collection

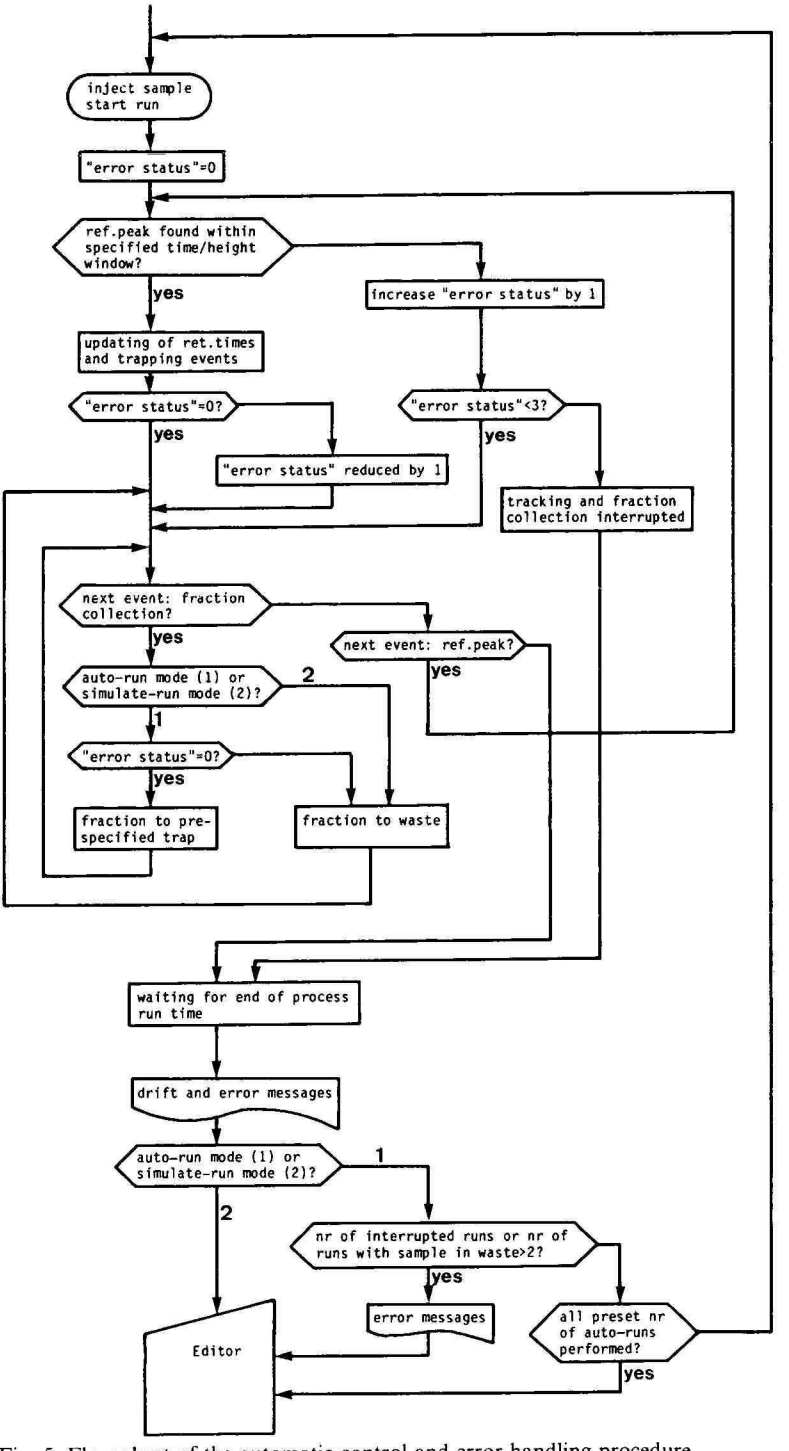

Fig. 5. Flow sheet of the automatic control and error handling procedure.

mode are established. This is particularly important when flow switching systems[6] are included in the splitter and manifold unit. Failure to track a reference peak activates an error status, and the remaining fractions to be collected during the ongoing run are switched to V2. The error status is reverted to normal when reference peaks are tracked again. The repetitive separation process will be halted if V2 has been activated in three consecutive runs. Fig. 5 shows a flow sheet where the error handling procedure is included.

Chromatographic equipment

A gas chromatograph (Varian Model 6000) equipped with a flame ionization detector and a split/splitless injector was used together with the described control and trapping unit. The electrically heated aluminium interface tube (length 175 mm, I.D. 14 mm) was inserted in the oven wall under the control box for the pneumatics. Automatic repetitive sample injection was accomplished using a modified autosampler (Varian Model 8000). The regular sample carousel was replaced by an automatic micro-dispenser (Hamilton Microlab-P), equipped with a 0.5-ml syringe. This syringe was coupled to the side inlet of the auto-injector syringe via a narrow-bore PTFE tube. The dispenser was actuated by a micro-switch when the plunger of the injection syringe reached the filling position. The micro-dispenser was set to fill the syringe of the auto-injector with sample portions of 5 μl. After 99 injections, the stock syringe was refilled with sample solution. For manual injections and fraction evaluation, an on-column injector (SGE-OCI-3) was used.

A computing integrator (Spectra-Physics SP-4270) was employed for area integration. A strip-chart recorder (Servogor 120), coupled in parallel, served as an additional monitor. The capillary columns used were prepared according to the procedure of Grob *et al.*[13]. The stationary phase (SE-54) was cross-linked with azoisobutyronitrile[14].

RESULTS AND DISCUSSION

Precision trapping

Several methods can be employed to ensure accurate fraction collection. In systems where packed columns are used, timer-based control devices without automatic retention adjustment are usually regarded as satisfactory[15,16], and a time resolution of the order of 1 s may be sufficient. A few systems for work with packed columns have employed a time correction procedure[17,18]. Hupe[19] employed a peak level detector, combined with a peak counting procedure. However, this technique is not suitable in cases where trace components are to be collected or in configurations where a flow switching splitter[6] is utilized. Additional advantages of time-based systems for fraction collection have been summarized by Roz *et al.*[20].

For high-resolution preparative work, stringent timing is necessary. Although a high degree of reproducibility is obtained with modern GC equipment, long-term deviations in retention can occur, *e.g.*, owing to accumulation of non-volatile material in the column, column deterioration, injection imperfections and sometimes also sample decomposition. Linear shifts in retention are frequently encountered when splitless or on-column injection in combination with the solvent effect is employed.

The present control system has the appropriate time resolution to be com-

patible with rapidly eluting compounds. Hence fused peaks can be "sliced" into optimized fractions. The real-time correction process ensures correct timing throughout long-term collection, and the error handling program allows safe unattended operation.

Proper selection of the reference peaks is important. The best trapping synchronization is obtained when reference peaks are chosen that elute just prior to the fractions to be trapped. Retention windows should be chosen large enough to allow for the maximum expected drift, even when the area embraces more than one peak. A mix-up of the peaks is not possible as long as the peaks can be discriminated in height. The signal obtained during collection can also be used for reference purpose. It is important to realise that the described retention correction system does not eliminate the need for precise control of the chromatographic variables (temperature, flow, etc.) Non-linear shifts are not fully corrected for, and it is hardly possible to provide a satisfactory algorithm that compensates for such errors. It would, of course, be possible (and simple) to include a level detector, which is activated in a defined retention window, but the advantages of the time-operated system are thereby sacrificed. However, as judged from the work carried out so far, no additional correction measures are necessary.

Optimization

In production-scale preparative GC, it is of vital importance to optimize the preparative efficiency[21], *i.e.*, to maximize the preparation of material of a defined purity per unit time. In this context, it is usually advantageous to use pre-fractionation procedures[22] or temperature programming. In principle, this approach should also be followed in preparative work using capillary columns. In fact, it is even more important here, considering the very limited sample capacity of capillary columns. Therefore, the strategy for the isolation of a compound from a complex mixture should include an extensive pre-fractionation on high-capacity systems (LC columns, packed GC columns).

However, in many situations, the total amount of available sample is limited to a few milligrams or less (*e.g.*, flavour concentrates, pheromone isolates, gland extracts). The collection of such material is usually a laborious procedure, and the preparation of substantially larger amounts involves an unreasonable amount of work or is simply not possible. Thus, the risk for losses due to sample work-up, adsorption, etc., must be reduced to a minimum, which largely prohibits the use of classical pre-fractionation methods. In such instances, preparative capillary GC has a unique potential.

Usually, it is desirable to isolate as many components as possible when dealing with limited amounts of important isolates, and a one-step preparative fractionation using an inert capillary column may be the preferred approach. If only a few target compounds are to be isolated, a preparative pre-separation on a capillary column with a different stationary phase may be advantageous. Column choice and optimization of microfractionation is a complex procedure, where many factors such as volatility, polarity and available amounts of starting material must be taken into consideration. In a forthcoming paper in this series, this subject will be considered in more detail.

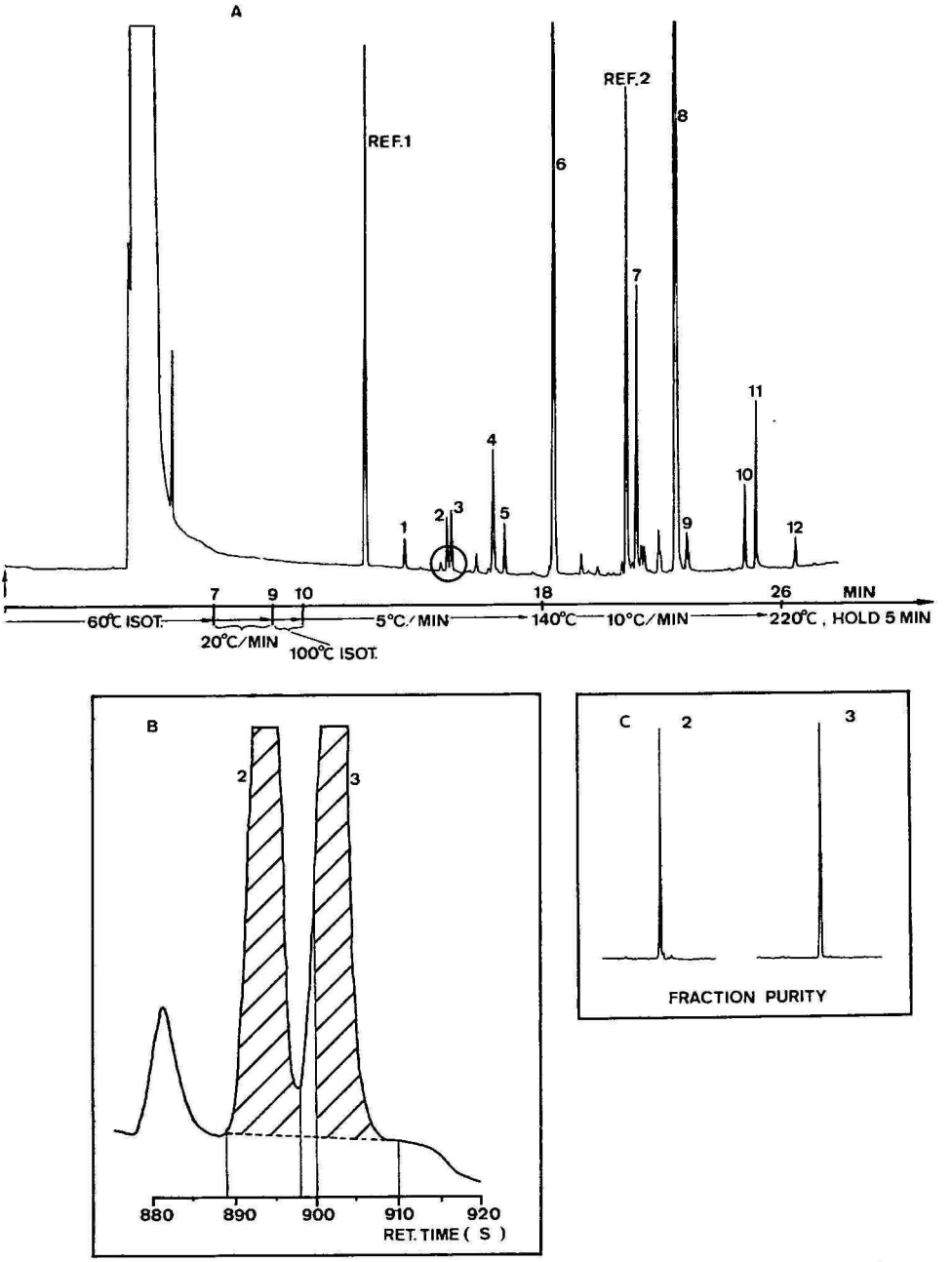

Fig. 6. (A) High-resolution preparative separation of the essential oil of Paraguay Petit Grain. The compounds collected are numbered 1–12. Nonane and dodecene (refs. 1 and 2) were added to the sample (125 μg/ml) and served as reference compounds for the retention synchronization. Chromatographic conditions: sample concentration, 1 mg/ml in hexane; injection, splitless, 1 μl; column, 50 m × 0.31 mm I.D., SE-54, 0.5 μm, cross-linked; carrier gas, nitrogen, head pressure, 100 kPa; time window for the reference peaks, 40 s; maximum allowed height variation of the reference peaks, 50%. (B) Enlargement of the encircled area around peaks 2 and 3. The hatched regions represent the areas of fraction collection, as defined in the stored reference chromatogram. (C) Chromatograms of compounds 2 and 3 after 76 repetitive collections.

System performance

In order to evaluate the performance of the control system, a direct fractionation of a complex mixture (the essential oil of Paraguay Petit-Grain) was carried out. Twelve components from this mixture were isolated from 76 repetitive automatic separations under temperature-programmed condition. A representative gas chromatogram and the corresponding operating conditions are shown in Fig. 6A.

Nonane and dodecene were used as reference compounds for the synchronization of the process. The setting of the identification windows employed allowed a maximum retention shift of 10 s in the forward or backward direction. The maximum drift observed was 4.5 s. The peak-height variations were not more than 30% from run to run. Hence faultless tracking of the reference peaks occurred. The retention correction was accomplished with a trapping precision of *ca.* 0.2 s, as could be observed from the event marks in the chromatograms. Fig. 6B shows an enlargement of the lower area around two closely spaced peaks (2 and 3). As can be seen, a drift of a few seconds would have caused appreciable cross-contamination. On comparing the chromatograms of the collected material (Fig. 6C) with the set points for the fractionation (Fig. 6B), an excellent correspondence in expected fraction purity is observed, which confirms the observed trapping accuracy.

It should be mentioned that the fractions collected were found to contain small amounts of impurities of a wide volatility range. The origin of this material is not known. It is possible that the fractions were contaminated during handling, transfer or re-injection, or that the impurities stem from the solvents employed. Another

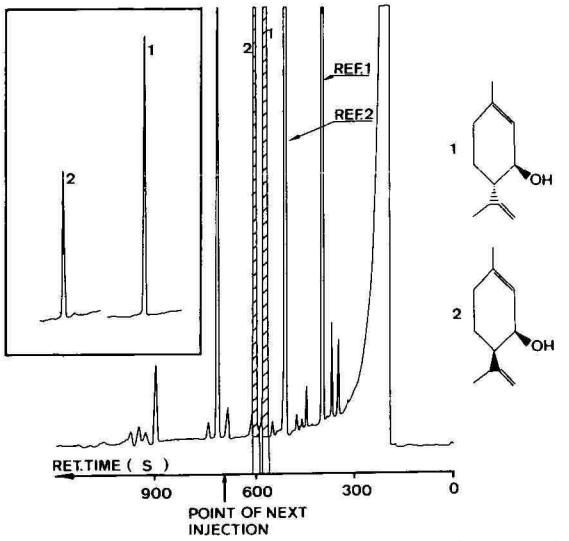

Fig. 7. Chromatogram of an automated preparative separation of *trans*- and *cis*-isopiperitenol. Undecane and dodecane (refs. 1 and 2) were used as reference compounds for the retention synchronization. Chromatographic conditions: column, glass capillary 25 m × 0.3 mm I.D.; film thickness 2 μm; stationary phase, SE-54, cross-linked; column temperature, 180°C, isothermal; carrier gas nitrogen; inlet pressure, 35 kPa; injection, 3 μl; split, 1:10 of a solution in hexane (this corresponds to a column load of 8 and 2 μg of components 1 and 2, respectively). The interspersed chromatograms depicted on the left-hand side show the purity of the fractions after 796 repeated collections.

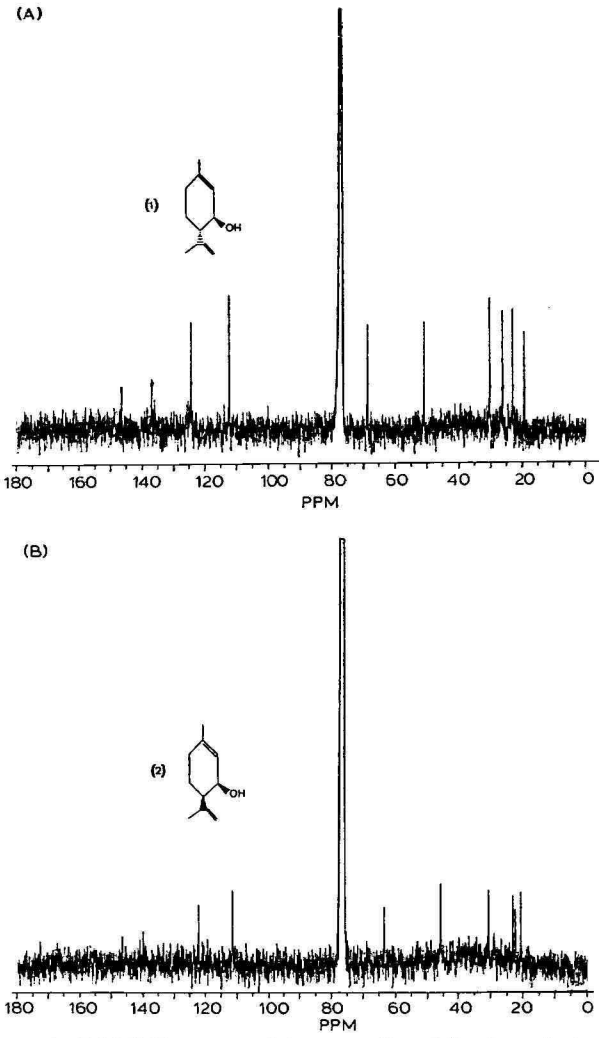

Fig. 8. ^{13}C NMR spectra of the two collected fractions. Instrument: Jeol GX-400; sample tube, 5 mm diameter; solvent, $CDCl_3$. (A) 6500 scans; (B) 25 000 scans.

problem concerns the sample recovery, which never exceeded 80%. This may be due to inefficient trapping, but could also be caused by losses in the injection system or during sample transfer. Both questions are at present being studied in detail.

Long-term collection

An additional experiment was undertaken to evaluate the long-term performance of the control system. Two isomers of isopiperitenol, obtained in a mixture from a synthesis, were subjected to automatic preparative fractionation. Two hydrocarbons (undecane and dodecane) were added to serve as references for the time synchronization. A chromatogram of the mixture and the corresponding chromatographic conditions are shown in Fig. 7. Optimization of the cycle time was accom-

plished by injecting the sample during the elution of the preceding injected material.

The average drift during the collection period was about 1 s. The maximum retention time deviation during a run from the nearly 800 unattended cycles proved to be 6 s, which demonstrates the need for the time correction system. Faultless tracking was observed throughout the experiment, and the collected material had the expected high purity. The extended preparative fractionation afforded several milligrams of the pure isomers, sufficient for ^{13}C NMR spectroscopy. Fig. 8 shows the spectra of both fractions. As can be seen, all the carbon atoms of the monoterpene structure can be assigned. The spectroscopic data obtained are at present being used in a structural study of the isomers.

CONCLUSIONS

The real-time retention correction system described provides an accurate and versatile means of control for automated preparative capillary GC. The automatic protection for collection errors allows reliable and unattended operation under extended periods. This opens up new opportunities for the straightforward isolation of trace components from complex mixtures, and makes it possible to obtain ^{1}H NMR or ^{13}C NMR spectral data for such components.

There should be several other applications of the described system, such as the control of multi-dimensional column switching or on-column trace enrichment and for preparative HPLC.

ACKNOWLEDGEMENTS

We are indebted to Dr. U. Jacobsson and Dr. L. Kenne for recording the NMR spectra. This work was financially supported by the Swedish National Research Council and the Swedish Board of Technical Development.

REFERENCES

1 H. T. Badings, J. J. van der Pol and J. G. Wassink, *Chromatographia*, 8 (1975) 440.
2 E. Gelpi, P. C. Wszolek, E. Yang and A. L. Burlingame, *J. Chromatogr. Sci.*, 9 (1971) 147.
3 P. Sandra, T. Saeed, G. Redant, M. Godefroot, M. Verstappe and M. Verzele, *J. High Resolut. Chromatogr. Chromatogr. Commun.*, 3 (1980) 107.
4 W. J. Williams, S. Vinson and J. Bradleigh, *J. Chem. Ecol.*, 6 (1980) 973.
5 B. V. Burger and Z. Munro, *J. Chromatogr.*, 262 (1983) 95.
6 J. Roeraade and C. R. Enzell, *J. High Resolut. Chromatogr. Chromatogr. Commun.*, 2 (1979) 123.
7 I. Klimes, W. Stünzi and D. Lamparsky, *J. Chromatogr.*, 136 (1977) 23.
8 R. Teranishi, R. A. Flath, K. L. Stevens and T. R. Mon, *J. Gas Chromatogr.*, 3 (1965) 206.
9 R. G. Clark and D. A. Cronin, *J. Sci. Food Agric.*, 26 (1975) 1009.
10 T. H. Parliment, *Anal. Chem.*, 45 (1973) 1792.
11 P. Sandra, M. Schelfaut and M. Verzele, *J. High Resolut. Chromatogr. Chromatogr. Commun.*, 6 (1983) 561.
12 J. Roeraade, S. Blomberg and G. Flodberg, *J. Chromatogr.*, 301 (1984) 454.
13 K. Grob, G. Grob, W. Blum and W. Walther, *J. Chromatogr.*, 244 (1982) 197.
14 S. R. Springston, K. Melda and M. V. Novotný, *J. Chromatogr.*, 267 (1983) 395.
15 H. Abegg, *J. Chromatogr.*, 25 (1966) 198.
16 T. H. Parliment, *J. Chromatogr.*, 58 (1971) 283.
17 *Publication No. 299366*, Pye Unicam, Cambridge, U.K.
18 V. E. Burton, T. R. Orr, A. M. Brearly and M. A. Kaiser, *Anal. Instrum.*, 13 (1984) 205.
19 K. P. Hupe, *J. Gas Chromatogr.*, 3 (1965) 92.
20 B. Roz, R. Bonmati, G. Hagenbach, P. Valentin and G. Guiochon, *J. Chromatogr. Sci.*, 14 (1976) 367.
21 V. Pretorius and K. de Clerk, in A. Zlatkis and V. Pretorius (Editors), *Preparative Gas Chromatography*, Interscience, New York, 1971, p. 1–51.
22 G. Schomburg, H. Kötter, D. Stoffels and W. Reissig, *Chromatographia*, 19 (1984) 382.

Journal of Chromatography, 356 (1986) 285–299
Elsevier Science Publishers B.V., Amsterdam — Printed in The Netherlands

CHROM. 18 399

GAS–LIQUID CHROMATOGRAPHIC ANALYSES

XLV*. RETENTION BEHAVIOUR OF C_1–C_{12} *n*-ALKYL ESTERS OF BENZOIC, 4-NITROBENZOIC AND 3,5-DINITROBENZOIC ACIDS ON SE-30 AND OV-351 CAPILLARY COLUMNS

ILPO O. O. KORHONEN
Department of Chemistry, University of Jyväskylä, Kyllikinkatu 1–3, SF-40100 Jyväskylä 10 (Finland)
(Received November 25th, 1985)

SUMMARY

The gas chromatographic separation of a mixture of C_1–C_{12} *n*-alkyl esters of benzoic, 4-nitrobenzoic and 3,5-dinitrobenzoic acids was studied on low-polarity (SE-30) and polar (OV-351) capillary columns under isothermal and temperature-programmed operating conditions. The relative retention data, the Kováts retention indices and the retention index increments for the methylene units and the nitro substituents were determined and the separation of the mixture is discussed. The results are compared with those reported earlier for aromatic esters.

INTRODUCTION

In contrast to aliphatic esters, there have been few studies on the gas chromatographic (GC) retention behaviour of aromatic esters[1], and most frequently they have concerned the GC of halogenated esters with substitution in either the acid[1–6] or the alcohol[4,7–12] moiety.

Nitrobenzoic acid isomers have been primarily analysed by using thin-layer[13,14], ion-exchange[15,16] or high-performance liquid chromatography[17]. GC on graphitized thermal carbon black has been used for the isomeric mononitrobenzoic acids[18] and packed columns coated with silicone oil[19] and five other stationary phases, *viz.*, Apiezon L, dodecyl dibenzoate and dodecyl 2-, 3- and 4-nitrobenzoate isomers[20] for the methyl esters. Higher esters, *viz.*, C_1–C_6 4-nitrobenzoates[21] and C_1–C_{10} 3,5-dinitrobenzoates[22], have been separated on low-polarity SE-30 and OV-17 packed columns, the purpose of these studies being to identify lower alkanols in the complex mixture as their nitrobenzoyl derivatives rather than a systematic GC study of the corresponding esters.

This paper describes the isothermal and temperature-programmed capillary GC of C_1–C_{12} *n*-alkyl esters of benzoic, 4-nitrobenzoic and 3,5-dinitrobenzoic acids

* For Part XLIV, see ref. 6.

0021-9673/86/$03.50

on low-polarity (SE-30) and highly polar (OV-351) stationary phases. The relative retentions and the Kováts retention indices of all 36 individual components in the three homologous series were determined and examined, together with the effects of alkyl chain length and acyl nitro substitution, shown by retention index increments. The results are compared with those reported earlier for aromatic esters[1,20–22].

EXPERIMENTAL

Materials

n-Alkyl benzoates (1–12), 4-nitrobenzoates (m1–m12) and 3,5-dinitrobenzoates (d1–d12) were synthesized from the C_1–C_{12} *n*-alkanols (Fluka, Buchs, Switzerland) and acid chlorides (Merck-Schuchart, Darmstadt, F.R.G.) as described earlier[23]. The mixture analysed contained suitable amounts of the individual components for the sensitivity of the flame ionization detector.

Mixtures of *n*-alkanes were obtained from different commercial sources.

Methods

GC analyses were carried out on a Perkin-Elmer Sigma 3 gas chromatograph under the following operating conditions: injection and flame-ionization detection (FID) temperatures, 280°C; nitrogen carrier gas velocities for methane at 180°C, 28.2 (SE-30) and 61.3 cm s^{-1} (OV-351); splitting ratio, 1:30; and chart speed, 10 mm min^{-1}. The columns used were a vitreous silica SE-30 wall-coated open-tubular (WCOT) column (25 m × 0.33 mm I.D.), supplied by SGE (North Melbourne, Australia), and a fused silica OV-351 WCOT column (25 m × 0.32 mm I.D.), supplied by Orion Analytica (Espoo, Finland). The column temperature was programmed from 100 to 310°C (SE-30) and from 100 to 220°C (OV-351) at 6°C min^{-1} and held on OV-351 at 220°C until elution of peaks had ceased. The isothermal data were determined at the temperatures indicated in Tables II and III.

The chromatographic data were recorded with a Hewlett-Packard Model 3390A reporting integrator using standard programs. The retention times were measured from the time of sample injection and the Kováts retention indices were calculated off-line by using two appropriate *n*-alkanes[24]; the dead volume was determined by the injection of methane. Owing to the incomplete resolution of a complex mixture of all compounds, each of the three groups of esters and *n*-alkanes were chromatographed separately in turn.

RESULTS AND DISCUSSION

Chromatograms of a mixture of C_1–C_{12} *n*-alkyl benzoates (1–12), 4-nitrobenzoates (m1–m12) and 3,5-dinitrobenzoates (d1–d12) are illustrated in Figs. 1 and 2, separated on SE-30 and OV-351 with temperature programming, respectively. The corresponding retention data of the compounds are given in Table I.

Fig. 1 shows a relatively good separation of the individual components in the mixture on the low-polarity SE-30 column. The elution order observed is C_{n-6}-alkyl 3,5-dinitrobenzoate < C_n-alkyl benzoate < C_{n-3}-alkyl 4-nitrobenzoate. Methyl 3,5-dinitrobenzoate (d1) is a diverging compound in this respect, eluting later than heptyl benzoate (7) and overlapping partly with butyl 4-nitrobenzoate (m4). Partially

TABLE I

RETENTION DATA FOR C_1–C_{12} *n*-ALKYL ESTERS OF BENZOIC, 4-NITROBENZOIC AND 3,5-DINITROBENZOIC ACIDS, DETERMINED ON SE-30 AND OV-351 CAPILLARY COLUMNS WITH TEMPERATURE PROGRAMMING

Conditions as in Figs. 1 and 2.

Peak No.	*Compound*	*Column*						
		SE-30			*OV-351*			
		*ART**	*RRT***	*RRT****	*ART**	*RRT***	*RRT****	*RRT*§
1	Methyl benzoate	3.37	0.41	1.00	3.62	1.98	1.00	1.07
2	Ethyl benzoate	4.20	0.51	1.00	4.13	2.26	1.00	0.98
3	Propyl benzoate	5.64	0.69	1.00	5.26	2.87	1.00	0.93
4	Butyl benzoate	7.35	0.90	1.00	6.70	3.66	1.00	0.91
5	Pentyl benzoate	9.21	1.13	1.00	8.22	4.49	1.00	0.89
6	Hexyl benzoate	11.02	1.35	1.00	9.84	5.38	1.00	0.89
7	Heptyl benzoate	12.91	1.58	1.00	11.51	6.29	1.00	0.89
8	Octyl benzoate	14.83	1.81	1.00	13.18	7.20	1.00	0.89
9	Nonyl benzoate	16.62	2.03	1.00	14.80	8.09	1.00	0.89
10	Decyl benzoate	18.40	2.25	1.00	16.32	8.92	1.00	0.89
11	Undecyl benzoate	20.08	2.45	1.00	17.80	9.73	1.00	0.89
12	Dodecyl benzoate	21.70	2.65	1.00	19.28	10.54	1.00	0.89
m1	Methyl 4-nitrobenzoate	8.61	1.05	2.55	13.02	7.11	3.60	1.51
m2	Ethyl 4-nitrobenzoate	9.99	1.22	2.38	13.46	7.36	3.26	1.35
m3	Propyl 4-nitrobenzoate	11.84	1.45	2.10	14.76	8.07	2.81	1.25
m4	Butyl 4-nitrobenzoate	13.76	1.68	1.87	16.30	8.91	2.43	1.18
m5	Pentyl 4-nitrobenzoate	15.65	1.91	1.70	17.78	9.72	2.16	1.14
m6	Hexyl 4-nitrobenzoate	17.49	2.14	1.59	19.23	10.51	1.95	1.10
m7	Heptyl 4-nitrobenzoate	19.23	2.35	1.49	20.73	11.33	1.80	1.08
m8	Octyl 4-nitrobenzoate	20.91	2.56	1.41	22.54	12.32	1.71	1.08
m9	Nonyl 4-nitrobenzoate	22.53	2.75	1.36	24.78	13.54	1.67	1.10
m10	Decyl 4-nitrobenzoate	24.08	2.94	1.31	27.61	15.09	1.69	1.15
m11	Undecyl 4-nitrobenzoate	25.58	3.13	1.27	31.31	17.11	1.76	1.22
m12	Dodecyl 4-nitrobenzoate	27.01	3.30	1.24	36.14	19.75	1.87	1.34
d1	Methyl 3,5-dinitrobenzoate	13.63	1.67	4.04	20.04	10.95	5.54	1.47
d2	Ethyl 3,5-dinitrobenzoate	14.80	1.81	3.52	20.10	10.98	4.87	1.36
d3	Propyl 3,5-dinitrobenzoate	16.51	2.02	2.93	20.77	11.35	3.95	1.26
d4	Butyl 3,5-dinitrobenzoate	18.27	2.23	2.49	22.40	12.24	3.34	1.23
d5	Pentyl 3,5-dinitrobenzoate	19.91	2.43	2.16	24.36	13.31	2.96	1.22
d6	Hexyl 3,5-dinitrobenzoate	21.54	2.63	1.95	26.87	14.68	2.73	1.25
d7	Heptyl 3,5-dinitrobenzoate	23.11	2.83	1.79	30.21	16.51	2.62	1.31
d8	Octyl 3,5-dinitrobenzoate	24.59	3.01	1.66	34.60	18.91	2.63	1.41
d9	Nonyl 3,5-dinitrobenzoate	26.04	3.18	1.57	40.15	21.94	2.71	1.54
d10	Decyl 3,5-dinitrobenzoate	27.41	3.35	1.49	47.50	25.96	2.91	1.73
d11	Undecyl 3,5-dinitrobenzoate	28.74	3.51	1.43	56.90	31.09	3.20	1.98
d12	Dodecyl 3,5-dinitrobenzoate	30.05	3.67	1.38	69.22	37.83	3.59	2.30
C_{14}	*n*-Tetradecane	8.18	1.00	–	1.83	1.00	–	0.22

* Absolute retention times (min) were measured from the time of sample injection (Figs. 1 and 2).

** Relative retention time for *n*-tetradecane (C_{14}) taken as 1.00.

*** Relative retention time for the corresponding *n*-alkyl benzoate (1–12) taken as 1.00.

§ Relative retention time for the corresponding compound on SE-30 taken as 1.00.

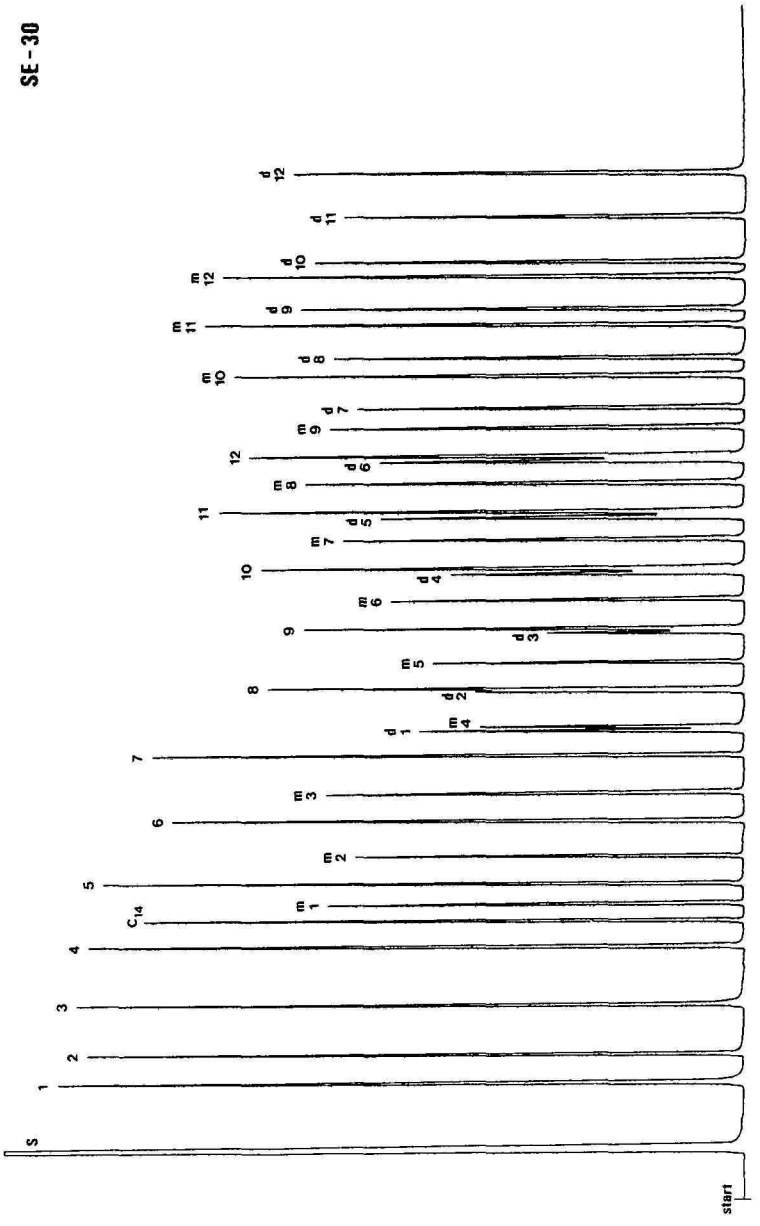

Fig. 1. Chromatogram of a mixture of C_1–C_{12} *n*-alkyl esters of benzoic (1–12), 4-nitrobenzoic (m1–m12) and 3,5-dinitrobenzoic (d1–d12) acids, separated on an SE-30 quartz capillary column with temperature programming from 100 to 310°C at 6°C min^{-1}. S = Solvent; C_{14} = *n*-tetradecane; m = mono-; d = di-; number = alkyl chain length.

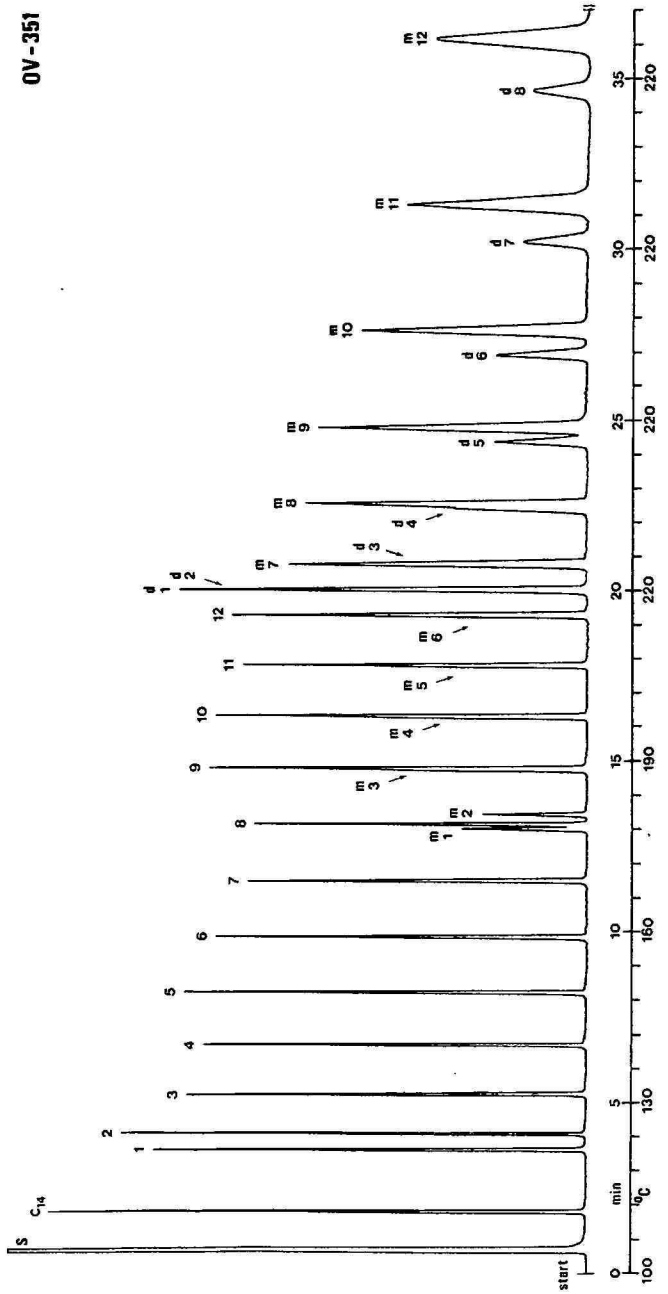

Fig. 2. Chromatogram of the same mixture as in Fig. 1, separated on an OV-351 quartz capillary column with temperature programming from 100 to 220°C at 6°C min^{-1} and held at the final temperature until elution of peaks had ceased. S = Solvent; C_{14} = *n*-tetradecane; m = mono-; d = di-; number = alkyl chain length.

TABLE II

RETENTION INDICES (I) FOR C_1–C_{12} *n*-ALKYL ESTERS OF BENZOIC, 4-NITROBENZOIC AND 3,5-DINITROBENZOIC ACIDS, DETERMINED ON SE-30 CAPILLARY COLUMN AT A VARIETY OF TEMPERATURES

n-Alkyl ester	*Chain length*	*Column (SE-30) temperature*						
		Programmed from 100 to 310°C at 6°C min^{-1}		*Isothermal*				
				160°C	*180°C*	*200°C*	*220°C*	*240°C*
		I	*E.T. (°C)**	*I*	*I*	*I*	*I*	*I*
Benzoate	C_1	1071	120.2	1067	1064	1063	–	–
	C_2	1145	125.2	1144	1142	1142	–	–
	C_3	1249	133.8	1249	1248	1248	1262	–
	C_4	1353	144.1	1356	1352	1353	1360	1386
	C_5	1455	155.3	1458	1454	1455	1465	1480
	C_6	1551	166.1	1556	1555	1557	1568	1572
	C_7	1651	177.5	1657	1657	1660	1670	1672
	C_8	1757	189.0	1755	1758	1762	1774	1777
	C_9	1860	199.7	1857	1859	1864	1874	1879
	C_{10}	1965	210.4	1957	1959	1964	1977	1981
	C_{11}	2068	220.5	2058	2059	2065	2076	2080
	C_{12}	2173	230.2	2157	2159	2166	2180	2184
4-Nitrobenzoate	C_1	1423	151.6	1432	1427	1449	1440	1411
	C_2	1497	159.9	1500	1501	1511	1522	1527
	C_3	1594	171.0	1600	1602	1612	1625	1636
	C_4	1697	182.6	1700	1704	1715	1727	1738
	C_5	1803	193.9	1799	1805	1817	1829	1839
	C_6	1911	204.9	1900	1907	1917	1930	1939
	C_7	2016	215.4	1999	2007	2018	2031	2039
	C_8	2121	225.5	2101	2108	2120	2131	2140
	C_9	2227	235.2	2200	2208	2220	2232	2241
	C_{10}	2333	244.5	2299	2308	2321	2333	2342
	C_{11}	2443	253.5	–	2408	2421	2435	2444
	C_{12}	2550	262.1	–	2509	2521	2536	2546
3,5-Dinitrobenzoate	C_1	1690	181.8	1694	1701	1714	1724	1745
	C_2	1755	188.8	1757	1760	1767	1781	1810
	C_3	1853	199.1	1846	1853	1860	1874	1892
	C_4	1957	209.6	1942	1950	1959	1975	1985
	C_5	2058	219.5	2039	2047	2058	2074	2083
	C_6	2162	229.2	2138	2146	2157	2173	2182
	C_7	2266	238.7	2236	2244	2256	2269	2281
	C_8	2370	247.5	–	2343	2355	2368	2380
	C_9	2476	256.2	–	2442	2454	2467	2478
	C_{10}	2581	264.5	–	2541	2552	2564	2578
	C_{11}	2686	272.4	–	–	2651	2663	2677
	C_{12}	2791	280.3	–	–	2750	2764	2777

* E.T. = Elution temperature.

TABLE III

RETENTION INDICES (I) FOR C_1–C_{12} *n*-ALKYL ESTERS OF BENZOIC, 4-NITROBENZOIC AND 3,5-DINITROBENZOIC ACIDS, DETERMINED ON OV-351 CAPILLARY COLUMN AT A VARIETY OF TEMPERATURES

n-Alkyl ester	*Chain length*	*Column (OV-351) temperature*					$I_{OV\text{-}351} - I_{SE\text{-}30}$** *(programmed)*
		Programmed from 100 to 220°C at 6°C min⁻¹		*Isothermal*			
				180°C	*200°C*	*220°C*	
		I	*E.T. (°C)**	*I*	*I*	*I*	
Benzoate	C_1	1612	121.7	1661	–	–	541
	C_2	1655	124.8	1706	–	–	510
	C_3	1742	131.6	1791	1812	–	493
	C_4	1841	140.2	1879	1901	–	488
	C_5	1943	149.3	1971	2000	1999	488
	C_6	2046	159.0	2069	2097	2093	495
	C_7	2151	169.1	2169	2198	2199	500
	C_8	2258	179.1	2270	2298	2300	501
	C_9	2366	188.8	2372	2400	2400	512
	C_{10}	2473	197.9	2474	2500	2504	508
	C_{11}	2583	206.8	2578	2601	2606	515
	C_{12}	2694	215.7	2681	2701	2708	521
4-Nitrobenzoate	C_1	2250	178.1	2273	2314	2314	827
	C_2	2280	180.8	2298	2334	2343	783
	C_3	2367	188.6	2376	2414	2426	773
	C_4	2474	197.8	2472	2511	2524	777
	C_5	2582	206.7	2572	2606	2620	779
	C_6	2689	215.4	2671	2704	2719	778
	C_7	2800	220.0	2771	2806	2824	784
	C_8	2911	220.0	2874	2910	2926	790
	C_9	3021	220.0	2979	3014	3029	794
	C_{10}	3130	220.0	3082	3117	3131	797
	C_{11}	3235	220.0	3185	3220	3235	792
	C_{12}	3342	220.0	3288	3326	3341	792
3,5-Dinitrobenzoate	C_1	2749	220.0	2729	2762	2780	1059
	C_2	2753	220.0	2739	2764	2781	998
	C_3	2803	220.0	2784	2809	2826	950
	C_4	2906	220.0	2873	2898	2915	949
	C_5	3007	220.0	2969	2993	3007	949
	C_6	3108	220.0	3067	3089	3103	946
	C_7	3210	220.0	3164	3189	3205	944
	C_8	3313	220.0	3265	3288	3305	943
	C_9	3413	220.0	3367	3390	3406	937
	C_{10}	3515	220.0	3469	3490	3505	934
	C_{11}	3616	220.0	–	3589	3605	930
	C_{12}	3719	220.0	–	3690	3708	928

* E.T. = Elution temperature.

** For the retention indices on SE-30, see Table II.

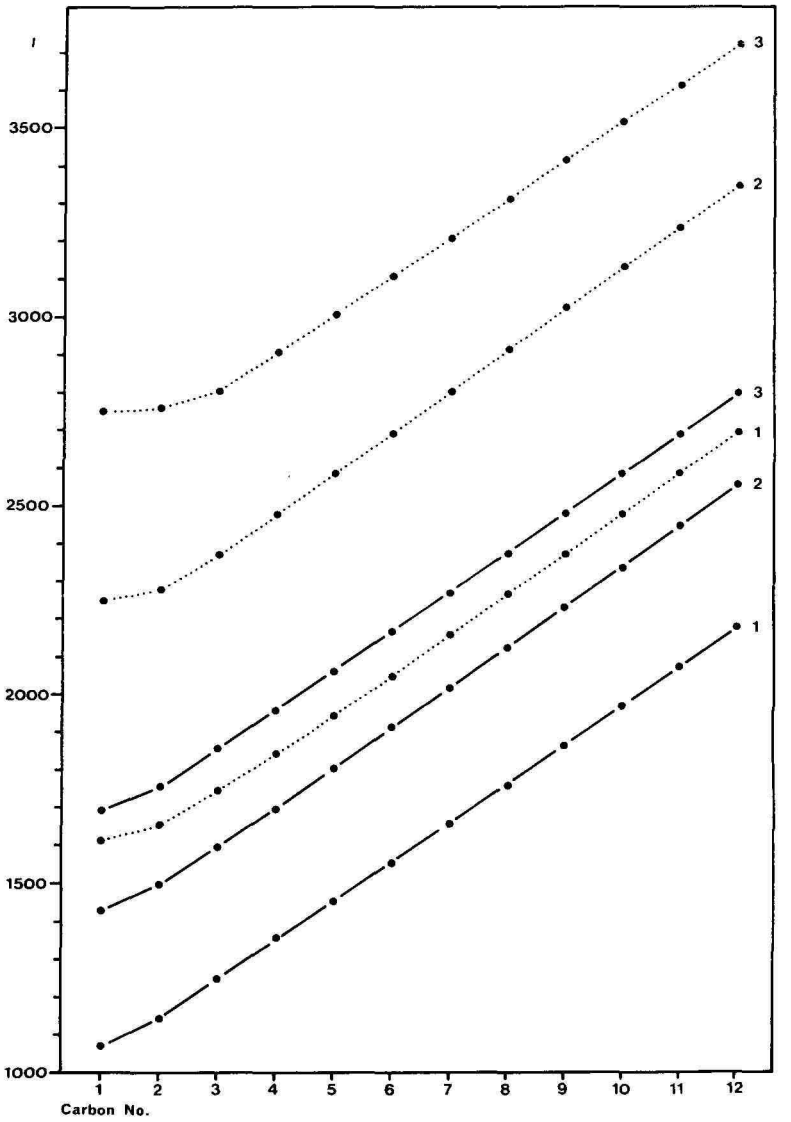

Fig. 3. Plot showing retention of C_1–C_{12} *n*-alkyl esters of benzoic (curve 1), 4-nitrobenzoic (curve 2) and 3,5-dinitrobenzoic (curve 3) acids, obtained on SE-30 (solid lines) and OV-351 (dotted lines) capillary columns with temperature programming (Figs. 1 and 2). *I* = Retention index units.

resolved peaks are also observed for the closely related 3,5-dinitrobenzoates (d2–d6) and benzoates (8–12). As would be expected, the retention order of the compounds is the same as on the packed column[21,22].

The analysis time of the mixture on OV-351 is more than double that on SE-30 in spite of the greatly increased carrier gas velocity used (Fig. 2). This is due to the polar column and the low thermal stability of the stationary phase. The retentions of the nitro isomers are markedly increased, the mixture showing the following elu-

tion orders: C_{n-6}-alkyl 4-nitrobenzoate $\leqslant C_n$-alkyl benzoate ($n \geqslant 9$) and C_{n-4}-alkyl 3,5-dinitrobenzoate $< C_n$-alkyl 4-nitrobenzoate ($n \geqslant 8$). The overlapping that occurred is more pronounced on OV-351 than on SE-30 and the peak shapes are broadened (but symmetrical) particularly with the 3,5-dinitro isomers (Fig. 2).

The retention indices of the compounds are shown in Tables II and III, determined on SE-30 and OV-351 at a variety of temperatures, respectively. Plots of the retention of the three homologous series on both phases are illustrated in Fig. 3. Tables IV and V give the incremental effects for the methylene units and the nitro substitution. A summary and correlation of the increments with the values for the corresponding 4-chloro esters[1] and a comparison between the highly polar and low-polarity columns are shown in Table VI.

The retention behaviour of methyl 4-nitrobenzoate on the SE-30 capillary column is in good agreement with that reported previously on a packed column coated with Apiezon L[20]; values for the higher esters and the 3,5-dinitro isomers, however, are not available.

The increased retention values on OV-351 with respect to SE-30 are shown in Table III, these being markedly higher than observed previously for the corresponding chlorinated esters[1], *viz.*, 773–827 retention index units (i.u.) with *n*-alkyl 4-nitrobenzoates and 928–1059 i.u. with *n*-alkyl 3,5-dinitrobenzoates.

As usual, the retention index increments for the methylene groups on both columns are close to 100 i.u., the temperature-programmed runs showing higher increments than the isothermal runs. The nitro substitution in the acid group seems to have a greater effect on the alkyl chain, as found previously with chlorine substitution[1], *i.e.*, the average increment for the 4-nitro isomers on both columns with isothermal runs is 101 i.u., decreasing to 98 i.u. with the 3,5-dinitro isomers (Tables IV and V). The greatest disparity (6 i.u.) between the nitro derivatives is shown on OV-351 with temperature programming.

The incremental effects of the nitro substitution shown in Tables IV (SE-30), V (OV-351) and VI (summary) are highest with the temperature-programmed runs. On SE-30 the average retention enhancement due to the 4-nitro substitution at 180°C is 351 i.u., which is markedly higher than with the corresponding 4-chloro esters (159 i.u.)[1], but lower than with nitrated polynuclear aromatic hydrocarbons (nitro-PAHs)[25]. On OV-351 the increment is increased to 602 i.u. (187 i.u.), with the value for the 4-chloro isomers[1] given in parentheses.

The retention enhancements due to the 3,5-dinitro substitution are further increased, *viz.*, to 594 i.u. on SE-30 and to 1006 i.u. on OV-351. The increase per nitro substituent, however, is lower than that with the 4-nitro isomers, being in agreement with the chlorine substitution in several aromatic series studied previously[9,10,26,27].

The retention increment ratios between the highly polar and low-polarity columns shown in Table VI indicate that the polar effects are maximal (1.72) with the 4-nitro isomers, although the disparity between the two groups of the esters investigated is negligible. The corresponding ratio with the 4-chloro isomers is markedly lower (1.18), but that of the most polar 2-chloro isomers is of the same magnitude, *viz.*, 1.68[1].

TABLE IV

INCREMENTAL EFFECTS FOR METHYLENE UNITS AND NITRO SUBSTITUTION ON SE-30 AT VARIOUS COLUMN TEMPERATURES

n-Alkyl ester	*Chain length*	*Column (SE-30) temperature*								
		Programmed from 100 to 310°C at 6°C min^{-1}			*Isothermal*					
					180°C			*200°C*		
		ΔI_{CH_2}	$\Sigma\Delta I_{nNO_2}^{*}$	$\Delta I_{1NO_2}^{**}$	ΔI_{CH_2}	$\Sigma\Delta I_{nNO_2}^{*}$	$\Delta I_{1NO_2}^{**}$	ΔI_{CH_2}	$\Sigma\Delta I_{nNO_2}^{*}$	$\Delta I_{1NO_2}^{**}$
Benzoate	C_1	–			–			–		
	C_2	74[§]			78[§]			79[§]		
	C_3	104			106			106		
	C_4	104			104			105		
	C_5	102			102			102		
	C_6	96			101			102		
	C_7	100			102			103		
	C_8	106			101			102		
	C_9	103			101			102		
	C_{10}	105			100			100		
	C_{11}	103			100			101		
	C_{12}	105			100			101		
	C_1–C_{12}	103***			102***			102***		

4-Nitrobenzoate	C_1	–	352	352	–	363§	363§	–	386§	386§
	C_2	74§	352	352	74§	359	359	62§	369	369
	C_3	97	345	345	101	354	354	101	364	364
	C_4	103	344	344	102	352	352	103	362	362
	C_5	106	348	348	101	351	351	102	362	362
	C_6	108	360	360	102	352	352	100	360	360
	C_7	105	365	365	100	350	350	101	358	358
	C_8	105	364	364	101	350	350	102	358	358
	C_9	106	367	367	100	349	349	100	356	356
	C_{10}	106	368	368	100	349	349	101	357	357
	C_{11}	110	375	375	100	349	349	100	356	356
	C_{12}	107	377	377	101	350	350	100	355	355
	C_1–C_{12}	105***	360***	360***	101***	351***	351***	101***	360***	360***
3,5-Dinitrobenzoate	C_1	–	619	310	–	637§	319§	–	651§	326§
	C_2	65§	610	305	59§	618	309	53§	625	313
	C_3	98	604	302	93	605	303	93	612	306
	C_4	104	604	302	97	598	299	99	606	303
	C_5	101	603	302	97	593	297	99	603	302
	C_6	104	611	306	99	591	296	99	600	300
	C_7	104	615	308	98	587	294	99	596	298
	C_8	104	613	307	99	585	293	99	593	297
	C_9	106	616	308	99	583	292	99	590	295
	C_{10}	105	616	308	99	582	291	98	588	294
	C_{11}	105	618	309	–	–	–	99	586	293
	C_{12}	105	618	309	–	–	–	99	584	292
	C_1–C_{12}	104***	612***	306***	98***	594***	297***	98***	598***	299***

* Total retention index increase.
** Retention index increase per nitro group.
*** Average value.
§ Not included in average values.

TABLE V

INCREMENTAL EFFECTS FOR METHYLENE UNITS AND NITRO SUBSTITUTION ON OV-351 AT VARIOUS COLUMN TEMPERATURES

n-Alkyl ester	*Chain length*	*Column (OV-351) temperature*								
		Programmed from 100 to 220°C at 6°C min^{-1}			*Isothermal*					
					180°C			*200°C*		
		ΔI_{CH_2}	$\Sigma\Delta I_{nNO_2}^{*}$	$\Delta I_{1NO_2}^{**}$	ΔI_{CH_2}	$\Sigma\Delta I_{nNO_2}^{*}$	$\Delta I_{1NO_2}^{**}$	ΔI_{CH_2}	$\Sigma\Delta I_{nNO_2}^{*}$	$\Delta I_{1NO_2}^{**}$
Benzoate	C_1	–			–			–		
	C_2	43[§]			45[§]			–		
	C_3	87			85			–		
	C_4	99			88			89		
	C_5	102			92			99		
	C_6	103			98			97		
	C_7	105			100			101		
	C_8	107			101			100		
	C_9	108			102			102		
	C_{10}	107			102			100		
	C_{11}	110			104			101		
	C_{12}	111			103			100		
	C_1–C_{12}	104***			98***			99***		

4-Nitrobenzoate	C_1	–	638	638	–	612	612	–	–	–
	C_2	30§	625	625	25§	592	592	20§	–	–
	C_3	87§	625	625	78§	585	585	80§	602	602
	C_4	107	633	633	96	593	593	97	610	610
	C_5	108	639	639	100	601	601	95	606	606
	C_6	107	643	643	99	602	602	98	607	607
	C_7	111	649	649	100	602	602	102	608	608
	C_8	111	653	653	103	604	604	104	612	612
	C_9	110	655	655	105	607	607	104	614	614
	C_{10}	109	657	657	103	608	608	103	617	617
	C_{11}	105	652	652	103	607	607	103	619	619
	C_{12}	107	648	648	103	607	607	106	625	625
	C_1–C_{12}	108***	643***	643***	101***	602***	602***	101***	612***	612***
3,5-Dinitrobenzoate	C_1	–	1137	569	–	1068	534	–	–	–
	C_2	4§	1098	549	10§	1033	517	2§	–	–
	C_3	50§	1061	531	45§	993	497	45§	997	499
	C_4	103	1065	533	89	994	497	89	997	499
	C_5	101	1064	532	96	998	499	95	993	497
	C_6	101	1062	531	98	998	499	96	992	496
	C_7	102	1059	530	97	995	498	100	991	496
	C_8	103	1055	528	101	995	498	99	990	495
	C_9	100	1047	524	102	995	498	102	990	495
	C_{10}	102	1042	521	102	995	498	100	990	495
	C_{11}	101	1033	517	–	–	–	99	988	494
	C_{12}	103	1025	513	–	–	–	101	989	495
	C_1–C_{12}	102***	1062***	531***	98***	1006***	503***	98***	992***	496***

* Total retention index increase.
** Retention index increase per nitro group.
*** Average value.
§ Not included in average values.

TABLE VI

SUMMARY AND CORRELATION BETWEEN RETENTION INCREMENTS OF 4-CHLORO-, 4-NITRO- AND 3,5-DINITROBENZOATES ON SE-30 AND OV-351

*Retention increment**	*Temperature*		
	*Programmed****	*Isothermal*	
		180°C	*200°C*
SE-30			
$\Delta I_{4\text{-Chloro}}$**	166	159	162
$\Delta I_{4\text{-Nitro}}$	360	351	360
$\Delta I_{3,5\text{-Dinitro}}$	612	594	598
$\Delta I_{4\text{-Nitro}} - \Delta I_{4\text{-Chloro}}$	194	192	198
$\Delta I_{3,5\text{-Dinitro}} - \Delta I_{4\text{-Nitro}}$	252	243	238
OV-351			
$\Delta I_{4\text{-Chloro}}$**	197	187	189
$\Delta I_{4\text{-Nitro}}$	643	602	612
$\Delta I_{3,5\text{-Dinitro}}$	1062	1006	992
$\Delta I_{4\text{-Nitro}} - \Delta I_{4\text{-Chloro}}$	446	415	423
$\Delta I_{3,5\text{-Dinitro}} - \Delta I_{4\text{-Nitro}}$	419	404	380
OV-351/SE-30			
$\Delta I_{4\text{-Chloro}}$**	1.19	1.18	1.17
$\Delta I_{4\text{-Nitro}}$	1.79	1.72	1.70
$\Delta I_{3,5\text{-Dinitro}}$	1.74	1.69	1.66
$\Delta I_{4\text{-Nitro}} - \Delta I_{4\text{-Chloro}}$	2.30	2.16	2.14
$\Delta I_{3,5\text{-Dinitro}} - \Delta I_{4\text{-Nitro}}$	1.66	1.66	1.60
OV-351 − SE-30			
$\Delta I_{4\text{-Chloro}}$**	31	28	27
$\Delta I_{4\text{-Nitro}}$	283	251	252
$\Delta I_{3,5\text{-Dinitro}}$	450	412	394
$\Delta I_{4\text{-Nitro}} - \Delta I_{4\text{-Chloro}}$	252	223	225
$\Delta I_{3,5\text{-Dinitro}} - \Delta I_{4\text{-Nitro}}$	167	161	142

* From Tables IV and V.
** From ref. 1.
*** Under conditions shown in Figs. 1 and 2 and ref. 1.

ACKNOWLEDGEMENTS

The author thanks the Ellen and Artturi Nyyssönen Foundation and the OL-VI-Foundation for grants.

REFERENCES

1 I. O. O. Korhonen and M. A. Lind, *J. Chromatogr.*, 322 (1985) 83; and references cited therein.
2 I. O. O. Korhonen and M. A. Lind, *J. Chromatogr.*, 323 (1985) 331.
3 I. O. O. Korhonen and M. A. Lind, *J. Chromatogr.*, 324 (1985) 113.
4 I. O. O. Korhonen and M. A. Lind, *J. Chromatogr.*, 325 (1985) 433.
5 I. O. O. Korhonen and M. A. Lind, *J. Chromatogr.*, 328 (1985) 325.
6 I. O. O. Korhonen, *J. Chromatogr.*, 329 (1985) 359.
7 I. O. O. Korhonen and J. Knuutinen, *J. Chromatogr.*, 256 (1983) 135; and references cited therein.
8 J. Knuutinen and I. O. O. Korhonen, *J. Chromatogr.*, 257 (1983) 127.

9 J. K. Haken and I. O. O. Korhonen, *J. Chromatogr.*, 257 (1983) 267.
10 I. O. O. Korhonen, *J. Chromatogr.*, 321 (1985) 115.
11 J. Knuutinen and E. Kolehmainen, *Chromatographia*, 15 (1982) 707.
12 J. Knuutinen, E. Kolehmainen, J. Tarhanen, J. Salovaara and M. Lahtiperä, *Chromatographia*, 15 (1982) 364.
13 G. Coppi, *Boll. Chim. Farm.*, 101 (1962) 225.
14 S. Hashimoto and T. Yamashita, *Kogyo Kagaku Zasshi*, 70 (1967) 1450.
15 O. R. Skorokhod and M. L. Tabulo, *Ionoobmen Tekhnol., Akad. Nauk SSSR, Inst. Fiz. Khim.*, (1965) 186; *C.A.*, 63 (1965) 10648.
16 O. R. Skorokhod and M. L. Tabulo, *Geterogennye Reaktsii i Reakts. Sposobnost Sb.*, (1964) 26; *C.A.*, 64 (1966) 11906.
17 T.-T. Su and Y.-C. Cheng, *J. Chromatogr.*, 241 (1982) 416.
18 T. B. Gavrilova, S. S. Krivolapov and V. G. Pastushenko, *J. Chromatogr.*, 245 (1982) 114.
19 A. Smith and F. Vernon, *J. Chromatogr.*, 43 (1969) 503.
20 F. Vernon, *J. Chromatogr.*, 87 (1973) 29.
21 D. W. Connell and C. R. Strauss, *J. Chromatogr.*, 72 (1972) 391.
22 W. G. Galetto, R. E. Kepner and A. D. Webb, *Anal. Chem.*, 38 (1966) 34.
23 J. D. Edwards, W. Gerrard and M. F. Lappert, *J. Chem. Soc.*, (1957) 353.
24 G. Guiochon, *Anal. Chem.*, 36 (1964) 661.
25 I. O. O. Korhonen and M. A. Lind, *J. Chromatogr.*, 322 (1985) 71.
26 I. O. O. Korhonen, *J. Chromatogr.*, 294 (1984) 99.
27 I. O. O. Korhonen, *J. Chromatogr.*, 315 (1984) 185.

Journal of Chromatography, 356 (1986) 301–309
Elsevier Science Publishers B.V., Amsterdam — Printed in The Netherlands

CHROM. 18 443

HIGH-PERFORMANCE LIQUID CHROMATOGRAPHIC QUANTITATION OF RHODAMINES 123 AND 110 FROM TISSUES AND CULTURED CELLS

ALBERT J. BANES*
Department of Surgery and Dental Research Center, 253 Clinical Sciences Building 229H, University of North Carolina, Chapel Hill, NC 27514 (U.S.A.)
and
G. WILLIAM LINK, WILLIAM C. BECKMAN, Jr., JOSEPH L. CAMPS and STEPHEN K. POWERS
Department of Surgery, University of North Carolina, Chapel Hill, NC 27514 (U.S.A.)
(Received December 19th, 1985)

SUMMARY

Rhodamine 123 is a fluorescent vital dye which has potential for therapeutic use in cancer treatment. The dye concentrates in mitochondria of normal and neoplastic cells but accumulates in and is toxic to neoplastic cells. When dye-treated cells are irradiated with blue laser light at 514 nm, mitochondrial injury or cell death results. Rhodamine concentration in cultured cells and tumor tissue was quantitated to correlate cell or tumor death with drug dose. A reversed-phase separation of rhodamine 123 was accomplished using a gradient of 0.05 *M* phosphate buffer pH 2.85 (mobile phase A) and acetonitrile (mobile phase B), 10–80% B in 15 min with a DuPont Golden Series C_8 column. Effluent was monitored with a fluorescence detector at 295 nm excitation and 520 nm emission. Stock rhodamine 123 contained approximately 6–8% of rhodamine 110, the parent compound, which eluted at 9.8 min whereas rhodamine 123 eluted at 11.7 min. Structural verification of both compounds by field desorption mass spectrometry was performed.

This is the first report of the chemical separation and quantitation of rhodamine 123 from cultured tumor cells or tumor tissue.

INTRODUCTION

The cationic lipophilic dye, rhodamine 123 (Rh123) has been used recently as a specific probe for the localization of mitochondria in the living cell[1], but has been used as a histologic stain for almost 50 years[2,3]. This compound and its cationic analogues enter the cell and are sequestered at or inside the mitochondria[2,4]. Many tumor cells concentrate the cationic dyes to a far greater extent than do normal cells and retain it for days under non-equilibrium conditions[5–9]. The mechanism of selective uptake and retention by tumor cells may be related to the greater negative membrane potential of tumor cells at the mitochondrial membranes (−180 mV), responsible for binding the cationic Rh123, *versus* −60 mV for the mitochondrial membrane

0021-9673/86/$03.50

of normal cells[7]. The rhodamine 123 concentration in the incubation medium correlated directly with photoradiation-induced killing of cultured, malignant cells[10].

All the published reports to date demonstrate quantitation of Rh123 in whole cells by epifluorescence, either in a flow cytometer or in histological preparations, or in a spectrofluorometer[1,4,11].

The current report utilizes a reversed-phase separation method to quantitate Rh123 sequestered in cells in culture and in control or tumor tissue from animals.

EXPERIMENTAL

Preparation of stock solutions

Rhodamine 123 and Rhodamine 110 preparations were gifts from Eastman Kodak (Rochester, NY, U.S.A.). Standard solutions of Rh123 or Rh110 were made separately by dissolving 100 mg of stock compound in 10 ml dimethylsulfoxide and bringing the solution to 100 ml in a volumetric flask. The stock solutions were protected from light in brown glass bottles covered with metal foil to minimize photobleaching and stored at −20°C. Stock solutions were stable under these conditions for at least three months. Stock solutions were diluted to 10^{-4} or 10^{-5} with deionized water to make working solutions for constructing standard curves.

Chromatography

Analytical separations of standard and experimental solutions containing rhodamine compounds were conducted using a C_8 reversed-phase column at a flow-rate of 2 ml per min (DuPont Golden Series, 8 × 0.62 cm, 3 μm particle size, 60 Å pore size). A linear gradient of 0.05 *M* phosphate buffer, pH 2.85 (mobile phase A), and acetonitrile (mobile phase B), 10–80% B in 15 min, followed by 90% B for 5 min then 10% B for 8 min was used. A Waters Assoc. WISP was used for autoinjection of samples (Waters Assoc., Milford, MA, U.S.A.). A DuPont 880 system controller and pump in conjunction with a Shimadzu (Columbia, MD, U.S.A.) RF 530 spectrofluorometer set at 300 nm excitation and 500 nm emission (optimized with rhodamine standard in the flow cell) were used. A Dynamic Solutions (Pasadena, CA, U.S.A.) integration system was used to store data and integrate peaks.

For preparative chromatography, a 2.0-ml fixed loop injector was used to introduce the stock rhodamine solution (1 mg/ml, 2 ml sample volume) onto the head of a DuPont preparative C_8 column (25 cm × 242 nm, P.N. 880952-106, DuPont, Wilmington, DE, U.S.A.). A flow-rate of 8 ml/min with a linear gradient of 10–80% B in 75 min was used. Detection was performed using a Waters 440 UV monitor at 260 nm. Peaks eluting at 41.3 (Rh110) and 51.2 min (Rh123) were collected and pooled from 4 separations. Acetonitrile was evaporated under a stream of nitrogen. The two compounds were dissolved in a small volume of *n*-butanol whereupon the phosphate precipitated from solution. The butanol was evaporated under a nitrogen stream and the latter process repeated three times until the salt concentration in the sample was minimal.

UV–VIS and fluorescence spectrophotometry

Ultraviolet to visible scans of rhodamine compounds were carried out using a UV-240 Shimadzu spectrophotometer. Fluorescence scans were performed using the Perkin Elmer (Stanford, CT, U.S.A.) MPF-66 spectrofluorometer.

Mass spectrometry

Samples solvated in dimethylsulfoxide (DMSO) were examined by field desorption mass spectrometry using a double focusing Varian (Sunnyvale, CA, U.S.A.) MAT-731 mass spectrometer.

Cell culture

For *in vitro* studies of the retention of Rh123, two sublines of the Dunning R3327 rat prostate adenocarcinoma were used. Dunning R3327 MatLu and MatLyLu cells were cultured as described[12,13]. Cultures in stationary phase were treated with 10 μg/ml Rh123 and incubated for various times (5, 15, 30, 60, 120 min) then washed 3 times with culture medium without serum. Cells were scraped from the plates with two 1-ml volumes of *n*-butanol. Samples were brought to a volume of 5 ml in a volumetric flask with *n*-butanol. The samples were extracted with vigorous manual shaking for 5 min, in glass tubes with PTFE-lined caps. This extraction removed 98% of the rhodamine from the sample. Samples were sedimented at 3000 *g* for 10 min then supernatant fluids were collected and a portion used for analytical analysis of rhodamine compounds by high-performance liquid chromatography (HPLC).

Animal care and tumor innoculation

Adult, male athymic (nude) mice of the beige strain (bg/bg) were utilized in this study. Animals were housed in the Department of Surgery Athymic Mouse Facility. All National Institute of Health guidelines regarding care and handling of laboratory animals were followed. Dunning R3327-MATLu and MATLyLu rat prostate adenocarcinomas transplanted surgically, under anesthesia, from solid tumors grown in other mice, or cultured cells were injected subcutaneously in the inguinal fat. Transplanted tumors were allowed to grow to 0.3–1.0 mm diameter before mice were sacrificed by cervical dislocation. Tissue samples were collected and stored at −20°C until used.

Rhodamine treatment and tissue extraction

Mice bearing tumors received intraperitoneal injections of 10 mg/kg body weight RH123 dissolved in 50% DMSO. Mice were sacrificed by cervical dislocation, 24 h after injection. Tumors were removed and frozen. Tumor samples weighing approximately 100 mg were removed for extraction and treated as follows: (1) samples were homogenized for 30 s in 0.5 ml distilled water at 4°C with a Polytron homogenizer; (2) the homogenate was collected, then step 1 was repeated twice with 0.5 ml water each time; (3) the homogenizer probe was washed twice for 30 s each time in 800 ml water, once for 10 s with 95% ethanol then rinsed with a stream of water and wicked dry prior to preparation of another extract. Following homogenization, rhodamine was extracted from the homogenate in the following way: 5 ml of HPLC grade *n*-butanol were added to 1.5 ml of homogenate. Samples were vortexed for 1 min, then 5 ml of *n*-butanol were added, followed by 1 min of vortexing. The extraction proceeded overnight in the dark at 4°C in stoppered tubes. The suspension was vortexed, then sedimented at 2000 *g* for 5 min. The supernatant fluid comprised of butanol–water was removed and saved, protected from light. The pellet was rinsed with 1 ml of *n*-butanol, the sample vortexed, sedimented and the second supernatant fluid added to the first supernatant fluid.

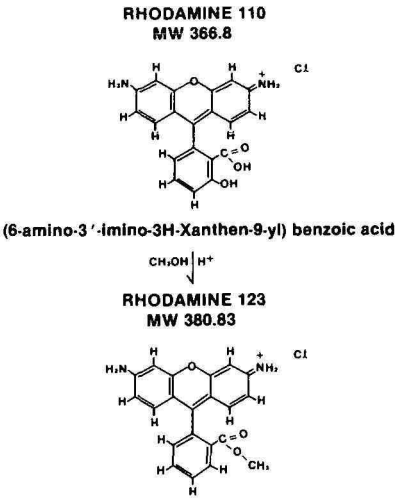

Fig. 1. Structures of rhodamines 123 and 110.

RESULTS

Fig. 1 depicts the structures of Rh123 [methyl O-(6-amino-3'-imino-3H-xanthen-9-yl) benzoate monochloride, molecular weight 380.83] and Rh110. Rh110 [6-amino-3'-imino-3H-xanthen-9-yl) benzoic acid, molecular weight 366.8] is the parent compound to Rh123. The positive charge of the 3'-imino group is responsible for the cationic nature of Rh123 at neutral pH. Rh110 has no charge at neutral pH.

Data in Fig. 2 indicate that detection of rhodamine is linear from 0.2 to 4.0 pmoles in the current system (correlation coefficient = 0.999).

Fig. 3a and b are spectral scans from 190 to 700 nm of stock solutions of Rh123 and Rh110. The stock Rh123 compound contains at least 6–8% of the parent

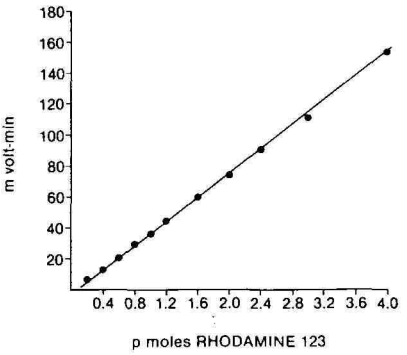

Fig. 2. A standard curve of rhodamine 123 was constructed by preparing standard rhodamine (100 mg) in 10 ml dimethylsulfoxide then diluting to 100 ml in a volumetric flask. Samples were diluted up to 10^{-5} in *n*-butanol then applied to the C_8 reversed-phase column and eluted with a linear gradient of acetonitrile (B), 10–80% B in 15 min, 2 ml/min, 25°C. Standard Rh123 eluted at 11.8 min whereas Rh110 eluted at 9.9 min.

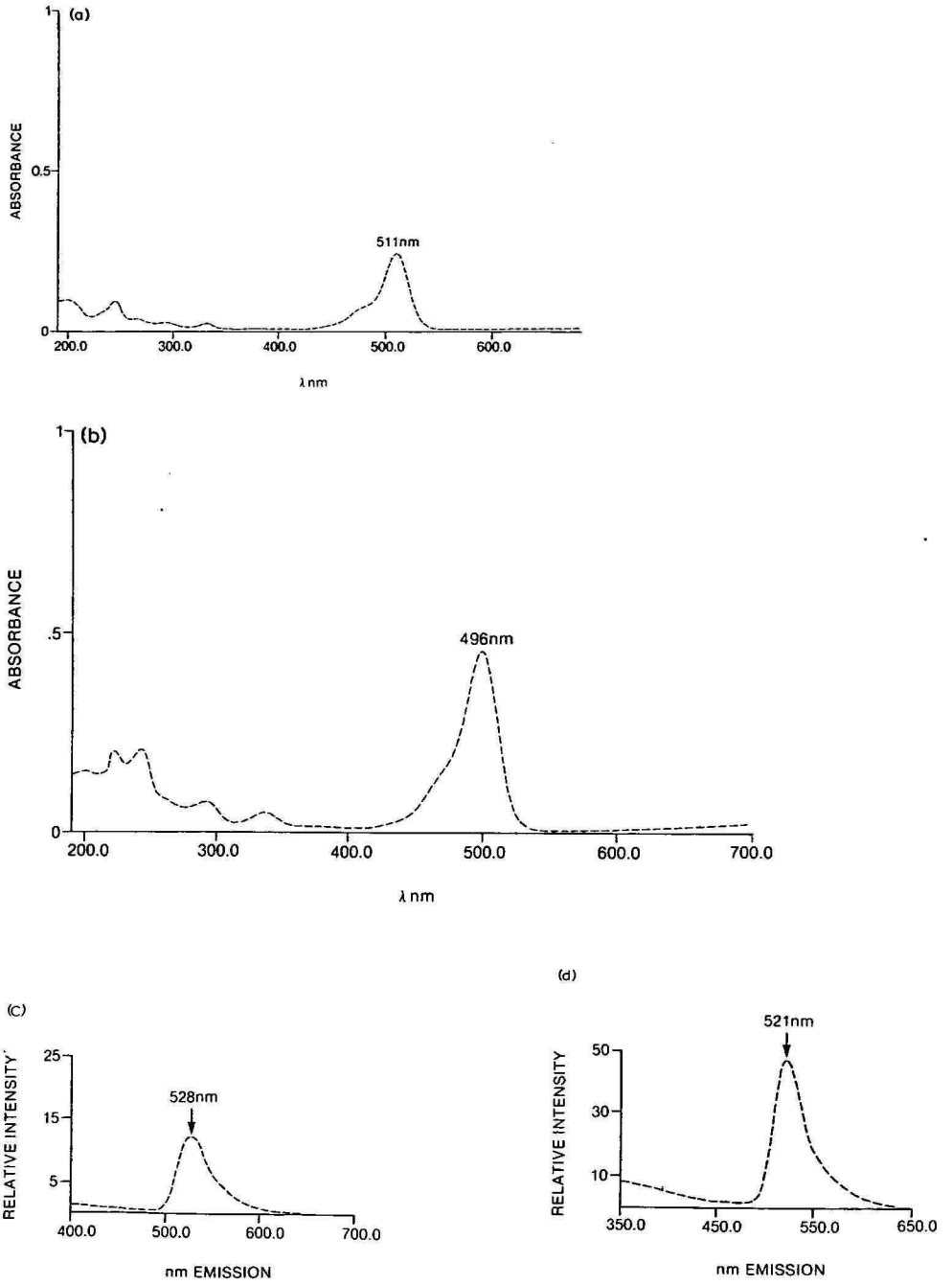

Fig. 3. (a) Spectral scan (UV–VIS), from 190 to 700 nm, of rhodamine 123 dissolved in ethanol. The absorbance peak was at 511 nm. (b) Spectral scan of Rhodamine 110 dissolved in ethanol. The absorbance peak was at 496 nm. (c) Fluorescence scan of rhodamine 123 in ethanol. Excitation was at 334 nm and the emission peak was at 528 nm. (d) Fluorescence scan of rhodamine 110 in ethanol. Excitation was at 294 nm and the emission peak was at 521 nm. Other excitation peaks were at 334 and 482 nm.

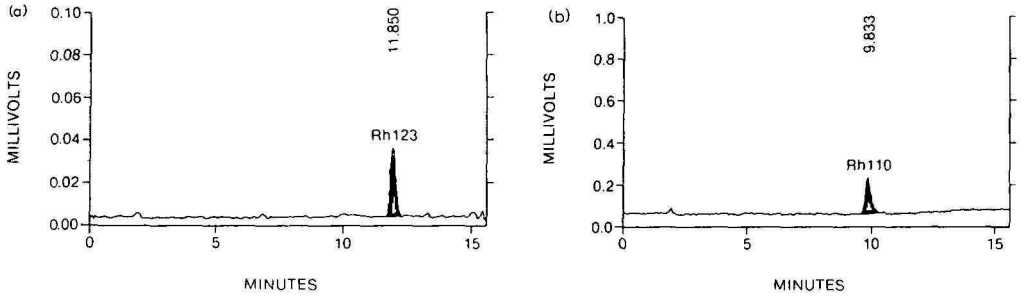

Fig. 4. (a) Chromatogram of a butanol extract of MLA prostatic cells grown in culture and incubated with 10 μg rhodamine 123/ml medium for 2 h at 37°C. Cells were then washed to remove unincorporated dye and extracted in *n*-butanol. A portion of the extract was subjected to chromatography to separate and quantitate the laser dye. A single peak of dye was detected. (b) Elution of stock rhodamine 110 under the same conditions as in (a).

compound, Rh110. The UV–VIS scan of Rh123 indicates a major peak at 511 nm. The scan of Rh110 indicates a major peak at 496 nm.

Fig. 3c and d are fluorescence scans of Rh123 and Rh110, respectively. Rh123 had an emission peak at 528 nm when excited at 334 nm (Fig. 3c). Rh110 had an emission peak at 521 nm when excited at 294 nm (Fig. 3d).

Fig. 4a indicates the peak of Rh123 eluting at 11.85 min in the linear gradient of phosphate–acetonitrile from a typical separation of 0.5 pmoles of standard. The contaminating Rh110 peak is not detectable at this level of sensitivity.

Fig. 4b is a separation of 2.5 picomoles of standard Rh110 which elutes at 9.83 min, approximately 2 min earlier than Rh123.

Fig. 5 is a chromatogram of a butanol extract of ML cells 24 h after a 2 h incubation with 10 μg Rh123/ml (5 ml medium per plate). Cell monolayers were washed three times with medium after the 2-h incubation to remove excess rhodamine. The peak eluting at 11.8 min is Rh123. The peak at 9.867 min coeluted with standard Rh110 and was the Rh110 metabolite of Rh123 that de-esterified.

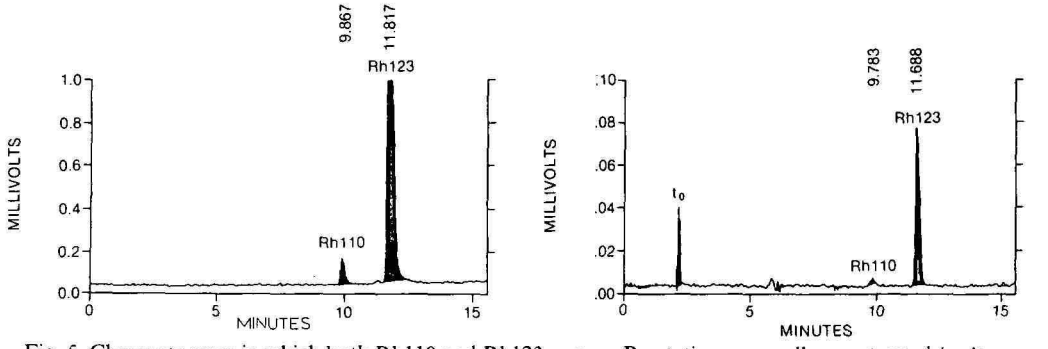

Fig. 5. Chromatogram in which both Rh110 and Rh123 appear. Prostatic cancer cells were treated *in vitro* with 10 μg Rh123/ml medium for 2 h. The resultant butanol extract contained both Rh110 and Rh123. Rh110 may have accrued from metabolism of Rh123 by de-esterification of the methyl group at the benzoate function of Rh123.

Fig. 6. Chromatogram of RH110 and Rh123 separated from a tumor comprised of human ML cells injected in the flank of a nude mouse.

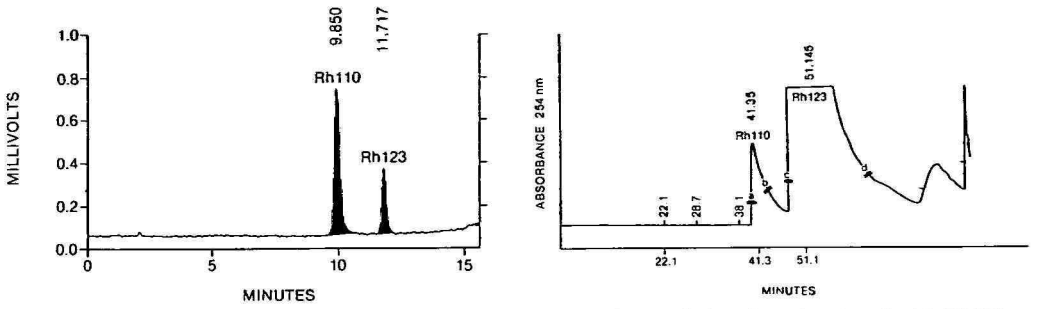

Fig. 7. Chromatogram with both Rh110 and Rh123 extracted from cells in culture incubated with Rh123. Standard Rh110 was added to the cell extract to verify the position of Rh110.

Fig. 8. Preparative separation of Rh110 and Rh123 after application of 2 mg of stock Rh123 to a C_8 Du-Pont preparative column and elution with 10–80% B in 75 min at 8 ml/min. Detection was at 254 nm. The major peaks of Rh123 and Rh110 were collected as shown by the double hash marks on the peak sides (R110 a–b; R123 c–d). Additional contaminating compounds were detected at 22.1, 28.7 and 38.1 min.

Fig. 6 is a chromatogram of a tissue extract of a solid tumor from the flank of a nude mouse previously injected with ML cells. The minor peak at 9.783 min was Rh110. The major peak at 11.688 min was Rh123. The material at 2.15 min was unretained.

Fig. 7 is a chromatogram of Rh123 and Rh110 from a cell extract with added standard Rh110, indicating coelution of standard Rh110 with the 9.85 min peak.

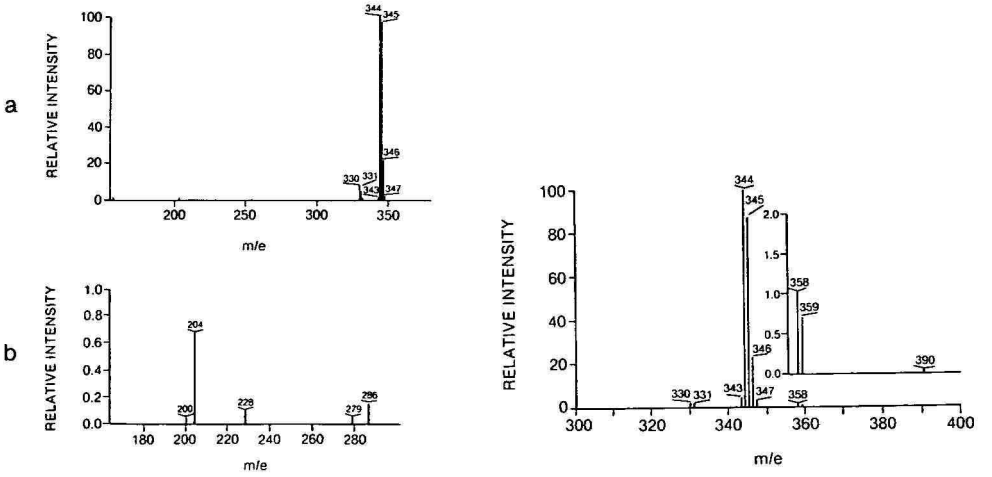

Fig. 9. Averaged field desorption mass spectrum for a commercial preparation of Rh123. The major ion peaks observed were m/e = 344 $(M)^+$ and m/e = 345 $[(M + 1)^+]$ (where m is mass and e is charge and M is the ion). (a) Shows an ion peak at m/e = 330, suggestive of Rh110, approximately 10% of m/e = 344 ion intensity; (b) shows other ions, each at less than 1% ion intensity of m/e = 344, at m/e = 28, 279 and 286.

Fig. 10. Field desorption mass spectrum for chromatographically purified Rh123. The major ion peaks observed were m/e = 344 (M^+) and m/e = 345 $[(M + 1)^+]$. Ion peak m/e = 330, suggestive of Rh110, is 1.8% of the m/e = 344 in intensity; m/e = 358, perhaps the ethyl ester, is less than m/e = 344 ion intensity.

Fig. 8 is a chromatogram showing the UV scan at 260 nm of the effluent from a DuPont C_8 preparative column loaded with 2 mg of Rh123. The primary peaks at 41.35 min and 51.145 min corresponded to Rh110 (a to b for further analysis) and Rh123 (c to d for further analysis), respectively. Other components were detected during the separation and were saved for later analysis. The presence of additional peaks, eluting at 22.1, 28.7 and 38.1 min, in the chromatogram of the preparative gradient elution confirmed the mass spectrographic data, indicating that contaminants other than Rh110 were present in the stock solution. The latter contaminants were detected as peaks when the absorbance scale was decreased.

Chromatographically pure Rh123 and Rh110 were subjected to mass spectrographic analysis to confirm structure. The data in Fig. 9a confirmed the presence of Rh123 [$M^+ = 344$ *m/e*; $(M + 1)^+ = 345$ *m/e*] as major ion peaks. This was the compound that eluted at 51.2 minutes in the preparative chromatogram (Fig. 8). Data in Fig. 9b and the inset of Fig. 10 indicated that ions of lower and higher mass respectively were also present as contaminants. The field desorption mass spectrographic data in Fig. 9a were consistent with the Rh123 structure (Fig. 9).

Data in Fig. 9a and 10 confirmed the presence of Rh110 as the ion peak at *m/e* = 330 in the Rh123 preparation. Rh110 was the compound that eluted at 41.35 min in the preparative chromatography (Fig. 8).

DISCUSSION

Rhodamine 123 is a laser dye that has a future as a therapeutic drug in the treatment of cancer[7]. The drug is toxic to tumor cells *in vitro* and to tumors *in vivo* as well. Moreover, dye treatment combined with application of laser light act synergistically to amplify the toxicity[10]. However, in order to be of use clinically, the constituents of the active material must be known. Commercially available Rh123 has been used principally as a mitochondrial stain and was not prepared commercially in highly purified form. Results of preparative chromatography indicated that at least 5 compounds were present in stock Rh123 at 1% or less concentration, including the parent compound Rh110 which represented approximately 6–8% of the total dye by weight (Figs. 9a and b, and 10). The phosphate–acetonitrile gradient elution system easily resolved the two principal rhodamines, with Rh110 eluting prior to Rh123 (Figs. 5, 7 and 8). The lesser contaminants were beyond the limits of detection in analytical separations but were readily detected in preparative separations (Fig. 8).

It has been stated that Rh110 is not biologically important because it does not enter the cell due to its lack of charge at neutral pH[7]. However, the compound may be formed by de-esterification of Rh123 inside the cell (Fig. 1). It appears that Rh110 is formed in cells incubated with Rh123 (Fig. 5). The effect of intracellular Rh110 on cellular metabolism is not known.

Preliminary experiments with Rh123 that contained 1.8% Rh110 indicated that cytotoxicity to cultured cells was reduced (data not shown). Higher concentrations of more pure Rh123 were also required to produce photoradiation-induced cell killing *in vitro*. These findings suggest the possibility that Rh110 may be a cytotoxic factor alone and/or in conjunction with Rh123.

Cells from human prostatic cancer grown *in vitro* can take up the dye. Studies

have shown that the dye is toxic to cells *in vitro* when they are exposed to blue-green light from an argon laser[14]. A solid tumor from the same cells, induced *in vivo* by inoculation of nude mice, will also incorporate the drug and necrose after administration of blue-green light. Therefore, toxicity in the *in vitro* culture system may be used as a predictor of efficacy *in vivo*. However, adequate tissue levels of Rh123 must be obtained to ensure tumor necrosis after light exposure. We are currently correlating the Rh123 concentration detected in cultured cells with that observed in solid tumors *in vivo*.

Future studies of this nature will employ pure Rh123 and cationic analogues that may be more selective and toxic for tumor cells than Rh123 alone.

ACKNOWLEDGEMENTS

The authors would like to thank Dr. Elsa Anders and Mr. Ken Ellington for technical assistance. Thanks also to Dr. Tom Crisswell of Eastman Kodak Co. for providing mass spectrometry data and reviewing the manuscript.

REFERENCES

1 L. V. Johnson, M. L. Walsh and L. B. Chen, *Proc. Natl. Acad. Sci. U.S.A.*, 77 (1980) 990.
2 L. Monne, *Protoplasma*, 30 (1938) 58.
3 L. Monne, *Protoplasma*, 32 (1939) 184.
4 J. S. Modica-Napolitano, M. J. Weisse, L. B. Chen and J. R. Aprille, *Biochem. Biophys. Res. Commun.*, 118 (1984) 717.
5 S. D. Bernal, T. J. Lampidis, I. C. Summerhayes and L. B. Chen, *Science (Washington, D.C.)*, 218 (1982) 1117.
6 S. D. Bernal, T. J. Lampidis, R. M. McIsaac and L. B. Chen, *Science (Washington, D.C.)*, 222 (1983) 169.
7 T. J. Lampidis, S. D. Bernal, I. C. Summerhayes and L. B. Chen, *Ann. N.Y. Acad. Sci.*, 397 (1982) 299.
8 T. J. Lampidis, S. D. Bernal, I. C. Summerhayes and L. B. Chen, *Cancer Res.*, 43 (1983) 716.
9 I. C. Summerhayes, T. J. Lampidis, S. D. Bernal, J. J. Nadakavukaren, K. K. Nadakavukaren, E. L. Shepard and L. B. Chen, *Proc. Natl. Acad. Sci. U.S.A.*, 79 (1982) 5292.
10 S. K. Powers, S. Pribil, G. Y. Gillespie and P. J. Watkins, *J. Neurosurg.*, in press.
11 Z. Darzynkiewicz, F. Traganos, L. Staino-Coico, J. Kapuscinski and M. R. Melamud, *Cancer Res.*, 42 (1982) 799.
12 J. Camps, S. K. Powers, W. C. Beckman, J. T. Brown and R. M. Weissman, *J. Urol.*, 134 (1985) 1.
13 J. T. Isaacs, G. W. Yu and D. S. Coffey, *Invest. Urol.*, 19 (1981) 220.
14 D. W. Lazan, W. D. W. Heston, D. Kadmon and W. R. Fair, *Cancer Res.*, 42 (1982) 1390.

Journal of Chromatography, 356 (1986) 311–319
Elsevier Science Publishers B.V., Amsterdam — Printed in The Netherlands

CHROM. 18 400

DETERMINATION OF BIOGENIC AMINES IN CHEESE AND SOME OTHER FOOD PRODUCTS BY HIGH-PERFORMANCE LIQUID CHROMATOGRAPHY IN COMBINATION WITH THERMO-SENSITIZED REACTION DETECTION

H. M. L. J. JOOSTEN* and C. OLIEMAN
Netherlands Institute for Dairy Research, Kernhemseweg 2, 6718 ZB Ede (The Netherlands)
(Received December 9th, 1985)

SUMMARY

A simple high-performance liquid chromatographic (HPLC) analysis is described for biogenic amines in cheese and other food products. The sample clean-up consists of a precipitation–extraction step with trichloroacetic acid, which gives recoveries of amines in cheese in the range of 85–105%. The HPLC analysis is performed by reversed-phase ion-pair chromatography, using a ninhydrin-containing eluent, which eliminates the need for an extra reagent pump for the post-column derivatization. Band broadening is minimized by using a poly(tetrafluoroethylene) knitted tube reactor at 145°C. The detection limit for amines is 2 mg/kg cheese and the method is linear for 0.1–4 μg of amine injected. Examples are given of the analysis of amines in cheese, wine and sauerkraut.

INTRODUCTION

During the ripening of cheese, proteins are degraded by enzymes, resulting in an increase of the free amino acid content. Decarboxylation of the amino acids by bacterial enzymes gives rise to the formation of biogenic amines[1–4]. While in most cheeses the content of biogenic amines is low, some have rather high levels. The consumption of large quantities of amines brings about symptoms of intoxication such as headache, nausea, hypo- or hypertension, cardiac palpitation and possibly shock[5,6]. The amines which may be found in cheese are tyramine, histamine, putrescine, cadaverine, tryptamine and phenylethylamine[7–11].

In order to prevent the formation of toxic amounts of biogenic amines in cheese, an investigation to reveal the essential parameters of the production of amines, was commenced. Therefore we needed a simple method for the quantitative detection of biogenic amines in cheese, making possible an automated analysis of many samples.

A variety of methods for estimating biogenic amines in foods has been described[12]. Most of these deal with the detection of only one or two amines[13–16]. Many methods have been developed for the determination of histamine in fish, since his-

0021-9673/86/$03.50

tamine is the causative agent of the food poisoning called "scombroïd fever"[17]. Generally applicable methods for the determination of biogenic amines other than histamine and tyramine are usually based on gas or high-performance liquid chromatography (GLC and HPLC respectively). GLC methods always require a derivatization step to make the amines volatile[18,19]. Derivatization, however, is cumbersome and is difficult to reproduce in the presence of an interfering matrix of compounds in food products like cheese. Pre-column derivatization with, *e.g.*, dansyl chloride, followed by HPLC analysis of the products thus formed, suffers from the same drawbacks.

The separation of underivatized amines by using ion-pair chromatography is a well known HPLC technique. UV detection permits the detection of tyramine and tryptamine at 280 nm, phenylethylamine at 254 nm and histamine at 215 nm. However, 215 nm gives no selectivity and the risk of interfering matrix components cannot be neglected. Putrescine and cadaverine, lacking a suitable chromophore, cannot be detected by UV spectroscopy.

Electrochemical detection of underivatized amines by oxidation of the amino group is a sensitive method but not a very useful one since the oxidation takes place only at pH > 7 and this means that the separation has to be carried out in an alkaline mobile phase, which excludes the use of silica-based columns. The use of a reagent pump has been discarded since electrochemical detection is far too sensitive for shifts of the eluent composition due to pulsation of the pumps. Reversed-phase packing materials, based on organic polymers, should enable the analysis of biogenic amines in the suppressed ion mode at pH > 8. Preliminary experiments with the PRP-1 column, packed with polystyrene, cross-linked with divinylbenzene, were disappointing. Tryptamine and phenylethylamine showed strongly tailing peaks, which could not be suppressed by manipulating the mobile phase.

Post-column derivatization of amines is a widely used technique. With ninhydrin a coloured product is formed[20], while with *o*-phthalaldehyde a highly fluorescent derivative[21] is obtained. A disadvantage of these methods is the requirement of a second pump to deliver the reagent.

Recently, LePage and Rocha[22] described a simple method for the determination of low-molecular-weight aliphatic amines which involved post-column derivatization with ninhydrin. The simplicity is due to the fact that ninhydrin is already dissolved in the mobile phase: the chemical reaction which yields a blue product does not take place until the eluent is heated in a reaction coil (after passage through the column).

The inherent simplicity of thermo-sensitized reaction detection makes this method highly suitable for routine analysis of biogenic amines, requiring in addition to a normal HPLC apparatus only a heated reaction coil. Therefore we have adapted this method for the determination of biogenic amines in cheese and some other food products.

EXPERIMENTAL

Chemicals

Tyramine (TA), histamine (HA), putrescine (PTR), cadaverine (CAD) and tryptamine (TPA) were obtained from Fluka (Buchs, Switzerland), phenylethylamine (PHEA) from Merck (Darmstadt, F.R.G.), ninhydrin and hydrindantin from Pierce

(Rockford, IL, U.S.A.) and sodium dodecyl sulphate (SDS) from Bio-Rad Labs. (Richmond, CA, U.S.A.). Other reagents were obtained from various suppliers.

HPLC equipment

A Waters M6000A pump (Waters Assoc., Milford, MA, U.S.A.) and a M440 absorbance detector (detection wavelength 546 nm) were used together with a Perkin-Elmer ISS 100 automatic sampler, equipped with a 1-ml sample loop, and a Sigma 15 B data system (Perkin-Elmer, Oak Brook, IL, U.S.A.). The separations were performed on a radial compression cartridge (10 × 0.8 cm I.D.), custom-packed with Nucleosil C_{18}, 10 μm (Macherey, Nagel & Co., Düren, F.R.G.), in combination with a Waters RCM module. The guard column (3 × 0.3 cm I.D.), was packed with Corasil C_{18} (Waters). The reaction coil consisted of 10 m of PTFE tubing (0.25 mm I.D., volume 0.49 ml) coiled in the form of a twisted figure eight, according to Engelhardt and Neue[23] and heated in an oil-bath to 145°C with a Colora KS ultrathermostat (Colora, Lorch/Württ, F.R.G.).

Mobile phase

Ninhydrin (16 g) and 1.2 g hydrindantin were dissolved in 322 ml dimethyl sulphoxide (DMSO) by sonication for 10 min, followed by the addition of 350 ml of 2.8 *M* sodium acetate buffer (pH 5.00). A 2-g amount of SDS was dissolved in a mixture of 618 ml DMSO and 710 ml water. The two solutions were combined and filtered through a 0.45-μm filter. The mobile phase was stored in a dark bottle and nitrogen was constantly passed through the solution. Under these circumstances it remained stable for at least 1 week. The HPLC system was equilibrated for *ca.* 4 h at 1.0 ml/min. The temperature of the RCM module was kept constant at 29°C by means of a small thermostat. A mixture of DMSO and water (1:1) was used to flush the HPLC system before shut-down.

Extraction of the amines

For the analysis of cheese and chocolate, 45 ml of a 0.07 *M* trisodium citrate solution (45°C) were added to 5 g of the ground sample and homogenized with a "stomacher" for 5 min. A portion (3 ml) of this suspension was mixed with 3 ml of 0.6 *M* trichloroacetic acid (TCA) and centrifuged for 10 min at 10 000 *g* and 4°C in a Sorvall centrifuge. The resulting pellet was resuspended in 3 ml of 0.3 *M* TCA and centrifuged. The combined supernatants were filtered through a 0.45-μm Gelman acrodisc and the volume was adjusted to 10 ml with water. Wine (3 ml) was treated with 3 ml of 0.6 *M* TCA. After centrifugation, the supernatant was filtered and injected. Fish and sauerkraut were prepared for analysis by adding 200 ml of water to 200 g of sample and blending in a household mixer for 3 min. To 3 ml of the suspension were added 3 ml of 0.6 *M* TCA. After centrifugation the supernatant was filtered.

Stock solutions of biogenic amines

Stock solutions containing about 0.2 mg amine per ml in water were kept refrigerated at −20°C. Tryptamine (TPA) solutions were prepared fresh weekly. The calibration mixture was prepared daily by mixing equal volumes of the stock solutions, diluted 1 to 10 in 0.3 *M* TCA solution.

RESULTS AND DISCUSSION

Optimization of the separation and detection

In order to make the method of LePage and Rocha[22] suitable for detection of biogenic amines in cheese, the composition of the mobile phase was adjusted. The composition of the ninhydrin-containing eluent, however, is restricted by the low solubility of hydrindantin: a DMSO content of at least 40% is required. This concentration makes necessary the use of a very non-polar ion-pair reagent in order to get sufficient retention of the amines. A second restriction is the pH dependence of the ninhydrin reaction: the pH should lie between 5.0 and 5.5. Other components of the mobile phase have a limited solubility, and finally the high viscosity of the DMSO–water mixture makes flow-rates of more than 1.5 ml/min impossible. Despite all these limitations we were able to find a set of conditions for a useful separation.

Fig. 1 shows an example of the optimization of the mobile phase. Eluents were prepared with different SDS and DMSO concentrations in such a way as to keep the retention time more or less constant. The effect of increasing the DMSO content can be counteracted by an increase of the SDS concentration. At 44.5% DMSO and 0.5

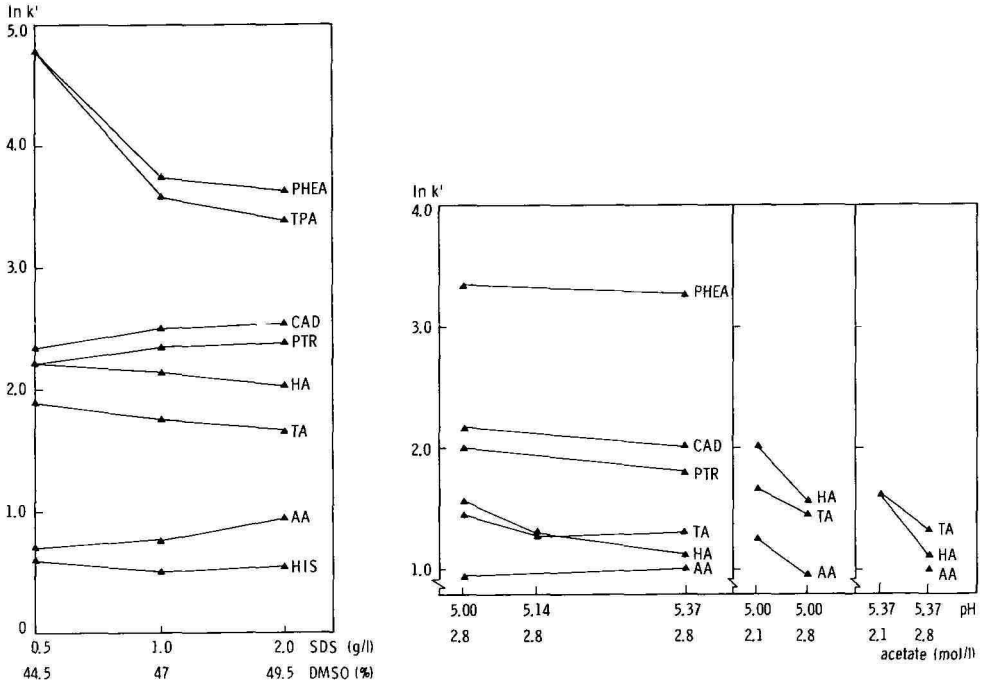

Fig. 1. Dependency of the capacity factor, k', on the mobile phase composition. Samples: mixture of six amines and histidine, 3.3 μg of each compound per ml and a cheese extract. AA = Last eluted amino acid. Mobile phase: pH = 5.00, 2.8 *M*.

Fig. 2. Dependency of the capacity factor on the pH and molarity of the acetate buffer. Sample: cheese extract spiked with TA, HA, PTR, CAD and PHEA. Mobile phase: DMSO–water (47:53), containing 1 g of SDS per litre.

g SDS/l, there is insufficient separation of putrescine and histamine and of phenylethylamine and tryptamine. With 49.5% DMSO and 2.0 g SDS/l these separations are much better, but this mixture proved to be less useful for cheese samples because of the presence of very large amounts of free amino acids, which interfered with the accurate measurement of the first amine (tyramine) eluted. The mobile phase containing 47% DMSO and 1 g SDS/l proved to be ideal: good separation of all amines and sufficient resolution between tyramine and the amino acids. During the experiments it became clear that the optimum composition was also dependent on the age of the column: after several months of use the DMSO percentage had to be gradually lowered to 43%. This phenomenon is most probably caused by the gradual hydrolysis of the bonded phase.

Another aspect of optimization is shown in Fig. 2. Eluents having small differences in pH and in the molarity of the sodium acetate buffer were prepared. Within the narrow pH range of 5.0–5.4 the degree of protonation of the amino groups of the amines hardly changes, but histamine is very sensitive to small pH shifts, because of the presence of the imidazole group with a pK_a of about 5.0. The 2.8 *M* buffer with pH 5.37 gave a good separation of the first three amines eluted, but analysis of cheese samples caused problems with the resolution of histamine and the amino acids of the cheese extract. Decreasing the molarity of the acetate buffer to 2.1 *M* at pH 5.00 resulted in retention times of more than 2 h for phenylethylamine, which is not a practical proposition, while the resolution between the amino acids and tyramine decreased. Optimum results were obtained with the 2.8 *M* buffer at pH 5.00.

The use of methylcellosolve, which is more toxic than DMSO, gave more problems in keeping the hydrindantin dissolved, while the separation of the amines was less satisfactory than with DMSO.

A reduction of the analysis time by using gradient elution was not possible, since an unacceptable baseline drift was observed. This might be caused by the slow

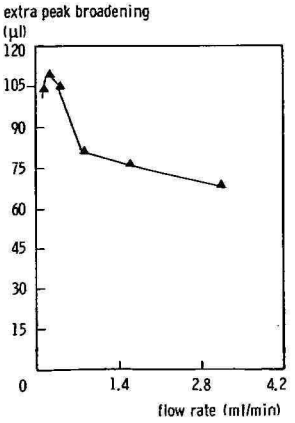

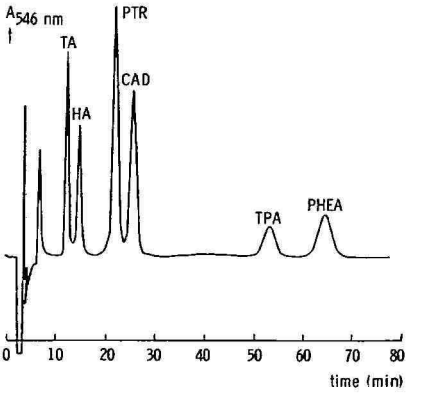

Fig. 3. Extra peak broadening of the knitted tube reactor at different flow-rates of water. A 5 µl volume of acetone was injected into a system with and without the knitted tube reactor.

Fig. 4. Separation of a mixture of biogenic amines, in combination with thermo-sensitized reaction detection with ninhydrin. Detection wavelength: 546 nm. Injected amount: 0.6 µg of each amine. For the column and conditions, see Experimental.

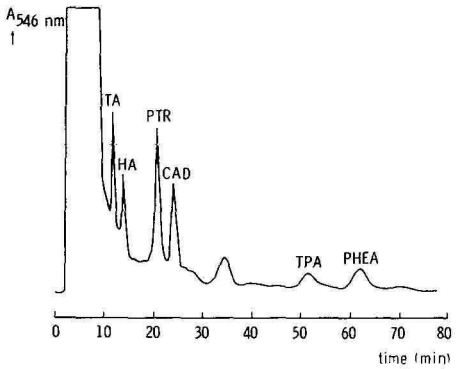

Fig. 5. Chromatogram of a cheese extract, spiked with the amine mixture (each 50 mg per kg cheese). Amino acids are eluted during the first 10 min.

equilibration of SDS with the stationary phase or by desorption of ninhydrin or hydrindantin during the gradient elution.

The band broadening caused by the post-column reaction coil as a function of the flow-rate is shown in Fig. 3 for water. At a flow-rate of 1.0 ml/min an extra band broadening of only 80 μl was measured, having no influence on the resolution. The optimum reaction temperature was found to be 145°C.

Analysis of biogenic amines

Figs. 4 and 5 show chromatograms of a standard mixture and of a Gouda cheese extract, spiked with a mixture of the amines. An analysis time of 1.5 h is needed for the complete separation of the important amines in cheese. Despite the long retention times of tryptamine and phenylethylamine, these compounds show good peak shapes and they have response factors comparable to those of the faster eluting amines. The rate of the reaction of ninhydrin with amines at 30°C is very low and does not interfere with the analysis. The amino acids are eluted during the first 10 min. Since these are present in very high amounts in cheese, massive peaks are observed on the chromatogram. By lowering the amount of extract injected it is also

TABLE I

RECOVERY OF AMINES BY THE TCA PRECIPITATION METHOD

n = 2. The cheese used contained 5 mg histamine and 5 mg putrescine per kg.

Added amount (mg/kg cheese)	*Recovery (%)*					
	TA	*HA*	*PTR*	*CAD*	*TPA*	*PHEA*
10	140	95	73	100	140	140
50	102	86	86	94	92	94
100	99	93	98	95	100	95
500	93	96	99	97	103	102
1000	92	94	97	95	102	102
2000	93	94	94	94	97	102

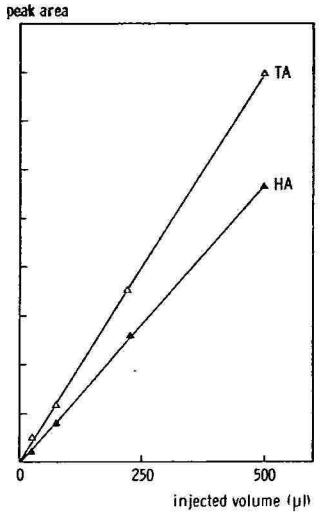

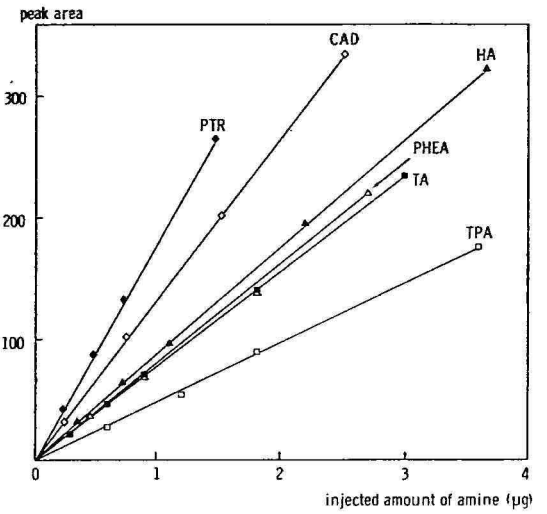

Fig. 6. Peak area as a function of the injected volume (25–500 µl). Sample: mixture of tyramine and histamine (each 3.3 µg/ml). For the column and conditions, see Experimental.

Fig. 7. Linear regression of peak area and the amount of injected amine. Samples of 200 µl were injected, containing 0–4 µg of each amine. Residual standard deviations: TA, 0.3; HA, 0.3; PTR, 2.2; CAD, 0.6; TPA, 5.4; PHEA, 22.6; statistically, the intercepts did not differ from zero.

possible to get an impression of the total amino acid formation in cheese. Histidine (HIS) can be detected selectively by decreasing the content of DMSO to 40% and lowering the molarity of the buffer to 0.7 *M*.

The recovery of amines was studied by homogenizing a three month-old Gouda type cheese with a low amine content ($\leqslant 10$ mg/kg). Portions of the suspension

TABLE II

REPEATABILITY

Two cheese samples were fortified with 50 and 500 mg of each amine per kg cheese, respectively. Extracts of these were each injected four times and peak areas were determined. The repeatability of the analysis is expressed as the relative standard deviation (R.S.D.).

Amine concn. (mg/kg cheese)	*Peak area*		*R.S.D. (%)*	*n*
	Mean	*Range*		
TA 50	25.9	25.59–26.27	1.21	4
500	310.4	304.6–315.9	1.58	4
HA 50	21.4	21.03–21.65	1.47	3
500	298.8	292.2–308.0	2.46	4
PTR 50	63.3	62.16–64.35	1.90	4
500	627.9	617.1–641.2	1.92	4
CAD 50	58.1	56.73–59.49	3.36	2
500	465.6	457.1–475.9	2.13	4
TPA 50	14.0	12.24–15.15	9.94	4
500	136.5	133.8–137.5	1.31	4

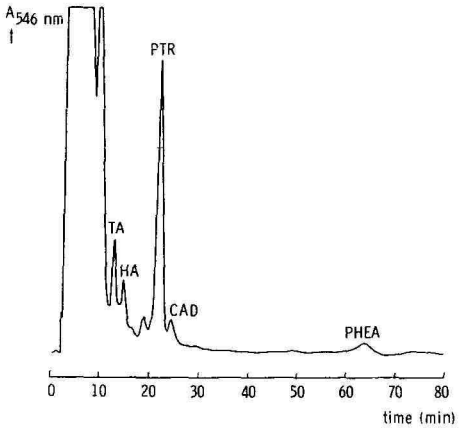

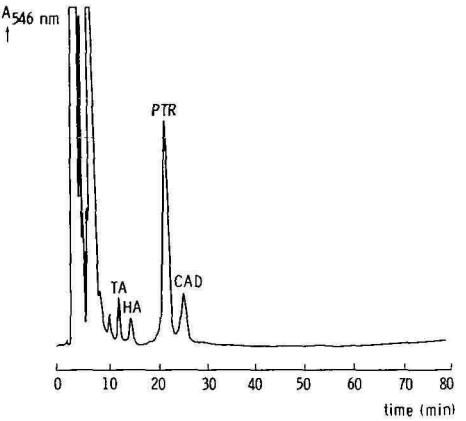

Fig. 8. Chromatogram of a wine extract. This sample contained tyramine (2.7 mg/l), histamine (2.0 mg/l), putrescine (6.9 mg/l) and also traces of cadaverine and phenylethylamine.

Fig. 9. Chromatogram of a sauerkraut extract, containing a large amount of putrescine (210 mg/kg). Tyramine, histamine and cadaverine were also detectable (69, 58 and 79 mg/kg respectively).

were spiked with amines at several concentrations. The results are summarized in Table I. The recoveries of the amines varied between 85 and 105%. Only at the lowest level (10 mg/kg added) was this range larger.

Attempts to make sample preparation easier by reducing the procedure to only one TCA precipitation failed, since recovery rates were about 10% lower. Neither did the addition of 20–40% DMSO to the TCA solution raise the efficiency of the first extraction.

The detection limit for biogenic amines in cheese is 2 mg/kg for each of the amines, which is sufficiently low for toxicological investigations. This low limit is also due to the large sample volume of 200 μl, which could be injected without any change in peak size and shape (Fig. 6). The amines are concentrated at the top of the column probably because they are dissolved in a weaker eluent (0.3 *M* TCA) than the mobile phase. They will not be eluted as long as the surrounding solution does not contain DMSO.

To investigate the repeatability, two Gouda cheese samples, one with a low and one with a high amine content (50 and 500 mg/kg, respectively), were each analysed four times. The results are summarized in Table II. The sample with the low amine content gave a relative standard deviation (R.S.D.)[24] of less than 10%. The sample with the high amine content showed a maximum R.S.D. of 2.5%.

Assuming a linear relationship between the amount of amine injected and its peak area, the residual standard deviation (Syx) was determined. Constant volumes of different diluted standard solutions were injected and the peak areas thus obtained were subjected to linear regression (Fig. 7).

This method was also tested on several other foodstuffs which are known to contain biogenic amines: fish (tuna), wine, sauerkraut and chocolate. Examples are shown in Figs. 8 and 9 for wine and sauerkraut respectively. The detection limit of the amines in sauerkraut is 0.8 mg/kg and in wine 0.3 mg/kg.

CONCLUSION

The described HPLC system permits the determination of biogenic amines in cheese and other foods with good sensitivity and specificity. By means of an automatic injector, this method is very useful for routine analysis.

ACKNOWLEDGEMENT

This work was supported by the Stichting J. Mesdagfonds, instituted by Kaascontrolestation Friesland, Leeuwarden, The Netherlands.

REFERENCES

1 S. L. Rice, R. R. Eitenmiller and P. E. Koehler, *J. Milk Food Technol.*, 39 (1976) 353.
2 A. Askar, *Ernährungs-Umschau*, 29 (1982) 143.
3 D. Beutling, I. Janz and G. Scheibner, *Mh.Vet.-Med.*, 39 (1984) 231.
4 S. T. Edwards and W. E. Sandine, *J. Dairy Sci.*, 64 (1981) 2431.
5 F. Franzen and K. Eysell, *Biologically Active Amines Found in Man*, Pergamon, New York, 1969.
6 W. Lovenberg, in *Toxicants Occurring Naturally in Foods*, Natl. Acad. Sci., Washington, DC, 1973, p. 170.
7 U. Pechanek, H. Woidich, W. Pfannhauser and G. Blaicher, *Ernährung/Nutrition*, 4 (1980) 58.
8 P. Koehler and R. Eitenmiller, *J. Food Sci.*, 43 (1978) 1245.
9 G. J. Silverman and F. V. Kosikowski, *J. Dairy Sci.*, 39 (1956) 1134.
10 M. Saxby, J. Chaytor and R. Reid, *Food Chem.*, 6 (1981) 281.
11 S. Ramantanis, *Arch. Lebensmittelhyg.*, 35 (1984) 75.
12 N. Seiler, *J. Chromatogr.*, 143 (1977) 221.
13 G. Suhren, W. Heeschen and A. Tolle, *Milchwissenschaft*, 37 (1982) 143.
14 M. Voigt, R. Eitenmiller, P. Koehler and M. Hamdy, *J. Milk Food Technol.*, 37 (1974) 377.
15 J. Chaytor, B. Crathorne and M. Saxby, *J. Sci. Food Agric.*, 26 (1975) 593.
16 T. Chambers and W. Staruszkiewicz, *J. Assoc. Off. Anal. Chem.*, 61 (1978) 1092.
17 S. Hudson-Arnold and W. Duane-Brown, *Adv. Food Res.*, 24 (1978) 113.
18 S. Wada, M. Takada and C. Koizumi, *Chem. Abstr.*, 98 (1983) 52033f.
19 J. Slemr and K. Beyermann, *J. Chromatogr.*, 283 (1984) 241.
20 S. Moore and W. Stein, *J. Biol. Chem.*, 176 (1948) 367.
21 M. Walters, *J. Assoc. Off. Anal. Chem.*, 67 (1984) 1040.
22 J. LePage and E. Rocha, *Anal. Chem.*, 55 (1983) 1360.
23 H. Engelhardt and U. Neue, *Chromatographia*, 15 (1982) 401.
24 *ISO 5725-1981*, International Organization for Standardization, Geneva, 1981.

Journal of Chromatography, 356 (1986) 320–325
Elsevier Science Publishers B.V., Amsterdam — Printed in The Netherlands

CHROM. 18 411

Note

Unified retention indices for arenes in gas chromatography

D. PAPAZOVA*
Economic Complex "Neftochim", Institute of Petroleum, Burgas 8104 (Bulgaria)
and
N. DIMOV
Chemical Pharmaceutical Research Institute, Analytical Department, Sofia 1156 (Bulgaria)
(First received September 19th, 1985; revised manuscript received December 12th, 1985)

Arenes are of great practical importance and often the sole reason for an analysis is to determine their individual contents. That is why in many cases the phases used for gas chromatographic (GC) separation are polar[1–3] and sometimes extremely polar[4]. In the latter case all of the non-aromatic compounds are eluted first and almost as one peak, while the arenes are retained and eluted separately. The resolution of C_9^+ arenes, however, is very poor on such phases and a less polar or even apolar phase may be preferred. If the identification of the arene peaks is necessary, one needs accurate retention indices, I, this is better than using standards. There are enough I_{exp} data in the literature, but their comparison often shows very great differences.

Recently, Dimov[5] proposed the so-called unified retention index calculated from the available literature data. The aim of the present study is to examine the possibility of unifying the retention indices for arenes using the available experimental data obtained on different phases.

EXPERIMENTAL

The statistical treatment of the experimental data is based on the least-squares approach and leads to the equation

$$UI_T = UI_0 + (dUI/dT)T \pm s$$

where UI_T is the unified index at a given temperature T, UI_0 is a constant value at an accepted standard temperature, *e.g.*, 0°C, and s is the standard deviation.

It is considered that, in routine analysis, differences of ± 1 index units (i.u.) between experimental indices from different laboratories are acceptable[6,7]. Any experimental data which differred from the calculated value of UI_T by more than ± 1 i.u. were excluded from the regression analysis. The values of the unified index, UI_T, obtained and its temperature increment were considered as reliable if the data included in the regression matrix were from two authors and at three temperatures at least and no more than 33% of all data were excluded.

0021-9673/86/$03.50

Experimental retention indices for arenes at different temperatures on squalane have been taken from eighteen sources[1,2,8–23]. Hively and Hinton[21] reported the retention of benzene, toluene, ethylbenzene and xylenes in the interval 27–86°C. Soják *et al.*[1,11,12,20] carried out a detailed study on the retention of arenes in the range 50–115°C. Švob and Deur-Šiftar[8] published experimental values at 100°C, while Kugucheva and Machinski[16] quoted data at 96 and 106°C. Papazova and Pankova[14] investigated the retention at 110°C.

Experimental retention indices for benzene and toluene on OV-101 at 50°C were reported by Johansen and Ettre[24]. Nabivach and co-workers[25,26] published retention indices for 56 alkylbenzenes on the same phase at 100, 120 and 140°C. Boneva *et al.*[27] investigated retention at 100°C.

Recently, experimental indices on Carbowax 20M have been reported by Tóth[28] at 70°C, by Döring *et al.*[3] at 90°C and by Engewald and Wennich[2] at 100°C.

The data on other phases are limited by the number of authors and do not meet the requirements for UI_T.

RESULTS AND DISCUSSION

A comparison of the literature data obtained by different authors using the same phase shows that even on the most apolar phase, squalane, the experimental data for arenes often differ greatly, in contrast to the retention of other classes of hydrocarbons. For example, the difference in the retention of benzene at 100°C is 4.6 i.u.[10,13], for toluene it is 5.0 i.u.[8,15] and for *p*-xylene it is 3.3 i.u.[17,19].

Much greater differences are found for the same hydrocarbons on polar phases. The interlaboratory reproducibility is so poor that it is impossible to use literature data for a reliable identification. In Table I we compare the values of UI_T calculated from all the available data with the values of I_{exp} from a given author. It is obvious that the I_{exp} value is of little use. The differences between UI_T and I_{exp} are less than ± 1 i.u. only on squalane. The more polar the phase, the greater are the differences: up to 3 i.u. on OV-101 and greater than 10 i.u. on Carbowax 20M.

Unfortunately, the calculated values of UI_T have an unacceptably high standard deviation and could not be used for identification purposes. The only data that

TABLE I

UNIFIED RETENTION INDICES AND EXPERIMENTAL INDICES FOR SOME ARENES ON SQUALANE, OV-101 AND CARBOWAX 20M AT 100°C

Hydrocarbon	*Squalane*			*OV-101*			*Carbowax 20M*		
	UI	I^{8}_{exp}	Δ	*UI*	I^{26}_{exp}	Δ	*UI*	I^{2}_{exp}	Δ
Benzene	650.45	650.5	0.05	662.59	663.6	−1.01	940.25	947.2	−6.95
Toluene	757.63	758.0	−0.37	764.88	766.4	−1.52	1035.40	1043.2	−7.80
Ethylbenzene	847.51	847.7	−0.19	857.62	858.9	−1.28	1119.56	1127.1	−7.54
p-Xylene	861.93	861.8	0.13	866.37	867.7	−1.33	1127.27	1134.8	−7.53
m-Xylene	864.39	863.2	1.19	865.30	866.6	−1.30	1133.02	1140.7	−7.68
o-Xylene	883.97	883.7	0.27	888.75	890.3	−1.55	1175.50	1183.9	−8.40

TABLE II

VALUES OF THE CALCULATED UNIFIED INDEX (UI_0) AT 0°C ON SQUALANE, CALCULATED TEMPERATURE INCREMENT (dUI/dT), STANDARD DEVIATION, s, NUMBER OF EXPERIMENTAL INDICES USED IN THE CALCULATION, n, AND EXPERIMENTAL VALUES OF dI/dT FROM DIFFERENT AUTHORS

No.	*Hydrocarbon*	UI_0	s	n	dUI/dT	dI/dT
1	Benzene	623.01	0.41	13	0.2744	0.24[1]; 0.30[2]; 0.24[12]; 0.23[15]; 0.247[21]; 0.29[29]
2	Toluene	732.98	0.35	15	0.2465	0.245[1]; 0.32[2]; 0.22[12]; 0.22[15]; 0.25[29]
3	Ethylbenzene	821.76	0.24	16	0.2575	0.265[1]; 0.32[2]; 0.24[12]; 0.25[15]; 0.261[29]
4	*p*-Xylene	836.00	0.45	17	0.2593	0.251[1]; 0.34[2]; 0.23[12]; 0.25[15]; 0.26[29]
5	*m*-Xylene	839.42	0.54	14	0.2497	0.245[1]; 0.27[2]; 0.23[12]; 0.30[15]; 0.23[17]; 0.255[29]
6	*o*-Xylene	855.61	0.47	16	0.2836	0.284[1]; 0.34[2]; 0.27[12]; 0.24[15]; 0.27[17]; 0.295[29]
7	Isopropylbenzene	883.56	0.58	10	0.2389	0.264[1]; 0.30[2]; 0.25[12]; 0.26[15]; 0.253[29]
8	*n*-Propylbenzene	911.61	0.40	11	0.2470	0.282[1]; 0.31[2]; 0.26[12]; 0.27[15]; 0.272[29]
9	1-Methyl-3-ethylbenzene	923.99	0.67	10	0.2474	0.242[1]; 0.25[2]; 0.22[12]; 0.25[15]
10	1-Methyl-4-ethylbenzene	928.67	0.33	10	0.2279	0.269[1]; 0.36[2]; 0.24[12]; 0.27[15]
11	1-Methyl-2-ethylbenzene	939.69	0.65	10	0.2559	0.282[1]; 0.29[2]; 0.26[12]; 0.28[15]; 0.35[29]
12	1,3,5-Trimethylbenzene	948.27	0.51	8	0.1944	0.239[1]; 0.25[9]; 0.20[12]; 0.23[15]
13	*tert.*-Butylbenzene	950.93	0.53	7	0.2240	0.29[1]; 0.20[9]; 0.28[14]; 0.31[29]
14	Isobutylbenzene	954.95	0.49	7	0.3497	0.301[1]; 0.23[9]; 0.321[29]
15	1,2,4-Trimethylbenzene	959.06	0.48	8	0.2726	0.228[1]; 0.28[9]; 0.28[12]; 0.30[15]
16	*sec.*-Butylbenzene	959.89	0.48	8	0.3007	0.308[1]; 0.29[9]; 0.30[15]; 0.321[29]
17	1,2,3-Trimethylbenzene	978.19	0.51	8	0.3418	0.337[1]; 0.35[2]; 0.31[15]
18	1-Methyl-2-isopropylbenzene	987.19	0.68	8	0.2968	0.264[1]; 0.25[2]

19	1-Methyl-3-isopropylbenzene	987.56	0.52	8	0.1521	0.216[1]; 0.22[2]; 0.15[9]
20	1-Methyl-4-isopropylbenzene	992.21	0.50	5	0.1824	0.267[1]; 0.22[2]
21	1,3-Diethylbenzene	1002.94	0.38	10	0.2584	0.244[1]; 0.18[2]; 0.23[12]
22	1-Methyl-4-*n*-propylbenzene	1007.63	0.54	5	0.3222	0.282[1]; 0.27[12]; 0.30[29]
23	1-Methyl-3-*n*-propylbenzene	1008.37	0.43	8	0.2522	0.255[1]; 0.23[12]
24	1,4-Diethylbenzene	1010.12	0.64	7	0.3063	0.277[1]; 0.27[12]; 0.362[29]
25	1,2-Diethylbenzene	1011.19	0.47	9	0.2816	0.289[1]; 0.362[29]
26	*n*-Butylbenzene	1012.67	0.54	12	0.2351	0.284[1]; 0.24[12]; 0.35[29]
27	1-Methyl-2-*n*-propylbenzene	1015.06	0.37	10	0.3104	0.298[1]; 0.25[2]; 0.29[12]
28	1,3-Dimethyl-5-ethylbenzene	1023.45	0.23	3	0.2493	0.218[1]
29	*tert.*-Pentylbenzene	1030.86	0.73	4	0.3985	0.369[1]
30	1,4-Dimethyl-2-ethylbenzene	1032.46	0.29	4	0.2745	0.26[1]; 0.32[2]
31	1,2-Dimethyl-4-ethylbenzene	1035.71	0.51	4	0.3677	0.286[1]; 0.31[2]
32	1,3-Dimethyl-4-ethylbenzene	1036.61	0.14	5	0.2979	0.281[1]; 0.24[2]
33	*sec.*-Pentylbenzene	1045.35	0.07	3	0.3280	0.286[1]
34	1-Methyl-4-*tert.*-butylbenzene	1045.50	0.71	4	0.3022	0.292[1]
35	1,2,4,5-Tetramethylbenzene	1071.14	0.32	4	0.3605	0.341[1]; 0.31[2]; 0.31[9]
36	1,2,3,5-Tetramethylbenzene	1077.48	0.37	5	0.3563	0.338[1]; 0.33[2]
37	1,2,3,4-Tetramethylbenzene	1083.84	0.18	5	0.5254	0.395[1]; 0.41[2]; 0.35[9]
38	1-Ethyl-4-*n*-propylbenzene	1093.94	0.07	3	0.3251	0.336[1]
39	1,3-Diisopropylbenzene	1095.19	0.35	4	0.2497	0.195[1]; 0.22[2]
40	*n*-Pentylbenzene	1102.29	0.52	3	0.3326	0.286[1]; 0.27[2]
41	1,3,5-Triethylbenzene	1161.79	0.86	3	0.3252	0.167[1]; 0.17[9]
42	Pentamethylbenzene	1241.75	0.20	4	0.4555	0.452[1]; 0.41[2]

might be used for UI_T calculation with an acceptable variance are those obtained on squalane.

Using the least-square approach, we evaluated the experimental retention indices of 42 arenes on squalane. The values of UI_0, dUI/dT, s and n are given in Table II. The hydrocarbons are arranged in order of increasing values of UI_0. The values of dUI/dT are compared with some of the most similar values of dI/dT cited in the literature.

Comparing the values of UI_0 and dUI/dT for C_6–C_8 aromatic hydrocarbons given here and in ref. 5, it can be concluded that in spite of the different number of input data, the results are adequate. Thus there is a real possibility to check the separation and identification properties of every squalane column for arenes, using the UI_T concept.

Using a limited set of arenes, the I_{exp} values are calculated and compared with UI_T. If they are coincident within ± 1 i.u. the I_{exp} values can be used for a reliable identification. In this case the values of UI_T could be used as a data bank and with the aid of suitable software a compouter-assisted identification might be possible.

Comparing dUI/dT with the experimental values of dI/dT obtained by different authors, it is evident that there are sometimes large differences. We consider the value of dUI/dT as the most reliable and should be used to calculate the optimum analysis temperature for separation of a given mixture of arenes. The I_{exp} values obtained from a given squalane column should be compared with the values of UI_T. We propose also a preliminary test of the column with a limited number of standards in order to determine whether it yields I_{exp} values that are statistically equal to UI_T. If this is not the case, the use of literature data may lead to an incorrect identification.

REFERENCES

1 L. Soják and J. A. Rijks, *J. Chromatogr.*, 119 (1976) 505.
2 W. Engewald and L. Wennrich, *Chromatographia*, 9 (1976) 540.
3 C. Döring, D. Estel and R. Fischer, *J. Prakt. Chem.*, 316 (1974) 1.
4 C. L. Stuckey, *J. Chromatogr. Sci.*, 7 (1969) 177.
5 N. Dimov, *J. Chromatogr.*, 347 (1985) 366.
6 T. Bellas, *Chromatographia*, 8 (1975) 38.
7 L. Soják, V. Berezkin and J. Janák, *J. Chromatogr.*, 209 (1979) 15.
8 V. Švob and D. Deur-Šiftar, *J. Chromatogr.*, 91 (1974) 677.
9 J. Macák, V. Nabivach, P. Buryan and Š. Sinder, *J. Chromatogr.*, 234 (1982) 285.
10 L. Hála, R. Lacko and K. Hegedüsova, *Ropa Uhlie*, 18 (1976) 140.
11 L. Soják and J. Hrivnak, *Ropa Uhlie*, 11 (1969) 361.
12 L. Soják, A. Bucinska and P. Skalák, *Ropa Uhlie*, 12 (1970) 1357.
13 N. Dimov, T. Petkova and D. Shapov, *J. Chromatogr.*, 91 (1974) 691.
14 D. Papazova and M. Pankova, *J. Chromatogr.*, 105 (1975) 411.
15 G. Mitra, G. Mohan and A. Sinha, *J. Chromatogr.*, 91 (1974) 633.
16 E. Kugucheva and V. Machinski, *Zh. Anal. Khim.*, 38 (1983) 2023.
17 G. Schomburg, in J. A. Rijks (Editor), *Thesis*, Eindhoven University of Technology, Eindhoven, 1973, p. 116.
18 J. Rijks and C. Cramers, *Chromatographia*, 7 (1974) 99.
19 J. Loewenguth and D. Tourres, *Fresenius' Z. Anal. Chem.*, 236 (1968) 170.
20 L. Soják and A. Bučinská, *J. Chromatogr.*, 51 (1970) 75.
21 R. Hively and R. Hinton, *J. Gas Chromatogr.*, 6 (1968) 203.
22 C. Döring, D. Estel, J. Weber, G. Zimmerman and D. Zschummel, *J. Prakt. Chem.*, 313 (1971) 1081.

23 D. Desty, A. Goldup and W. Swanton, in N. Breuner *et al.*(Editors), *Gas Chromatography*, Academic Press, New York, 1962, p. 105.
24 N. Johansen and L. Ettre, *Chromatographia*, 15 (1982) 625.
25 V. Gerasimenko, A. Kirilenko and V. Nabivach, *J. Chromatogr.*, 208 (1981) 9.
26 V. Gerasimenko and V. Nabivach, *Zh. Anal. Khim.*, 37 (1982) 110.
27 S. Boneva, D. Papazova and N. Dimov, *God. Vissh. Khim. Tekhnol. Inst. Burgas, Bulg.*, 18 (1983) 143.
28 T. Tóth, *J. Chromatogr.*, 279 (1983) 157.
29 N. Dimov, T. Petkova and D. Shopov, *J. Chromatogr.*, 74 (1972) 165.

Journal of Chromatography, 356 (1986) 326–330
Elsevier Science Publishers B.V., Amsterdam — Printed in The Netherlands

CHROM. 18 419

Note

Determination of biotin in multivitamin pharmaceutical preparations by high-performance liquid chromatography with electrochemical detection

KUNIHIRO KAMATA*, TERUHIKO HAGIWARA, MISAKO TAKAHASHI, SHINICHI UEHARA, KYOKO NAKAYAMA and KAZUYUKI AKIYAMA

Tokyo Metropolitan Research Laboratory of Public Health, 24-1, Hyakunincho 3-chome, Shinjuku-ku, Tokyo, 160 (Japan)

(First received November 18th, 1985; revised manuscript received December 16th, 1985)

Biotin (vitamin H, coenzyme R) is widely distributed in animals and plants, and was first isolated from egg yolk[1]. It is one of the most active biological substances known, being a coenzyme essential in amino acid metabolism and in the maintenance of skin, hair and nerves, with an important rôle in growth, decarboxylation of amino acids and carbohydrate metabolism.

Microbiological methods are generally used to determine small amounts of biotin[2–7]. However, these methods require an incubation period of 18–24 h in addition to the sample preparation. The chemical methods reported comprise spectrophotometric assays based on the binding of a dye with avidin[8–10], oxidation with potassium iodate[11] or reaction with 4-dimethylaminocinnamaldehyde[12,13]. None is applicable to multivitamin pharmaceutical preparations because of a lack of sensitivity, or due to interferences from other water-soluble vitamins. Several gas chromatographic procedures have been reported[14,15], but all involve volatilizing biotin by silation. Therefore, other methods for the determination of biotin in multivitamin pharmaceutical preparations are needed.

It has recently been demonstrated that high-performance liquid chromatography (HPLC) is suitable for the analysis of many drugs, and numerous applications of this technique to multivitamin pharmaceutical preparations have been reported[16–21]. Biotin is difficult to determine by conventional HPLC techniques, because it does not have an adequate UV chromophore. It must be measured at a low UV wavelength when direct UV detection is applied. Thomas *et al.*[22] described a procedure for the quantitative analysis of biotin in pharmaceutical products by using a reversed-phase column, and an UV monitor operating at 230 nm. Kanazawa *et al.*[23] described a method for determining biotin as its 9-anthryl ester by HPLC with fluorometric detection.

We have applied HPLC with electrochemical detection (ED) to the determination of biotin in multivitamin pharmaceutical preparations, and describe here some factors affecting the analysis.

0021-9673/86/$03.50

EXPERIMENTAL

Chemicals

Biotin (Wako), acetonitrile (HPLC grade; Wako), ethanol (95%, v/v; Wako), potassium dihydrogen phosphate (KH_2PO_4), phosphoric acid (analytical reagent grade; Wako) and deionized water were used.

Instrumentation

The HPLC apparatus consisted of a JASCO pump Model BIP-I (Japan Spectroscopic, Tokyo, Japan), a Rheodyne injector Model 7125 equipped with a 20-μl loop (Rheodyne, CA, U.S.A.) and an electrochemical detector Model VMD-101A (Yanagimoto, Kyoto, Japan). The potential of the detector was set at +1.4 V *versus* a silver–silver chloride reference electrode. Prepacked LiChrosorb RP-18 Hiber (7 μm, 250 × 4.6 mm I.D., Cica Merck) was used under ambient conditions. Acetonitrile–0.05 *M* KH_2PO_4 (adjusted to pH 2.0 with phosphoric acid) (15:85) was used as a mobile phase at a flow-rate of 1 ml/min. It was filtered through a Millipore membrane filter (0.45 μm; Millipore, Bedford, MA, U.S.A.) and degassed under vacuum prior to use. Samples of 5 μl were injected. The results were evaluated by the Shimadzu Chromatopac C-R1A digital integrator. The ultrasonic bath was from Kyoto Daichi Kagaku (Kyoto, Japan).

Sample preparation

A representative number (usually 20) of tablets were accurately weighed and finely powdered so as to pass through a 60-mesh sieve. A suitable amount of the powder was placed in a 50-ml volumetric flask. The final biotin concentration was *ca.* 50 μg/ml. Approximately 30 ml of 0.05 *M* KH_2PO_4 (pH 2) were added and the flask was placed in an ultrasonic bath for 10 min. After cooling to room temperature, the contents were diluted to the volume with 0.05 *M* KH_2PO_4 (pH 2). A portion of the sample solution was filtered through a 0.45-μm filter, discarding the first 10 ml of filtrate. A 5-μl volume of the filtrate was injected for HPLC.

RESULTS AND DISCUSSION

The relationship between the applied potential and sensitivity was examined first by changing the potential from +0.9 to +1.6 V *versus* the silver–silver chloride reference electrode, other conditions being held constant. The results are shown in Fig. 1. The sensitivity of the detector increased with increasing potential between +0.9 and +1.4 V, but was almost constant in the range +1.4 to +1.6 V. The large background current arising at high detector potentials led to baseline drift and higher noise. From these results, the potential was chosen a +1.4 V *versus* silver–silver chloride reference electrode.

The effects of the mobile phase pH and the concentration of KH_2PO_4 on the sensitivity were then examined. As is seen from Figs. 2 and 3, the sensitivity of the detector increased with decreasing mobile phase pH, and with increasing concentration of KH_2PO_4 between 0.005 and 0.05 *M*. The sensitivity was almost constant in the range 0.05–0.1 *M* KH_2PO_4. Therefore, pH 2.0 and 0.05 *M* KH_2PO_4 were adopted.

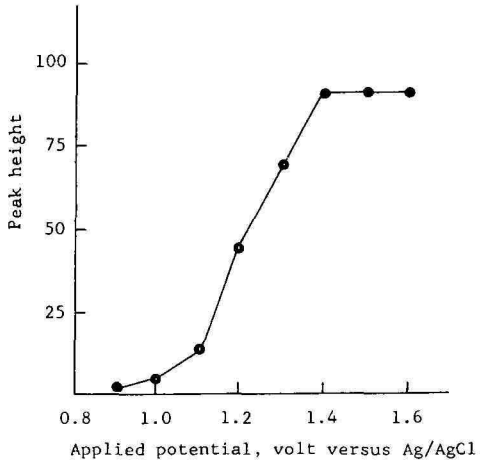

Fig. 1. Dependence of the electrochemical detector response upon the applied potential. Mobile phase: 15% acetonitrile–0.05 *M* KH_2PO_4 (pH 2.0); flow-rate, 1.0 ml/min.

The solvent had a very strong influence on the HPLC separation. Various mixtures of acetonitrile and 0.05 *M* KH_2PO_4 (pH 2.0) were used on the LiChrosorb RP-18 column. For sufficiently rapid elution a content of about 15% acetonitrile was needed. At lower acetonitrile percentages the retention time was increased.

The effects of the mobile phase pH and the concentration of KH_2PO_4 on the retention time are shown in Table I. The retention time decreased with increasing pH, and with increasing concentration of KH_2PO_4.

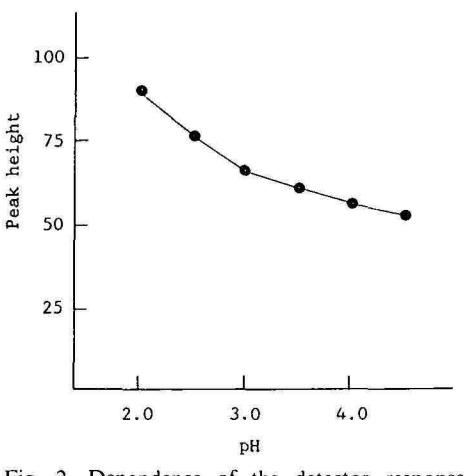

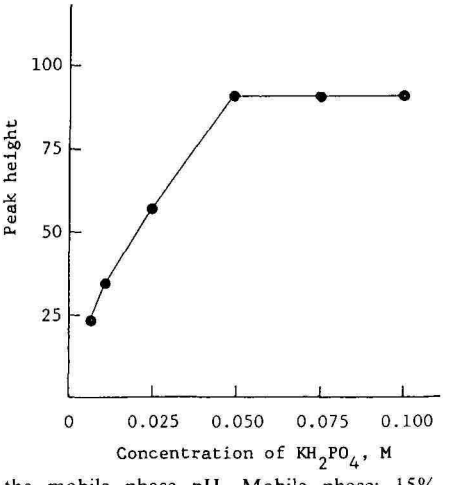

Fig. 2. Dependence of the detector response upon the mobile phase pH. Mobile phase: 15% acetonitrile–0.05 *M* KH_2PO_4, adjusted to the appropriate pH by titration with H_3PO_4; flow-rate, 1.0 ml/min. Electrode potential: +1.4 V *vs.* Ag/AgCl.

Fig. 3. Dependence of the detector response upon mobile phase ionic strength. Mobile phase: various concentrations of KH_2PO_4 (pH 2.0) with 15% acetonitrile; flow-rate, 1.0 ml/min. Electrode potential: +1.4 V *vs.* Ag/AgCl.

TABLE I

EFFECTS OF MOBILE PHASE pH AND CONCENTRATION OF KH_2PO_4 ON THE RETENTION TIME OF BIOTIN

Content of acetonitrile is 15%.

pH	*Concentration of KH_2PO_4 (M)*	*Retention time (min)*
2	0.01	9.60
2	0.05	8.92
2	0.10	8.57
3	0.05	8.23
4	0.05	7.27

The electrochemical detector was found to be more sensitive than an UV detector operating at 230 nm by at least a factor of ten. The limits of detectability for biotin range between 5 and 10 ng, based on twice the noise level. The linearity of the detector response to biotin was tested by injecting 5 μl of 5–50 μg/ml solutions of biotin. The plot of the peak height *versus* the amount of biotin was linear (correlation coefficient, 0.998). The precision of the chromatographic system was tested by five injections of the biotin: a standard deviation of 0.45% for 50 μg of biotin is typical. Thus this method can be used for quantitation.

Studies were conducted on the separation of six water-soluble vitamins which are widely used in multivitamin pharmaceutical preparations. The chromatographic behaviour of these compounds is summarized in Table II.

Thomas *et al.*[22] suggested that the HPLC determination of biotin in pharmaceutical products by direct injection without clean-up was difficult, because the coexisting riboflavin interfered with the determination. Our method was free from interference by riboflavin.

In order to investigate its applicability, the present method was applied to some multivitamin pharmaceutical preparations. A typical chromatographic separation of biotin is shown in Fig. 4. The chromatograms of all the other samples also showed a sharp peak for biotin with no interference from other substances. The

TABLE II

CHROMATOGRAPHIC BEHAVIOUR OF BIOTIN AND SOME WATER-SOLUBLE VITAMINS

Compound	*Retention time (min)*	
	ED	*UV 254 nm*
Biotin	8.92	8.89
Calcium pantothenate	–	3.24
Riboflavin	–	7.22
Niacinamide	–	2.52
Pyridoxine hydrochloride	2.68	2.57
Ascorbic acid	2.47	2.46
Thiamine hydrochloride	–	2.77

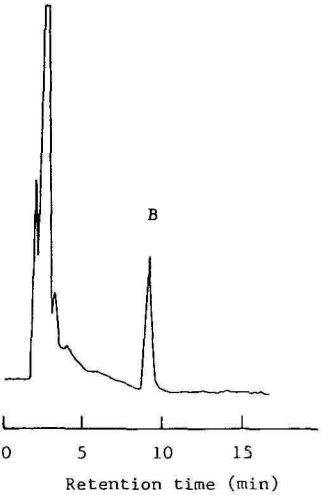

Fig. 4. Chromatogram of a multivitamin tablet extract. Peak B is biotin. Conditions as in the text.

results indicate that this method is suitable for the determination of biotin in multivitamin pharmaceutical preparations.

REFERENCES

1 W. G. Bateman, *J. Biol. Chem.*, 26 (1916) 263.
2 E. E. Snell, R. E. Eakin and R. J. Williams, *J. Am. Chem. Soc.*, 62 (1940) 175.
3 L. D. Wright and H. R. Skeggs, *Proc. Soc. Exp. Biol. med.*, 56 (1944) 95.
4 G. G. Villela and A. Cury, *Proc. Soc. Exp. Biol. Med.*, 76 (1951) 341.
5 K. Dittmer and V. du Vigneaud, *J. Biol. Chem.*, 169 (1947) 63.
6 M. N. Voigt, R. R. Eitenmiller and G. O. Ware, *J. Food Sci.*, 43 (1978) 1418.
7 M. N. Voigt, R. R. Eitenmiller and G. O. Ware, *J. Food Sci.*, 44 (1979) 729.
8 N. M. Green, *Biochem. J.*, 94 (1965) 23C.
9 J. H. Lin and F. J. Kirsch, *Anal. Biochem.*, 81 (1977) 442.
10 A. Jameel and K. K. Verma, *Talanta*, 26 (1979) 1025.
11 C. Plinton, F. P. Mahn, M. Hawrylshyn, V. S. Venturella and B. Z. Senkowski, *J. Pharm. Sci.*, 58 (1969) 875.
12 K. Shimada, Y. Nagase and U. Matsumoto, *Yakugaku Zasshi*, 89 (1969) 436.
13 D. B. McCormick and J. A. Roth, *Anal. Biochem.*, 34 (1970) 226.
14 M. G. Horning, E. A. Boucher and A. M. Moos, *J. Gas Chromatogr.*, 5 (1967) 297.
15 V. Viswanathan, F. P. Mahn, V. S. Venturella and B. Z. Sennkowski, *J. Pharm. Sci.*, 59 (1970) 400.
16 R. B. H. Wills, C. G. Shaw and W. R. Day, *J. Chromatogr. Sci.*, 15 (1977) 262.
17 R. P. Kwok, W. P. Rose, R. Tabor and T. S. Pattison, *J. Pharm. Sci.*, 70 (1981) 1014.
18 R. L. Kirchmeir and R. P. Upton, *J. Pharm. Sci.*, 67 (1978) 1444.
19 R. Vanhaelen-Fastré and M. Vanhaelen, *J. Chromatogr.*, 153 (1978) 219.
20 C. Mackay, J. Tillman and D. T. Burns, *Analyst (London)*, 104 (1979) 626.
21 S. A. Barnett, L. W. Frick and H. M. Baine, *Anal. Chem.*, 52 (1980) 610.
22 H. S. Thomas, S. Shyamala and A. J. Rebecca, *J. Assoc. Off. Anal. Chem.*, 67 (1984) 994.
23 Y. Kanazawa, T. Nakano and H. Tanaka, *Nippon Kagaku Kaishi*, 3 (1984) 434.

Journal of Chromatography, 356 (1986) 331–333
Elsevier Science Publishers B.V., Amsterdam — Printed in The Netherlands

CHROM. 18 429

Note

Separation and identification of phenol–formaldehyde condensates by gas chromatography–mass spectrometry

IV*. Application of a stationary phase of intermediate polarity to the analysis of methylolated dihydroxydiphenylmethanes

LÁSZLÓ PRÓKAI
Hungarian Oil and Gas Research Institute, József A. u. 34, H-8200 Veszprém (Hungary)
(Received December 10th, 1985)

Previous studies on the composition of the condensation products of phenol with formaldehyde have revealed that gas chromatography–mass spectrometry (GC–MS) using trimethylsilylation has considerable potential in the characterization of many low-molecular-weight compounds found in different resins[1–6]. In investigations of the reaction mechanisms, several types of oligomeric species have received attention, especially those formed by the condensation of two or more phenolic nuclei. In certain instances not all the possible positional isomers of a given structure were detected. For instance, Lindner[1] identified 2,2′- and 4,4′-dihydroxydiphenylmethane in a product obtained under base-catalysed conditions and on applying an excess of formaldehyde the 2,4′-isomer was found to be absent.

The assignment of methylolated dihydroxydiphenylmethane positional isomers present in resol-type resins has been attempted based on the fact that the number of components separated by apolar stationary phases was less than the number of possible isomers and provided that complete separation has been achieved, the best matching was achieved by considering only two of the three possible types of connections of phenolic units via methylene bridges (*viz.*, 2,2′- and 4,4′-dihydroxy compounds).

Reversed-phase high-performance liquid chromatographic (HPLC) separation of the title compounds has been reported recently by Mechin *et al.*[7]. ^{1}H and ^{13}C NMR spectrometric investigations revealed the predominant formation of 2,4′- and and 4,4′-connections for the methylolated dimers.

This study was undertaken to reinvestigate the effectiveness of GC analyses in the field concerned.

EXPERIMENTAL

Gas chromatograms were recorded on a JGC-20K (JEOL, Tokyo, Japan) instrument equipped with a flame ionization detector and using an SP-4000 chromato-

* For Part III, see ref. 6.

0021-9673/86/$03.50

graphy data system (Spectra-Physics, San Jose, CA, U.S.A.). The mass spectrometer interfaced to the gas chromatograph as described earlier[4,5]. Borosilicate glass column of 30 m × 0.25 mm I.D. coated with SP-2250 stationary phase of 0.20 μm film thickness (Supelco, Bellefonte, PA, U.S.A.) was used. Helium was applied as the carrier gas with a linear velocity of 30 cm/min. The injection port and detector temperatures were maintained at 280°C. Split injection with a ratio of *ca.* 1:100 was used. The column oven was held at 120°C for 3 min, then programmed to 280°C at 12°C/min.

The preparation and trimethylsilylation of resol with N,O-bis(trimethylsilyl) trifluoroacetamide (BSTFA) were carried out as described previously[5].

RESULTS AND DISCUSSION

Using a stationary phase of intermediate polarity [SP-2250; methylsilicone–phenylsilicone (50:50)] in the analysis of trimethylsilylated resol obtained with a 1:1.5 phenol to formaldehyde molar ratio, in contrast with apolar stationary phases[5], trinuclear phenols and methylolated trinuclear phenols were not present in the chromatogram under the conditions described above. Mononuclear methylolated phenols showed similar retention properties in both instances.

Further separation of the methylolated dihydroxydiphenylmethanes was achieved, however, as is shown by the relevant part of the chromatogram in Fig. 1. GC and GC–MS investigations of the unsubtituted dimers revealed that only 2,4'- and 4,4'-dihydroxydiphenylmethane were present. From a chemical point of view it

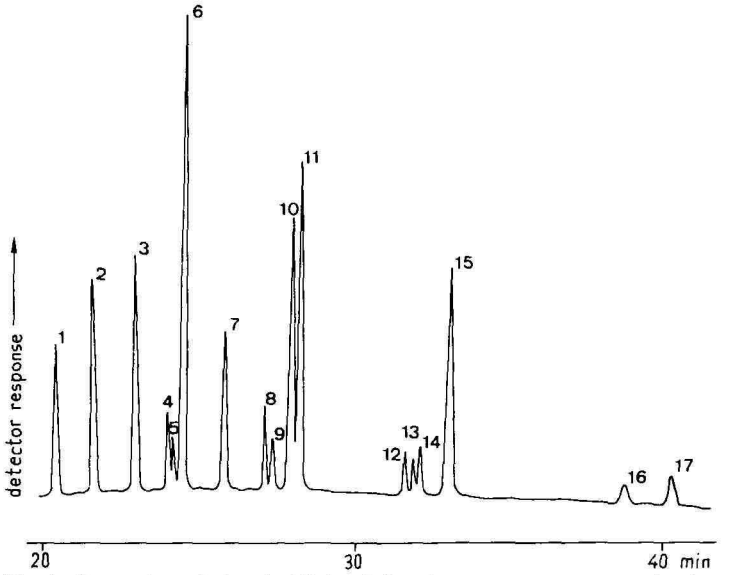

Fig. 1. Separation of trimethylsilylated dinuclear compounds present in phenol–formaldehyde resol. Column, 30 m × 0.25 mm I.D. coated with 0.20 μm SP-2250. Carrier gas, helium, linear velocity 30 cm/min. Split injection (1:100); port temperature, 280°C. Flame ionization detector; temperature, 280°C. GC oven, initial hold for 3 min at 120°C then programmed to 280°C at 12°C/min. For peak assignments, see in Table I.

TABLE I

IDENTIFICATION OF COMPONENTS HAVING THE DIHYDROXYDIPHENYLMETHANE SKELETON AS TRIMETHYLSILYL DERIVATIVES

Peak No.	*Compound*
1	2,4'-Dihydroxydiphenylmethane
2	4,4'-Dihydroxydiphenylmethane
3	3'-Methylol-2,4'-dihydroxydiphenylmethane
4	3-Methylol-2,4'-dihydroxydiphenylmethane
5	5-Methylol-2,4'-dihydroxydiphenylmethane
6	3-Methylol-4,4'-dihydroxydiphenylmethane
7	3',5'-Dimethylol-2,4'-dihydroxydiphenylmethane
8	3,3'-Dimethylol-2,4'-dihydroxydiphenylmethane
9	5,3'-Dimethylol-2,4'-dihydroxydiphenylmethane
10	3,3'-Dimethylol-4,4'-dihydroxydiphenylmethane
11	3,5-Dimethylol-4,4'-dihydroxydiphenylmethane
12	3,3',5'-Trimethylol-2,4'-dihydroxydiphenylmethane
13	5,3',5'-Trimethylol-2,4'-dihydroxydiphenylmethane
14	3,5,3'-Trimethylol-2,4'-dihydroxydiphenylmethane
15	3,5,3'-Trimethylol-4,4'-dihydroxydiphenylmethane
16	3,5,3',5'-Tetramethylol-2,4'-dihydroxydiphenylmethane
17	3,5,3',5'-Tetramethylol-4,4'-dihydroxydiphenylmethane

is obvious that these compounds can be accepted as skeletons of methylol-substituted components. This conclusion is confirmed by ^{13}C NMR spectrometric results. Based on mass spectra, the two distinct groups of isomers are readily distinguishable. The only problem is the assignment of components possessing the 2,4'-dihydroxydiphenylmethane skeleton but substituted by only one methylol in the ring having an *ortho*-hydroxy group relative to the methylene bridge in the parent compound (*i.e.*, for peaks 4 and 5, 8 and 9, 12 and 13). These pairs of isomer structures produce similar mass spectra as expected from the fragmentation pattern[5].

Obviously, the position of the substituent introduced by the condensation with formaldehyde can be *ortho* or *para* as in mononuclear compounds where the order of retention for trimethylsilyl derivatives has been ascertained previously[1,3,5]. Accepting the rule that *ortho* isomers precede *para* isomers in the present compounds also, the tentative identification of components containing two aromatic nuclei is made as listed in Table I. These assignments are in agreement with the results of HPLC separation followed by NMR spectroscopy[7]; hence GC can also be applied effectively for the characterization of dimer condensation products present in resol-type resins.

REFERENCES

1 W. Lindner, *J. Chromatogr.*, 151 (1978) 406.
2 R. Gnauck and D. Habisch, *Plaste Kautsch.*, 27 (1980) 485.
3 G. M. Anthony and G. Kemp, *Angew. Makromol. Chem.*, 115 (1983) 183.
4 L. Prókai, *J. Chromatogr.*, 329 (1985) 290.
5 L. Prókai, *J. Chromatogr.*, 331 (1985) 91.
6 L. Prókai, *J. Chromatogr.*, 333 (1985) 161.
7 B. Mechin, D. Hanton, J. Le Goff and J. P. Tanneur, *Eur. Polym. J.*, 20 (1984) 333.

Journal of Chromatography, 356 (1986) 334–340
Elsevier Science Publishers B.V., Amsterdam — Printed in The Netherlands

CHROM. 18 409

Note

Comparison between high-performance thin-layer chromatography–densitometry and high-performance liquid chromatography for the determination of ajmaline, reserpine and rescinnamine in *Rauwolfia vomitoria* root bark

P. DUEZ and S. CHAMART

Laboratoire de Chimie Analytique, Chimie Pharmaceutique Inorganique et Toxicologie, CP 205/1, Université Libre de Bruxelles, Campus Plaine, 1050 Bruxelles (Belgium)

M. VANHAELEN* and R. VANHAELEN-FASTRÉ

Laboratoire de Pharmacognosie, CP 205/4, Université Libre de Bruxelles, Campus Plaine, 1050 Bruxelles (Belgium)

and

M. HANOCQ and L. MOLLE

Laboratoire de Chimie Analytique, Chimie Pharmaceutique Inorganique et Toxicologie, CP 205/1, Université Libre de Bruxelles, Campus Plaine, 1050 Bruxelles (Belgium)

(Received December 12th, 1985)

A number of alkaloids have been isolated from Rauwolfia root barks[1]. Reserpine and rescinnamine are ester alkaloids related to the principal medicinal use of the drug, *i.e.*, the treatment of hypertension and mental disorders[2]; ajmaline is a non-esterified alkaloid and is widely used as an anti-arrhythmic compound, but also as a precursor of semi-synthetic drugs[3].

A number of methods have been proposed for the standardization of Rauwolfia. [They include: total alkaloids gravimetry[4,5], spectrometry of the reserpine-like ester alkaloids[5,6], separation by paper chromatography and spectrometric measurement of reserpine and rescinnamine[7,8]. For these last compounds, thin-layer chromatography (TLC)[9,10], electrophoresis[11], TLC–densitometry[12–14], high-performance liquid chromatography (HPLC)[15,16] have also been used. Assays of ajmaline have been performed by TLC–densitometry[14] and by gas–liquid chromatography (GLC)[3].] Most of these methods were unsatisfactory so that rapid and reliable methods had to be developed in order to study the effects of ecophysiological conditions on the alkaloid production of *Rauwolfia vomitoria* Afz.

An extensive degradation of reserpine and rescinnamine occurs on silica gel so that the addition of α-tocopherol acid succinate to standard solutions was found essential in order to perform the accurate determination of these two alkaloids. Most of the previously described TLC assays for reserpine and rescinnamine were probably biased because of the non-consideration of this degradation.

A new HPLC method, performed on an octadecylsilane column, has allowed the analysis of the three alkaloids in crude plant extracts and the ascertainment of the results obtained by the described HPTLC densitometric methods. All methods

0021-9673/86/$03.50

required a two-step analysis because of the wide difference in the chromatographic behaviours of ajmaline and reserpine–rescinnamine.

EXPERIMENTAL

As far as possible, all the described operations were effected in darkness.

The Perkin-Elmer chromatograph was equipped with a pump (Model 601), a sample loop (Rheodyne 7105), an UV detector (Model LC-55 equipped with the scanner LC-55S, operating at 250 nm for the analysis of reserpine–rescinnamine and at 292 nm for ajmaline) and a 250 × 4 mm I.D. Lichrocart cartridge prepacked with LiChrosorb RP-18, 7 μm (Merck, Darmstadt, F.R.G.). The flow-rate was 1 ml/min. For the analysis of reserpine–rescinnamine, the mobile phase was phosphate buffer (0.04 *M* NaH_2PO_4 and 0.01 *M* Na_2HPO_4)–acetonitrile–1-propanol–tetrahydrofuran (70:13:13:4) and the column was maintained at 40°C while for the ajmaline assays the mobile phase was phosphate buffer (0.04 *M* NaH_2PO_4 and 0.01 *M* Na_2HPO_4)–1-propanol–tetrahydrofuran (95:1:4) and the column temperature was 45°C.

HPTLC pre-coated plates of silica gel 60 F 254 (20 × 10 cm) were obtained from Merck. The solutions (1 μl, standards or crude extracts) were applied 15 mm from the lower edge of the plates and then developed with petroleum benzine (b.p. 40–60°C)–acetone–diethylamine (70:20:10), for reserpine–rescinnamine analysis, or with chloroform–cyclohexane–diethylamine (70:20:10) for ajmaline assays; these mobile phases were allowed to migrate a distance of 100 mm when the plates were placed in unsaturated tanks at a temperature of 20°C. After drying at 105°C for 15 h (reserpine/rescinnamine) or for 2 h (ajmaline), the spots were measured with a Shimadzu high speed TLC scanner CS-930 equipped with a fluorescence attachment. The following settings were used: zigzag stroke width, 9 mm; swing width, 0.2 mm; beam size, 0.4 × 0.4 mm; fluorescence-reflection mode with λ (excitation) = 365 nm, filter 3 (UV cut-off = 480 nm) for reserpine–rescinnamine analysis; absorption-reflection mode with λ (absorption) = 292 nm for ajmaline assays. In both cases, the mean values were calculated by integration of nine spots corresponding to three different standard concentrations, each analysed twice, and three spots of the solution of unknown concentration.

A 100-mg amount of a *Rauwolfia vomitoria* root bark powder (315 μm) was weighed in a 10-ml glass-stoppered centrifuge-tube and 10 mg of calcium hydroxide, 0.2 ml of water and 5 ml of methanol were added. This suspension was shaken for 15 min and centrifuged at 2000 *g*, these two steps being repeated thrice with 5 ml methanol. The supernatants were combined and evaporated to dryness under reduced pressure; the residue was dissolved in 1 ml of methanol and filtered through a Millipore HV-4 filter.

Standards for HPLC were 1/10 to 8/10 dilutions in methanol of a stock solution prepared by dissolving either 10 mg of reserpine base (Boehringer) and 5 mg of rescinnamine base (Inverni & Della Beffa) or 25 mg of ajmaline (Sigma, St. Louis, MO, U.S.A.) in 50 ml of methanol–chloroform (96:4).

For HPTLC, the same standard solutions could be used in the case of ajmaline, whereas for reserpine and rescinnamine other solutions were prepared according to the same modus operandi but using 2% α-tocopherol acid succinate in "hydro-methanolic solution" instead of methanol.

RESULTS AND DISCUSSION

HPLC

There have been few reports on the HPLC separation of Rauwolfia alkaloids in plant material, probably because of low efficiency and peak tailing, both on normal and reversed phases. The chromatographic conditions initially proposed by Robinson[15] were modified so as to obtain the reserpine and rescinnamine separation in

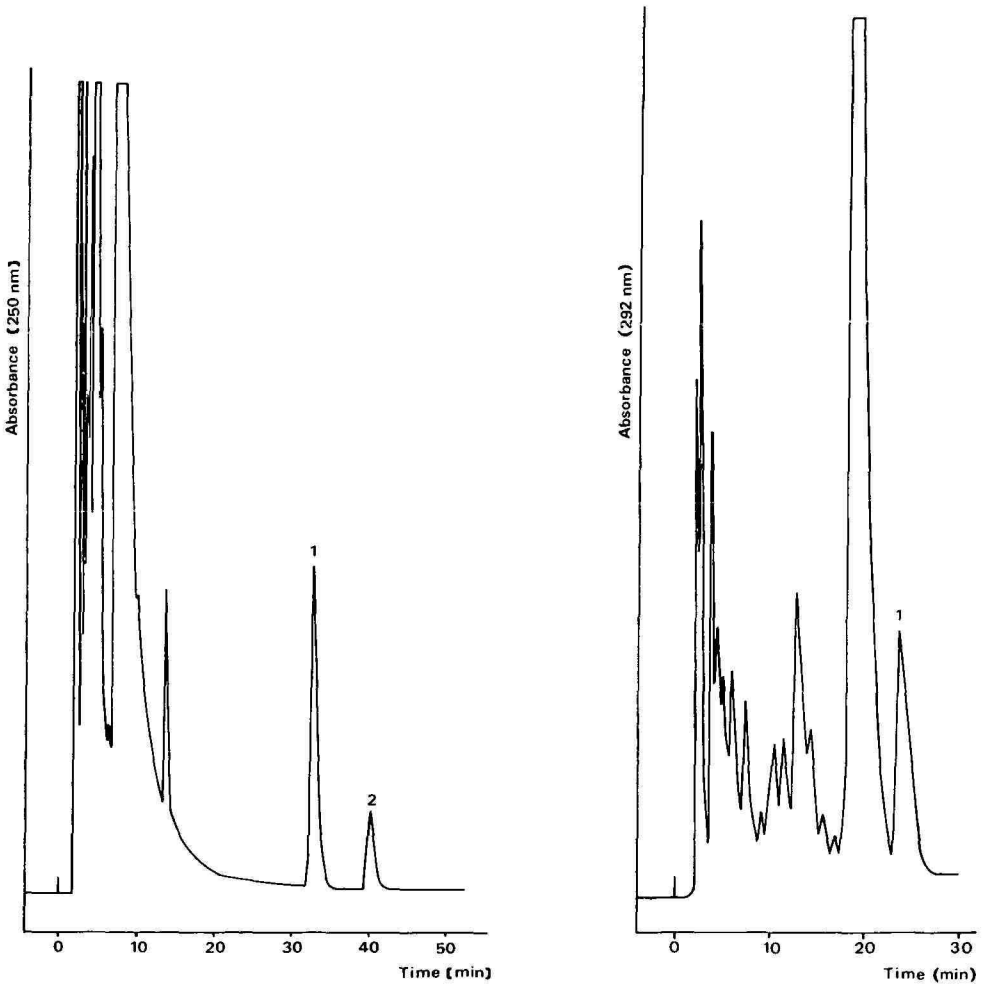

Fig. 1. HPLC chromatogram of a *Rauwolfia vomitoria* stem bark extract. Column packing: Lichrosorb RP-18, 7 μm. Mobile phase: phosphate buffer (0.04 *M* NaH_2PO_4 and 0.01 *M* Na_2HPO_4)–acetonitrile–1-propanol–tetrahydrofuran (70:13:13:4) at a flow-rate of 1 ml/min. Column temperature: 40°C. Detection: UV at 250 nm. Peaks: 1 = reserpine; 2 = rescinnamine.

Fig. 2. HPLC chromatogram of a *Rauwolfia vomitoria* stem bark extract. Column packing: Lichrosorb RP-18, 7 μm. Mobile phase: phosphate buffer (0.04 *M* NaH_2PO_4 plus 0.01 *M* Na_2HPO_4)–1-propanol–tetrahydrofuran (95:1:4) at a flow-rate of 1 ml/min. Column temperature: 45°C. Detection: UV at 292 nm. Peak: 1 = ajmaline.

crude plant extracts (Fig. 1) and further adapted to allow an efficient ajmaline retention on the RP-18 column (Fig. 2).

For the analysis of reserpine–rescinnamine, the insufficient selectivity of binary systems such as acetonitrile–buffer was improved by addition of 1-propanol to the mobile phase; the introduction of tetrahydrofuran and higher temperatures allowed an important reduction of the peak tailing without any loss of resolution.

Concerning the analysis of ajmaline, the described conditions are to be considered as "limit conditions", leading to a rapid saturation of the columns with random peaks from previous injections which interfere in the chromatograms, so that frequent washings of the column with methanol–water (50:50) were required, at least twice a day. As described, these assays were only employed to confirm the HPTLC results.

The purity of ajmaline, reserpine and rescinnamine peaks obtained from plant extracts was tested by UV spectroscopy.

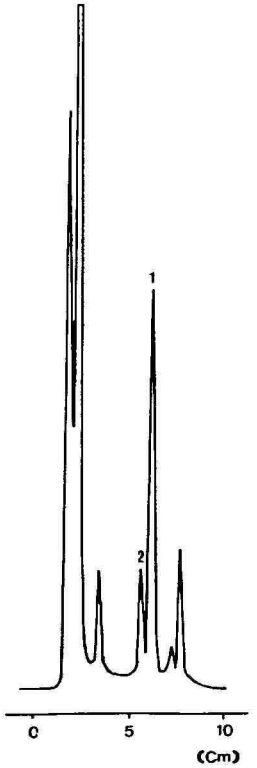

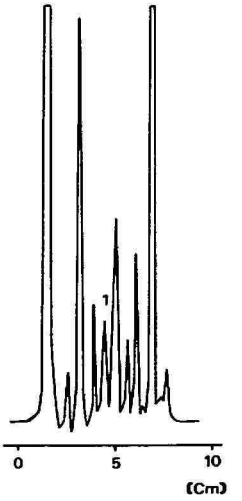

Fig. 3. Scanning profile of an HPTLC chromatogram of a *Rauwolfia vomitoria* stem bark extract. Adsorbent: silica gel 60 F 254. Mobile phase; petroleum benzine (b.p. 40–60°C)–acetone–diethylamine (70:20:10). λ(excitation) = 365 nm; filter 3 (UV cut-off 480 nm). Peaks as in Fig. 1.

Fig. 4. Scanning profile of an HPTLC chromatogram of a *Rauwolfia vomitoria* stem bark extract. Adsorbent: silica gel 60 F 254. Mobile phase: chloroform–cyclohexane–diethylamine (70:20:10). λ(absorption) = 292 nm. Peaks as in Fig. 2.

HPTLC

From the previous studies on the TLC of Rauwolfia alkaloids[17], it became evident that it would not be possible to determine all three alkaloids with a one-step chromatographic development because of the large basicity and polarity differences between ajmaline and reserpine–rescinnamine.

Reserpine and rescinnamine were resolved with one of the solvent systems described by Court and Hubib[18] but using unsaturated tanks at 20°C (Fig. 3). The separation was extremely dependent on the saturation conditions and development temperature.

The purity of the ajmaline spot was uncertain because of the number of substances having similar R_F values and UV spectra; this explains the need for an HPLC method allowing comparison of assay results. An efficient separation was realized

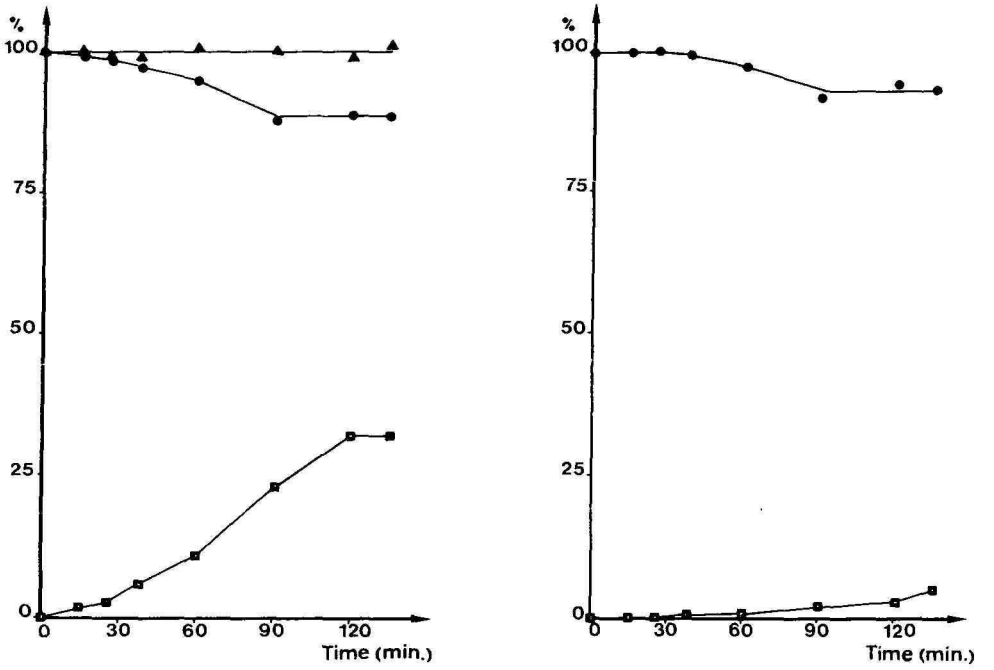

Fig. 5. Degradation of reserpine between the time of application on the silica gel plate and development (time 0): Chromatographic conditions as in Fig. 3; between each application of spots, the plates were left at ambient temperature. ▲—▲; The ratio of the reserpine signal at time t to the reserpine signal at time 0 (percentage) for a *Rauwolfia vomitoria* stem bark extract as a function of the time between application and development. ●—●; Plot as above for a standard. ■—■, The ratio of the signal at time t of the reserpine degradation product (3-dehydro according to Frijns[12]) and to the reserpine signal at time t (percentage) for a standard.

Fig. 6. Degradation of reserpine, in the presence of α-tocopherol acid succinate, between the time of application on the silica gel plate and development (time 0). Chromatographic conditions as in Fig. 3; between each application of spots, the plates were left at ambient temperature. ●—●, The ratio of the reserpine signal at time t to the reserpine signal at time 0 (percentage) for a standard containing α-tocopherol acid succinate as a function of the time between application and development. ■—■, The ratio of the signal at time t of the reserpine degradation product (3-dehydro according to Frijns[12]) to the reserpine signal at time t (percentage) for a standard containing α-tocopherol acid succinate.

TABLE I

DETERMINATION OF RESERPINE, RESCINNAMINE AND AJMALINE IN *RAUWOLFIA VOMITORIA* Afz. EXTRACTS: COMPARISON OF DENSITOMETRIC AND HPLC RESULTS

Alkaloid	*Sample*	*HPTLC with densitometry*		*HPLC*	
		Mean alkaloid (dried powder) (%)	*R.S.D. (%)*	*Mean alkaloid (dried powder) (%)*	*R.S.D. (%)*
Reserpine	1	0.16	6	0.19	2
	2	0.20	2	0.20	4
	3	0.60	3	0.69	4
	4	1.07	2	1.15	2
	5	0.86	1	1.00	4
Rescinnamine	1	0.04	5	0.04	3
	2	0.13	2	0.13	3
	3	0.10	5	0.11	5
	4	0.50	5	0.53	2
	5	0.33	1	0.37	5
Ajmaline	1	0.37	2	0.38	4
	2	0.68	4	0.69	2
	3	1.34	5	1.31	4
	4	0.29	3	0.26	7
	5	0.91	3	0.93	4

using a solvent system described by Kaess and Mathis[19], once again working with unsaturated tanks at 20°C (Fig. 4).

The fluorescence of the reserpine and rescinnamine spots was best developed by keeping the plates at 105°C in the dark for 15 h which yielded stable fluorescent derivatives, probably 3-dehydro[12]; this was preferred to Frijns' method[12] (exposure to light for 2 h), because of its easier reproducibility.

To our knowledge, Frijns[12] is the only author to have noticed the degradation of reserpine and rescinnamine that occurs between application of the spots and the development of the silica gel plates. This degradation probably does not occur during the chromatographic process because no tailing of the spots could be observed; it was noticed only for standard solutions and not for the plant extracts (Fig. 5). From our results, the addition of α-tocopherol acid succinate to the standard solutions was found essential to delay this degradation (Fig. 6). Thus assay errors are reduced if the standard spots are applied moments before development, the time between the first standard spot and development being less than 20 min. Curves similar to those shown in Figs. 5 and 6 were obtained for rescinnamine.

Concentrations of 20–200 ng reserpine, 20–100 ng rescinnamine and 50–500 ng ajmaline per μl spotted afforded linear calibration graphs with r values (correlation coefficients) typically greater than 0.999; the detection limits were 5, 5 and 20 ng respectively.

Extraction procedure and comparison between HPTLC–densitometric and HPLC results

A four-step extraction procedure assured that at least 99% of the total alkaloids were extracted without any degradation. The proposed densitometric HPTLC methods were applied to reserpine, rescinnamine and ajmaline determination in the root bark of *Rauwolfia vomitoria* from Africa. The data were compared (Table I) with those obtained by HPLC, from which it was concluded that these HPTLC–densitometric methods are of interest for the rapid determination of these alkaloids in plants.

ACKNOWLEDGEMENTS

We thank Mr. A. Livaditis for his very skilful technical assistance. This work was supported by the Administration General de Cooperation au Developpement of Ministere des Affaires Etrangeres de Belgique and by the United Nations Industrial Development Organization (Vienna).

REFERENCES

1 W. E. Court, *Planta Med.*, 48 (1983) 228.
2 W. Martindale, *The Extra Pharmacopoeia*, The Pharmaceutical Press, London, 28th ed., 1982, pp. 162–164.
3 G. P. Forni, *J. Chromatogr.*, 176 (1979) 129.
4 K. A. Hamied and V. M. Bakshi, *Indian J. Pharm.*, 18 (1956) 190.
5 *Pharmacopee Francaise*, Ministere de la Santé Publique et de la Securité Sociale, Paris, 9th ed., 1982.
6 J. Poisson, *Ann. Pharm. Fr.*, 16 (1958) 611.
7 W. H. McMullen, J. Pazdera, S. R. Missan, L. L. Ciaccio and T. C. Grenfell, *J. Am. Pharm. Assoc.*, 44 (1955) 446.
8 B. P. Korzum, A. F. St. Andre and P. R. Ulshafer, *J. Am. Pharm. Assoc.*, 46 (1957) 720.
9 M. J. Harris, A. F. Stewart and W. E. Court, *Planta Med.*, 16 (1968) 217.
10 M. S. Habib and W. E. Court, *Can. J. Pharm. Sci.*, 8 (1973) 81.
11 E. H. Sakal and E. J. Merrill, *J. Am. Pharm. Assoc.*, 43 (1954) 709.
12 J. M. G. J. Frijns, *Pharm. Weekbl.*, 106 (1971) 605.
13 V. F. Hammerstein and F. Kaiser, *Planta Med.*, 21 (1972) 5.
14 M. Ktic, E. Kucan, M. Prosek and M. Bano, *J. High Resolut. Chromatogr. Chromatogr. Commun.*, 3 (1980) 149.
15 J. W. Robinson, *Edro Sarap. Res. Tech. Rep.*, 2 (1977) 1035.
16 U. R. Cieri, *J. Assoc. Off. Anal. Chem.*, 66 (1983) 867.
17 Svendsen, A. Baerheim and R. Verpoorte, *Chromatography of Alkaloids part A*, Elsevier, Amsterdam, 1983, p. 310.
18 W. E. Court and M. S. Habib, *J. Chromatogr.*, 80 (1973) 101.
19 A. Kaess and C. Mathis, *Ann. Pharm. Fr.*, 23 (1965) 739.

Journal of Chromatography, 356 (1986) 341–345
Elsevier Science Publishers B.V., Amsterdam — Printed in The Netherlands

CHROM. 18 405

Note

Preparative separation of diastereoisomeric 2-arylpropionic acid derivatives by centrifugal thin-layer chromatography

Comparison with preparative liquid chromatography

JEAN-MICHEL MAÎTRE, GILLES BOSS, BERNARD TESTA* and KURT HOSTETTMANN
School of Pharmacy, University of Lausanne, CH-1005 Lausanne (Switzerland)
(Received December 10th, 1985)

Metabolic studies of chiral drugs and other xenobiotics can be performed using the racemates or the isolated enantiomers. The latter can be obtained by stereospecific synthesis or by resolution. Although resolution by crystallization of diastereoisomeric salts or other derivatives is frequently used, it is time consuming and does not usually yield enantiomeric percentages much greater than 95%.

The separation of diastereoisomers by liquid chromatography (LC) provides a valuable alternative to fractional crystallization. Preparative LC is considered to be the method of choice for the gram-scale separation of stereoisomers[1], although it requires expensive equipment and large volumes of solvents. In this study, we found that centrifugal thin-layer chromatography[2] (CTLC) allows the rapid separation of diastereoisomers on the decigram scale with good yields and minimal solvent consumption. To the best of our knowledge, this is the first time that this technique has been used for the preparative separation of stereoisomers.

The compounds investigated were chiral 2-arylpropionic acids, including ibuprofen and cicloprofen, which are non-steroidal antiinflammatory agents. The resolution of these drugs is of biomedical interest as they display enantioselective activity[3] and metabolism[4].

EXPERIMENTAL

Chemicals

The structures of the 2-arylpropionic acids investigated are shown in Fig. 1. 2-(2-Naphthyl)propionic acid (III) and 2-(4-biphenyl)propionic acid (V) have been described previously[5]. Racemic ibuprofen and cicloprofen were generous gifts from Boots (Nottingham, U.K.) and Squibb (Princeton, NJ, U.S.A.), respectively.

The (−)-(*S*)-1-phenylethylamides of these acids were synthesized by reaction of the acyl chloride with the amine in chloroform or toluene (for ibuprofen)[6,7]. The amides were recrystallized from *n*-hexane–ethanol (95:5) or methanol (for the cicloprofen amide). The NMR spectra confirmed the identities and purities of the compounds. However, the amides of III and V were contaminated with *ca.* 10% of the phenylethylamide of 2-naphthylacetic acid and 4-biphenylacetic acid, respectively.

0021-9673/86/$03.50

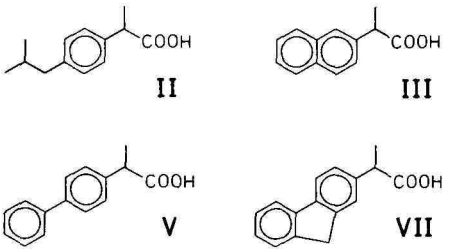

Fig. 1. 2-Arylpropionic acids investigated: (II) ibuprofen: (III) 2-(2-naphthyl)propionic acid; (V) 2-(4-biphenyl)propionic acid; (VII) cicloprofen. The numbering of compounds is taken from a previous study[5].

The chromatographic solvents (Merck, Darmstadt, F.R.G.) were of analytical-reagent grade for centrifugal TLC and of purum grade for preparative LC.

Centrifugal TLC

A Chromatotron Model 7924 (Harrison Research, Palo Alto, CA, U.S.A.) equipped with an FMI Model RPG 150 pump was used. The silica layer was 2 mm thick and was prepared from a mixture of 60 g of silica gel 60 GF_{254}, 8 g of calcium sulphate hemihydrate and 120 ml of water. The plates were dried at 70°C for 12 h, then rinsed and stabilized with the eluent (chloroform–cyclohexane–tetrahydrofuran, 54.2:45:0.8, v/v). The mixture to be separated (0.100 g) was dissolved in 1.5 ml of the eluent. The flow-rate of the eluent was maintained at 3.5 ml/min and the separation on the plates was monitored with a UV lamp. Samples (4–6 ml) were collected and directly analysed by analytical high-performance liquid chromatography (HPLC) as described previously[5].

Preparative LC

A Jobin-Yvon Chromatospac instrument equipped with an LKB 2238 Uvicord SII UV detector operating at 254 nm and an LKB 2210 two-channel recorder was used. The column (500 mm × 40 mm I.D.) was freshly prepared before each separation using silica H60 for TLC (15 μm) (Merck). The eluent was cyclohexane–isopropanol (97:3, v/v). The flow-rate was 23 ml/min corresponding to a pressure of 9 bar. Samples to be analysed (1.0–1.2 g) were dissolved in 10 ml of the eluent. Fractions of various volumes were collected and directly analysed by analytical HPLC[5].

RESULTS

Preliminary studies

Preliminary studies were necessary in order to choose suitable eluents for both centrifugal TLC and preparative LC. (a) The compounds to be separated must have good solubility in the eluent system, typically 1 part or more in 10 parts. (b) TLC (employing the same or similar stationary phases) must be used to optimize the eluent composition. The migration of the solutes must lie within the range $0.1 < R_F < 0.3$, with $\Delta R_F > 0.05$. Thus, on TLC plates made with 60 F_{254} silica, the following ΔR_F values were obtained with chloroform–cyclohexane–tetrahydrofuran (54.2:45:0.8) eluent: amides of 2-(2-naphthyl)propionic acid, 0.05; amides of

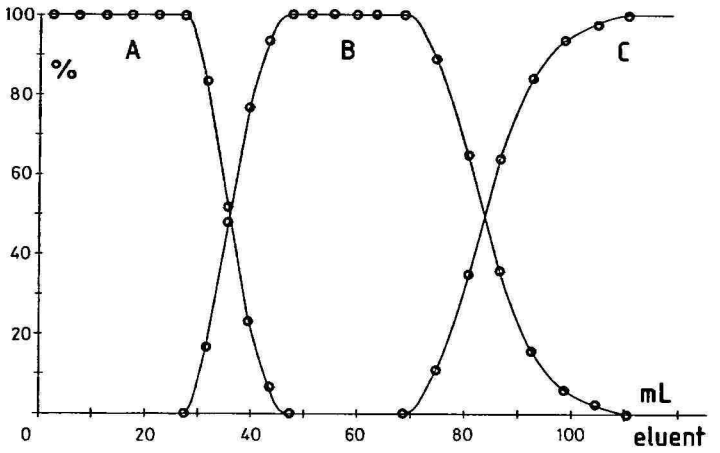

Fig. 2. Centrifugal TLC separation of the (*S*)-1-phenylethylamides of (*R*)- and (*S*)-2-(2-naphthyl)propionic acid and 2-naphthylacetic acid (A, B and C, respectively). The results are expressed in terms of the percentage composition (A + B + C = 100%) in each 4–6 ml fraction collected. The origin of the abcissa (0 ml of eluent) is arbitrarily fixed at the appearance of A.

2-(4-biphenyl)propionic acid, 0.07; and amides of cicloprofen, 0.06. For the amides of ibuprofen in the cyclohexane–isopropanol (97:3) eluent, the ΔR_F value was 0.08. The final R_F values in this study were between 0.12 and 0.25.

Centrifugal TLC

In a single passage (70–90 min, 250–300 ml of eluent), the Chromatotron allowed a good separation of diastereoisomeric phenylethylamides. When the mixture contained the amide of the arylacetic acid as an impurity, the latter eluted last and was also well separated. Fig. 2 exemplifies a typical separation obtained with 2-(2-naphthyl)propionic acid (A and B) contaminated with 2-naphthylacetic acid.

For the three arylpropionamides investigated, *ca.* 80% of the starting material

TABLE I

TYPICAL YIELDS AND STEREOISOMERIC PERCENTAGES OF THE DIASTEREOISOMERIC (−)-(*S*)-1-PHENYLETHYLAMIDES OF 2-ARYLPROPIONIC ACIDS SEPARATED BY CENTRIFUGAL TLC

Sample: 100 mg.

(−)-(S)-1-Phenylethylamide	*Yield (mg)*	*Stereoisomeric percentage*
(*R*)-2-(2-Naphthyl)propionic acid	40	99.8
(*S*)-2-(2-Naphthyl)propionic acid	35	99.0
(*R*)-2-(4-Biphenyl)propionic acid	40	99.4
(*S*)-2-(4-Biphenyl)propionic acid	40	98.9
(*R*)-Cicloprofen	41	99.8
(*S*)-Cicloprofen	38	99.1

TABLE II

TYPICAL YIELDS AND STEREOISOMERIC PERCENTAGES OF THE DIASTEREOISOMERIC (−)-(*S*)-1-PHENYLETHYLAMIDES OF IBUPROFEN SEPARATED BY PREPARATIVE LC

Sample: 1200 mg.

Run	*Parameter*	*Amide*	
		(R)-Ibuprofen	*(S)-Ibuprofen*
First	Yield (mg)	400	250
	Stereoisomeric percentage	99.8	99.5
Second	Yield (mg)	150	80
	Stereoisomeric percentage	99.2	98.4

was consistently recovered after separation, each fraction being contaminated with 1% or less of its diastereoisomer. Typical results are presented in Table I.

Preparative LC

The 1-phenylethylamides of ibuprofen were separated by preparative LC. Samples of 1–1.2 g were used. After a first run (*ca.* 60 min, and 1 l of eluent), *ca.* 50% of the sample was recovered as two pure fractions. The impure fractions were pooled and recycled (*ca.* 60 min, 0.8 l of eluent), yielding two pure fractions amounting to *ca.* 40% of the recycled material. Results of a typical experiment are given in Table II.

DISCUSSION

The two chromatographic methods have their advantages and disadvantages. In this study, the resolving power of preparative LC appears to be inferior to that of centrifugal TLC, although we did not compare the same pairs of diastereoisomers. The amides of ibuprofen showed the best separation in the preliminary TLC analyses; nevertheless, their separation by preparative LC was only partial and necessitated a second cycle in order to achieve yields (75–80%) comparable to those obtained with centrifugal TLC.

The volumes of solvent needed to separate 1 g of starting material are comparable for the two techniques, namely 2–3 l. However, preparative LC consumes much larger amounts of stationary phase.

It therefore appears that centrifugal TLC is a rapid, efficient and cost-effective technique for the decigram-scale separation of diastereoisomers. For gram-scale separations, preparative LC has advantages.

The separated diastereoisomers have to be hydrolysed if the purpose of the work is to obtain pure enantiomers of 2-arylpropionic acids. Acid hydrolysis (*e.g.*, with sulphuric acid–dioxane) is time-consuming and always leads to racemization[8]. For example, we found the racemization to be moderate with cicloprofen, but complete with of ibuprofen. The method of choice, which destroys the amine but leaves the acid enantiomerically pure, is diazotation with N_2O_4 followed by cleavage of the amide bond[9–12].

ACKNOWLEDGEMENT

J.-M.M. and B.T. are indebted to the Swiss National Science Foundation for research grant 3.723-0.80.

REFERENCES

1 K.-H. Rimböck, F. Kastner and A. Mannschreck, *J. Chromatogr.*, 329 (1985) 307.
2 K. Hostettmann, M. Hostettmann-Kaldas and O. Sticher, *J. Chromatogr.*, 202 (1980) 154.
3 R. A. Appleton and K. Brown, *Prostaglandins*, 18 (1979) 29.
4 A. J. Hutt and J. Caldwell, *J. Pharm. Pharmacol.*, 35 (1983) 693.
5 J.-M. Maître, G. Boss and B. Testa, *J. Chromatogr.*, 299 (1984) 397.
6 *Organikum, Organisch-chemisches Grundpraktikum*, VEB DVW, Berlin, 15. Aufl., 1977, pp. 523–529.
7 A. I. Vogel, *A Textbook of Practical Organic Chemistry*, Longmans, London, 3rd ed., 1961, pp. 361–368.
8 G. Helmchen, G. N. D. Flockerzi and M. S. K. Yossef, *Angew. Chem., Int. Ed. Engl.*, 18 (1979) 63.
9 E. H. White, *J. Am. Chem. Soc.*, 77 (1955) 6008, 6011, 6014.
10 G. Haas and V. Prelog, *Helv. Chim. Acta*, 52 (1969) 128.
11 G. Helmchen and V. Prelog, *Helv. Chim. Acta*, 55 (1972) 2599.
12 S. Naruto and A. Terada, *Chem. Pharm. Bull.*, 26 (1978) 1486; 31 (1983) 4286.

Journal of Chromatography, 356 (1986) 346–348
Elsevier Science Publishers B.V., Amsterdam — Printed in The Netherlands

CHROM. 18 404

Note

Silicic acid column chromatography of phosphinolipids

II*. Study of the column chromatographic properties of bis(diacyloxypropyl) phosphinate

MICHAEL C. MOSCHIDIS
Sancorin Laboratories, 6 Aglawrou Street, Koukaki 117 41, Athens (Greece)
(Received December 12th, 1985)

The column chromatographic properties of the direct phosphinate analogues of lecithin and cephalin have been reported[1], where it was noted that the two analogues were eluted rapidly with 20% methanol in chloroform. In this paper is reported the column chromatographic behaviour of bis(diacyloxypropyl) phosphinate in the presence of the phosphonate analogue of bis(diacylglycero) phosphate, of the direct phosphinate analogues of lecithin and cephalin, of phosphatidylcholine and of the phosphono analogue of cephalin. The collected fractions were analysed by thin-layer chromatography (TLC) and IR spectroscopy to confirm identification of the components.

EXPERIMENTAL

Instrumentation

IR spectra were recorded on a Perkin-Elmer 197 double-beam grating spectrophotometer. A glass column (35 × 1.6 cm I.D.) was employed for the chromatographic experiment.

Reagents

Solvents for column chromatography and TLC were of analytical-reagent grade and were purchased from Merck (Darmstadt, F.R.G.) and Vioryl (Kifissia, Athens, Greece). All solvents were distilled before use. Silicic acid for column chromatography was purchased from Sigma (St. Louis, MO, U.S.A.).

Standards

The phosphino analogues of lecithin, cephalin and bis(diacylglycero) phosphate and the phosphonate analogues of cephalin and bis(diacylglycero) phosphate were synthetic products. Phosphatidylcholine was purchased from Koch-Light (Colnbrook, U.K.).

* For Part I, see ref. 1.

0021-9673/86/$03.50

TABLE I

CHROMATOGRAPHIC CONDITIONS

The column (35 × 1.6 cm I.D.) was packed with 11.0 g of silicic acid to a height of 10.0 cm and a total volume of 26 ml. Flow-rate, 1.4–1.8 ml/min. Fractions of *ca.* 5.0 ml were collected.

Methanol in chloroform (%)	*No. of column volumes*	*Total volume of solvent (ml)*	*Fractions collected*
5	3	75	1–18
20	5	130	19–48
40	7	180	49–78

Procedure

The procedure used was similar to that reported earlier[1,2]. Column elution was effected with methanol–chloroform mixtures as indicated in Table I.

IR spectra of the various pilot fractions were recorded as thin films from dry chloroform or KBr discs. Thin-layer chromatograms were obtained on 20 × 20 cm silica gel G plates coated in this laboratory to a thickness of 0.30 mm. Development of the chromatograms was carried out in a chamber of dimensions 20 × 8 cm and the run normally took 55 min. The solvents used were chloroform–methanol–water (65:25:4) (system A) and methanol–water (2:1) (system B). The spots were rendered visible with molybdenum blue and iodine sprays and the Stillway–Harmon procedure[3]. Standards were also spotted to aid in the detection of the developed spots.

RESULTS AND DISCUSSION

Column elution was effected with various methanol–chloroform mixtures. The

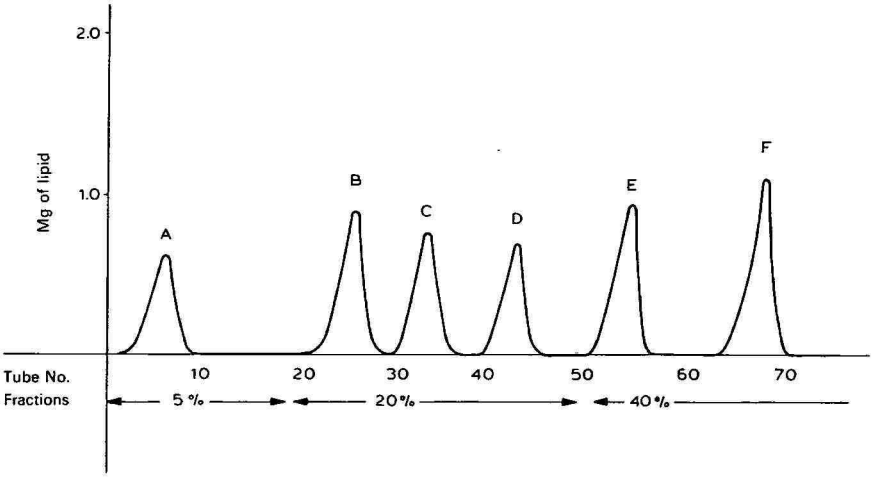

Fig. 1. Chromatography of phosphinolipids and phosphonolipids on silicic acid. Solvents as indicated. (A) Phosphono analogue of bis(diacylglycero) phosphate, 2.1 mg; (B) bis(diacyloxypropyl) phosphinate, 2.4 mg; (C) phosphinate analogue of cephalin, 2.4 mg; (D) phosphinate analogue of lecithin, 2.0 mg; (E) phosphonocephalin, 3.2 mg; (F) phosphatidylcholine, 4.5 mg. The lipids were applied in 3.5 ml of chloroform.

TABLE II

COMPOSITION OF FRACTIONS OBTAINED BY CHROMATOGRAPHY OF PHOSPHINOLIPIDS AND PHOSPHONOLIPIDS ON SILICIC ACID

16.6 mg of lipids were applied to the column. The total recovery was 100%.

Solvent	*Fractions collected*	*TLC R_F values*		*Components identified by IR spectroscopy*
		System A	*System B*	
5% methanol in chloroform	3–8	0.71*	0.93	1,2-Diacyloxypropyl-3-(1',2'-diacyl-*sn*-glycero) phosphonate
20% methanol in chloroform	22–27	0.73*	0.95	Bis(diacyloxypropyl) phosphinate
	32–36	0.60	0.85	Phosphinate analogue of cephalin
	39–45	0.46	0.90	Phosphinate analogue of lecithin
40% methanol in chloroform	52–57	0.65	0.86	Phosphonocephalin
	64–72	0.42	0.00	Phosphatidylcholine

* Silica gel H.

fractionation pattern of the phosphino- and phosphonolipids is depicted in Fig. 1. Fractions were identified by TLC and IR spectroscopy (Table II).

Under the above experimental conditions and with the solvents used, 100% of the lipids applied to the column could be recovered.

Bis(diacyloxypropyl) phosphinate was eluted with 20% methanol in chloroform and very early in the process. This feature distinguishes this compound from its structurally related phosphono analogue of bis(diacylglycero) phosphate, as both compounds exhibit similar thin-layer chromatographic properties[4,5].

This project, concerned with the silicic acid column chromatography of phosphinolipids, is continuing.

REFERENCES

1 M. C. Moschidis, *J. Chromatogr.*, 329 (1985) 160.
2 M. C. Moschidis, *J. Chromatogr.*, 261 (1983) 181.
3 L. W. Stillway and S. J. Harmon, *J. Lipid Res.*, 21 (1980) 1141.
4 M. C. Moschidis, *Chem. Phys. Lipids*, 36 (1985) 297.
5 M. C. Moschidis, *Chem. Phys. Lipids*, in press.

Journal of Chromatography, 356 (1986) 349–353
Elsevier Science Publishers B.V., Amsterdam — Printed in The Netherlands

CHROM. 18 422

Note

High-performance liquid chromatographic determination of sugar phosphates and sugar acids, applied to the oxidation of glucose 1-phosphate

H. E. VAN DAM*, P. DUIJVERMAN and F. VAN RANTWIJK
Laboratory of Organic Chemistry, Delft University of Technology, P.O. Box 5045, 2600 GA Delft (The Netherlands)
(Received December 17th, 1985)

Oxidation of glucose 1-phosphate (α-D-glucopyranosyl phosphate, I), by means of oxygen and a supported platinum catalyst yields mainly glucuronic acid 1-phosphate (α-D-glucopyranuronic acid 1-phosphate, II). Hydrolysis results in the formation of inorganic phosphate (III), glucose (IV) and glucuronic acid (VI). The last two products are rapidly oxidised to gluconic acid (V) and glucaric acid (VII), respectively. In the course of our investigation of the oxidation of I, we required a simple method for the determination of I–III, V and VII.

Anion-exchange chromatography has been used for the separation of phosphate esters[1–4]. However, in most instances complex salt and pH gradients had to be applied, which necessitated post-column colorimetric detection. I and III can be separated in an isocratic system[5], but broad peaks are obtained, and application of this method to the analysis of the complex oxidation mixtures seemed not to be feasible. In our laboratory, ion-pair reversed-phase chromatography has been used for the determination of I and II in oxidation mixtures[6]. Although a baseline separation can be obtained, this method is less practical when large numbers of samples, or small sample volumes, are involved. Ion-moderated partitioning (IMP) chromatography has been used for the determination of I in the presence of fructose and sucrose[7] and for the analysis of sugar acids[8].

We have reinvestigated the application of IMP chromatography to the analysis of I–III, V and VII. A cation-exchange resin in the hydrogen form was used as the stationary phase. In order to determine the scope of this method, the investigation also included D-glucose 6-phosphate (VIII) and D-fructose 6-phosphate (IX).

To avoid corrosion problems[7], the aqueous mobile phase was acidified with trifluoroacetic acid (TFA) rather than sulphuric acid. TFA is a moderately strong acid; the literature provides pK_a values ranging from 0.5 up to 1.1[9,10]. As this range is wide, the dissociation of TFA in the mobile phases used in this work was calculated (more directly) from pH measurements.

EXPERIMENTAL

Chemicals

Glucose 1-phosphate, glucose 6-phosphate, fructose 6-phosphate (dipotassium

0021-9673/86/$03.50

salts) and TFA were obtained from Janssen Chimica (Beerse, Belgium). Glucuronic acid was purchased from Fluka (Buchs, Switzerland). Glucuronic acid 1-phosphate (tripotassium salt, pentahydrate) and monopotassium glucarate were prepared in our laboratory. Other chemicals were obtained from Merck (Darmstadt, F.R.G.). The compounds were injected as salts; lactones were not present in the samples.

Aminex A-7 sulphonic acid resin (polystyrene–8% divinylbenzene, 9 ± 2 μm) was obtained from Bio-Rad Labs. (Richmond, CA, U.S.A.).

Chromatography

The chromatographic system consisted of the following elements: a Waters Assoc. M45 pump, a Perkin-Elmer ISS-100 autosampler, a slurry-packed[11] Aminex A-7 column (200 × 9 mm I.D.) and a thermostated Waters Assoc. R401 refractive index detector. The flow-rate was 0.4 ml/min. A faster flow-rate resulted in a less efficient separation and a decrease in the flow-rate gave no improvement. The column temperature was kept constant at 35°C. Higher temperatures resulted in significant hydrolysis of I when 0.2 *M* TFA was used as the mobile phase.

Owing to difficulties in defining and reliably measuring the void volume of the ion-exchange resin column, the results are presented in terms of retention times instead of capacity factors.

System peaks and sample preparation

When a high TFA concentration in the mobile phase was used (*e.g.*, 0.2 *M*), direct injection of reaction mixtures (or water) resulted in a large negative system peak. This peak, caused by the absence of TFA from the samples, interfered with the peak of I. Therefore, the samples were made 0.2 *M* in trifluoroacetate by the addition (Finn pipette) of concentrated aqueous potassium trifluoroacetate. This correction eliminated the negative peak without affecting the neutral pH of the samples.

When the corrected system was used and the TFA concentration in the mobile phase exceeded 0.01 *M*, chromatograms of samples containing (moderately) strong acids (*e.g.*, sugar phosphates) exhibited a small positive TFA peak. We ascribe this effect to the expulsion of undissociated TFA from the mobile phase into the stationary phase.

Glycerol was added to the samples as an internal standard for quantitative analysis (retention time 20 min).

pH measurements and dissociation calculations

A Cole Parmer standard combined glass electrode was used for pH measurements in TFA solutions (mobile phase). The electrode was calibrated at pH 2.00 and checked with 0.1 *M* hydrochloric acid (observed pH 1.085; calculated[12] pH 1.08). The extended Debye–Hückel equation[12] was used to calculate the activity coefficients, f_{H^+}. The results are given in Table I, together with the calculated H^+ concentrations and the extent of dissociation of TFA.

RESULTS AND DISCUSSION

Fig. 1 shows the retention times of the compounds under investigation *versus* the TFA concentration in the mobile phase. In all instances an increase in retention

TABLE I

pH VALUES, H^+ ACTIVITY COEFFICIENTS AND DISSOCIATION OF AQUEOUS TRIFLUOROACETIC ACID

[TFA] (M)	*pH**	*f_{H^+}***	*$[H^+]$*** (M)*	*Dissociation (%)*
0.20	0.88	0.80	0.165	83
0.10	1.125	0.83	0.090	90
0.050	1.385	0.86	0.048	96
0.010	2.04	0.91	0.010	100

* Measured (20°C).
** Calculated[12].
*** Log $[H^+] = -pH - \log f_{H^+}$.

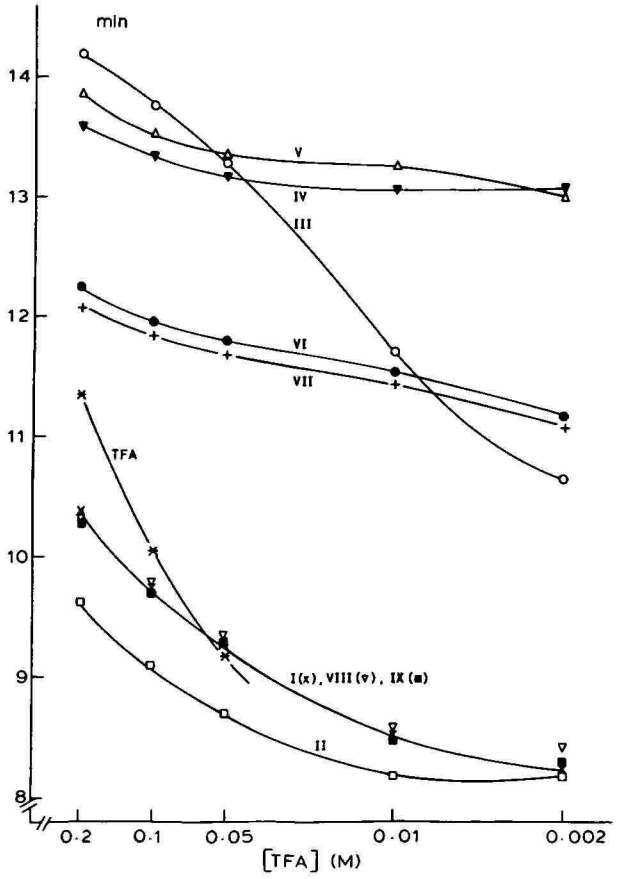

Fig. 1. Retention times of I–IX and TFA *versus* the TFA concentration in the mobile phase: I, glucose-1-phosphate; II, glucuronic acid 1-phosphate; III, inorganic phosphate; IV, glucose; V, gluconic acid; VI, glucuronic acid; VII, glucaric acid; VIII, glucose-6-phosphate; IX, fructose-6-phosphate; TFA (system peak).

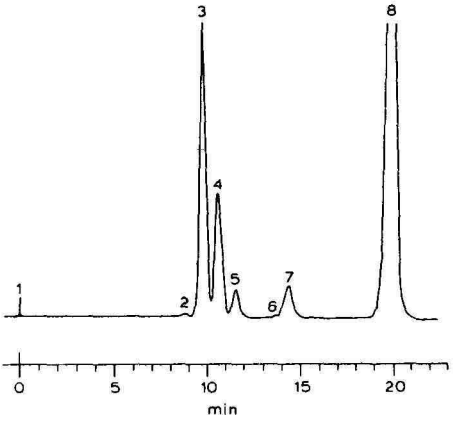

Fig. 2. Chromatographic analysis of oxidation mixtures: Peaks: 1 = injection; 2 = solvent front; 3 = glucuronic acid 1-phosphate (II); 4 = glucose-1-phosphate (I); 5 = system peak (TFA); 6 = gluconic acid (V); 7 = inorganic phosphate (III); 8 = glycerol (internal standard).

is observed at the highest TFA concentrations (0.05–0.2 *M*). This effect is probably connected with the dissociation of TFA, which is incomplete below pH 2 (Table I).

The internal H^+ concentration in the stationary phase (sulphonic acid resin) is approximately 1.7 *M*. In such media, the investigated compounds exist solely as undissociated acids. This implies that the retention of the acidic compounds increases when their dissociation in the mobile phase decreases. The sugar acids (gluconic, glucuronic and glucaric acid) have $pK_{a,1}$ values of about 3.6[9,10]. They are still partially dissociated in 0.002 *M* TFA (pH 2.7), but are virtually undissociated in the more concentrated mobile phases. The sugar phosphates are stronger acids ($pK_{a,1}$ = 1–1.5[9,10]) and are almost completely ionized in 0.002 *M* TFA. Retention of these compounds starts at pH 2, and increases rapidly in more acidic mobile phases. The TFA system peak, which appears only when the more concentrated mobile phases are used, shows the same behaviour (TFA, pK_a 0.5–1.1[9,10]; *cf.*, Table I). As expected, phosphoric acid ($pK_{a,1}$ = 2.1) shows an increased retention around 0.01 *M* TFA (pH 2).

As can be concluded from Fig. 1, samples taken during the oxidation of I can be analysed for I and II when 0.2 *M* TFA is used as the mobile phase. An example is given in Fig. 2. A near-baseline separation of I, II and the TFA system peak is obtained. Quantitative peak height analysis is possible (accuracy 3% absolute for 50 m*M* samples). III, V and VII can be analysed when 0.02 *M* TFA is used. I, VIII and IX cannot be separated from each other.

REFERENCES

1 M. H. Simatupang, *J. Chromatogr.*, 180 (1979) 177.
2 S. P. Bessman, P. J. Geiger, T.-C. Lu and E. R. B. McCabe, *Anal. Biochem.*, 50 (1974) 533.
3 H. J. Duncan, *J. Chromatogr.*, 62 (1971) 391.
4 P. J. Geiger, S. Alm and S. P. Bessman, *Methods Carbohydr. Chem.*, 8 (1980) 21.
5 K. Brunt and H. Hokse, *J. Chromatogr.*, 268 (1983) 131.
6 T. T. Tjioe, J. P. van der Wiel, R. M. Stikkelman, A. J. J. Straathof and F. van Rantwijk, *J. Chromatogr.*, 330 (1985) 412.

7 R. M. Stikkelman, T. T. Tjioe, J. P. van der Wiel and F. van Rantwijk, *J. Chromatogr.*, 322 (1985) 220.
8 K. B. Hicks, P. C. Lim and M. J. Haas, *J. Chromatogr.*, 319 (1985) 159.
9 G. Kortüm, W. Vogel and K. Andrusson, *Dissociationskonstanten Organischer Säuren in Wässeriger Lösung*, Butterworths, London, 1961.
10 E. P. Serjeant and B. Dempsey, *Ionisation Constants of Organic Acids in Aqueous Solution*, IUPAC Chemical Data Series, 23, Pergamon Press, Oxford, 1979.
11 L. A. Th. Verhaar and B. F. M. Kuster, *J. Chromatogr.*, 210 (1981) 279.
12 J. Kielland, *J. Am. Chem. Soc.*, 59 (1937) 1675.

Journal of Chromatography, 356 (1986) 354–358
Elsevier Science Publishers B.V., Amsterdam — Printed in The Netherlands

CHROM. 18 408

Note

Enantiomer separation of phenolic α- and β-receptor active drugs by chiral capillary gas chromatography after derivatization with diazomethane and phosgene

WILFRIED A. KÖNIG*
Institut für Organische Chemie der Universität, D-2000 Hamburg 13 (F.R.G.)
and
OLLE GYLLENHAAL and JÖRGEN VESSMAN
Analytical Chemistry, AB Hässle, S-43183 Mölndal (Sweden)
(Received December 12th, 1985)

α- and β-adrenergic stimulants of the adrenaline type are important and widely used drugs with antiasthmatic or cardial activity[1]. Although it is known that the *S*-enantiomer of adrenaline (epinephrine) has 10–100 fold and of isoprenaline (aludrine) up to 1500 fold higher activity than the corresponding *R*-isomer[2], most of these drugs are still used in the racemic form. Nevertheless, there is a strong tendency to use enantiomerically pure pharmaceuticals, and techniques for determining their optical purity have received much attention.

In recent communications[3–6] we have shown that the enantiomers of pharmaceuticals of the amino alcohol type can be separated by capillary gas chromatography (GC) with the chiral stationary phase XE-60-L-valine-(*R*)-α-phenylethylamide after formation of the oxazolidin-2-one derivatives using phosgene as a reagent. In this work we have extended this approach to amino alcohols with phenolic substituents.

EXPERIMENTAL

Chemicals and derivatization

Samples of adrenaline and its analogues were either commercially available or supplied by the Department of Organic Chemistry, AB Hässle. A saturated solution of diazomethane in diethyl ether was prepared in a micro-reactor[7] from N-methyl-N-nitroso-*p*-toluenesulphonamide in 40% aqueous potassium hydroxide solution.

An excess of the diazomethane solution was added to a solution of 0.5–1 mg of sample in 200 μl of methanol and kept for 3 h at room temperature. The excess of reagent and of the solvent were then removed in a stream of nitrogen. To the residue, 400 μl of diethyl ether, 50 μl of 0.5 *M* aqueous sodium hydroxide solution and 50 μl of a 20% solution of phosgene in toluene were added. The mixture was shaken occasionally and kept for 1 h at room temperature. The organic phase was transferred to a dry vial and the solvent and excess of reagent were removed in a stream of nitrogen. A 400-μl volume of dichloromethane was added to the residue, and the solution again taken to dryness in a stream of nitrogen. Finally, the sample was dissolved in 200 μl of dichloromethane for GC analysis.

0021-9673/86/$03.50

Gas chromatography

A Carlo Erba Model 2101 gas chromatograph with a split inlet and a flame ionization detector was used. The preparation of the chiral stationary phases[8] and coating of the glass capillary columns has been described elsewhere[9].

RESULTS AND DISCUSSION

Phosgene is a versatile and convenient reagent for enantiomer separation of mainly bifunctional compounds, namely diols, amino alcohols, aminothiols, N-methylamino acids and hydroxy acids[3–6]. According to our experience, this derivatization method produces chemically and configurationally stable derivatives. This is particularly important for pharmaceuticals like ephedrine and its analogues, which tend to racemize when perfluoroacylation is used to form volatile derivatives for enantiomer separation[10,11]. For ephedrine, racemization of the chiral centre next to the hydroxy group was observed after formation of the N,O-bis(heptafluorobutyryl) derivative[12]. It is also known that these derivatives are highly sensitive to humidity and to active sites in the GC system[13].

Phenolic amino alcohols react with phosgene and methanol at pH 12 to yield a methyl carbonate oxazolidin-2-one derivative[14]. This type of derivative, however, has an unduly long retention time in the chromatographic system, *e.g.*, 90 min for prenalterol at 190°C (1.3 bar H_2).

Catechols such as adrenaline react with phosgene in an aqueous buffer to give a cyclic carbonate oxazolidin-2-one derivative[15]. Due to the polar nature of the cyclic carbonate, this derivative partially decomposed in the chromatographic system. Under the strongly alkaline conditions (sodium hydroxide), used to form oxazolidin-2-one derivatives, the phenolic residue forms a salt and again sufficient volatility cannot be achieved. To avoid these problems, diazomethane is used to form methyl ether derivatives prior to the reaction with phosgene (Scheme 1). This approach has been used before in the stereochemical analysis of a new amino acid isolated from a hydrolyzate of nikkomycin B, an antibiotic with antifungal and insecticidal properties[16].

Using this procedure it was possible to obtain sufficiently volatile derivatives of many sympathomimetic drugs (Table I), which could all be baseline separated on a 15-m glass capillary column containing the chiral phase XE-60-L-valine-(*R*)-α-phenylethylamide. An example is shown in Fig. 1. Some N-methylation was observed in the treatment with diazomethane of compounds having primary amino groups. This may result in ambiguities when synephrine and octopamine or phenylephrine and norfenefrine are present in the same sample. Also, adrenaline and metadrenaline with a 3-OCH_3 group at the aromatic ring give identical derivatives after treatment with diazomethane. For these cases diazoethane may be used in order to distinguish between the original compounds. In all cases gas chromatography–mass spectrometry was applied to confirm the structure of the derivatives.

The separation factors (Table II) are almost identical in each case, independent of the kind of substituent present at the amino group. Except for adrenaline analogues, the enantiomers of the phenolic metabolite of the β-receptor blocking agent alprenolol and the β-receptor agonist prenalterol and its antipode could be separated under the same conditions.

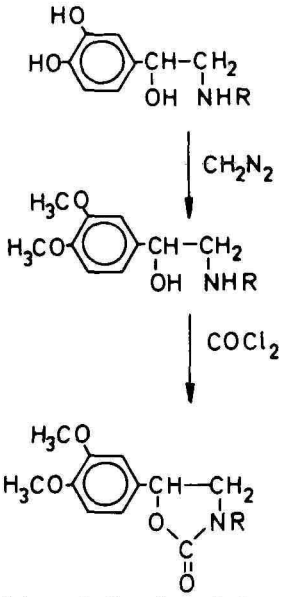

Scheme 1. Reaction of adrenaline and analogues with diazomethane and phosgene.

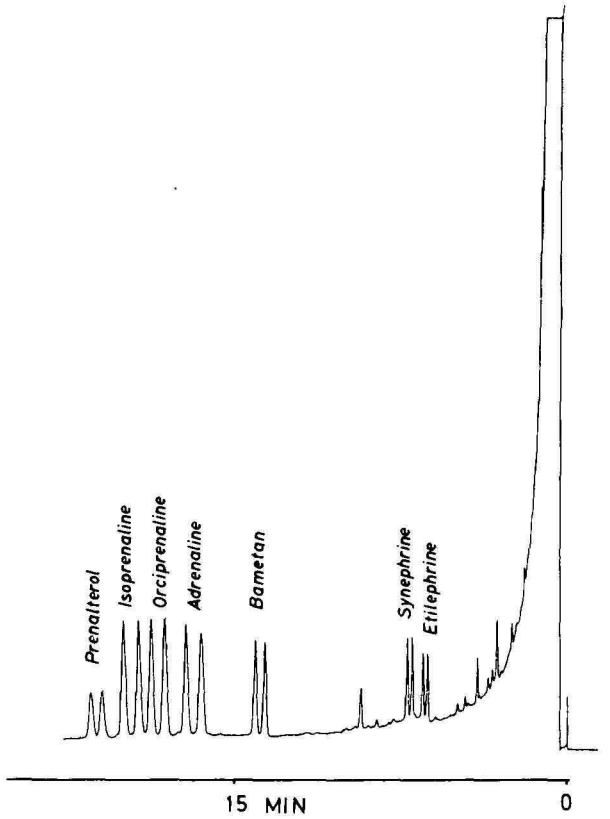

Fig. 1. Separation of the enantiomers of etilephrine, synephrine, bametan, adrenaline, orciprenaline, isoprenaline and prenalterol after reaction with diazomethane and phosgene. Column: 15-m glass capillary containing XE-60-L-valine-(*R*)-α-phenylethylamide; temperature, 190°C. Carrier gas: 1 bar H_2.

TABLE I

STRUCTURES OF RACEMIC COMPOUNDS SEPARATED BY CAPILLARY GAS CHROMATOGRAPHY ON XE-60-L-VALINE-(*R*)-α-PHENYLETHYLAMIDE

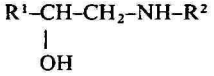

Compound	*R*¹	*R*²
Synephrine	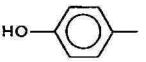	CH_3
Etilephrine	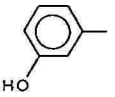	CH_3CH_2
Bametan	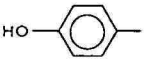	$CH_3(CH_2)_3$
Octopamine	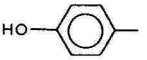	H
Norfenefrine	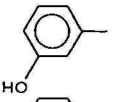	H
Phenylephrine	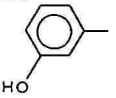	CH_3
Adrenaline	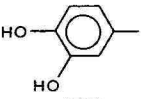	CH_3
Isoprenaline	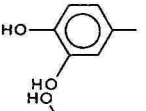	$(CH_3)_2CH$
Orciprenaline	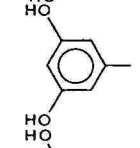	$(CH_3)_2CH$
Terbutaline	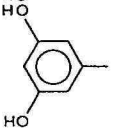	$(CH_3)_3C$
Salbutamol	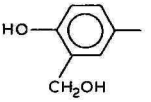	$(CH_3)_3C$
Prenalterol	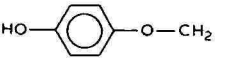	$(CH_3)_2CH$
4-Hydroxyalprenolol	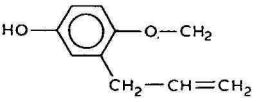	$(CH_3)_2CH$

TABLE II

SEPARATION FACTORS, α, AND COLUMN TEMPERATURES FOR ENANTIOMER SEPARATION OF RACEMIC PHARMACEUTICALS AFTER DERIVATIZATION WITH DIAZOMETHANE AND PHOSGENE (ACCORDING TO SCHEME 1)

Column: 15-m glass capillary containing XE-60-L-valine-(*R*)-α-phenylethylamide.

Compound	α	*Column temp. (°C)*
Synephrine	1.033	190
Etilephrine	1.036	190
Bametan	1.033	190
Octopamine	1.033	200
Norfenefrine	1.042	190
Phenylephrine	1.044	190
Adrenaline	1.041	190
Isoprenaline	1.036	190
Orciprenaline	1.033	190
Terbutaline	1.033	200
Salbutamol	1.029	190
Prenalterol/*R*-antipode	1.026	190
4-Hydroxyalprenolol	1.024	190

In some examples, pure enantiomers were available and the order of elution could be investigated. As already shown for β-receptor blocking drugs[3], the stereoisomers with negative optical rotation are eluted after the (+)-isomers.

ACKNOWLEDGEMENT

We thank Mr. M. Preusse, University of Hamburg, for his help in the preparation of the derivatives.

REFERENCES

1 N. Kucharczyk and F. H. Segelman, *J. Chromatogr.*, 340 (1985) 243.
2 W. Schunack, K. Mayer and M. Haake, *Arzneistoffe, Lehrbuch der Pharmazeutischen Chemie*, Vieweg, Braunschweig/Wiesbaden, 2nd ed., 1983, p. 102.
3 W. A. König, K. Ernst and J. Vessman, *J. Chromatogr.*, 294 (1984) 423.
4 W. A. König, E. Steinbach and K. Ernst, *J. Chromatogr.*, 301 (1984) 129.
5 W. A. König, E. Steinbach and K. Ernst, *Angew. Chem.*, 96 (1984) 516; *Angew. Chem., Int. Ed. Engl.*, 23 (1984) 527.
6 O. Gyllenhaal, W. A. König and J. Vessman, *J. Chromatogr.*, 350 (1985) 328.
7 H. M. Fales and T. M. Jaouni, *Anal. Chem.*, 45 (1973) 2302.
8 W. A. König, I. Benecke and S. Sievers, *J. Chromatogr.*, 217 (1981) 71.
9 W. A. König, K. Stölting and K. Kruse, *Chromatographia*, 10 (1977) 444.
10 H. Frank, G. J. Nicholson and E. Bayer, *J. Chromatogr.*, 146 (1978) 197.
11 W. A. König and K. Ernst, *J. Chromatogr.*, 280 (1983) 135.
12 W. A. König and K. Ernst, unpublished results (1982).
13 M. Ahnoff, M. Ervik and L. Johansson, in R. E. Kaiser (Editor), *Proceedings Fourth International Symposium on Capillary Chromatography, Hindelang, 1981*, Institute for Chromatography, Bad Dürkheim and Hüthig, Heidelberg, 1981, p. 487.
14 O. Gyllenhaal, *J. Chromatogr.*, 349 (1985) 447.
15 O. Gyllenhaal and J. Vessman, unpublished results (1980).
16 G. Zimmermann, W. Hass, H. Faasch, H. Schmalle and W. A. König, *Liebigs Ann. Chem.*, (1985) 2165.

Journal of Chromatography, 356 (1986) 359–366
Elsevier Science Publishers B.V., Amsterdam — Printed in The Netherlands

CHROM. 18 401

Note

Analysis of phomenone in cultures of *Phoma destructiva* and *Phoma betae* by high-performance liquid and thin-layer chromatography

RENATO CAPASSO*, GIACOMINO RANDAZZO and ALBERTO RITIENI
Dipartimento di Chimica Organica e Biologica dell'Università, Via Mezzocannone 16, Naples (Italy)
ELVIRA DELLA CASA
Istituto di Medicina Pubblica e Sicurezza Sociale, Facoltà di Medicina e Chirurgia dell'Università, Naples (Italy)
and
ANTONIO LOGRIECO
Istituto Tossine e Micotossine da Parassiti Vegetali del Consiglio Nazionale delle Ricerche, Via G. Amendola 97/F, Bari (Italy)
(First received October 15th, 1985; revised manuscript received December 2nd, 1985)

Phomenone (Fig. 1) is an eremofilanic sesquiterpene with wide biological activity[1–6]. It was identified as phytotoxin of *Phoma exigua* var. *inoxidabilis* Boerema et Vegh[7] and recently as phytotoxin of *Phoma destructiva* Plowr., the causal agent of wilt disease of tomato[8]. Some attempts have been made to identify it in culture filtrates of twenty phytopathogenic *Phoma* species[9] by high-performance liquid chromatography (HPLC), on account of its possible property as taxonomic marker for these species.

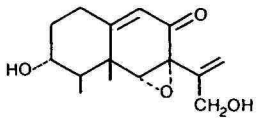

Fig. 1. Structure of phomenone.

We applied an HPLC method as described previously[10] to check the occurrence of phomenone in infected tomato plants, but this method failed to detect with reliability the occurrence of the phytotoxin in the *Phoma* species mentioned above. However, a more sophisticated investigation, utilizing both a partially modified HPLC method and a high-performance thin-layer chromatographic (HPTLC) method, as described in this paper, excluded the presence of phomenone in cultures of *Phoma betae* Frank, in contrast with previous findings[9].

The methods were applied to *P. destructiva*, to determine quantitatively the toxin, and to *P. betae* from diseased leaf-beet (*Beta vulgaris* var. *cycla* L.) and *P. betae* from diseased spinach (*Spinacia oleracea* L.) culture filtrate extracts, to check its occurrence. The procedure was based on two steps: (1) extraction of culture filtrates with ethyl acetate and (2) analysis by HPLC and HPTLC.

0021-9673/86/$03.50

EXPERIMENTAL

Reagents

All reagents were of analytical reagent grade. HPLC-grade ethanol, acetonitrile, methanol, ethyl acetate, *n*-hexane and chloroform for use as eluting solvents were purchased from Fluka. HPLC-grade water was prepared by double distillation over $KMnO_4$ and filtration on Millipore filters (GSWP, 0.22 μm).

A pure sample of phomenone was purified from culture filtrates of *P. destructiva*, as described previously[8]. Solutions of 1.9 and 0.09 mg of phomenone in 1 ml of methanol for HPLC and HPTLC analysis, respectively, were used as standards.

Culture filtrates

The culture filtrates of *P. destructiva* and *P. betae* isolates were obtained as described previously[8].

Extraction of phomenone from culture filtrates of P. destructiva and extraction of culture filtrates of P. betae from leaf-beet and spinach

Culture filtrates of *P. destructiva* (220 ml), *P. betae* from leaf-beet (1250 ml) and *P. betae* from spinach (1325 ml) were extracted with ethyl acetate (4 × 150 ml for *P. destructiva*, 4 × 900 ml for *P. betae* from leaf-beet and 4 × 900 ml for *P. betae* from spinach). The organic extracts were combined, dried over anhydrous sodium sulphate and evaporated under reduced pressure. The dry residues (15 mg for *P. destructiva*, 28.3 mg for *P. betae* from leaf-beet and 46 mg for *P. betae* from spinach) were dissolved in methanol (1 ml) and analysed by HPLC and HPTLC. The solutions used for HPTLC analysis were diluted 1:100.

HPLC

A Perkin-Elmer Series 3B liquid chromatograph equipped with a Perkin-Elmer LC-75 variable-wavelength UV–visible spectrophotometric detector was used in connection with a Perkin-Elmer Sigma 10B chromatographic data station.

Experimental conditions for the determination of phomenone in the extracts of *P. destructiva* and *P. betae* culture filtrates are reported in Table I.

HPTLC

HPTLC was performed on silica gel-coated aluminium plates (Merck 5547, 20 × 20 cm, 0.25 mm layer), previously washed with ethyl acetate–*n*-hexane (90:10, v/v) and heated at 100°C for 1 h. The plates were eluted for a distance of 10 cm with the same solvent.

A Camag TLC/HPTLC scanning densitometer set at 240 nm was used to analyse the phomenone spots *in situ*. The corresponding peaks were recorded with a Perkin-Elmer 56 recorder and the areas were calculated in square millimetres by graphic integration. Each sample was loaded twice on the plate by an automatic loader under a nitrogen flow as 4 mm spaced narrow bands 4 mm long.

For qualitative HPTLC controls plates of various lengths were used, eluted with chloroform–methanol (85:15, v/v), the phomenone spot showing $R_F = 0.6$.

The plates were analysed by UV detection at 240 nm and by visible detection, by spraying the plates first with 10% sulphuric acid in methanol and then with 3% phosphomolybdic acid in methanol, followed by heating for 10 min at 110°C.

RESULTS

HPLC

The standard deviation of the phomenone determination was 3% for eight replicate injections using two different volumes. When phomenone was analysed using an RP-18 column eluted with the mixtures described in Table I and a UV detector set at 240 nm, the detection limit was 5.5 ng. However, using a silica gel column eluted with ethyl acetate–*n*-hexane (90:10) and a UV detector set at 248 nm (Table I), the detection limit was 100 ng.

The retention time of phomenone is dependent on the experimental conditions and the values obtained are reported in Table I. The analysis of a semi-synthetic liquid medium[11] spiked with phomenone led to an average recovery of 95.1 ± 1.6% in four independent experiments.

The determination of the toxin in crude extracts of *P. destructiva* culture filtrates was accomplished by preparing two calibration graphs of average peak area versus amount of pure compound, and were linear in the range 0.1–8 μg (Fig. 2a and b). The content of phomenone in *P. destructiva* extracts, characterized by the chromatograms in Fig. 3a and b, corresponded to 5.5 μg/ml of culture.

The chromatograms of crude extracts of *P. betae* from beet and spinach culture filtrates, obtained using an RP-18 column as reported in Table I (experimental conditions 1 and 1a–e, showed peaks with the same retention time as phomenone. In contrast, the chromatograms of the same extracts obtained using a silica gel column eluted with ethyl acetate–*n*-hexane (90:10) (experimental conditions 2 and 2a in Table I) showed peaks with retention times different from that of phomenone, as shown in Fig. 4a–d.

TABLE I

EXPERIMENTAL CONDITIONS FOR THE DETERMINATION OF PHOMENONE IN *IN VITRO* CULTURES OF *P. DESTRUCTIVA* AND *P. BETAE* BY HPLC

No.	*Column*	*Chromatographic eluent (v/v)*	*Flow-rate (ml/min)*	*Retention time of phomenone (min)*	*UV detector (nm)*
1	RP-18*	Water–ethanol (70:30)	1.5	3.51	240
1a		Water–ethanol (70:30)	0.8	3.65	240
1b		Water–acetonitrile (50:50)	0.8	3.75	240
1c		Water–methanol (50:50)	0.8	4.78	240
1d		Water–acetonitrile (5:95 to 50:50 over 20 min)**	0.9	3.45	240
1e		Water–acetonitrile (15:85 to 50:50 over 10 min)***	0.8	3.32	240
2	Silica gel*	Ethyl acetate–*n*-hexane (90:10)	2.5	3.09	248
2a		Ethyl acetate–*n*-hexane (90:10)	1.2	7.60	248

* 25 × 0.46 cm I.D., 10 μm (Hibar-LiChrochart stainless steel, Merck).
** Linear gradient.
*** Concave gradient.

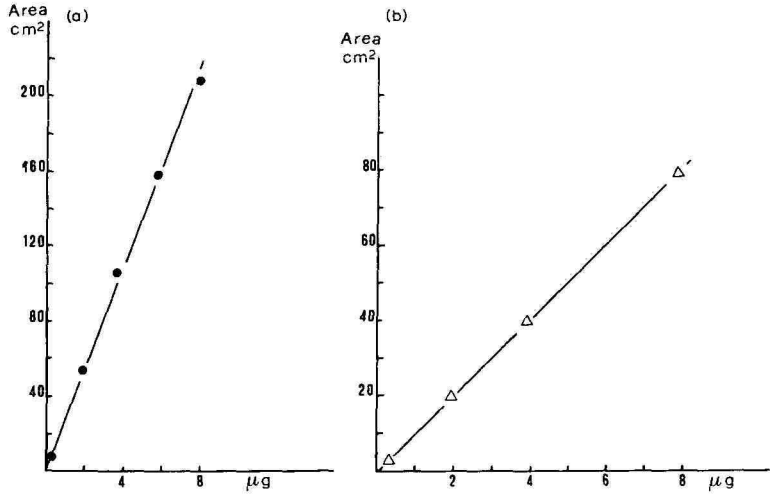

Fig. 2. (a) Calibration graph for phomenone obtained on a Merck RP-18 column. Mobile phase, water–ethanol (70:30, v/v); flow-rate, 1.5 ml/min; detector, 240 nm. (b) Calibration graph for phomenone obtained on a Merck Si-60 column. Mobile phase, ethyl acetate–*n*-hexane (90:10, v/v); flow-rate, 2.5 ml/min; detector, 248 nm.

HPTLC

The detection limit when using a UV detector set at 240 nm was 10 ng, whereas the blue spot of phomenone obtained by spraying the plates first with 10% sulphuric acid in methanol and then with 3% phosphomolybdic acid in methanol followed by heating 10 min at 110°C was detectable at levels up to 19 ng. The standard deviation calculated for ten loadings [5 μl (0.013 μg/μl)] on a plate was found to be 7.8%. The linear calibration graph obtained in the range 10–200 ng is shown in Fig. 5.

The thin-layer chromatogram of a culture filtrate of *P. destructiva* is shown in Fig. 6. Phomenone appeared at R_F 0.42 with UV and visible range development

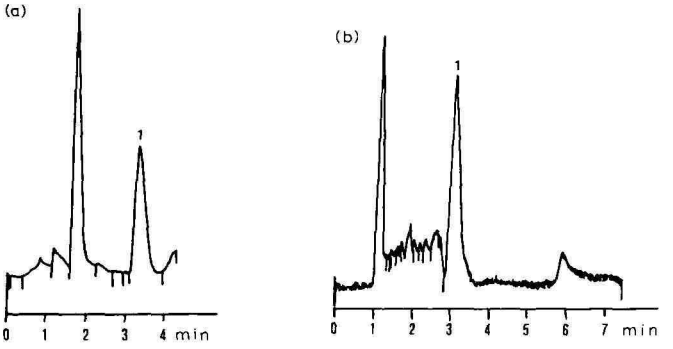

Fig. 3. (a) Chromatogram of extract from *P. destructiva* culture filtrates obtained on a Merck RP-18 column (25 × 0.46 cm I.D., 10 μm) at 20°C. Mobile phase, water–ethanol (70:30, v/v); flow-rate, 1.5 ml/min; detector, 240 nm. Peak 1, phomenone (3.51 min). (b) Chromatogram of extract from *P. destructiva* culture filtrates, obtained on a Merck silica gel column (25 × 0.46 cm I.D., 10 μm) at 20°C. Mobile phase, ethyl acetate–*n*-hexane (90:10, v/v); flow-rate, 2.5 ml/min; detector, 248 nm. Peak 1, phomenone (3.09 min).

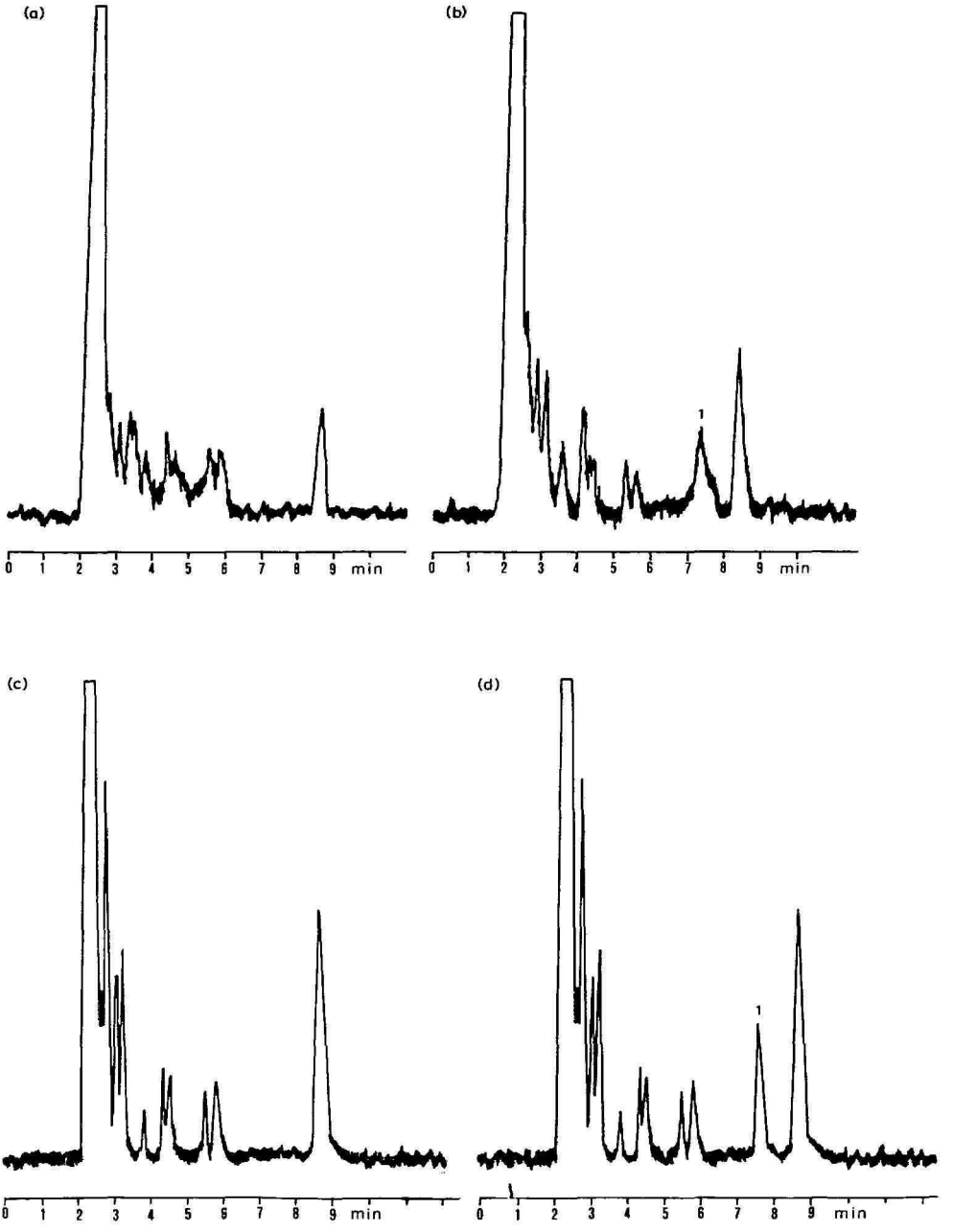

Fig. 4. (a) Chromatogram of extract from culture filtrates of *P. betae* from diseased beet. (b) Chromatogram of extract from culture filtrates of *P. betae* from diseased beet, after co-injection of phomenone. Peak 1, phomenone (7.60 min). (c) Chromatogram of extract from culture filtrates of *P. Betae* from diseased spinach beet. (d) Chromatogram of extract from culture filtrates of *P. betae* from diseased spinach beet, after co-injection of phomenone. Peak 1 phomenone (7.60 min). Merck silica gel column (25 × 0.46 cm I.D., 10 μm) at 20°C. Mobile phase, ethyl acetate–*n*-hexane (90:10, v/v). flow-rate 1.2 ml/min; detector, 248 nm.

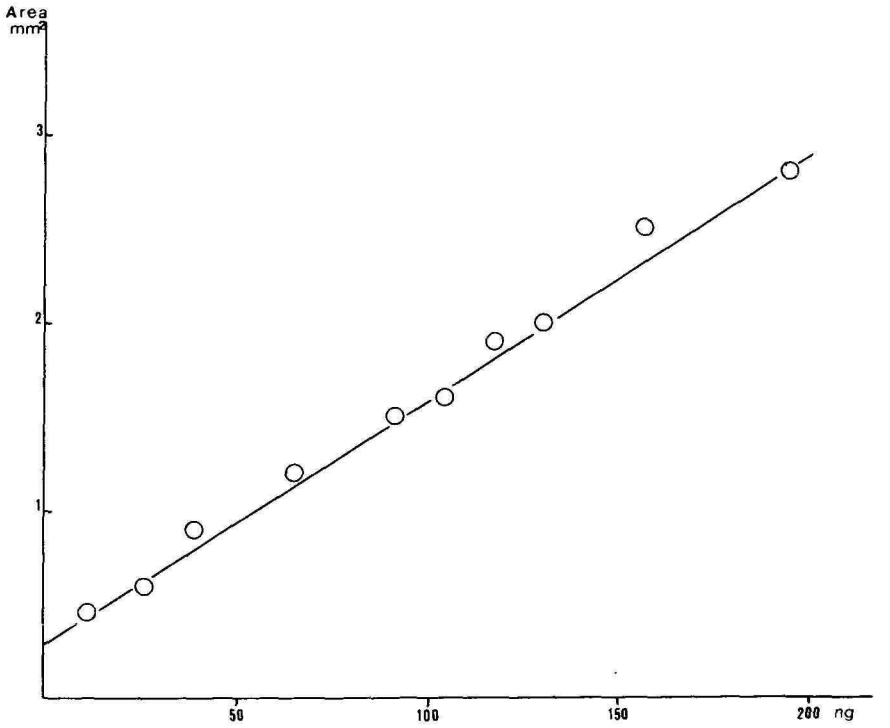

Fig. 5. Calibration graph for phomenone. Merck HPTLC plate (20 × 20 cm, 0.25 mm). Mobile phase, ethyl acetate–*n*-hexane (90:10, v/v). UV detector, 240 nm.

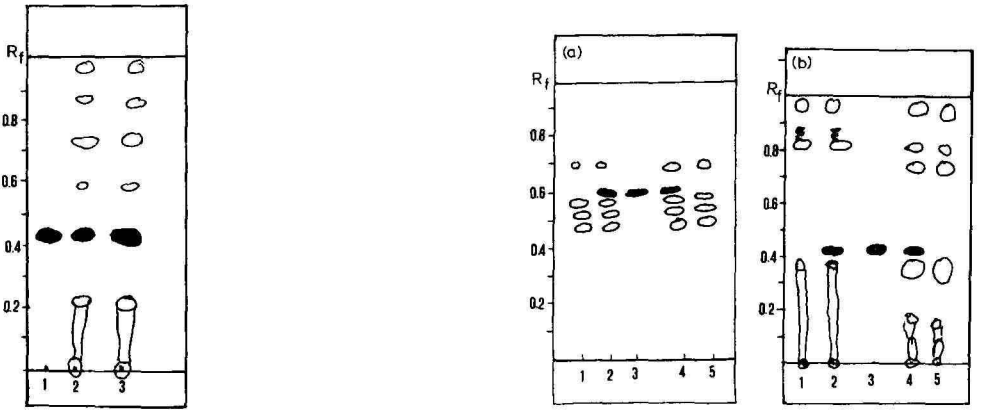

Fig. 6. Chromatogram of extract from *P. destructiva* culture filtrates. 1, Phomenone as reference (R_F 0.42); 2, *P. destructiva* extract by co-loading of phomenone; 3, *P. destructiva* extract. Mobile phase, ethyl acetate–*n*-hexane (90:10, v/v); detector, 240 nm; visible detection by development with 10% sulphuric acid and 3% phosphomolybdic acid in methanol by heating for 10 min at 100°C.

Fig. 7. Chromatograms of extracts from culture filtrates of the two isolates of *P. betae*. Detector, 240 nm; visible detection by development with 10% sulphuric acid and 3% phosphomolybdic acid in methanol by heating for 10 min at 100°C. 1, *P. betae* extract from beet; 2, *P. betae* extract from beet by co-loading of phomenone; 3, phomenone as reference; 4, *P. betae* extract from spinach beet by co-loading of phomenone; 5, *P. betae* extract from spinach beet. Mobile phase: (a) chloroform–methanol (85:15, v/v); (b) ethyl acetate–*n*-hexane (90:10, v/v).

[when chloroform–methanol (85:15, v/v) was used as the eluent, phomenone appeared at R_F 0.60]. Quantitative analysis, performed as described under Experimental, gave an amount of phomenone up to 5.5 μg/ml of (*P. destructiva*) culture.The thin-layer chromatograms of culture filtrate extracts of *P. betae* are shown in Fig. 7a and b; the phomenone spot could not be detected with either a UV or a visible-range detector.

DISCUSSION

Reversed-phase and adsorption TLC methods were not suitable, because compounds with the same R_F as phomenone were not separated. On the other hand, the HPTLC method allowed the separation of phomenone from compounds having an R_F value similar to that of phomenone (Figs. 6, 7a and 7b). This method showed a resolution higher than that of reversed-phase HPLC, although its sensivity was similar (10 and 5 ng, respectively). Finally, the HPLC method with a UV detector and a silica gel column gave good resolution, but it exhibited a low sensitivity (100 ng) on account of the interference of the UV absorbance of the solvent (ethyl acetate–*n*-hexane) with phomenone. Therefore, by combining the use of HPTLC plates with a scanning densitometer and an automatic loader, it was possible to perform rapid and sensitive analyses with a precision comparable to that of HPLC.

The two methods were used independently for the analysis of *P. destructiva* cultures, whereas HPTLC was used in combination with HPLC to determine phomenone in *P. betae* cultures. Using HPLC on silica gel the detection limit of the toxin was 100 ng, whereas using silica gel HPTLC it was 10 ng, because in the latter instance ethyl acetate was removed by evaporation on the plate and the analysis was performed *in situ*. Such conditions should be considered when an eluent interferes in UV detection. Moreover, if a scanning densitometer is not available, HPTLC can be used in a preliminary step to establish a suitable mobile phase for the HPLC column to be used.

In conclusion, for the analysis of *Phoma* phytopathogenic species, the application of these two methods, separately or together, should provide reliable results.

ACKNOWLEDGEMENTS

We thank Dr. Giovanni Di Pascale for its helpful discussions. This work was supported by the Italian Research Council, Special ad hoc Programme Chimica Fine e Secondaria Subproject Ca.

REFERENCES

1 J. F. Bousquet and N. Barbier, *Phytopathol. Z.*, 75 (1972) 365.
2 Y. Moulé, S. Moreau and J. F. Bousquet, *Chem.-Biol. Interact.*, 17 (1977) 185.
3 S. Moreau, Y. Moulé and F. Bousquet, *Ann. Nutr. Aliment.*, 31 (1977) 881.
4 A. Bottalico, S. Frisullo, N. S. Iacobellis, R. Capasso, E. Corrado and G. Randazzo, *Phytopathol. Mediterr.*, 22 (1983) 116.
5 R. Capasso, N. S. Iacobellis, A. Bottalico and G. Randazzo, *Phytochemistry*, 23 (1984) 2781.
6 N. S. Iacobellis and A. Bottalico, *Phytopathol. Mediterr.*, 23 (1985) in press.
7 C. Riche, C. Pascard-Billy, M. Devys, A. Gaudemer and M. Barbier, *Tetrahedron Lett.*, 32 (1974) 2765.

8 A. Bottalico, S. Frisullo, P. Lerario, G. Randazzo and R. Capasso, *Phytopathol. Mediterr.*, 21 (1982) 39.
9 A. Bottalico, S. Frisullo, N. S. Iacobellis, R. Capasso, A. Evidente, I. Iasiello and G. Randazzo, *Phytopathol. Mediterr.*, 22 (1983) 120.
10 R. Capasso, E. Corrado, G. Randazzo and A. Bottalico, *J. Liq. Chromatogr.*, 7 (1984) 935.
11 A. Nachmias, I. Barash, Z. Solel and G. Strobel, *Physiol. Plant Pathol.*, 10 (1977) 147.

Journal of Chromatography, 356 (1986) 367–371
Elsevier Science Publishers B.V., Amsterdam — Printed in The Netherlands

CHROM. 18 483

Note

Analysis of the radiochemical purity of [^{14}C]chloroform and dibromo[1,2-$^{14}C_2$]ethane by radiomonitored high-performance liquid chromatography

DAVID A. WELLS
Graduate Center for Toxicology, University of Kentucky, Lexington, KY 40536-0078 (U.S.A.)
and
GEORGE A. GARBOLAS and GEORGE A. DIGENIS*
Division of Medicinal Chemistry, College of Pharmacy, University of Kentucky, Lexington, KY 40536-0081 (U.S.A.)
(Received January 15th, 1986)

The determination of the radiochemical purity of a synthesized radioactive compound has traditionally involved a separation by thin-layer chromatography, column chromatography or gas chromatography (GC), with subsequent quantitation of radioactivity. In recent years, high-performance liquid chromatography (HPLC) has been recognized as a sensitive and rapid method for the separation and quantitation of radiolabeled compounds[1–5].

In order to examine the radiochemical purity of two commercially obtained products, [^{14}C]chloroform and dibromo[1,2-$^{14}C_2$]ethane, a chromatographic system of first choice would be GC, since methods for the separation of these compounds are well documented in the literature. However, a radioactivity detector on-line with a GC system was not available to us. As an alternative method, an HPLC assay was developed which separated chloroform from the expected chemical contaminants arising from its synthesis, namely dichloromethane and carbon tetrachloride, and which also separated 1,2-dibromoethane from bromoethane. The HPLC assay involved UV detection of the effluent at 205 nm followed by quantitation of radioactivity using a flow-through radioactivity detector. This paper details the use of radiomonitored HPLC in the determination of the radiochemical purity of commercially obtained [^{14}C]chloroform and dibromo[1,2-$^{14}C_2$]ethane.

EXPERIMENTAL

Chemicals and reagents

[^{14}C]Chloroform (2.5 mCi, 4.6 mCi/mmol; lot No. 1844-056) and dibromo[1,2-$^{14}C_2$]ethane (2.5 mCi, 3.8 mCi/mmol; lot No. 2157-031) were obtained from New England Nuclear (Boston, MA, U.S.A.). Dichloromethane, chloroform and methanol were of HPLC grade and purchased from Fisher Scientific (Fairlawn, NJ, U.S.A.). Carbon tetrachloride, bromoethane and 1,2-dibromoethane were of Gold Label grade and were purchased from Aldrich (Milwaukee, WI, U.S.A.). Solvents were filtered through a 0.45-μm Millipore filter and degassed before use.

0021-9673/86/$03.50

Instrumentation and chromatographic conditions

Identification of chemicals and evaluation of radiochemical purities were determined using an HPLC system consisting of an Altex 110A solvent metering pump (Altex, Berkeley, CA, U.S.A.), a Varian Vari-Chrom analytical UV detector (Varian, Palo Alto, CA, U.S.A.) and a Linear Instruments dual-channel recorder (Linear, Reno, NV, U.S.A.). Samples were injected via a Rheodyne Model 7125 injector (Rheodyne, Cotati, CA, U.S.A.) fitted with a 20-μl loop onto an Altex 5-μm Ultrasphere ODS column (25 cm × 4.6 mm I.D.). The mobile phase consisted of methanol–water (75:25, v/v), delivered at a flow-rate of 1.0 ml/min with UV detection at 205 nm. The effluent passed through the UV detector and then into a Flo-One HP flow-through radioactivity detector (Radiomatic, Tampa, FL, U.S.A.). The programmable detector mixed scintillation cocktail (Flo-Scint III, Radiomatic) with effluent in a ratio of 3:1 (v/v). The UV output was recorded on one channel of the recorder and the radioactivity output was recorded simultaneously on the second channel.

Sample preparation

The sealed glass ampule containing the neat sample of [^{14}C]chloroform (65 mg) or dibromo[1,2-$^{14}C_2$]ethane (123.5 mg) was cooled in dry ice and then broken open, and the contents were transferred to an empty glass ampule by using a micropipet. The glass ampule containing the transferred liquid sample was cooled in dry ice and then sealed by using a gas flame. The residue remaining adsorbed to the glass of the original ampule was dissolved in methanol and the successive rinses were combined into a volumetric flask (5 or 10 ml) to make a stock solution. An aliquot of each stock solution was added to 15 ml of scintillation cocktail (Scintiverse II, Fisher Scientific) and counted for radioactivity in a Packard Model 3255 liquid scintillation counter (Packard, Downers Grove, IL, U.S.A.). Another aliquot was injected into the HPLC system for the determination of radiochemical purity.

RESULTS AND DISCUSSION

Retention times of unlabeled standards

Stock solutions of the chemical standards were prepared in methanol (1, 2 or 10 mg/ml) and analyzed by HPLC (for conditions, see Experimental). The chromatogram representing chloroform and its derivatives is shown in Fig. 1 and the retention times are as follows: dichloromethane (a), 3.7 min; chloroform (b), 4.5 min; and carbon tetrachloride (c), 8.3 min. Fig. 2 illustrates the chromatogram of bromoethane (a) and 1,2-dibromoethane (b), having retention times of 4.8 and 5.4 min, respectively. Note that in each chromatogram the first two mass peaks (UV detection) are from the methanol solvent used. This was confirmed by injecting methanol alone and observing the identical peaks on the chromatogram.

Radiomonitored HPLC analysis of [^{14}C]chloroform

A 20-μl aliquot of the stock solution of [^{14}C]chloroform in 5 ml methanol (17.3 μCi/ml, 0.45 mg/ml) was analyzed by radiomonitored HPLC and the corresponding chromatogram is shown in Fig. 3. Five significant radioactive peaks (upper tracing on chromatogram) were identified which together account for 99.7% of the total radioactivity present in the sample. The identities of peaks 1 and 4 are unknown and

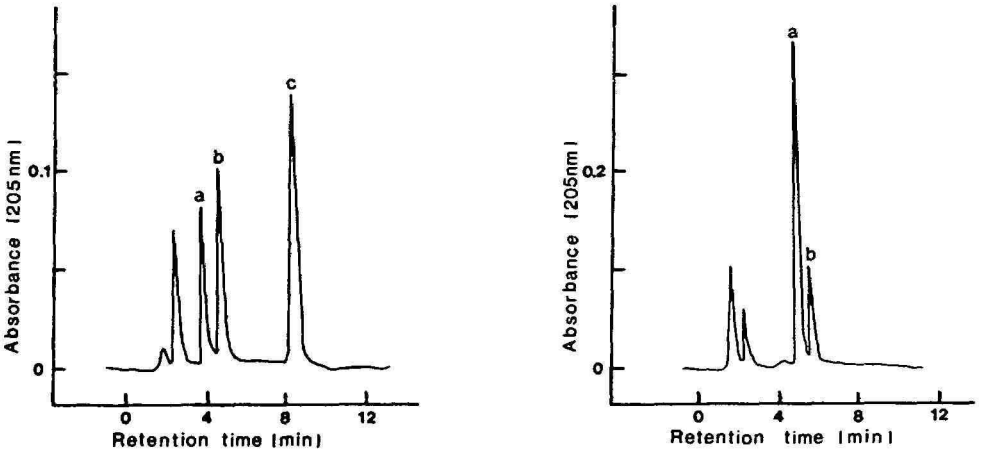

Fig. 1. HPLC chromatogram of a mixture of dichloromethane (a), chloroform (b) and carbon tetrachloride (c). The first two UV peaks are from the methanol solvent used in preparing the stock solutions. See Experimental for chromatographic conditions.

Fig. 2. HPLC chromatogram of a mixture of bromoethane (a) and 1,2-dibromoethane (b). The first two UV peaks are from the methanol solvent used in preparing the stock solutions. See Experimental for chromatographic conditions.

together represent 2.2% of the total radioactivity. Peak 2 was determined to be dichloromethane, based on the retention time of the radioactive peak compared to that of the unlabeled standard, although no definitive UV absorption peak is detectable. This impurity represents 3.5% of the total radioactivity. Peak 5 is also an impurity, determined (in the same manner as described for dichloromethane) to be carbon tetrachloride, present as 0.8% of the total radioactivity. Peak 3 represents [^{14}C]chloroform and is detectable by UV absorption as peak c (lower tracing on chromatogram), having a retention time of 4.5 min. The radiochemical purity of [^{14}C]chloroform was determined to be 93.2%. The two UV peaks designated as a and b are from the methanol solvent used in preparing the stock solutions.

Radiomonitored HPLC analysis of dibromo[1,2-$^{14}C_2$]ethane

A 20-μl aliquot of the stock solution of dibromo[1,2-$^{14}C_2$]ethane in 10 ml methanol (6.8 μCi/ml, 0.34 mg/ml) was analyzed by radiomonitored HPLC and the corresponding chromatogram is shown in Fig. 4. Two major radioactive peaks (upper tracing on chromatogram) were identified which together account for 99.9% of the total radioactivity present in the sample. Peak 1 was determined to be bromoethane, based on the retention time of the radioactive peak compared to that of the unlabeled standard, although no definitive UV absorption peak is detectable. Peak 2 was determined to be dibromo[1,2-$^{14}C_2$]ethane, confirmed by UV absorption as peak c (lower tracing on chromatogram) with a retention time of 5.4 min. The radiochemical purity of dibromo[1,2-$^{14}C_2$]ethane was determined to be 99.6%. Radioactivity peaks 3 and 4 arising at about 9 min are unidentified but are likely to be polybrominated derivatives and are known to collectively contain less than 0.1% of the total radioactivity in the sample. The two UV peaks designated as a and b are from the methanol solvent used in preparing the stock solutions.

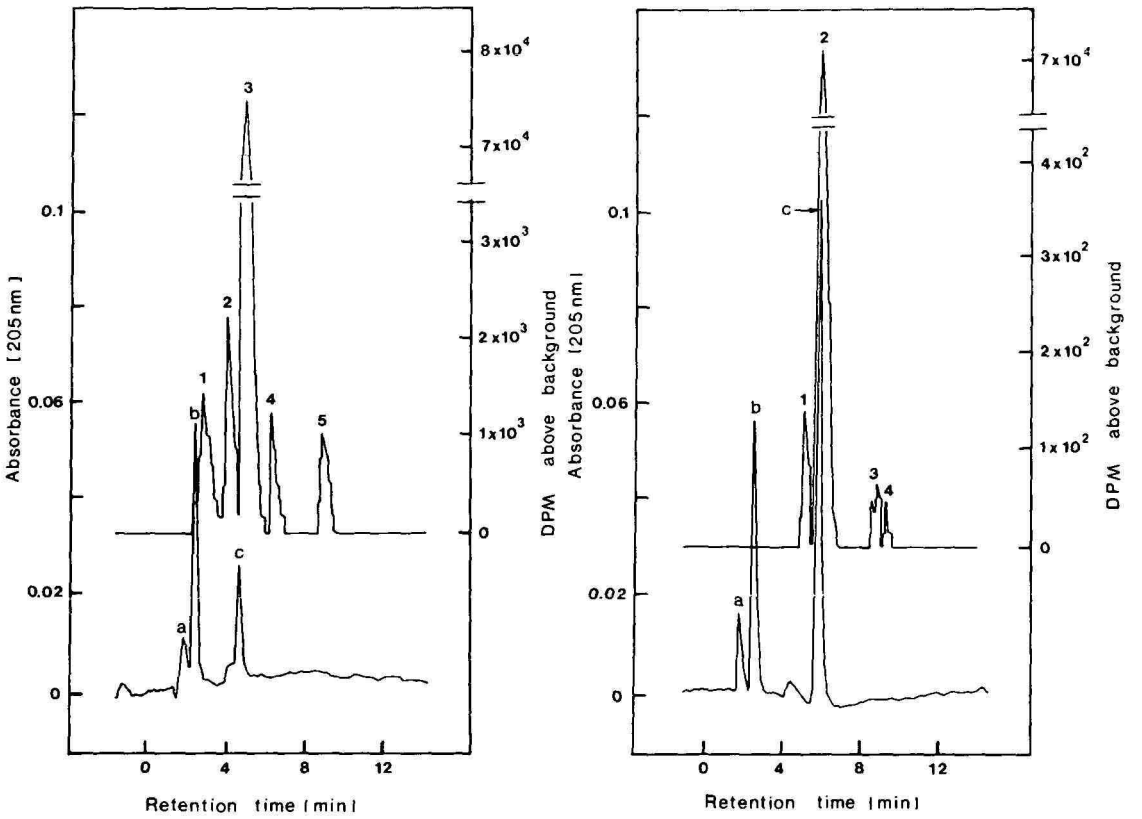

Fig. 3. Lower tracing: HPLC chromatogram of [^{14}C]chloroform (c) in methanol (a, b) by UV detection at 205 nm. Upper tracing: Radiochromatogram; ^{14}C-detection by direct analysis of column effluent using a flow-through radioactivity detector (see Experimental for details and chromatographic conditions). Peaks: 1 = unidentified; 2 = dichloromethane; 3 = chloroform; 4 = unidentified; 5 = carbon tetrachloride.

Fig. 4. Lower tracing: HPLC chromatogram of dibromo[1,2-$^{14}C_2$]ethane (c) in methanol (a, b) by UV detection at 205 nm. Upper tracing: Radiochromatogram; ^{14}C-detection by direct analysis of column effluent using a flow-through radioactivity detector (see Experimental for details and chromatographic conditions). Peaks: 1 = bromoethane; 2 = 1,2-dibromoethane; 3, 4 = unidentified.

CONCLUSIONS

[^{14}C]Chloroform and dibromo[1,2-$^{14}C_2$]ethane were commercially obtained and their radiochemical purities were evaluated. In the case of [^{14}C]chloroform, the manufacturer reported a radiochemical purity of 97.4% using GC with flame ionization detection, with the system coupled to an undescribed radioactivity detector. A radiomonitored HPLC analysis of the same sample determined that the radiochemical purity was only 93.2%. The results for the dibromo[1,2-$^{14}C_2$]ethane sample were more closely comparable between the GC and HPLC radiomonitored systems. By GC analysis, also with flame ionization detection and an undescribed radioactivity

detector, the manufacturer reported 99% radiochemical purity, while HPLC analysis determined the purity to be 99.6%.

In the determination of the radiochemical purity of synthesized radiolabeled products, it has been shown in this report that radiomonitored HPLC is a very sensitive method and can yield more accurate results than those obtainable by radio-gas chromatography. It is suggested that HPLC be used more routinely in evaluations of the radiochemical purities of labeled compounds. A flow-through radioactivity detector can easily be added to any existing HPLC system and its usefulness can be extended to radioactivity quantitation of biological samples from radiotracer experiments.

REFERENCES

1 D. R. Reeve and A. Crozier, *J. Chromatogr.*, 137 (1977) 271.
2 W. J. Rzeszotarski, in G. L. Hawk (Editor), *Biological/Biomedical Applications of Liquid Chromatography*, Marcel Dekker, New York, 1979, p. 475.
3 B. M. Frey and F. J. Frey, *Clin. Chem.*, 28 (1982) 689.
4 M. J. Kessler, *J. Chromatogr.*, 255 (1983) 209.
5 R. F. Roberts and M. J. Fields, *J. Chromatogr.*, 342 (1985) 25.

Journal of Chromatography, 356 (1986) 372–378
Elsevier Science Publishers B.V., Amsterdam — Printed in The Netherlands

CHROM. 18 473

Note

Anwendung der indirekten photometrischen Detektion mit Gradientenelution

Charakterisierung technischer Alkansulfonate

GÜNTER EPPERT* und GERT LIEBSCHER*
VEB Leuna-Werke "Walter Ulbricht", 4220 Leuna (D.D.R.)
(Eingegangen am 1. August 1985; geänderte Fassung eingegangen am 7. Januar 1986)

Insbesondere Small und Miller[1] zeigten die Leistungsfähigkeit der indirekten photometrischen Detektion (IPD) zur Visualisierung von an Ionentauschern getrennten anorganischen Anionen und Kationen. Zunehmend breitere Anwendung findet das Prinzip der IPD auch in der Umkehrphasenchromatographie UV-transparenter ionogener und nichtionogener Verbindungen[2–23]. Alle diese Arbeiten bedienen sich der isokratischen Arbeitsweise, die im allgemeinen aber nur auf einfache Gemische angewendet werden kann. Für die chromatographische Trennung kompliziert (komplex) zusammengesetzter Gemische ist zur Erzielung einer maximalen Information in der Mehrzahl der Fälle Gradientenelution notwendig.

Anliegen der vorliegenden Arbeit ist es deshalb zu zeigen, daß sich die IPD unter geeigneten Bedingungen mit der Gradientenelution kombinieren lässt, wodurch man ein allgemein anwendbares Detektionsprinzip erhält. Elutionssysteme und Visualisierungsreagens (VR) müssen allerdings stoffklassenspezifisch auf weitgehend empirischer Grundlage ausgewählt werden.

Die Anwendung der IPD mit Gradientenentwicklung auf komplexe Gemische wird von uns nachfolgend am Beispiel der Charakterisierung technischer Alkanmonosulfonate dargestellt.

Über die flüssigchromatographische Trennung technischer Alkanmonosulfonate mittels Hochleistungs-Flüssigkeitschromatographie (HPLC) berichteten zuerst Ullner *et al.*[24]. Sie wendeten die Umkehrphasen-Ionenpaarchromatographie isokratisch in einem System Methanol–Wasser–Tetrabutylammoniumhydrogensulfat an. Trennungen vergleichbarer Qualität und kürzerer Analysenzeit gelangen in einem ähnlichen System mit Lithiumacetat[25]. Die Detektion musste in beiden Fällen aufgrund der UV-Transparenz der Alkansulfonate mit dem Differentialrefraktometer erfolgen.

Smedes *et al.*[26] untersuchten technische Alkansulfonate auch durch Gradientenelution. Um allerdings unter diesen Bedingungen eine Detektion zu erreichen,

* Vorgetragen zum "4. Diskussionstreffen HPLC" der Chemischen Gesellschaft der D.D.R., Arbeitsgemeinschaft Chromatographie, am 20.9.1984 in Halle/Saale, D.D.R.

0021-9673/86/$03.50

nutzten sie die Ionenpaarbildung via post-Säulen UV-Detektion und umgingen so die Kombination der Gradientenelution mit der Ionenpaarchromatographie.

EXPERIMENTELLER TEIL

Für die experimentellen Untersuchungen stand ein Flüssigchromatograph des Typs 1084 B (Hewlett-Packard) mit Detektor variabler Wellenlänge Typ 79875 A zur Verfügung.

Die chromatographischen Trennungen erfolgten an 200 × 4.6 mm I.D. Säulen mit LiChrosorb RP-8, 10 μm (Merck). Methanol, rein, (VEB Leuna-Werke, Leuna, D.D.R.) und frisch destilliertes Wasser wurden vor der Chromatographie über G4-Fritten filtriert.

Die Herstellung der verwendeten N-Alkylpyridiniumsalze erfolgte aus Pyridin und den entsprechenden Alkylhalogeniden[27].

Zur Untersuchung gelangten endständige Alkanmonosulfonate verschiedener Hersteller sowie C-Zahl-reine Sulfonatgemische, die durch Laborsulfochlorierung präpariert wurden. Als technische Aniontenside wurden Emulgator E 30 (VEB Leuna-Werke), K 30 (Bayer, Leverkusen, B.R.D.) und Hostapur SAS (Hoechst, Frankfurt/Main, B.R.D.) eingesetzt.

ERGEBNISSE UND DISKUSSION

Voraussetzungen zur Gradientenelution

Im Mittelpunkt der jüngeren Arbeiten zur Trennung UV-transparenter ionogener Spezies an Umkehrphasen und IPD stehen die Untersuchung systemspezifischer Effekte und das Responseverhalten[8–12]. Diese Arbeiten beschäftigen sich mit der Lage des durch das VR induzierten Systempeaks im Chromatogramm mit dem Ziel, eine maximale Nachweisempfindlichkeit zu erreichen.

Wir versuchten hingegen, experimentelle Bedingungen zu finden, unter denen der Systempeak das chromatographische System möglichst nicht beeinflusst und die Voraussetzungen für eine störungsfreie Chromatogrammauswertung mit einfachem Responseverhalten gegeben sind. Dafür sollten besonders günstige Voraussetzungen bestehen, wenn der Systempeak zur Totzeit t_M eluiert wird und seine Lage weitestgehend unabhängig von der Zusammensetzung der fluiden Phase ist. Deshalb orientierten wir uns von vornherein auf ein stark hydrophiles Reagens, das nach unserer Auffassung die entscheidende Voraussetzung zur Anwendbarkeit der indirekten photometrischen Detektion mit programmierter Elution in einem wässrigen Umkehrphasensystem darstellt.

Um ein solches Reagens zu finden, untersuchten wir zunächst das chromatographische Verhalten verschiedener N-Alkylpyridiniumsalze unter Standardbedingungen an RP-8 in Abhängigkeit vom Methanolgehalt in der fluiden Phase. Wie in Fig. 1 zu sehen ist, steigt die Retention des Systempeaks mit zunehmender Länge der Alkylkette stark an. Das erwünschte Verhalten zeigt nur N-Methylpyridiniumchlorid (MPC), das zudem einfach aus Pyridin mit Methyliodid und anschliessendem Ionentausch herstellbar ist.

Weitere Versuche galten der Ermittlung der günstigsten MPC-Konzentration und Detektionswellenlänge. Bewertungskriterien waren hierbei Peakschärfe und

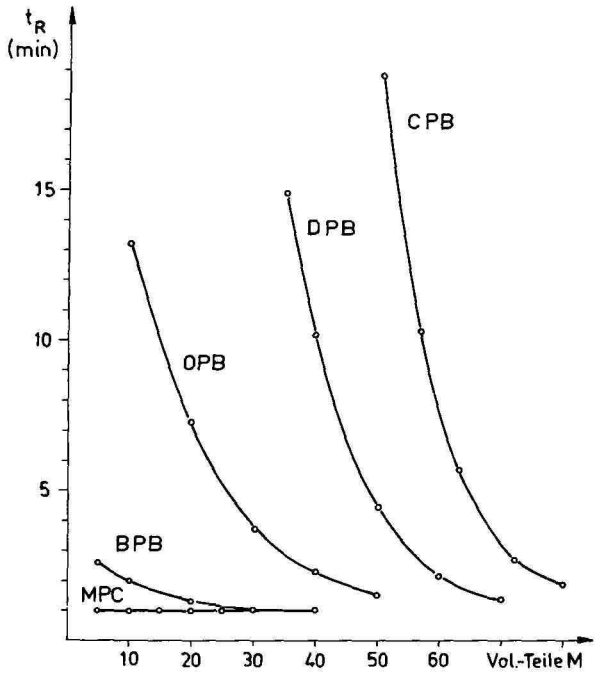

Fig. 1. Bruttoretentionszeit t_R des Systempeaks in Abhängigkeit vom Methanolanteil in der fluiden Phase. MPC = N-Methylpyridiniumchlorid, BPB = N-Butylpyridiniumbromid, OPB = N-Octylpyridiniumbromid, DPB = N-Dodecylpyridiniumbromid, CPB = N-Cetylpyridiniumbromid.

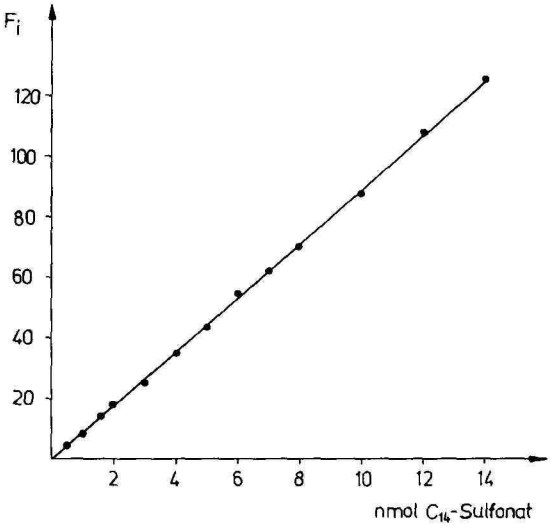

Fig. 2. Zusammenhang zwischen der Peakfläche F_i und der Menge an Tetradecan-1-sulfonat. Isokratische Arbeitsweise mit 50% Methanol. Übrige Bedingungen siehe Tabelle I.

TABELLE I

CHROMATOGRAPHISCHE BEDINGUNGEN

Probelösungen	1%ige Lösungen in Methanol–Wasser oder Eluens
Dosiervolumen	5 oder 10 µl
Fluide Phase A	30% Methanol (v/v) + 0.25 mmol MPC/l
Fluide Phase B	80% Methanol (v/v) + 0.25 mmol MPC/l
Fluss	2 ml/min
Säulenraumtemperatur	313 K
Wellenlänge	260 nm
Papiergeschwindigkeit	0.5 cm/min
Signalabschwächung	2^7 (2^6)
Gradient	25–95% B/20 min (42.5–77.5% Methanol/20 min)

Peakfläche eines definierten Alkanmonosulfonates im System Methanol–Wasser–VR. Im Ergebnis dieser Versuche wurde eine Messwellenlänge von 260 nm (das entspricht etwa dem Absorptionsmaximum von Pyridin[28]) und eine VR-Konzentration von 0.25 mmol/l Eluens festgelegt. Linearität zwischen Signal und Konzentration besteht bis 15 nmol Alkansulfonat (Fig. 2) und darüber hinaus. Die untere Detektionsgrenze lag für die untersuchten Alkansulfonate bei 0.2 nmol. Unter den Bedingungen der Gradientenelution (Tabelle I) traten keine Schwierigkeiten auf. Blindgradienten zeigten für den in Frage kommenden Bereich (siehe Tabelle I) keine Drift.

Ermittlung von Responsefaktoren

Die quantitative Chromatogrammauswertung erwies sich als überraschend einfach, denn die molaren Responsefaktoren wurden (anhand endständiger Alkansulfonate) im Bereich C_{10}–C_{18} als weitgehend konstant ermittelt (Tabelle II).

Zur Prüfung auf eventuelle Abhängigkeit des Responseverhaltens vom organischen Anteil in der fluiden Phase dienten Elutionsmittel unterschiedlichen Methanolgehaltes im Bereich von 30–75% Methanol. Der Nachweis konstanter Peakflächen erfolgte in 5%-Intervallen mit Decan-1-sulfonat (30–45% Methanol), Tetra-

TABELLE II

RESPONSEVERHALTEN DEFINIERTER ENDSTÄNDIGER ALKANMONOSULFONATE

C-Zahl	*Hersteller*	*% Methanol**	*F_i (cm^2)***	*s_w (% rel.)****
10	Schuchardt	38	1.629	0.3
12	Schuchardt	43	1.620	1.0
12	Leuna	43	1.562	0.8
13	Schuchardt	50	1.466	1.3
14	Schuchardt	52	1.446	1.2
14	Merck	52	1.665	0.5
15	Leuna	54	1.588	1.1
16	Schuchardt	58	1.658	1.0
18	Merck	64	1.652	1.0

* Methanolgehalt bei isokratischer Arbeitsweise (vgl. Text).

** Peakflächen F_i für jeweils gleiche molare Sulfonatmengen. Die niedrigeren Responsefaktoren sind auf ungenügende Reinheit der Produkte zurückzuführen.

*** Standardabweichung der Einzelbestimmungen.

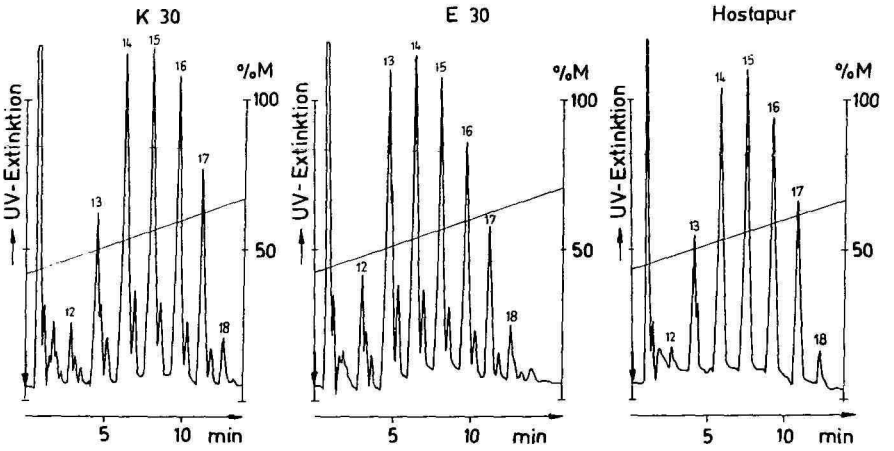

Fig. 3. Untersuchung technischer Alkansulfonate. Bedingungen siehe Tabelle I; je 5 µl 1%iger Lösungen. K 30, Bayer; E 30, Leuna-Werke; Hostapur SAS, Hoechst. Die Zahlen kennzeichnen die C-Zahl der betreffenden Peakgruppe.

TABELLE III

ERGEBNISSE DER UNTERSUCHUNGEN AN EMULGATOR E 30

Bedingungen siehe Tabelle I, M_i = relative Molekülmasse der Komponente(n), F_i = Peakfläche der Komponente(n) in elektronischen Flächeneinheiten × 10^{-3}, Ma(%) = Masseprozent der Komponente(n), bezogen auf die Summe aller Alkanmonosulfonate.

C-Zahl	M_i	*Alkansulfonate*	F_i	s_w *(% rel.)*	*Ma(%)*
11	258	Gesamt	27.2	7.3	1.68
		Nicht endständig			1.43
		Endständig			0.25
12	272	Gesamt	112.6	3.0	6.62
		Nicht endständig			5.04
		Endständig			1.58
13	286	Gesamt	488.8	0.8	27.33
		Nicht endständig			23.14
		Endständig			4.19
14	300	Gesamt	476.4	1.1	25.39
		Nicht endständig			21.77
		Endständig			3.62
15	314	Gesamt	378.8	1.9	19.28
		Nicht endständig			16.71
		Endständig			2.57
16	328	Gesamt	244.2	2.2	11.90
		Nicht endständig			10.53
		Endständig			1.37
17	342	Gesamt	117.2	1.9	5.47
		Nicht endständig			4.97
		Endständig			0.50
18	356	Gesamt	39.2	3.6	1.76
		Nicht endständig			1.53
		Endständig			0.23
19	370	Gesamt	13.2	8.9	0.56

decan-1-sulfonat (45–60% Methanol) und Octadecan-1-sulfonat (60–75% Methanol). Die Werte der einzelnen Messreihen wurden einer Varianzanalyse unterworfen. Dabei ergaben sich zwischen den Mittelwerten der Messreihen keine signifikanten Unterschiede, so dass unter den gewählten Bedingungen ein vom Methanolgehalt und damit vom Gradienten unabhängiges Responseverhalten der einzelnen Sulfonate angenommen werden kann.

Untersuchungen an technischen Alkansulfonaten

Fig. 3 zeigt die Anwendung der IPD mit Gradientenelution auf verschiedene technische Alkansulfonate. Aus den Chromatogrammen lassen sich Informationen über C-Zahl-Verteilung und mittlere C-Zahl der Produkte einzelner Hersteller sowie die Anteile an endständigen Monosulfonaten ermitteln.

Der letzte Peak jeder Peakgruppe entspricht dem endständigen Monosulfonat, der erste Peak enthält das Gemisch aller nichtendständigen Monosulfonate, die im vorderen C-Zahlbereich (C_{11}–C_{13}) weiter aufgelöst werden. Die Produkte K 30 und E 30 sind durch Sulfochlorierung hergestellt, Hostapur SAS hingegen über Sulfoxidation. Bei letzterem Produkt treten endständige Monosulfonate nur in geringen Mengen auf. Di- und Polysulfonate erscheinen in allen Chromatogrammen im ersten Peak. Eine detaillierte Auswertung enthält Tabelle III am Beispiel des Emulgators E 30, wobei Di- und Polysulfonate nicht berücksichtigt worden sind.

Die Zuordnung der Peaks erfolgte mit Hilfe definierter Alkanmonosulfonate und C-Zahl-reiner Sulfonatgemische.

SCHLUSSFOLGERUNGEN

Die IPD erwies sich als ein mit der Gradientenelution kompatibles Untersuchungs- und Detektionsprinzip. Um das zu erreichen, müssen für einzelne Stoffklassen spezifische Bedingungen und geeignete Visualisierungsreagenzien ermittelt werden, insbesondere so, dass der Systempeak mit der Totzeit erscheint. Am Beispiel der bekannten Methoden zur Untersuchung von technischen Alkansulfonaten ergibt die neue Methode eine Reihe von Vorteilen, die vor allem in der hohen Empfindlichkeit, der kurzen Analysenzeit sowie einer schnellen Regenerierbarkeit und einem vorteilhaften Responseverhalten des chromatographischen Systems zu sehen sind.

Die Anwendung der Methode auf andere Stoffklassen und weitere Tenside ist Gegenstand von Untersuchungen, über die an anderer Stelle berichtet wird.

LITERATUR

1 H. Small und T. E. Miller, Jr., *Anal. Chem.*, 54 (1982) 462.
2 B. A. Bidlingmeyer, *J. Chromatogr. Sci.*, 18 (1980) 525.
3 N. A. Parris, *J. Liq. Chromatogr.*, 3 (1980) 1743.
4 T. Gnanasambandan und H. Freiser, *Anal. Chem.*, 53 (1981) 909.
5 T. Gnanasambandan und H. Freiser, *Anal. Chem.*, 54 (1982) 2379.
6 T. Gnanasambandan und H. Freiser, *Anal. Chem.*, 54 (1982) 1282.
7 M. Dreux, M. Lafosse und M. Pequignot, *Chromatographia*, 15 (1982) 653.
8 L. Hackzell und G. Schill, *Chromatographia*, 15 (1982) 437.
9 J. J. Stranahan und S. N. Deming, *Anal. Chem.*, 54 (1982) 1540.
10 B. A. Bidlingmeyer und F. V. Warren, Jr., *Anal. Chem.*, 54 (1982) 2351.
11 B. Sachok, S. N. Deming und B. A. Bidlingmeyer, *J. Liq. Chromatogr.*, 5 (1982) 389.

12 L. Hackzell, T. Rydberg und G. Schill, *J. Chromatogr.*, 282 (1983) 179.
13 P. Helboe, *J. Chromatogr.*, 261 (1983) 117.
14 W. E. Barber und P. W. Carr, *J. Chromatogr.*, 260 (1983) 89.
15 W. E. Barber und P. W. Carr, *J. Chromatogr.*, 301 (1984) 25.
16 M. Dreux, M. Lafosse und P. Agbo-Hazoume, *Chromatographia*, 18 (1984) 15.
17 P. R. Haddad und A. L. Heckenberg, *J. Chromatogr.*, 300 (1984) 357.
18 J. Andrasko, *J. Chromatogr.*, 314 (1984) 429.
19 A. Trujillo, T. Gnanasambandan und H. Freiser, *Anal. Chim. Acta*, 162 (1984) 333.
20 G. Vigh und A. Leitold, *J. Chromatogr.*, 312 (1984) 345.
21 J. E. Parkin, *J. Chromatogr.*, 287 (1984) 457.
22 J. E. Parkin, *J. Chromatogr.*, 303 (1984) 436.
23 J. E. Parkin und H. T. Lau, *J. Chromatogr.*, 314 (1984) 488.
24 H. Ullner, I. König, C. Sander und U. Schwenk, *Tenside*, 17 (1980) 169.
25 G. Eppert und G. Liebscher, unveröffentlichte Ergebnisse.
26 F. Smedes, J. C. Kraak, C. F. Werkhoven-Goewie, U. A. Th. Brinkman und R. W. Frei, *J. Chromatogr.*, 247 (1982) 123.
27 F. Korte, *Methodicum Chimicum*, Band 6, G. Thieme Verlag, Stuttgart, 1974, S. 637.
28 R. A. Friedel und M. Orchin, *UV-Spectra of Aromatic Compounds*, Wiley, New York, Chapman and Hall, London, 1951.

Journal of Chromatography, 356 (1986) 379–381
Elsevier Science Publishers B.V., Amsterdam — Printed in The Netherlands

CHROM. 18 481

Note

Determination of alkyl sulfonates by liquid chromatography with indirect photometric detection

J. R. LARSON
Analytical Laboratories, The Dow Chemical Company, 574 Building, Midland, MI 48667 (U.S.A.)
(Received December 30th, 1985)

Indirect photometric liquid chromatography (IPC) is the name given to a technique which uses a UV-absorbing counter-ion in an ion-exchange mode with an UV detector to determine ionic species. IPC, as described in detail by Small and Miller[1,2], was first used for the determination of inorganic ions. Later Larson and Pfeiffer used IPC for the determination of UV-transparent quaternary ammonium salts[3], and alkylamines and alkanolamines[4]. This paper describes an IPC technique for the determination of a class of UV-transparent organic anions, *viz.* alkyl sulfonates. In the past these compounds have been determined by time-consuming derivatization techniques[5]. More recently, reversed-phase ion-pair chromatography with UV-absorbing ion-pair reagents has been used for determination of these compounds[6–8].

EXPERIMENTAL

Chemicals

Distilled-in-glass acetonitrile was obtained from Burdick and Jackson Labs. (Muskegon, MI, U.S.A.). Potassium biphthalate was obtained from Aldrich (Milwaukee, WI, U.S.A.). Sulfosalicylic acid and *m*-sulfobenzoic acid were obtained from ICN Pharmaceuticals (Plainview, NY, U.S.A.).

High-performance liquid chromatographic conditions

The liquid chromatograph used consisted of a Laboratory Data Control Constametric III pump, a Rheodyne Model 7125 injection valve equipped with a 20-μl loop, a Perkin-Elmer LC-75 variable-wavelength UV detector and a Sargent-Welch Model SRG recorder. The column used was a 250 × 4.6 mm I.D. Partisil 10 SAX (Whatman).

RESULTS AND DISCUSSION

In IPC the UV-absorbing counter-ion has the dual role of (1) selectively displacing the sample ions from the ion-exchange column and (2) revealing the UV-transparent sample ions as negative peaks in an elevated baseline as they are displaced from the column. Three compounds, potassium biphthalate, sulfosalicylic acid and *m*-sulfobenzoic acid were evaluated for use as the UV-absorbing counter-ion for the

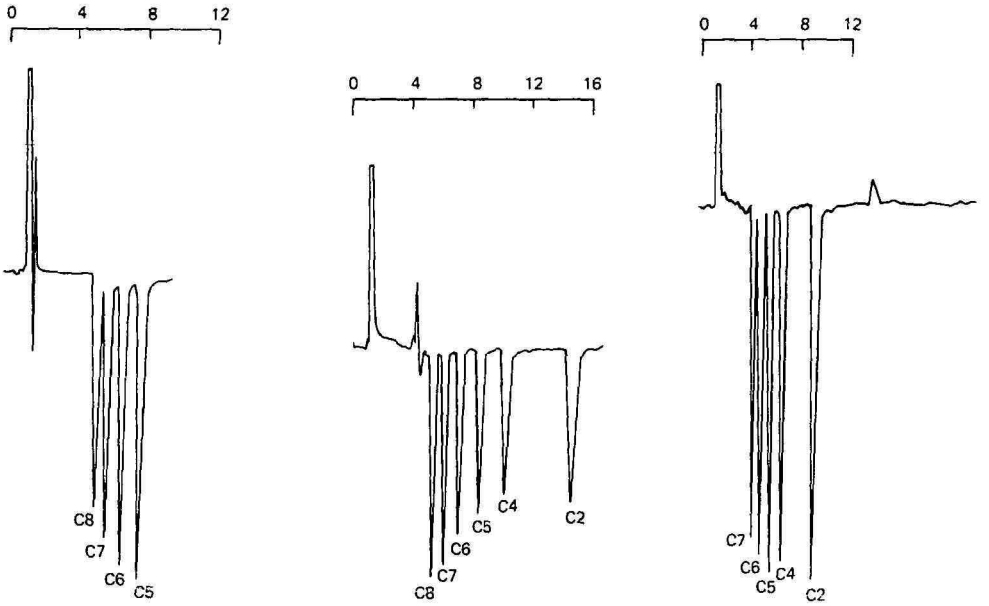

Fig. 1. Separation of octanesulfonate (C8), heptanesulfonate (C7), hexanesulfonate (C6) and pentanesulfonate (C5). Column: 250 × 4.6 mm I.D. Partisil-10 SAX. Mobile phase: acetonitrile–water (60:40) with 0.005 *M* potassium biphthalate, pH 5; flow-rate, 2.0 ml/min. Detection: UV at 297 nm and 0.16 a.u.f.s. Injection: 20 μl of 1.0 mg/ml of each alkylsulfonate in mobile phase.

Fig. 2. Separation of octanesulfonate (C8), heptanesulfonate (C7), hexanesulfonate (C6), pentanesulfonate (C5), butanesulfonate (C4) and ethanesulfonate (C2). Mobile phase: acetonitrile–water (60:40) with 0.005 *M* sulfosalicylic acid, pH = 2.4. Detection: UV at 320 nm and 0.16 a.u.f.s. Other conditions as in Fig. 1.

Fig. 3. Separation of heptanesulfonate (C7), hexanesulfonate (C6), pentanesulfonate (C5), butanesulfonate (C4), and ethanesulfonate (C2). Mobile phase: acetonitrile–water (60:40) with 0.005 *M* *m*-sulfobenzoic acid, pH = 3.6. Detection: UV at 298 nm and 0.16 a.u.f.s. Other conditions as in Fig. 1.

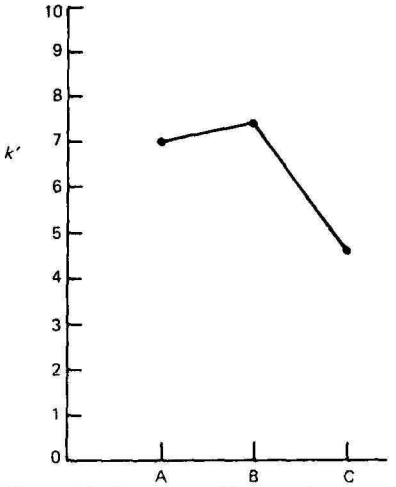

Fig. 4. *k'* of pentanesulfonate with: (A) biphthalate; (B) sulfosalicylic acid; (C) *m*-sulfobenzoic acid.

separation of alkyl sulfonates. Separations obtained using identical counter-ion and organic modifier concentrations are shown in Figs. 1–3. As illustrated in Fig. 4, which is a plot of capacity factor (k') *versus* choice of counter-ion, *m*-sulfobenzoic acid is the strongest counter-ion while potassium biphthalate and sulfosalicylic are approximately equal in strength. Thus, for speed of analysis *m*-sulfobenzoic acid would be the counter-ion of choice.

As noted by Small and Miller[1], the sensitivity of IPC improves as the concentration of counter-ion decreases up to the point where increased k' and band spreading negate this beneficial effect. This means that *m*-sulfobenzoic acid could also be used for increased sensitivity, since its concentration in the mobile phase could be reduced and still maintain k' equivalent to the other two counter-ions.

A linear response and constant k' were observed for the alkyl sulfonates over a range of 10–1000 ppm with a detection limit of 0.3 μg.

The IPC approach has several advantages compared to a reversed-phase ion-pair technique using a UV-absorbing ion-pair reagent[7]. These include improved peak shape, increased linear range, ease of calibration (peak height or peak area), and selectivity. Since retention times using the ion-pair approach decrease as volume injected or concentration injected increases, peak identification is difficult and calibration is limited to peak areas. Since the mode of separation in IPC is ion exchange, ionic compounds are retained while neutral compounds elute on the solvent front. This selectivity of IPC for ionic compounds is also an advantage, because alkyl sulfonates are often used in complex non-ionic matrixes.

REFERENCES

1 H. Small and T. E. Miller, *Anal. Chem.*, 54 (1982) 462.
2 *U.S. Pat.*, No. 4,414,842.
3 J. R. Larson and C. D. Pfeiffer, *Anal. Chem.*, 55 (1983) 393.
4 J. R. Larson and C. D. Pfeiffer, *J. Chromatogr.*, 259 (1983) 519.
5 T. Nakagawa, K. Miyajima and T. Uno, *J. Gas Chromatogr.*, 6 (1968) 292.
6 M. Denkert, L. Hackzell, G. Schill and E. Sjögren, *J. Chromatogr.*, 218 (1981) 31.
7 B. Sachok, S. N. Deming and B. A. Bidlingmeyer, *J. Liquid Chromatogr.*, 5 (1982) 389.
8 B. A. Bidlingmeyer and F. V. Warren, Jr., *Anal. Chem.*, 54 (1982) 2351.

HPLC columns for optical resolution

CHIRALPAK
CHIRALCEL

Daicel Chemical Industries, Ltd. has developed excellent chiral columns for the separation of optical isomers. "CHIRALPAK" or "CHIRALCEL" in combination with High Performance Liquid Chromatography has proven to be a highly successful technique for separation of optical isomers and for the determination of enantiomeric purity of compounds. Now a wide variety of optically pure compounds are readily available without laborious resolution techniques!

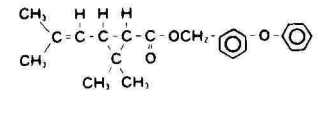

CHIRALPAK OT(+)
25cm×0.46cm I.D.
eluent: methanol
flow rate: 0.5ml/min
detection: UV 254nm

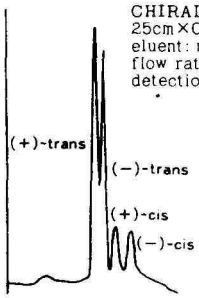

J. Am. Chem. Soc., 103, 6971 (1981)

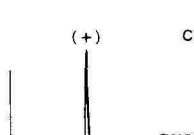

CHIRALCEL OC
25cm×0.46cm I.D.
eluent:
hexane-2-propanol
flow rate: 1.5ml/min
detection: UV 220nm

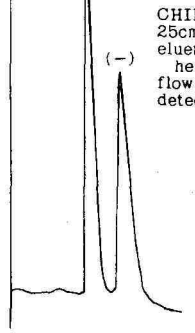

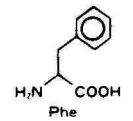

CHIRALPAK WH
12.5cm×0.46cm I.D.
eluent:
aq. 0.25mM $CuSO_4$
flow rate: 1.5ml/min
detection: UV 254nm

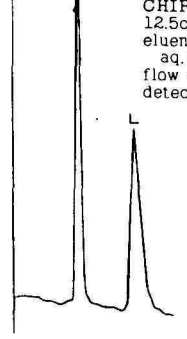

For more details about HPLC columns, please contact:

DAICEL CHEMICAL INDUSTRIES, LTD.

Tokyo
8-1, Kasumigaseki 3-chome,
Chiyoda-ku, Tokyo 100, Japan
Phone: 03 (507) 3173, 3178
Telex: 222-4632 DAICEL J

Düsseldorf
Königsallee 92a,
4000 Düsseldorf 1, F.R. Germany
Phone: (0211) 134158
Telex: (41) 8588042 DCEL D

New York
Pan-Am Bldg., 200 Park Avenue,
New York, N.Y. 10166-0130, U.S.A.
Phone: (212) 878-6765, 6766
Telex: (23) 236154 DCC UR

DAICEL (U.S.A.), INC.
611 west 6th Street, Room 2152
Los Angeles California 90017, U.S.A.
Phone: (213) 629-3656
Telex: 215515 DCIL UR

PUBLICATION SCHEDULE FOR 1986

Journal of Chromatography (incorporating *Chromatographic Reviews*) and *Journal of Chromatography, Biomedical Applications*

MONTH	O 1985	N 1985	D 1985	J	F	M	A	M	J	
Journal of Chromatography	346 347/1	347/2 347/3 348/1	348/2 349/1 349/2 350/1 350/2	351/1 351/2 351/3	352 353 354	355/1 355/2 356/1	356/2 356/3 357/1	357/2 357/3 358/1 358/2 359		The publication schedule for further issues will be published later
Chromatographic Reviews								373/1		
Bibliography Section					372/1		372/2		372/3	
Biomedical Applications				374/1 374/2	375/1	375/2	376 377	378/1	378/2 379	

INFORMATION FOR AUTHORS

(Detailed *Instructions to Authors* were published in Vol. 329, No. 3, pp. 449–452. A free reprint can be obtained by application to the publisher.)

Types of Contributions. The following types of papers are published in the *Journal of Chromatography* and the section on *Biomedical Applications:* Regular research papers (Full-length papers), Short communications and Notes. Short communications are preliminary announcements of important new developments and will, whenever possible, be published with maximum speed. Notes are usually descriptions of short investigations and reflect the same quality of research as Full-length papers, but should preferably not exceed four printed pages. For review articles, see page 2 of cover under Submission of Papers.

Submission. Every paper must be accompanied by a letter from the senior author, stating that he is submitting the paper for publication in the *Journal of Chromatography*. Please do not send a letter signed by the director of the institute or the professor unless he is one of the authors.

Manuscripts. Manuscripts should be typed in double spacing on consecutively numbered pages of uniform size. The manuscript should be preceded by a sheet of manuscript paper carrying the title of the paper and the name and full postal address of the person to whom the proofs are to be sent. Authors of papers in French or German are requested to supply an English translation of the title of the paper. As a rule, papers should be divided into sections, headed by a caption (*e.g.*, Summary, Introduction, Experimental, Results, Discussion, etc.). All illustrations, photographs, tables, etc., should be on separate sheets.

Introduction. Every paper must have a concise introduction mentioning what has been done before on the topic described, and stating clearly what is new in the paper now submitted.

Summary. Full-length papers and Review articles should have a summary of 50–100 words which clearly and briefly indicates what is new, different and significant. In the case of French or German articles an additional summary in English, headed by an English translation of the title, should also be provided. (Short communications and Notes are published without a summary.)

Illustrations. The figures should be submitted in a form suitable for reproduction, drawn in Indian ink on drawing or tracing paper. Each illustration should have a legend, all the *legends* being typed (with double spacing) together on a *separate sheet.* If structures are given in the text, the original drawings should be supplied. Coloured illustrations are reproduced at the author's expense, the cost being determined by the number of pages and by the number of colours needed. The written permission of the author and publisher must be obtained for the use of any figure already published. Its source must be indicated in the legend.

References. References should be numbered in the order in which they are cited in the text, and listed in numerical sequence on a separate sheet at the end of the article. Please check a recent issue for the layout of the reference list. Abbreviations for the titles of journals should follow the system used by *Chemical Abstracts.* Articles not yet published should be given as "in press", "submitted for publication", "in preparation" or "personal communication".

Dispatch. Before sending the manuscript to the Editor please check that the envelope contains three copies of the paper complete with references, legends and figures. One of the sets of figures must be the originals suitable for direct reproduction. Please also ensure that permission to publish has been obtained from your institute.

Proofs. One set of proofs will be sent to the author to be carefully checked for printer's errors. Corrections must be restricted to instances in which the proof is at variance with the manuscript. "Extra corrections" will be inserted at the author's expense.

Reprints. Fifty reprints of Full-length papers, Short communications and Notes will be supplied free of charge. Additional reprints can be ordered by the authors. An order form containing price quotations will be sent to the authors together with the proofs of their article.

Advertisements. Advertisement rates are available from the publisher on request. The Editors of the journal accept no responsibility for the contents of the advertisements.

HPLC columns for optical resolution

CHIRALPAK
CHIRALCEL

Daicel Chemical Industries, Ltd. has developed excellent chiral columns for the separation of optical isomers. "CHIRALPAK" or "CHIRALCEL" in combination with High Performance Liquid Chromatography has proven to be a highly successful technique for separation of optical isomers and for the determination of enantiomeric purity of compounds. Now a wide variety of optically pure compounds are readily available without laborious resolution techniques!

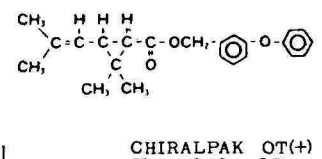

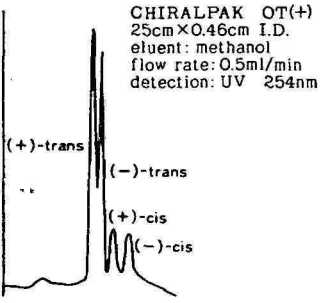

CHIRALPAK OT(+)
25cm×0.46cm I.D.
eluent: methanol
flow rate: 0.5ml/min
detection: UV 254nm

J. Am. Chem. Soc., 103, 6971 (1981)

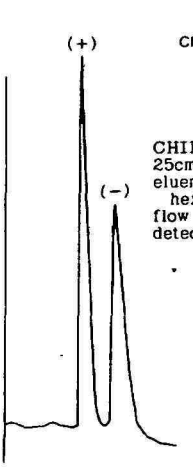

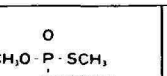

CHIRALCEL OC
25cm×0.46cm I.D.
eluent:
hexane-2-propanol
flow rate: 1.5ml/min
detection: UV 220nm

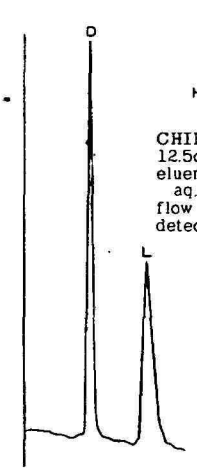

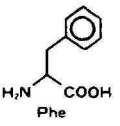

CHIRALPAK WH
12.5cm×0.46cm I.D.
eluent:
aq. 0.25mM $CuSO_4$
flow rate: 1.5ml/min
detection: UV 254nm

For more details about HPLC columns, please contact:

DAICEL CHEMICAL INDUSTRIES, LTD.

Tokyo
8-1, Kasumigaseki 3-chome,
Chiyoda-ku, Tokyo 100, Japan
Phone: 03 (507) 3173, 3178
Telex: 222-4632 DAICEL J

Düsseldorf
Königsallee 92a,
4000 Düsseldorf 1, F.R. Germany
Phone: (0211) 134 158
Telex: (41) 8588042 DCEL D

New York
Pan-Am Bldg., 200 Park Avenue,
New York, N.Y. 10166-0130, U.S.A.
Phone: (212) 878-6765, 6766
Telex: (23) 236154 DCC UR

DAICEL (U.S.A.), INC.
611 west 6th Street, Room 2152
Los Angeles California 90017, U.S.A.
Phone: (213) 629-3656
Telex: 215515 DCIL UR